

Toward personalized medicine: human adipose-derived stem cells (ASCs) and xenogenic-free media as enabling tools in tendon tissue engineering strategies.

Original

Toward personalized medicine: human adipose-derived stem cells (ASCs) and xenogenic-free media as enabling tools in tendon tissue engineering strategies / Stanco, Deborah. - (2020 Jul 02), pp. 1-208.

Availability:

This version is available at: 11583/2839845 since: 2020-07-14T10:36:47Z

Publisher:

Politecnico di Torino

Published

DOI:

Terms of use:

Altro tipo di accesso

This article is made available under terms and conditions as specified in the corresponding bibliographic description in the repository

Publisher copyright

(Article begins on next page)



UNIVERSITÀ
DEGLI STUDI
DI TORINO



ScuDo
Scuola di Dottorato -- Doctoral School
WHAT YOU ARE, TAKES YOU FAR



Doctoral Dissertation

Doctoral Program in Bioengineering and Medical-Surgical Sciences XXXII Cycle

**Toward personalized medicine:
human adipose-derive stem cells
(ASCs) and xenogenic-free media as
enabling tools in tendon tissue
engineering strategies.**

Deborah Stanco

Supervisors

Prof Gianluca Ciardelli
Dr Gianni Soldati

Doctoral Examination Committee:

Prof Mauro Alini, Referee, AO Research Institute Davos
Dr Enrico Lucarelli, Referee, Istituto Ortopedico Rizzoli
Prof Valeria Chiono, Politecnico di Torino
PD Dr Alexandre Lädermann, Geneva University Hospitals
Prof. Livia Visai, Università degli Studi di Pavia

Politecnico di Torino
April 2020

I hereby declare that, the contents and organisation of this dissertation constitute my own original work and does not compromise in any way the rights of third parties, including those relating to the security of personal data.

Deborah Stanco

April 2020

*To my adorable parents and my sister for their love,
words of encouragement, and endless support
pushing me to be the best version of myself every day.*

Grazie.

Acknowledgements

The work presented in this thesis would not have been possible without the close association with many people. I take this opportunity to extend my sincere gratitude and appreciation to all those who made this PhD thesis possible.

This thesis was carried out in collaboration with Swiss Stem Cell Foundation (SSCF), in Lugano, Switzerland, and with Joint Research Center (JRC) of European Commission, in Ispra, Italy.

First of all, I wish to thank my supervisors Gianluca Ciardelli, Full Professor at the Department of Mechanical and Aerospace Engineering (DIMEAS) of Politecnico of Turin and Dr Gianni Soldati, President of SSCF. They each fulfilled different roles as mentors during my PhD program. I would also to thank the distinguished reviewers of this PhD thesis, Dr Enrico Lucarelli from Istituto Ortopedico Rizzoli, and Dr Mauro Alini, Vice Director of AO Research Institute Davos, for their comments and appreciations.

I am extremely grateful to Prof Gianluca Ciardelli for his guidance and continuous support throughout my PhD in terms of time, mentorship, patience and also to economically sustain the second part of my PhD fellowship. I found very stimulating the periodic internal group meetings to debate about own experimental activity, results and concerns with a multitude of PhD students, Post-doc researchers and technicians (it is a very big and young team!). I would also express my congratulation to the School of Doctorate of the Politecnico (Scudo) for the high profile and multi-disciplinary courses that he has offered during this XXXII cycle of PhD program. I also found the possibility to attend congresses and external advance courses a very stimulating experience and opportunity. It allowed me to meet top-level worldwide researchers in person as in occasion of the Advance Course of Tissue Engineering at the Rice University in Houston hosted by Prof Antonios Mikos in August 2018 and during the Advance course of Immunology hosted by Dr Francesco Iacono at Messina in July 2018.

I wish to thank Dr Gianni Soldati for introducing me to this PhD program and to give me the great opportunity to join in the research and development team in his stem cell bank facility in Switzerland. Here I could collaborate in the development

of the clinical application of adipose-derived stem cells by the in vitro research work described in chapter 4. It was also very unique and instructive experience to be part on the International Congress on Adipose Stem Cell Treatments (ICAST) fully organized by the SSCF and held at the Technopark of Zurich in 2017 and 2018.

During these years, several people of the research staff at the Biomedical Lab of DIMEAS and at the SSCF have been very kind to help and teach me. In particular I would like to thank Dr Monica Boffito for her availability, kind support and to discuss and editing my work and Dr Christian Caprara for his supervision and to share with me criticisms as well as intuitions contributing positively to my work. I would also thank to all team of the SSCF including Silvia and Jean Mark for their kind welcome in the Swiss land and the informal nice moments provided of break out of the lab. I always found in all of them both scientific and moral support, fundamental to achieve the results reported in this thesis.

I want also to express my deep gratitude to all staff from the Health, Consumers & Reference Materials Unit F2 at JRC. The Joint Research Centre is the European Commission's department operating in Belgium, Germany, Italy, Spain and the Netherlands, with 2000 researchers and it is responsible for creating and managing much of the knowledge used to support the European Commission's policies. The multicultural and multi-disciplinary environment provided me it was an experience that will leave marks beyond this thesis. I am grateful to the team leader Dr Josepha Barrero and the Unit director's Arnd Hoeveler, that make this collaboration possible and to both the Medical Device and Nanobiotechnology teams that help me to investigate 3D bioprinting technology in terms of both regulatory and scientific point of view. I would also thank Dr Salvatore Tirendi and Dr Patricia Urbán for their constant support, availability and constructive suggestions and Dr Alessia Bogni, who was very kind to have always given me a hand to deal with the practicalities of working in the Nanobiotechnology facility. I would also to thank my first office/lab mate Dorelia for her kind welcome and availability. They have always gone off their way to make me feel integrated and were determinant for the accomplishment of the work presented in chapter 5, 6, and 7.

Finally, I would like to thank my adorable family and all my very special friends who support me during the challenging moments of this PhD program, uplift me, comfort me and bring joy to my soul. Special thanks also to Edoardo, locked down with me during Coronavirus emergency, is the best partner any writer could ever hope to have, for his love, constant support and confidence in me and, for sure, also for the delicious meals that he cooked for me. Thank you.

Summary

Tendon injuries affect millions of people worldwide annually and still remain a major challenge for clinicians. Tendon tissue is a connective tissue mainly composed by collagen fibrils organized with a hierarchical structure. Considering the scarce functionality of healed tendons and the unsuccessful clinical outcome of current conventional treatments, the development of tissue engineering and regenerative medicine (TERM) approaches have been proposed. To this end, a multidisciplinary strategy that resemble the specific 3D architecture, biological (e.g. progenitor cells) biophysical (e.g. stiffness and mechanical-sensitivity) and biochemical (growth factors, matrix proteins) characteristics of the microenvironment of tendon is strictly required. Three-dimensional (3D) bioprinting represents a promising tool in this contest, since it may allow production of highly precise 3D-structures by controlled placement of cells and biomaterials mimicking morphology and functionality of the native target tissue. However, the most advanced studies for its application in musculoskeletal system are mainly focused on bone and cartilage reconstruction. Among mesenchymal stem cell (MSC) sources, adipose derived stem cells (ASCs) have been already successfully employed *in vivo* for a wide range of pathological conditions including the treatment of tendon injuries. The precious hallmarks of ASCs for their use in TERM applications include, among others, multipotency, anti-inflammatory and immune-modulation properties as well as trophic and angiogenic effects. Some of the growth factors (GFs) known to be involved in the tendon healing process, have been proven to trigger MSC tenogenesis *in vitro*. However, the literature lacks a consensus about the exact medium culture composition that efficiently drives MSC tenogenesis *in vitro*. Moreover, optimization of standards and culture protocols, cell density and the use of clinical grade reagents are urgently needed to achieve their clinical application.

In order to meet these needs and move toward clinical scale-up of the use of ASCs in regenerative cell-based therapies for tendon treatment, in this Ph.D. thesis a bottom-up approach has been adopted encompassing three main steps: i) the development of xenogenic-free protocol for adipose-derived stem cell culture and differentiation toward a tenocyte-like phenotype in 2D *in vitro* condition; ii) the design of a 3D bioprinted construct fabricated with a precise positioning of ASCs

within a natural-based bioink for tendon TERM; and iii) the thorough analysis of regulatory aspects, availability of standards and guidelines within the current legislation framework about the possible clinical use of 3D bioprinting.

First, ASC cultured with the novel chemically defined serum-free and xenogenic-free (SF) medium and human platelet lysate (hPL) medium maintained MSC features, including the expression of stem-cell markers. Both SF and hPL tenogenic media (TENOs) consisting in the supplementation of AA (ascorbic acid), CTGF (connective tissue GF), TGF β -3 (transforming GF beta-3) and BMP-12 (bone morphogenic protein-12), efficiently triggered the differentiation of ASCs in 2D *in vitro* condition as demonstrated by the statistically significant up-regulation of specific tendon-related genes and proteins. Finally, for the first time in literature, ASCs were embedded in a nanofibrillar cellulose/alginate (NFC/A) hydrogel and 3D bioprinted into grid square structures suitable for tendon TERM application. 3D printed cells showed good cell viability suggesting the safety of the printing protocol and high tendon-related proteins synthesis when TENOs induced. The absence of ASC inflammatory response to the 3D NFC/A scaffold ensured the safety of the xeno-free FDA approved hydrogel constituents and of the xeno-free GMP-compliant tenogenic differentiation protocol. In addition, the careful examination of the existing regulation in the European Union indicated that a 3D bioprinted product could be classified as a tissue engineered combined medicinal product that would fall under the scope of the ATMP Regulation, although, as an emerging field, there is still a lack of bioprinting-related standards. In conclusion, the first attempt on the suitability of ASC-laden hydrogel for tendon TERM showed successful preliminary results on the applicability of 3D bioprinting of ASCs, suggesting, also, novel insight about tendon development. The evaluation of MSCs in a tissue-like construct is another key aspect to better understand their behavior in 3D-environments. Finally, there is an urgent need for an adequate standard to ensure that a bioprinted product can be reproducibly had a high quality and is effective and safe.

Contents

.....	0
Acknowledgements	7
Summary	10
Chapter 1	17
General Introduction	17
Goal and thesis scope	18
PART I	20
Chapter 2	21
Stem cells in tissue engineering and regenerative medicine	21
2.1 Abstract	22
2.2 Toward personalized medicine	23
2.3 Stem Cells in Regenerative Medicine and Tissue Engineering	26
2.3.1 Induced Pluripotent Stem Cells.....	27
2.3.2 Mesenchymal Stem/Stromal Cells	30
2.4 References	43
Chapter 3	53
Tendon Tissue Engineering	53
3.1 Abstract	54
3.1 Basic science of tendon.....	55
3.2 Conventional treatments	62
3.3 Tendon tissue engineering and regeneration.....	63
3.4 References	72
PART II	78
Chapter 4	79
<i>In vitro</i> tenogenic differentiation of ASCs in GMP-compliant xenogenic-serum free media	79
4.1 Abstract	80
4.2 Introduction	81
4.3 Materials and Methods.....	86
4.4 Results and Discussion.....	95
4.5 Conclusions	111
4.6 References	113
Chapter 5	120
3D bioprinting technology: current advances and limits for bone and cartilage tissue engineering applications and its mapping by TIM	120

5.1 Abstract	121
5.2 Introduction	122
5.3 Research strategy	124
5.4 Results and Discussion.....	125
5.5 Conclusions	139
5.6 References	140
Chapter 6	148
3D Bioprinting of Adipose-derived Stem Cells with Nanocellulose-Alginate bioink for tendon tissue Engineering applications	148
6.1 Abstract	149
6.2 Introduction	150
6.3 Materials and Methods.....	153
6.4 Results and Discussion.....	164
6.5 Conclusions	187
6.6 References	189
PART III.....	195
Chapter 7	196
The regulatory framework and available standards for 3D bioprinted products	196
7.1 Abstract	197
7.2 Classification of 3D bioprinted products under EU regulatory framework	198
7.3 Regulatory framework for 3D bioprinting outside Europe	203
7.4 Conclusions	205
7.5 References	206
Conclusions and future perspectives.....	209

List of Figures

Figure 2.1. The main aim of regenerative medicine and tissue engineering approaches	24
Figure 2.2 3D bioprinting	25
Figure 2.3. Stem cell classification	26
Figure 2.4. Potential of induced pluripotent stem cells (iPSC) for regenerative medicine, disease modelling, and drug discovery.	28
Figure 2.5. MSC activation in the perivascular region	32
Figure 2.6. Mechanical MSC memory effects on their multipotency	33
Figure 2.7. Preclinical studies of human MSC-derived EV.	35
Figure 2.8. MSC clinical trials registered internationally from 2011 through 2019.	37
Figure 2.9. Comparison between BMSCs and ASCs harvest	39
Figure 3.1. Ligament structure.....	55
Figure 3.2. Tendon hierarchical structure	56
Figure 3.3. Histology of tendon.	57
Figure 3.4. Stress–strain curve of tendon tissue.	58
Figure 3.5. Tendon healing process.	60
Figure 3.6. Tendon tissue engineering approach.	63
Figure 3.7. Preparation of platelet-rich plasma (PRP).....	65
Figure 3.8. Natural polymers.	67
Figure 4.1. Schematic diagram depicting svf isolation and characterization.	87
Figure 4.2. Determination of the number of viable cells with nucleocounter	89
Figure 4.3. Morphological appearance.	95
Figure 4.4. Immunophenotype profile of hPL-ASCs and SF-ASCs.....	96
Figure 4.5. Cell morphological appearance during tenogenic induction compared to undifferentiated cells cultured in CTRL conditions.	97
Figure 4.6. Cell viability.	98
Figure 4.7. Gene expression of cell proliferation and embryonic stem cell markers in control media conditions	99
Figure 4.8. Gene expression of cell proliferation and embryonic stem cell markers after tenogenic differentiation and in ctrl cell culture conditions.....	101
Figure 4.9. Scleraxis, tenascin-c and decorin expression.	103
Figure 4.10. Collagen type I, type III and COMP gene expression.....	105
Figure 4.11. MMP3, MMP13 and TIMP2 gene expression.	106
Figure 4.12. Scleraxis expression and collagen matrix deposition after tenogenic differentiation.	108
Figure 4.13. Tenomodulin expression on ASC surfaces.	110
Figure 5.1. 3D bioprinting strategy.....	123
Figure 5.2. Search strategy	124
Figure 5.3. Classification of bioprinting techniques.....	128
Figure 5.4. Tim platform (scopus, patstat, cordis) search.....	136
Figure 5.5. Scientific publication production trend from 2007 to 2019	137

Figure 5.6. Network analyses.	138
Figure 6.1. 3D printing equipment.....	153
Figure 6.2. 3D scaffold design.....	154
Figure 6.3. 3d bioprinting procedure.	159
Figure 6.4. Rheological characterization of the bioink.....	165
Figure 6.5. Rheological characterization of the bioink before and after cross-linking.....	166
Figure 6.6. Rheological characterization of cross-linked bioink at 25 °c and 37 °c	167
Figure 6.7. 3D printed NFC/A scaffold	168
Figure 6.8. Artefacts formation during printing.	169
Figure 6.9. Ultrastructure morphology of the scaffold	171
Figure 6.10. Swelling ratio	172
Figure 6.11. Live-dead staining of ASCs printed in the NFC/A hydrogel at different cell densities.....	176
Figure 6.12. Cell viability of ASCs in the NFC/A hydrogel	177
Figure 6.13. Asc distribution in the NFC/A hydrogel	178
Figure 6.14. Live and dead staining of CTRL- and TENO-cultured 3d bioprinted constructs.....	180
Figure 6.15. Cell viability of CTRL- and TENO-cultured ASCs printed in the NFC/A hydrogel	181
Figure 6.16. Fluorescence imaging.....	182
Figure 6.17. ASC cytokines release in the 3D NFC/A cultures.	185
Figure 7.1. Applicable regulations through the 3D bioprinting process.....	200

List of Tables

Table 3.1. Scaffolding strategies for tendon tissue engineering	68
Table 4.1. Primers used in this study.	93
Table 5.1. Recent in vitro and in vivo studies using 3d bioprinting for bone tissue engineering applications.....	130
Table 5.2. Recent in vitro and in vivo studies using 3d bioprinting for cartilage tissue engineering applications.....	134
Table 6.1. 3D bioprinting parameters	158

Chapter 1

General Introduction

Goal and thesis scope

This thesis provides insights into the potential clinical application of human adipose-derived stem cells (ASCs) in regenerative cell-based therapy for the treatment of tendon disorders.

In particular, this thesis's work was carried out in the framework of three main inter-correlated projects: i) "Development of clinical grade standard media and standardized protocols for *in vitro* culture expansion and tenogenic differentiation of human cryopreserved ASCs in stem cell bank facility" (in collaboration with Swiss Stem Cell Foundation, SSCF, Lugano, Switzerland), ii) "Development of a three-dimensional (3D) bioprinted ASC-laden construct suitable for tendon tissue engineering and regenerative medicine applications" (in collaboration with SSCF and the Joint Research Center's service of European Commission, JRC, Ispra, Italy), and iii) "in-depth analysis of regulatory aspects, availability of standards and guidelines of the current legislation framework inside and outside European Union (EU) about 3D bioprinting technology" (in collaboration with JRC, Ispra, Italy, in the framework of the EU Medical Converging Technologies project).

Consequently, this thesis is organized in three main parts subdivided into seven chapters.

Part I: Chapter 2 presents the state-of-the-art concerning the classification of stem cells and the impact of past and recent stem cell-based therapies applied in regenerative medicine and tissue engineering; Chapter 3 describes the state-of-the-art on tendon tissue biology and on current conservative and alternative strategies that have been proposed to ensure regeneration and repair of injured tendons.

Part II: Chapter 4 describes the achievements obtained in this thesis in the development of serum- and xenogenic-free media to culture cryoconserved ASCs and trigger tenogenesis in two-dimensional (2D) condition *in vitro*; Chapter 5 describes the original work in the development and *in vitro* validation of a 3D bioprinted ASC-laden scaffold using clinical-grade reagents and natural based hydrogel in order to drive tenogenic differentiation of the embedded ASCs; Chapter 6 presents an in depth-analysis by literature search on PUBMED of the

main advances in 3D bioprinting technology and applications in bone and cartilage tissue engineering as well as of the main players, countries or regions, worldwide that currently act toward the development of this technology using the innovative Tool for Innovation Monitoring (TIM) software developed by European Commission that allow to combine and analyze results from SCOPUS, Cordis, PATSTAT databases at the same time.

Part III: Chapter 7 analyses 3D bioprinting products identifying the procedures that would be applicable throughout the whole fabrication process and providing specific regulatory guidance for bioprinting.

PART I

Chapter 2

Stem cells in tissue engineering and regenerative medicine

2.1 Abstract

In the era of personalized medicine, novel therapeutic approaches raise many expectations for solutions that address currently unmet medical needs by developing patient-customized treatments. A leading role in this contest is played by tissue engineering and regenerative medicine approaches that combine stem cells, growth factors and biomaterials to treat a wide range of pathological conditions including tissue injury, trauma, cancers, and other degenerative diseases. Mesenchymal stem cells are the main cell types currently used in this approach. Thorough understanding of the potential and limits in stem cell application is crucial for the selection of the appropriate culture parameters as well as the trophic cues that guide proliferation and differentiation. In this chapter, challenges and advances for stem-cell based therapies are discussed, including the state-of-the-art technologies in advanced preclinical phase as well as those undergoing clinical trials.

2.2 Toward personalized medicine

The 'Vitruvian Man' was created by the Italian polymath Leonardo da Vinci around the year 1487. The drawing is a cornerstone of Leonardo's attempts to represent the ideal proportion of human body and its harmony with the universe to demonstrate its physical and regenerative capabilities. The Leonardo's fascination with the *figura istrumentale dell'omo* ("man's instrumental figure") is expressed also in the famous anatomical drawings, which are among the most significant achievements of Renaissance science (from Encyclopedia Britannica). Nowadays, at the time of the celebration of 500th anniversary of Leonardo's death, new frontiers in medicine are exploited to bear individual-based approaches and to ensure better patient-centered care. Since the mapping of the human genome in 2003, the development of synthetic biology and genomic editing techniques has been contributing to a better definition of disease mechanisms and importantly to the development of personalized therapeutic approaches. In contrast to the conventional treatments that straightened towards the general population, personalized medicine is based on targeted therapeutic approaches such as individual genetics, needs and lifestyle, to maximize the therapeutic efficacy as well as disease prevention and earlier diagnoses reducing the risk of adverse effects (1). A leading role in this contest is played by tissue engineering and regenerative medicine (TERM) approaches that combine stem cells, growth factors and biomaterials with the aim to repair or regenerate damaged tissues after tissue injury, trauma, cancers, and age-related and other degenerative diseases, restoring or establishing their normal function (2,3) (Fig 2.1). Moreover, TERM pursue the ambitious long-term goal to grow tissues or entire organs in laboratory to implant them in the human body. From the advancements in stem cell biology, biochemistry, material science and bio-fabrication it might be possible to mimic the complexity of human tissues in order to finely tune the patient individual requirements by producing a biocompatible and cellularized scaffold suitable for *in vivo* implantation. This would potentially overcome the limited efficacy of current available treatments and the problem of organ availability for transplant and immune rejection (4). Besides the benefit for the patient and in the follow-up therapies management, customized approaches also represent the next step toward

the realization of off the-shelf solutions with important socio-economic impact by reducing healthcare costs.

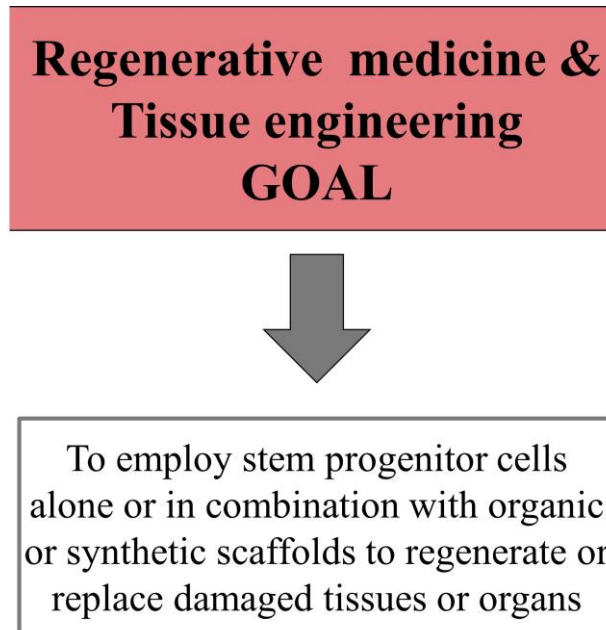


Figure 2.1. The main aim of regenerative medicine and tissue engineering approaches

In particular, the continuous improvement of methodology in this area includes (5):

- discovery of methods to generate functional cells such as the induced pluripotent stem cells (iPSCs) and adult stem cells from different sources
- substrate stiffness as physical cues to modulate stem cell differentiation and phenotypes
- advanced synthetic strategies to obtain biomaterial conjugations for precise patterning of biomolecules and biomaterials
- soluble factors delivery mechanisms of growth factors and cytokines to improve the bio-functionality of tissue constructs
- rational design of biomaterials to elude the immune system and minimize inflammatory responses
- development of new biomaterials and scaffolds to achieve biomimetic tissues fabrication

- advances in bio-fabrication technologies as three-dimensional (3D) bioprinting (Fig 2.2), illustrated in detail in chapter 5, to the generation of complex biological structures with high spatial resolution for 3D functional tissue reconstruction (6).

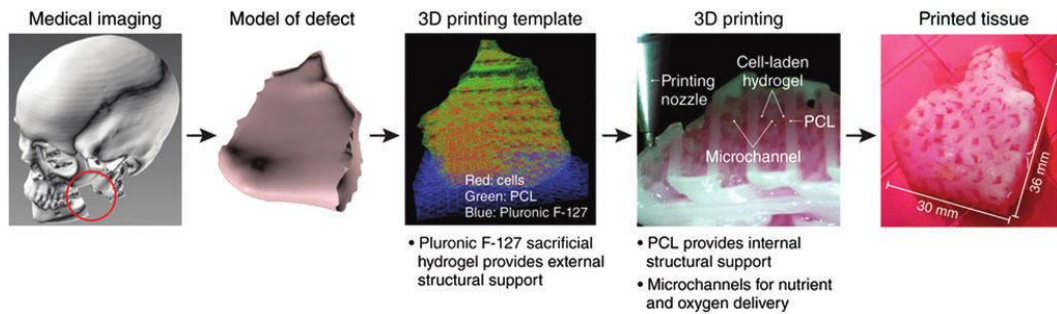


Figure 2.2 3D Bioprinting

Multi-step approach developed by Kang et al for tissue construct fabrication starting from clinical imaging of a tissue defect through the bioprinting of cells and polymeric materials in the desired shape. Reprinted by permission (7).

Regenerative medicine and tissue engineering strategies based on scaffold-free or scaffold-based approaches use tissue-derived cells that may consist in stem cells, although no consensus has been reached so far. The understanding of the potential and limits of each stem cell type is crucial for the selection of the appropriate cells and the optimal culture conditions as well as the trophic cues that guide proliferation and differentiation. The appealing of stem cells as cell source to improve tissue repair and regeneration and their translational use in clinical setting are illustrated in this chapter. Challenges and advances for stem-cell based therapies will be also discussed.

2.3 Stem Cells in Regenerative Medicine and Tissue Engineering

The regenerative potential of stem cells and/or progenitor stem cells is based on their capacity to elicit functional repair of damaged tissues or organs. They are defined by their capacity to preserve the undifferentiated stem state and extensive proliferation, named self-renewal, and differentiative potential into one or multiple cell types (8–11). Stem cells are classified in two categories according to their ability to differentiate and on the tissue of origin (Fig 2.3).

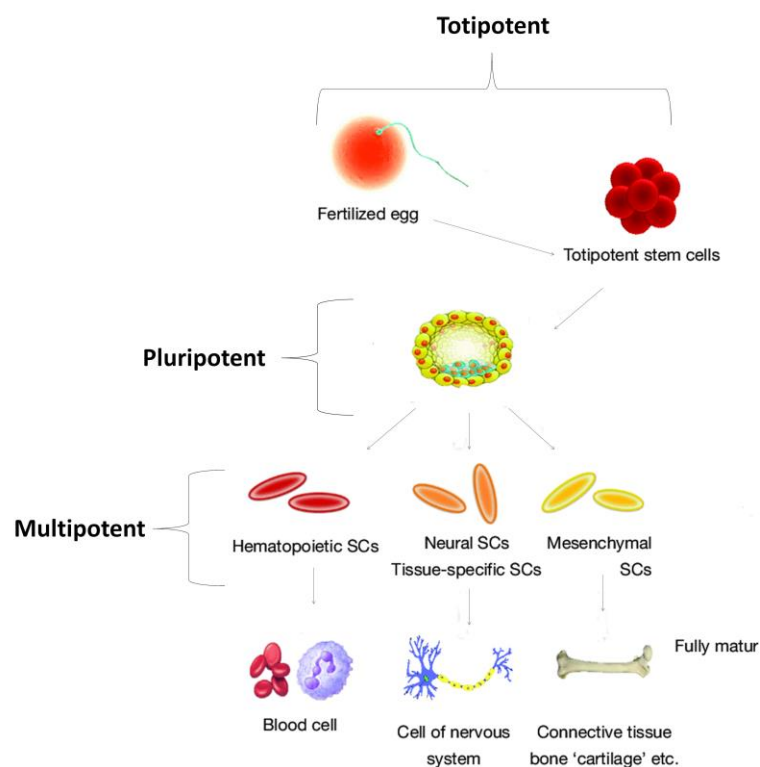


Figure 2.3. Stem cell classification

Totipotent cells, embryonic stem cells (ESCs), form all three germ layers and extra-embryonic tissue or placental cells. Pluripotent cells of the blastocyst stage form all 3 germ layers while multipotent cells (adult or somatic stem cells) can generate cells limited to 1 germ layer and include hematopoietic, tissue-specific and mesenchymal stem cells (SCs). Adapted with permission (12).

Categorization based on the differentiation potency includes totipotent, pluripotent, multipotent or unipotent stem cells. Totipotent cells can differentiate into embryonic and extra-embryonic cell types, as placenta, and are able to form a complete and viable organism. Pluripotent stem cells have the potential to generate all cells of germ cells: ecto-, endo- and mesoderm. Multipotent cells are capable of generating some tissue cell types limited to a germinal layer, included mesenchymal stem cells (MSCs), or a specific cell line such as hematopoietic stem cells (HSCs). Unipotent cells are able to generate a single cell type. Based on the tissue of origin, stem cell could be also defined as embryonic stem cells (ESCs) and tissue derived (somatic) stem cells. Tissue derived stem cells can be isolated from fetal tissues (i.e. placenta, amniotic fluid, umbilical cord blood) or adult tissues including bone marrow (BMSCs), adipose tissue (ASCs), tendon (TSPCs), dental pulp, skeletal muscle and others (5,13–18). Recently, two more sub-divisions of tissue-derived stem cells have been reported: induced pluripotent stem cells (iPSCs) and induced tissue specific stem (iTSCs) cells (19,20).

Given the recent advances in stem cell biology and their major contribution in regenerative medicine and tissue engineering approaches for the development of personalized treatments, the use of the pluripotent stem cells iPSCs and the multipotent adult stem cells are reported in details below.

2.3.1 Induced Pluripotent Stem Cells

Successfully reprogrammed in 2006, iPSCs are generated from adult human fibroblasts by the overexpression of embryonic genes or transcription factors named “Yamanaka factors”, from the Nobel laureate Yamanaka and his group, that consisting in OCT 4/3 (octamer-binding transcription factor 4/3), SOX-2 (sex determining region Y), KLF-4 (kruppel-like factor 4) and c-Myc (Avian Myelocytomatosis virus oncogene cellular homologue) (20,21). Likely to ESCs, iPSCs possess the capacity to indefinitely self-renewal and differentiate into any tissue of the body. In addition, iPSCs represent an abundant adult cell source, overcoming the ethical restrictions to use that ESCs possess (22). From 2007, iPSCs have received a great deal of attention as emerging technology useful for regenerative medicine applications as well as in the field of disease modelling and

drug discovery giving a boost to the advancements of personalized medicine treatments (23). A general approach is summarized in Figure 2.4.

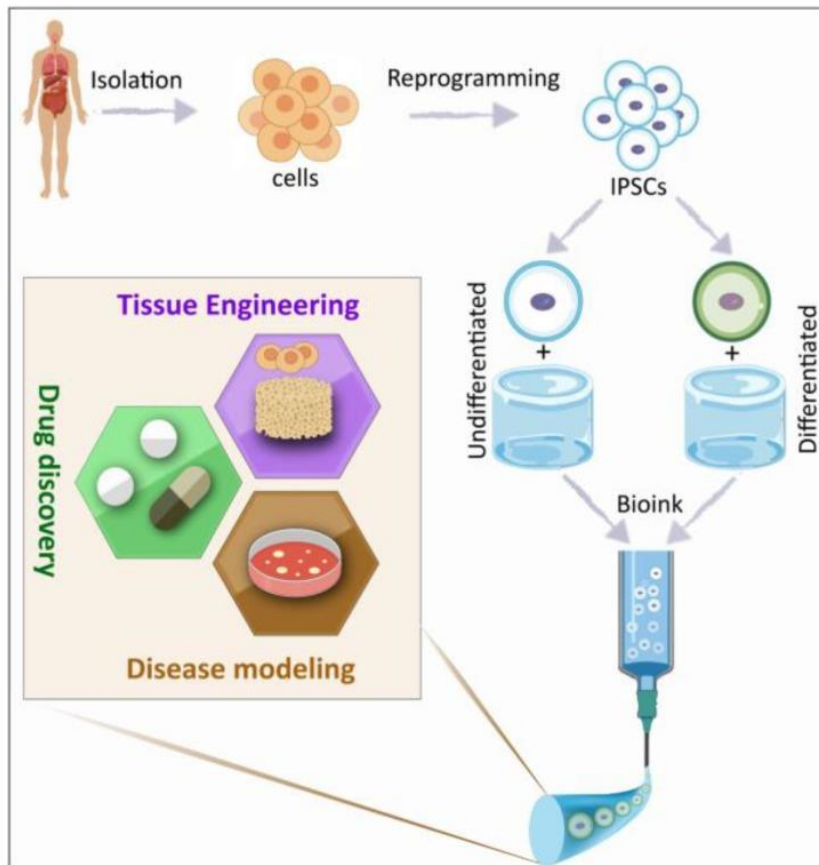


Figure 2.4. Potential of induced pluripotent stem cells (iPSC) for regenerative medicine, disease modelling, and drug discovery.
Reprinted with permission (24)

Patient-derived iPSCs could provide large quantities of disease-relevant cells and a variety of different cell types useful for three-dimensional (3D) organoids formation applied in personalized disease modelling, for screening the drug efficacy and toxicity as well as to assess human organ development models (23). Moreover, the recent gene editing technology like CRISPR-Cas9 system has improved the efficacy to introduce disease-causing mutations ensuring the reliable identification of the true pathology (25,26). Considerable interest in iPSCs was also gained for their potential application as cell-therapy product for regenerative

medicine. At present, one clinical study started in 2014 using patient-derived iPSCs from retinal pigment epithelial (RPE) cells to treat macular degeneration, reported positive results in improving the patient's vision. However, the trial was subsequently interrupted due to the identification of two genetic variants in the iPSCs (27). Tissue engineering approaches based on the combination of iPSCs with biomaterials for musculoskeletal regeneration are still at the beginning. Studies have been mainly focused on the *in vitro* differentiation of iPSCs into bone and cartilage progenitor cells (28–30). Some reports highlighted that MSC derived from iPSC have a more identical gene expression profile to BMSCs, compared to ESCs derived MSCs. Recently, 3D bioprinting technology was applied in one *in vitro* study related to cartilage tissue engineering with precisely positioned iPSCs. In this study, the authors successfully co-printed chondrocytes and iPSCs derived from patients undergoing knee surgery in a nano-fibrillated cellulose composite bio-ink (31). However, even with the integration of such technologies, differentiation to target cells still remains a challenge. Moreover, although iPSCs possess a great potential in cell therapy, several obstacles will need to be overcome before their clinical application. Main problems are related with iPSCs differentiation into target cells, tumorigenicity and genomic instability (32,33).

2.3.2 Mesenchymal Stem/Stromal Cells

Adult stem cells were described for the first time more than 50 years ago in the mouse bone marrow with the discovery of HSCs (34,35). Then, in the 1970s, Friedenstein and colleagues found a unique stem cell population with characteristics of plastic adherence and multilineage differentiation capacity and named them colony forming unit fibroblasts (CFU-F) (36). In the early 1990s they become known as mesenchymal stem cells (MSCs) because of their multilineage differentiation capacity, immunomodulation, and regenerative ability. Over the past decades, MSCs have generated global interest becoming the stem cell source mostly studied and employed for experimental cell therapy. The nomenclature used to define MSCs is still debated today because of their heterogeneous non-clonal nature, consisting in a mix of committed progenitors and differentiated cells, and their various biological functions. Additionally, other recently proposed names for MSCs are mesenchymal stromal cells, multipotent progenitor cells or medicinal signalling cells (37,38). In 2006, the Mesenchymal and Tissue Stem Cell Committee of International Society for Cellular Therapy (ISCT) published the minimum criteria for the identification of MSCs (39). ISCT recommendations include (i) the ability to adhere on plastic, (ii) specific flow-cytometric cell surface expression (> 95%) of cluster of differentiation (CD)73/5'-nucleotidase, CD90/Thy-1, and CD105/endoglin and lack (< 2%) of CD45, CD34, CD14, CD11b, CD79 α , CD19, and HLA-DR (hematopoietic cell markers), and (iii) multipotency, ability to differentiate into the mesodermal cell lineages osteoblasts, chondroblasts and adipocytes *in vitro*. However, the MSC identification criteria are not yet standardized and are frequently changing. Significant differences in proliferation, differentiation and molecular phenotype were observed in MSCs isolated from different tissues (40,41). This variability should be taken into consideration when planning their use in clinical protocols. For instance, surface markers CD13, CD29, and CD44 should be constitutively expressed by >80% of adipose-derived MSCs (ASCs), while CD31, CD45, and CD235a, which are primarily negative markers, should be expressed by less than 2% of cells (42). Additionally, the expression of CD34 as negative marker, is still controversial and debated in literature (43). Other specific MSC *in vitro* stemness markers including stromal precursor antigen-1 (Stro-1), stage-specific embryonic antigen (SSEA-4), CD271, and CD146 have been also proposed. However, the stemness marker

Stro-1, is reported positive in dental and bone marrow MSCs whereas is negative for ASCs (44–47). Moreover, the recent discovery of the ability of MSCs to trans-differentiate into ectodermal and endodermal cell lineages and the inclusion of novel surface markers (CD165, CD276 and CD82) clearly demonstrate that their biology is still to be completely understood (48–50).

In general, MSCs could be defined as: i) genomically stable, ii) highly accessible, iii) easy to isolate and expand, iv) immune-privileged and, importantly, v) non-teratogenic and ethically conforming, unlikely to ESCs and iPSCs (51,52). Additionally, a number of reports showing that BMSCs and ASCs from healthy and/or younger donors perform better in proliferation, differentiation and secretion ability compared to cells derived from osteoarthritic or obese suggesting that MSCs play a physiological role in homeostatic tissue maintenance (53–55).

Since their homing ability, engraftment, multilineage potential, secretion of anti-inflammatory molecules and immunoregulatory effects, MSC-based therapy has raised remarkable interest for the treatment for several disorders including autoimmune, inflammatory and degenerative diseases (48,56).

MSCs are localized in almost all tissues including bone marrow, adipose tissue, tendons, dental pulp, peripheral blood, menses blood, amniotic fluid, placenta, and umbilical cord, as they origin by perivascular cells (pericytes) (48,56–59). Since their broad distribution in all vascularized tissues of the body, MSCs are primary involved in the response to injury, infection or disease by sensing and secreting in their microenvironment trophic (mitogenic, angiogenic, anti-apoptotic or scar reduction), immunomodulatory and anti-microbial factors (Fig. 2.5) (56).

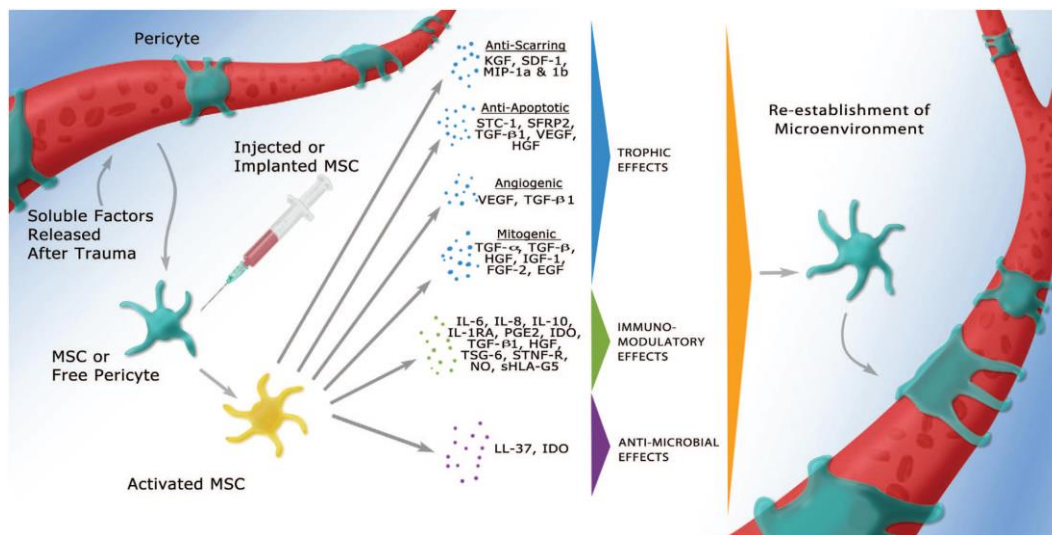


Figure 2.5. MSC activation in the perivascular region

After trauma growth factor and chemokines release in the microenvironment induce pericytes to become MSCs enabling them to release trophic (mitogenic, angiogenic, anti-apoptotic or scar reduction), immunomodulatory or antimicrobial factors. With the resolution of injury state, MSCs return to their native pericyte state attached to blood vessels. Courtesy of (56)

In particular, it is known that when MSCs of the bone marrow reside in their *in vivo* niches, the stem cell state is maintained by cell contacts mediated by N-cadherins and by the use of the essential interacting peptide His-Ala-Val-Asp domains. Further, when MSCs move away from their niche, they establish mainly extracellular matrix (ECM) interactions. In *in vitro* culture, cells interact with ECM molecules, such as fibronectin, laminins, and collagens, by integrin focal adhesion sites and they form extensive cytoskeletal networks on the plate surface. However, the hard plastic of polystyrene dishes or flasks may not be an ideal substrate to express their multipotency capability (60). For instance, BMSCs in their niche show a dendritic shape and express some specific neuro markers including CD271, TRK mRNAs, while BMSCs cultured in soft gels mimicking the environment of marrow or neural tissues, expressed other neuro-typic markers (61,62). Moreover, in both 2D and 3D culture conditions of BMSCs it has been observed that soft gels favour adipogenesis pathway whilst stiff substrates induced prevalingly the osteogenesis (63–68). MSC surface-mediated commitment toward a specific cell-lineage is currently under investigation and still remains to be identified (Fig. 2.6). MSCs respond to the substrate with a proper adhesion by acto-myosin motility, thus their cytoskeletal contraction and differentiation is influenced by forces exerted by the substrate.

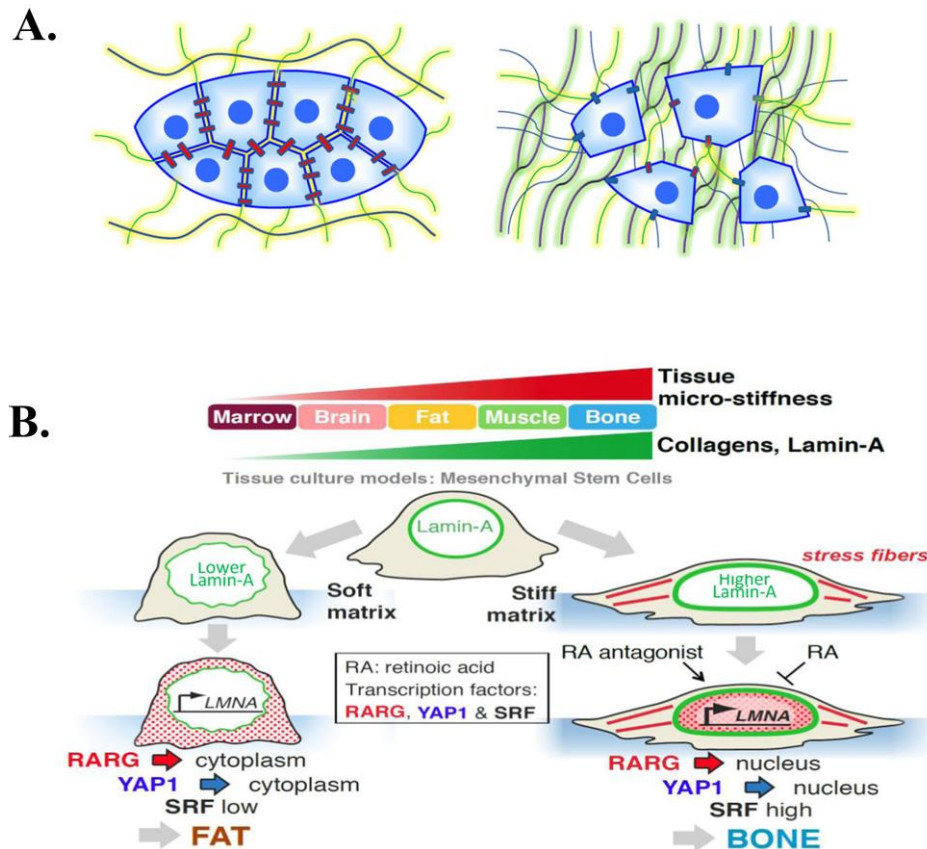


Figure 2.6. Mechanical MSC memory effects on their multipotency

A. MSCs are condensed in their niche environment and the culture *in vitro* change the intercellular connections mediated by cadherins and connexions with substrate and matrix cell interactions and more extracellular matrix production. **B.** MSC response to stiffness surface and the surface curvature by alter gene expression and MSC potential. Reprinted by permission (68)

It has been observed that the structural protein of nuclear membrane laminin-A interacts with MSCs cytoskeleton stress fibres. In particular, higher levels of this protein and the nuclear translocation of the transcriptional co-activators YAP and TAZ were found in MSC cultured in stiff tissues respect to soft-tissue cultures suggesting to promote specific osteogenic gene expression rather than adipogenic lineage (Fig. 2.5B). Moreover, in the presence of rigid surface curvature, MSC express more stress-fibres that determined a flattened shape of the nucleus and high levels of laminin-A, and thus favour osteogenesis, whereas in presence of concave surface, cells share more motility, less stress-fibres and lower levels laminin-A. Also, dynamic stretching and 3D matrix materials can provide new approaches to understand MSC responses and their potential therapeutic applications.

The homing property of MSCs derive also from their capacity to express a variety of adhesion molecules, endopeptidases, and growth factors responsible of vessel migration and transmigration to tissues (69). Numerous studies reported the ability of infused MSCs to reach several organs including bone marrow, heart and liver for prolonged periods of time by their chemokine and toll-like receptor (TLRs). Moreover, MSCs can also response to several stimuli, such as growth factors and xenobiotics, before engrafting into tissues where they either (trans)differentiate to the target cell lineage or secrete various growth factors, cytokines, chemokines, with (i) trophic, (ii) antiapoptotic, and (iii) pro-angiopoietic effects (52,70–74).

The regenerative potential of MSCs derives by biologically active molecules as a part of “secretome” or secreted extracellular microvesicles (EV) has recently received much attention. EV are nano-sized membrane-bound vesicles (size range from 30 nm to 1 μ m in diameter) that shuttle important biomolecules like mRNA/miRNA, to modulate tissue function and influence pathogenesis by establish cell-to-cell communication. Several preclinical evidences suggests the beneficial therapeutic effects of MSC-derived EV, as summarized in Figure 2.7; however the positive clinical outcome still remain to be elucidated (75).

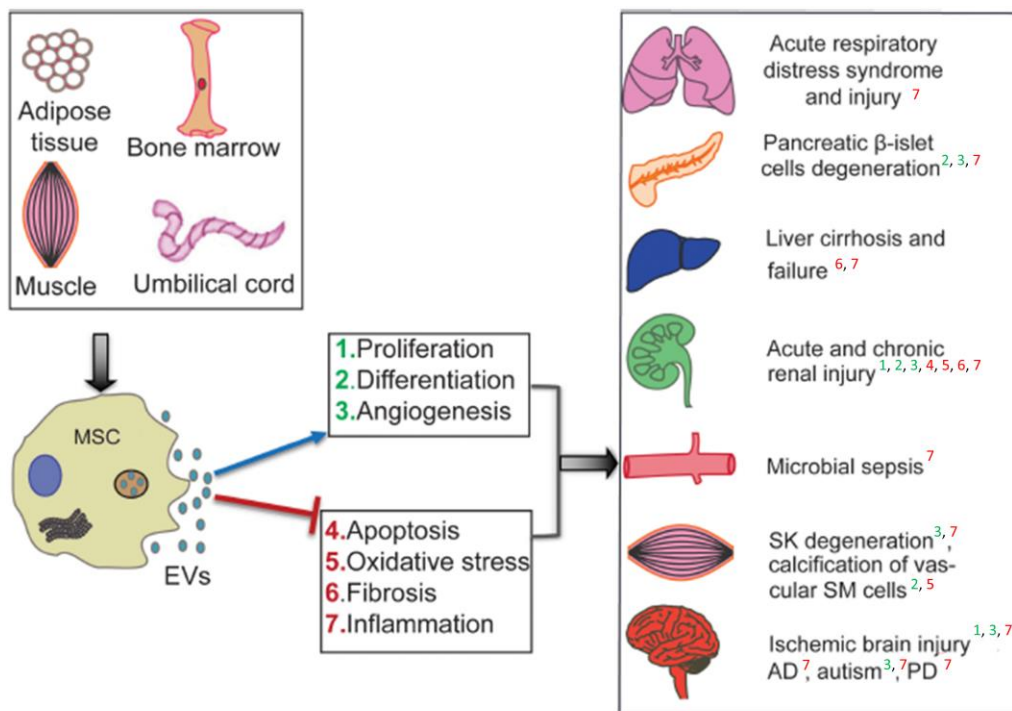


Figure 2.7. Preclinical studies of human MSC-derived EV.

Extracellular microvesicles derived from umbilical cord, muscle, bone marrow and adipose tissue were successfully applied in *in vitro* and *in vivo* studies to the treatment of many diseases and injuries such as acute respiratory distress and injury, pancreatic degeneration, cirrhosis, chronic and acute renal injury, microbial ischemic brain injury, skeletal muscle (SK) degeneration, calcification of smooth muscle (SM) cells, Alzheimer (AD) and Parkinson (PD). The positive and negative regulation is shown by the blue arrow and the red line, respectively (74).

The immune-privileged characteristics of MSCs consists in the expression of TLRs, key components of the immune system, and the low expression of MHC class I and the lack expression of MHC class II along with co-stimulatory molecules, like CD80, CD40 and CD86. These factors make MSCs unable to activate alloreactivity in the host and, at the same time, protect them from natural killer (NK) invasion (76). Moreover, the soluble immunosuppressive molecules released by the MSC secretome are of key importance to induce the suppression of NK cells and cytotoxic T-cells. Overall, immunosuppressive MSCs, contribute to tissue healing and regeneration also by inducing macrophages, via IL-6 release, toward a proangiogenic M2 phenotype that regulate anti-inflammatory T-cell responses (52,77).

Together with other properties, the immunomodulatory features shown by MSCs make them one of the viable stem-cell source for cell-based therapy. Moreover, preclinical successful results have been obtained without signs of toxicity or tumorigenicity allowing the transit to human studies using good manufacturing

practice (GMP)-compliant human MSCs suitable for clinical trial applications, particularly in the last decade (78,79). Notable, two recent studies conducted in China to treat COVID-19 pneumonia of patients in severe-critical conditions by infusion of GMP-compliant MSCs, revealed remarkable reversal of symptoms even in severe-critical conditions (80–82). One case report consisted in the treatment of a critical COVID-19 patient with evident liver injury, by using three intravenous infusions of 5×10^7 human umbilical cord MSCs. Authors reported that already four days after the second infusion, the patient was off the ventilator and able to walk with normal parameters and no side effects (81). The second pilot study on 7 enrolled patients in total (1 critically severe, 4 severe, and 2 non-severe) treated by a single intravenous injection of clinical grade MSCs, 1×10^6 cells per kilogram of weight, showed no adverse effects with significantly improved pulmonary function, including patients with severe COVID-19 pneumonia (81).

Over the past 25 years, the infusion procedures have exhibited an excellent safety profile, so much so that there has been an exponential growth in the use of MSC based therapies. Up to this date, 849 clinical studies employing MSCs as the primary intervention have been registered, 45 of which hit the Phase III, with 15 completed, and 4 of which in Phase IV (83). Worldwide, 1199 MSC clinical trials were registered internationally from 2011 through 2019, as shown in Figure 2.8, for the treatment of several pathologies including ischemic heart diseases, cirrhosis, diabetic foot ulcers, knee and hip osteoarthritis, knee cartilage defects, muscle injury after hip fracture or arthroplasty, atopic dermatitis, stroke, perianal fistula, cerebral palsy and Graft-versus-host diseases (GvHD) (MSC search performed at <https://celltrials.org/public-cells-data/msc-trials-2011-2018/65>).

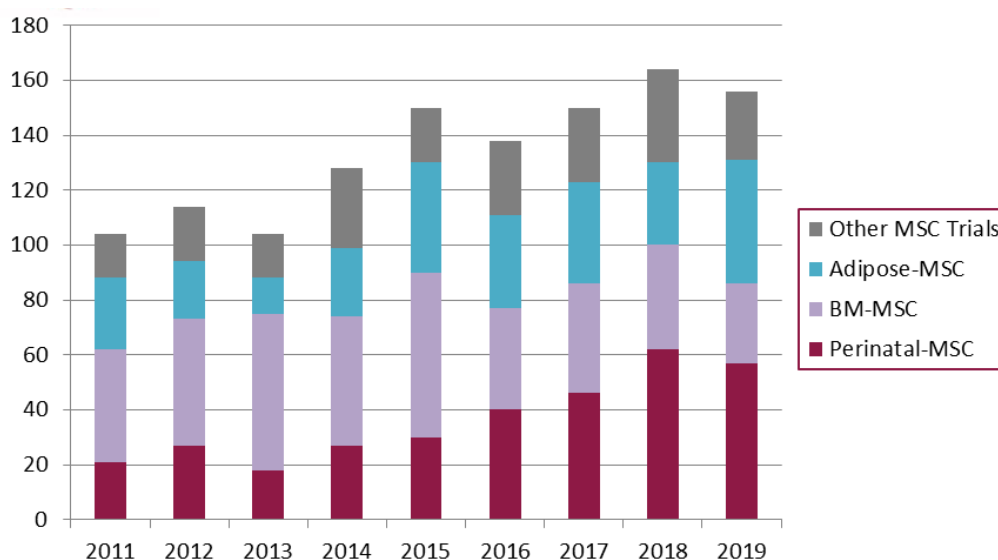


Figure 2.8. MSC clinical trials registered internationally from 2011 through 2019.

Only trials with isolated MSCs are included, from any source and whether the mesenchymal cells are considered to be stem cells, stromal cells, signalling cells, etc. (<https://celltrials.org/public-cells-data/msc-trials-2011-2018/65>)

This booming, particularly in the last decade, is indicative of MSC potential to ameliorate a plethora of degenerative diseases in various organs and tissues and above all for bone and cartilage treatments. Nevertheless, several limitations have to be addressed to completely free the clinical application of MSCs; including cell source availability, cellular dose, clinical-grade production compliance with GMP, scalability, administration timing and technique, engraftment rate, localization post-transplant and tissue persistence (52). This is explanatory of the limited number of MSC-based therapies at the final trial stage and the lack of approvals by the regulatory agencies in the United States and Europe as biopharmaceutical products (84–86). For these reasons, compelling clinical evidence from reliable well-controlled trials, stronger policy compliance, and extensive premarket reviews are urgently needed. Indeed, the gap between reputable clinical evidences and premature public marketing of stem cell products has led to a confused scenario (68). In May 2017, more than 700 clinics in the United States alone were offering directly to consumer so-called stem cell treatments, the vast majority of which for musculoskeletal injuries (87). A first attempt to improve standardization and transparency of cell therapies, has been offered in an international expert consensus by Murray et al, where strategies and parameters needed to improve cell therapy outcomes for both patients and

practitioners are described, suggesting the use of the acronym DOSES (87): (D)onor (autologous, allogeneic, xenogenic), (O)origin tissue, (S)eparation from other cell types/preparation method, (E)xhibited characteristics, (S)ite of Delivery. Although MSC properties make them an optimal cell source for tissue regeneration, several challenges have to be overcome for their clinical applications. Some of their specific properties, such as their immunomodulatory mechanism, still remain to be elucidated. Moreover, different methods of purification, culture protocols and supplementations, such as FBS, cell density and concentration of oxygen, may affect MSC functionality and potential. For these reasons, standard protocols for the *in vitro* culture are needed. Moreover, other factors such as cryopreservation, the age of donors and the site of harvest can influence the therapeutic potential of MSCs. Optimization of standards and culture conditions together with the implementation of biochemical stimulating factors and mechanical stimuli may be effective strategies toward effective MSC-based therapies for tissue regeneration.

2.3.2.1 Adipose-Derived Stem Cells (ASCs)

Among MSC tissue sources, bone marrow and adipose tissue derived MSCs are the most commonly employed MSCs in cell-based therapy; only recently, perinatal-MSCs (umbilical cord and placenta derived MSCs) have also gained attention in clinical applications procedure (Fig.2.9). An added value in the use of BMSCs and ASCs is that they can be harvested at any stage of human life. However, the use of BMSCs for therapeutic purpose involved some limitations in comparison to ASCs (5). First of all, the BMSC harvest typically requires large amount of tissue to obtain the high number of cells needed for therapeutic applications while the extensive cell expansion increases cellular senescence risks (88). Bone marrow aspiration procedure is commonly performed from the sternum or posterior iliac crest and is generally considered safe, however fatal complications have been also registered (89). On the other hand, adipose tissue is present in abundance in the body; its harvest consists in a simple liposuction procedure with minor adverse effects and ethical restrictions. Considerable cellular yield can be obtained from a small amount of tissue (25-100 ml) and with

about 100–500 folds higher in comparison to MSC yield by bone marrow (54,89–92). ASCs are isolated from adipose tissue by enzymatic or mechanical treatment, to obtain the stromal vascular fraction (SVF). The SVF consist in a heterogeneous population of stromal and vascular cells including various immune cells, including preadipocytes, fibroblasts, vascular smooth muscle cells, endothelial cells, resident monocyte, and lymphocytes, but mature adipocytes are absent (93). The regenerative cells of SVF are able to promote cartilage and subchondral bone regeneration and to the deposit of new cartilage matrix.

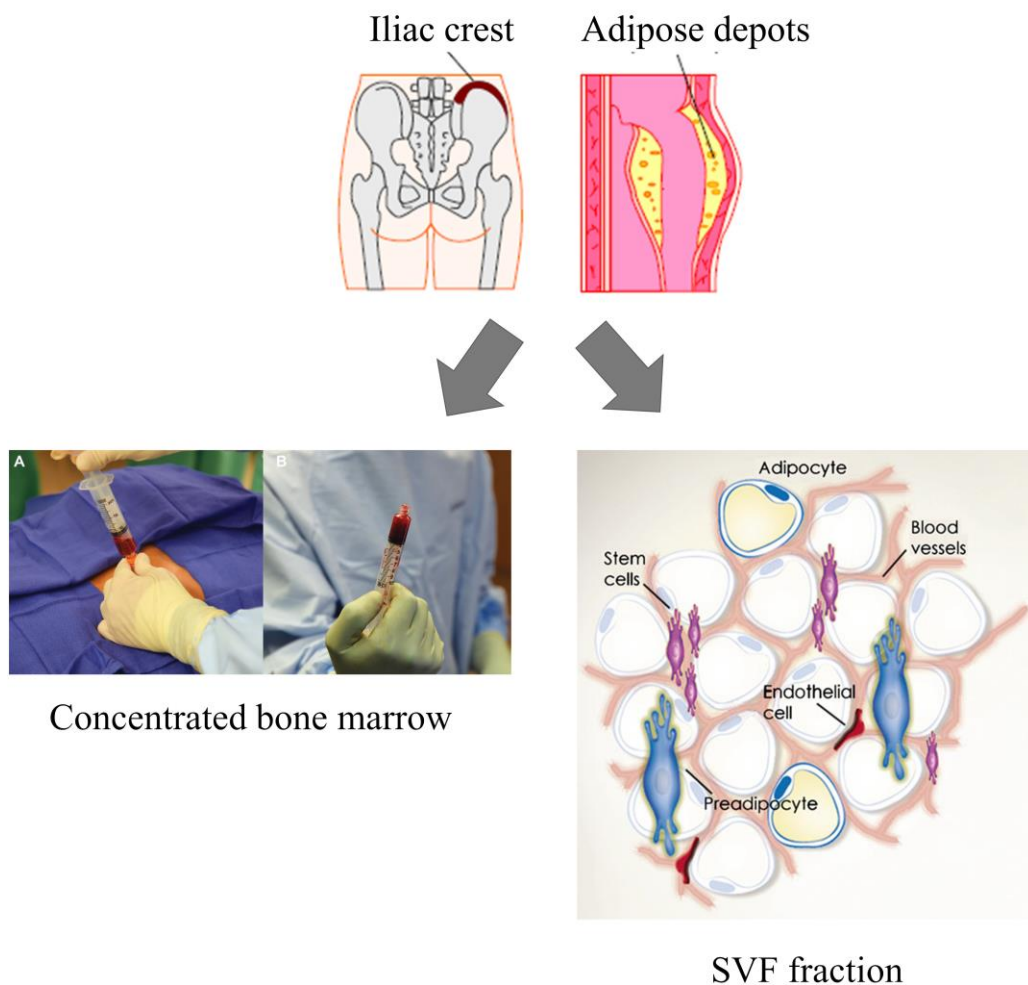


Figure 2.9. Comparison between BMSCs and ASCs harvest.

Bone marrow is commonly harvested from iliac crest; in orthopaedics bone marrow is often concentrated by centrifugation prior to injection into joints, tissue or blood system. Adipose tissue is isolated by subcutaneous fat and then the stromal vascular fraction (SVF), a heterogeneous set of cell populations that include stromal cells and ASCs, is isolated before ASC application. Adapted by Murray et al, and Lindroos et al, (87,94).

Classification of ASCs is based on specific markers screened by flow cytometry (95). In accordance to ISCT and the International Fat Applied Technology Society (IFATS) ASCs can express the specific MSC marker CD90 and other markers such as CD34, CD73, and CD105 whereas they are negative for CD45 and CD31(39,42). During culture, ASCs are isolated for plastic adhesion, are stable and are capable to differentiate into adipocytes, osteoblasts, chondroblasts, hepatocytes and tendon cells (54,94,96,97). Moreover they possess other MSC characteristics including anti-inflammatory effect, immune-modulation, trophic and angiogenic effects that have been reported in numerous preclinical studies (18,54,92,94,98–100). Both SVF cells and ASCs are currently used in clinical applications. For collection, isolation, cultivation, and storage, ASCs should satisfy, for their use in the clinics, the GMP guidelines are reported and validated by Hamid-Reza Aghayan et al (101,102).

In the last decades, the differentiative potential of ASCs, into multilineage cells such as adipocytes, osteocytes and chondrocytes has been also extensively investigated. Growth factors have a significant role to drive the differentiation capability of ASCs *in vitro*. For instance, IBMX and insulin supplementation promote ASCs into adipogenic lineage, bone morphogenetic protein-2 (BMP-2), β -glycerol phosphate, ascorbic acid are commonly used for osteogenesis whilst BMP-2/-4, insulin-like growth factor (IGF)-1, and transforming growth factor- β I/III (TGF- β 1/- β 3) are common stimulating factors for chondrogenesis (18,55,92).

Numerous preclinical studies have explored the regenerative potential of ASCs in tissue engineering strategies to support healing for several pathologies including the orthopaedic field. For instance, several randomized controlled trials reported the positive results of using ASCs injections in knee and hip osteoarthritis (OA) patients with no side effects (103–106). Currently the only one Phase III clinical trial study concerning the use of ASC application for knee OA disorder (83). Remarkable advances in stem cell clinical application were achieved in the last decades, although no optimal cellular dose is available to date as a standard. Moreover, a high number of cells is needed to be implanted into the patient because of the low engraftment and survival rates of cells after infusion (107). Bioengineering strategies represents a valid ally for the improvement of cell-based therapy. More attention has been paid to study ASCs in a 3D environment using

tissue engineered scaffolds, considering their capacity to closely mimic *in vivo* cellular environments. The fabrication of 3D scaffolds by combining biomaterials, molecular growth factors, and extracellular matrix can provide mechanical and chemical cues suitable for enhanced cell viability, proliferation and differentiation (108–111).

The ideal scaffold should possess (112):

- i) biocompatible properties to not elicit adverse immune system reactions
- ii) biodegradability to ensure controlled scaffold degradation whilst maintaining sufficient support and completed tissue ingrowth
- iii) bioactivity to interact with the host tissue and retain cells at the injection site encouraging endogenous repair and new tissue formation
- iv) 3D structure and architecture with interconnected pores tailored to target tissue and cells and enabling nutrient diffusion and cell migration
- v) mechanical properties resembling the native target tissue and able to regulate biochemical, biomechanical and biological functions

Several studies have proven the ability of ASCs to attach and proliferate, and thus to colonize 3D scaffolds. In clinical trials their potential employment for wound healing, cardiovascular grafts, orthopaedic tissue repair, and plastic tissue reconstruction after surgery was indicated (113). Natural and synthetic materials have been employed in clinical practice. For example, injection of hyaluronic acid (HA), a polysaccharide present in the body, at the knee joint of OA patients allow to ensure chondro-protective and anti-inflammatory effects. Several clinical trials have investigated HA or collagen as cell carrier to enhance cell retention at the site of injection (107). In addition, pre-clinical studies have also demonstrated that natural biomaterials such as collagen, hyaluronic acid and silica nanoparticles induce ASC proliferation and differentiation after implantation, while synthetic polymers allow better cell retention at the transplanted site (101).

2.3.2.2 Tendon stem/progenitor cells (TSPCs)

A stem/progenitor cell population (TSPCs) resident in tendons has been recently discovered by Bi and co-workers in human hamstrings tendon (114). TSPCs possess the peculiar MSC features like the ability to form colonies, the cytofluorimetric expression of surface MSC markers, the three-lineage differentiative potential (adipogenic, osteogenic and chondrogenic) and self-renewal capacity (18,114). They also express specific markers related to tendon tissue, such as scleraxis and tenomodulin, and are able to induce new tissue formation after implantation *in vivo* (114). In a previous study *in vitro*, we demonstrated the feasibility of the TSPC isolation procedure and their differentiative ability in comparison with ASCs. In particular, TSPCs showed more chondrogenic potential but lower adipogenic and osteogenic ability of TSPCs (18). Currently, due to the lack of specific molecular markers, it is difficult to perform comparative studies regarding TSPCs and the terminally differentiated cells resident in tendon (tenocytes). In another work, we purified TSPCs by the heterogeneous tendon resident cell population (mainly composed by TSPCs and tenocytes) by colony isolation in culture. That clone exhibited a more undifferentiated phenotype and showed higher osteogenic and chondrogenic ability than the whole population (40). In conclusion, although TSPCs could represent a potential cell source for treating injured tendons, the low average number of isolated TSPCs limits their potential use for clinical intervention. Moreover, a more complete understanding of tendon biology and TSPC nature and function is required as described in chapter 3.

2.4 References

1. Vogenberg FR, Barash CI, Pursel M. Personalized medicine - Part 1: Evolution and development into theranostics. *P and T*. 2010.
2. Langer R, Vacanti JP. Tissue engineering. *Science* (80-). 1993;
3. Gao G, Cui X. Three-dimensional bioprinting in tissue engineering and regenerative medicine. *Biotechnol Lett*. 2016;38(2):203–11.
4. Gomes ME, Rodrigues MT, Domingues RMA, Reis RL. Tissue engineering and regenerative medicine: new trends and directions - A year in review. *Tissue Eng - Part B Rev*. 2017;23(3):211–24.
5. Ntege EH, Sunami H, Shimizu Y. Advances in regenerative therapy: A review of the literature and future directions. *Regenerative Therapy*. 2020.
6. Murphy S V., Atala A. 3D bioprinting of tissues and organs. *Nature Biotechnology*. 2014.
7. Kang HW, Lee SJ, Ko IK, Kengla C, Yoo JJ, Atala A. A 3D bioprinting system to produce human-scale tissue constructs with structural integrity. *Nat Biotechnol* [Internet]. 2016;34(3):312–9. Available from: <http://dx.doi.org/10.1038/nbt.3413>
8. Filomeno P, Dayan V, Touriño C. Stem cell research and clinical development in tendon repair. *Muscles, Ligaments and Tendons Journal*. 2012.
9. Lerou PH, Daley GQ. Therapeutic potential of embryonic stem cells. *Blood Rev*. 2005;
10. Caplan AI. Adult mesenchymal stem cells for tissue engineering versus regenerative medicine. *Journal of Cellular Physiology*. 2007.
11. Kolios G, Moodley Y. Introduction to stem cells and regenerative medicine. *Respiration*. 2012.
12. Rajabzadeh N, Fathi E, Farahzadi R. Stem cell-based regenerative medicine. *Stem Cell Investig*. 2019;
13. Barisas DAG, Stappenbeck TS. Intestinal Stem Cells Live Off the Fat of the Land. *Cell Stem Cell*. 2018.
14. Klopsch C, Skorska A, Lemcke H, Kleiner G, Gaebel R, Beyer M, et al. Epicardial Erythropoietin Preserves Heart Function after Myocardial Infarction

- through Synergistic Angiogenesis and TGF-beta/WNT Signaling Trigger in Cardiac Mesenchymal Stem Cells. *Thorac Cardiovasc Surg*. 2018;
15. Zhang J, Lu X, Feng G, Gu Z, Sun Y, Bao G, et al. Chitosan scaffolds induce human dental pulp stem cells to neural differentiation: potential roles for spinal cord injury therapy. *Cell Tissue Res*. 2016;
 16. Willemse J, Lieshout R, van der Laan LJW, Versteegen MMA. From organoids to organs: Bioengineering liver grafts from hepatic stem cells and matrix. *Best Practice and Research: Clinical Gastroenterology*. 2017.
 17. Arrigoni E, Lopa S, De Girolamo L, Stanco D, Brini AT. Isolation, characterization and osteogenic differentiation of adipose-derived stem cells: From small to large animal models. *Cell Tissue Res*. 2009;
 18. Stanco D, Viganò M, Perucca Orfei C, Di Giancamillo A, Peretti GM, Lanfranchi L, et al. Multidifferentiation potential of human mesenchymal stem cells from adipose tissue and hamstring tendons for musculoskeletal cell-based therapy. *Regen Med*. 2015;10(6).
 19. Noguchi H, Saitoh I, Tsugata T, Kataoka H, Watanabe M, Noguchi Y. Induction of tissue-specific stem cells by reprogramming factors, and tissue-specific selection. *Cell Death Differ*. 2015;
 20. Takahashi K, Yamanaka S. Induction of Pluripotent Stem Cells from Mouse Embryonic and Adult Fibroblast Cultures by Defined Factors. *Cell*. 2006;
 21. Takahashi K, Tanabe K, Ohnuki M, Narita M, Ichisaka T, Tomoda K, et al. Induction of Pluripotent Stem Cells from Adult Human Fibroblasts by Defined Factors. *Cell*. 2007;
 22. Bilic J, Izpisua Belmonte JC. Concise review: Induced pluripotent stem cells versus embryonic stem cells: Close enough or yet too far apart? *Stem Cells*. 2012.
 23. Shi Y, Inoue H, Wu JC, Yamanaka S. Induced pluripotent stem cell technology: A decade of progress. *Nature Reviews Drug Discovery*. 2017.
 24. Romanazzo S, Nemeč S, Roohani I. iPSC bioprinting: Where are we at? *Materials*. 2019.
 25. Perez-Pinera P, Kocak DD, Vockley CM, Adler AF, Kabadi AM, Polstein LR, et al. RNA-guided gene activation by CRISPR-Cas9-based transcription factors. *Nat Methods*. 2013;

26. Shalem O, Sanjana NE, Hartenian E, Shi X, Scott DA, Mikkelsen TS, et al. Genome-scale CRISPR-Cas9 knockout screening in human cells. *Science* (80-). 2014;
27. Trounson A, DeWitt ND. Pluripotent stem cells progressing to the clinic. *Nature Reviews Molecular Cell Biology*. 2016.
28. Dogaki Y, Lee SY, Niikura T, Iwakura T, Okumachi E, Waki T, et al. Efficient derivation of osteoprogenitor cells from induced pluripotent stem cells for bone regeneration. *Int Orthop*. 2014;
29. Guzzo RM, O'Sullivan MB. Human Pluripotent Stem Cells: Advances in Chondrogenic Differentiation and Articular Cartilage Regeneration. *Curr Mol Biol Reports*. 2016;
30. Tsumaki N, Okada M, Yamashita A. iPS cell technologies and cartilage regeneration. *Bone*. 2015;
31. Nguyen D, Hgg DA, Forsman A, Ekholm J, Nimkingratana P, Brantsing C, et al. Cartilage Tissue Engineering by the 3D Bioprinting of iPS Cells in a Nanocellulose/Alginate Bioink. *Sci Rep*. 2017;
32. Merkle FT, Ghosh S, Kamitaki N, Mitchell J, Avior Y, Mello C, et al. Human pluripotent stem cells recurrently acquire and expand dominant negative P53 mutations. *Nature*. 2017;
33. Ben-David U, Benvenisty N. The tumorigenicity of human embryonic and induced pluripotent stem cells. *Nature Reviews Cancer*. 2011.
34. Till JE, McCulloch EA. A Direct Measurement of the Radiation Sensitivity of Normal Mouse Bone Marrow Cells. *Radiat Res*. 1961;
35. Siminovitch L, McCulloch EA, Till JE. The distribution of colony-forming cells among spleen colonies. *J Cell Comp Physiol*. 1963;
36. Friedenstein AJ, Chailakhjan RK, Lalykina KS. THE DEVELOPMENT OF FIBROBLAST COLONIES IN MONOLAYER CULTURES OF GUINEA-PIG BONE MARROW AND SPLEEN CELLS. *Cell Prolif*. 1970;
37. Caplan AI. Mesenchymal stem cells: Time to change the name! *Stem Cells Transl Med*. 2017;
38. Caplan AI. Mesenchymal Stem Cells in Regenerative Medicine. In: *Handbook of Stem Cells*. 2013.
39. Dominici M, Le Blanc K, Mueller I, Slaper-Cortenbach I, Marini FC, Krause DS, et al. Minimal criteria for defining multipotent mesenchymal stromal

- cells. The International Society for Cellular Therapy position statement. *Cytotherapy*. 2006;
40. Viganò M, Perucca Orfei C, Colombini A, Stanco D, Randelli P, Sansone V, et al. Different culture conditions affect the growth of human tendon stem/progenitor cells (TSPCs) within a mixed tendon cells (TCs) population. *J Exp Orthop*. 2017;4(1).
41. Stanco D, Viganò M, Perucca Orfei C, Di Giancamillo A, Peretti GM, Lanfranchi L, et al. Multidifferentiation potential of human mesenchymal stem cells from adipose tissue and hamstring tendons for musculoskeletal cell-based therapy. *Regenerative Medicine*. 2015.
42. Bourin P, Bunnell BA, Casteilla L, Dominici M, Katz AJ, March KL, et al. Stromal cells from the adipose tissue-derived stromal vascular fraction and culture expanded adipose tissue-derived stromal/stem cells: A joint statement of the International Federation for Adipose Therapeutics and Science (IFATS) and the International So. *Cytotherapy*. 2013;
43. Lin CS, Ning H, Lin G, Lue TF. Is CD34 truly a negative marker for mesenchymal stromal cells? *Cytotherapy*. 2012.
44. Gronthos S, Franklin DM, Leddy HA, Robey PG, Storms RW, Gimble JM. Surface protein characterization of human adipose tissue-derived stromal cells. *J Cell Physiol*. 2001;
45. Gronthos S, Graves SE, Ohta S, Simmons PJ. The STRO-1+ fraction of adult human bone marrow contains the osteogenic precursors. *Blood*. 1994;
46. Stewart K, Walsh S, Screen J, Jefferiss CM, Chainey J, Jordan GR, et al. Further characterization of cells expressing STRO-1 in cultures of adult human bone marrow stromal cells. *J Bone Miner Res*. 1999;
47. Kadar K, Kiraly M, Porcsalmy B, Molnar B, Racz GZ, Blazsek J, et al. Differentiation potential of stem cells from human dental origin - promise for tissue engineering. *J Physiol Pharmacol*. 2009;
48. Ullah I, Subbarao RB, Rho GJ. Human mesenchymal stem cells - Current trends and future prospective. *Bioscience Reports*. 2015.
49. Al-Nbaheen M, vishnubalaji R, Ali D, Bouslimi A, Al-Jassir F, Megges M, et al. Human Stromal (Mesenchymal) Stem Cells from Bone Marrow, Adipose Tissue and Skin Exhibit Differences in Molecular Phenotype and Differentiation Potential. *Stem Cell Rev Reports*. 2013;

50. Wu M, Zhang R, Zou Q, Chen Y, Zhou M, Li X, et al. Comparison of the Biological Characteristics of Mesenchymal Stem Cells Derived from the Human Placenta and Umbilical Cord. *Sci Rep.* 2018;
51. Wei XX, Fong L, Small EJ. Prostate Cancer Immunotherapy with Sipuleucel-T: Current Standards and Future Directions. *Expert Rev Vaccines.* 2015;
52. Shammaa R, El-Kadiry AEH, Abusarah J, Rafei M. Mesenchymal Stem Cells Beyond Regenerative Medicine. *Frontiers in Cell and Developmental Biology.* 2020.
53. Murphy JM, Dixon K, Beck S, Fabian D, Feldman A, Barry F. Reduced chondrogenic and adipogenic activity of mesenchymal stem cells from patients with advanced osteoarthritis. *Arthritis Rheum.* 2002;
54. De Girolamo L, Stanco D, Salvatori L, Coroniti G, Arrigoni E, Silecchia G, et al. Stemness and Osteogenic and Adipogenic Potential are Differently Impaired in Subcutaneous and Visceral Adipose Derived Stem Cells (ASCs) Isolated from Obese Donors. *Int J Immunopathol Pharmacol.* 2013;
55. Girolamo L De, Lopa S, Arrigoni E, Sartori MF, Baruffaldi Preis FW, Brini AT. Human adipose-derived stem cells isolated from young and elderly women: Their differentiation potential and scaffold interaction during in vitro osteoblastic differentiation. *Cytotherapy.* 2009;
56. Murphy MB, Moncivais K, Caplan AI. Mesenchymal stem cells: Environmentally responsive therapeutics for regenerative medicine. *Experimental and Molecular Medicine.* 2013.
57. Caplan AI. New MSC: MSCs as pericytes are Sentinels and gatekeepers. *Journal of Orthopaedic Research.* 2017.
58. Ding DC, Shyu WC, Lin SZ. Mesenchymal stem cells. *Cell Transplantation.* 2011.
59. Bianco P, Robey PG, Simmons PJ. Mesenchymal Stem Cells: Revisiting History, Concepts, and Assays. *Cell Stem Cell.* 2008.
60. Pelham RJ, Wang YL. Cell locomotion and focal adhesions are regulated by substrate flexibility. *Proc Natl Acad Sci U S A.* 1997;
61. Engler AJ, Sen S, Sweeney HL, Discher DE. Matrix Elasticity Directs Stem Cell Lineage Specification. *Cell.* 2006;

62. Méndez-Ferrer S, Michurina T V., Ferraro F, Mazloom AR, MacArthur BD, Lira SA, et al. Mesenchymal and haematopoietic stem cells form a unique bone marrow niche. *Nature*. 2010;
63. Dupont S, Morsut L, Aragona M, Enzo E, Giulitti S, Cordenonsi M, et al. Role of YAP/TAZ in mechanotransduction. *Nature*. 2011;
64. Yang C, Tibbitt MW, Basta L, Anseth KS. Mechanical memory and dosing influence stem cell fate. *Nat Mater*. 2014;
65. Fu J, Wang YK, Yang MT, Desai RA, Yu X, Liu Z, et al. Mechanical regulation of cell function with geometrically modulated elastomeric substrates. *Nat Methods*. 2010;
66. Alakpa E V., Jayawarna V, Lampel A, Burgess K V., West CC, Bakker SCJ, et al. Tunable Supramolecular Hydrogels for Selection of Lineage-Guiding Metabolites in Stem Cell Cultures. *Chem*. 2016;
67. Dingal PCDP, Bradshaw AM, Cho S, Raab M, Buxboim A, Swift J, et al. Fractal heterogeneity in minimal matrix models of scars modulates stiff-niche stem-cell responses via nuclear exit of a mechanorepressor. *Nat Mater*. 2015;
68. Pittenger MF, Discher DE, Péault BM, Phinney DG, Hare JM, Caplan AI. Mesenchymal stem cell perspective: cell biology to clinical progress. *npj Regenerative Medicine*. 2019.
69. De Becker A, Van Riet I. Homing and migration of mesenchymal stromal cells: How to improve the efficacy of cell therapy? *World Journal of Stem Cells*. 2016.
70. Wei X, Yang X, Han ZP, Qu FF, Shao L, Shi YF. Mesenchymal stem cells: A new trend for cell therapy. *Acta Pharmacologica Sinica*. 2013.
71. Prockop DJ, Kota DJ, Bazhanov N, Reger RL. Evolving paradigms for repair of tissues by adult stem/progenitor cells (MSCs). *Journal of Cellular and Molecular Medicine*. 2010.
72. Asahara T, Takahashi T, Masuda H, Kalka C, Chen D, Iwaguro H, et al. VEGF contributes to postnatal neovascularization by mobilizing bone marrow-derived endothelial progenitor cells. *EMBO J*. 1999;
73. Llevadot J, Murasawa S, Kureishi Y, Uchida S, Masuda H, Kawamoto A, et al. HMG-CoA reductase inhibitor mobilizes bone marrow-derived endothelial progenitor cells. *J Clin Invest*. 2001;

74. Niada S, Giannasi C, Gomasasca M, Stanco D, Casati S, Brini AT. Adipose-derived stromal cell secretome reduces TNF α -induced hypertrophy and catabolic markers in primary human articular chondrocytes. *Stem Cell Res.* 2019;38.
75. Gowen A, Shahjin F, Chand S, Odegaard KE, Yelamanchili S V. Mesenchymal Stem Cell-Derived Extracellular Vesicles: Challenges in Clinical Applications. *Frontiers in Cell and Developmental Biology.* 2020.
76. Rasmusson I, Ringdén O, Sundberg B, Le Blanc K. Mesenchymal stem cells inhibit the formation of cytotoxic T lymphocytes, but not activated cytotoxic T lymphocytes or natural killer cells. *Transplantation.* 2003;
77. Eggenhofer E, Hoogduijn MJ. Mesenchymal stem cell-educated macrophages. *Transplantation Research.* 2012.
78. Tappenbeck N, Schröder HM, Niebergall-Roth E, Hassinger F, Dehio U, Dieter K, et al. In vivo safety profile and biodistribution of GMP-manufactured human skin-derived ABCB5-positive mesenchymal stromal cells for use in clinical trials. *Cytotherapy.* 2019;
79. Stanco D, Caprara C, Ciardelli G, Mariotta L, Gola M, Minonzio G, et al. Tenogenic differentiation protocol in xenogenic-free media enhances tendon-related marker expression in ASCs. *PLoS One.* 2019;
80. Metcalfe SM. Mesenchymal stem cells and management of COVID-19 pneumonia. *Med Drug Discov.* 2020;
81. Liang B, Chen J, Li T, Wu H, Yang W, Li Y, et al. Clinical remission of a critically ill COVID-19 patient treated by human umbilical cord mesenchymal stem cells. *ChinaXiv.* 2020;
82. Leng Z, Zhu R, Hou W, Feng Y, Yang Y, Han Q, et al. Transplantation of ACE2- Mesenchymal Stem Cells Improves the Outcome of Patients with COVID-19 Pneumonia. *Aging Dis.* 2020;
83. U.S. National Institutes of Health. *ClinicalTrials.gov Background.* *ClinicalTrials.gov.* 2014.
84. Halme DG, Kessler DA. FDA regulation of stem-cell-based therapies. *N Engl J Med.* 2006;
85. FDA (Food and Drug Administration). Statement from FDA Commissioner Scott Gottlieb, M.D. on the FDA's new policy steps and

enforcement efforts to ensure proper oversight of stem cell therapies and regenerative medicine. FDA Statement August 28, 2017. 2017.

86. Center for Biologics Evaluation and Research. Approved Cellular and Gene Therapy Products. US Food Drug Adm. 2018;

87. Murray IR, Chahla J, Safran MR, Krych AJ, Saris DBF, Caplan AI, et al. International Expert Consensus on a Cell Therapy Communication Tool: DOSES. *J Bone Jt Surg - Am Vol.* 2019;

88. Chen Y, Tang L. Stem Cell Senescence: the Obstacle of the Treatment of Degenerative Disk Disease. *Curr Stem Cell Res Ther.* 2019;

89. Miyagi-Shiohira C, Kurima K, Kobayashi N, Saitoh I, Watanabe M, Noguchi Y, et al. Cryopreservation of Adipose-Derived Mesenchymal Stem Cells. *Cell Med.* 2015;

90. Gimble JM, Katz AJ, Bunnell BA. Adipose-derived stem cells for regenerative medicine. *Circulation Research.* 2007.

91. Zuk PA, Zhu M, Ashjian P, De Ugarte DA, Huang JI, Mizuno H, et al. Human adipose tissue is a source of multipotent stem cells. *Mol Biol Cell.* 2002;

92. Arrigoni E, Lopa S, De Girolamo L, Stanco D, Brini AT. Isolation, characterization and osteogenic differentiation of adipose-derived stem cells: From small to large animal models. *Cell Tissue Res.* 2009;338(3).

93. Matsumoto D, Sato K, Gonda K, Takaki Y, Shigeura T, Sato T, et al. Cell-assisted lipotransfer: Supportive use of human adipose-derived cells for soft tissue augmentation with lipoinjection. In: *Tissue Engineering.* 2006.

94. Lindroos B, Suuronen R, Miettinen S. The Potential of Adipose Stem Cells in Regenerative Medicine. *Stem Cell Reviews and Reports.* 2011.

95. Zuk PA, Zhu M, Mizuno H, Huang J, Futrell JW, Katz AJ, et al. Multilineage cells from human adipose tissue: Implications for cell-based therapies. In: *Tissue Engineering.* 2001.

96. Bunnell BA, Flaat M, Gagliardi C, Patel B, Ripoll C. Adipose-derived stem cells: Isolation, expansion and differentiation. *Methods.* 2008;

97. Stanco D, Caprara C, Ciardelli G, Mariotta L, Gola M, Minonzio G, et al. Tenogenic differentiation protocol in xenogenic-free media enhances tendon-related marker expression in ASCs. *PLoS One.* 2019;14(2).

98. Tobita M, Orbay H, Mizuno H. Adipose-derived stem cells: current findings and future perspectives. *Discovery medicine.* 2011.

99. Arrigoni E, De Girolamo L, Di Giancamillo A, Stanco D, Dellavia C, Carnelli D, et al. Adipose-derived stem cells and rabbit bone regeneration: Histomorphometric, immunohistochemical and mechanical characterization. *J Orthop Sci.* 2013;
100. Lopa S, Colombini A, Stanco D, de Girolamo L, Sansone V, Moretti M. Donor-matched mesenchymal stem cells from knee infrapatellar and subcutaneous adipose tissue of osteoarthritic donors display differential chondrogenic and osteogenic commitment. *Eur Cells Mater.* 2014;
101. Chu D-T, Nguyen Thi Phuong T, Tien NLB, Tran DK, Minh LB, Thanh V Van, et al. Adipose Tissue Stem Cells for Therapy: An Update on the Progress of Isolation, Culture, Storage, and Clinical Application. *J Clin Med.* 2019;
102. Aghayan H-R, Goodarzi P, Arjmand B. Stem Cells and Good Manufacturing Practices. *Methods in molecular biology (Clifton, N.J.).* 2015.
103. Roato I, Belisario DC, Compagno M, Lena A, Bistolfi A, Maccari L, et al. Concentrated adipose tissue infusion for the treatment of knee osteoarthritis: clinical and histological observations. *Int Orthop.* 2019;
104. Dall'Oca C, Breda S, Elena N, Valentini R, Samaila EM, Magnan B. Mesenchymal stem cells injection in hip osteoarthritis: Preliminary results. *Acta Biomed.* 2019;
105. Jones IA, Wilson M, Togashi R, Han B, Mircheff AK, Thomas Vangsness C. A randomized, controlled study to evaluate the efficacy of intra-articular, autologous adipose tissue injections for the treatment of mild-to-moderate knee osteoarthritis compared to hyaluronic acid: A study protocol. *BMC Musculoskelet Disord.* 2018;
106. Lee WS, Kim HJ, Kim K Il, Kim GB, Jin W. Intra-Articular Injection of Autologous Adipose Tissue-Derived Mesenchymal Stem Cells for the Treatment of Knee Osteoarthritis: A Phase IIb, Randomized, Placebo-Controlled Clinical Trial. *Stem Cells Transl Med.* 2019;
107. Loebel C, Burdick JA. Engineering Stem and Stromal Cell Therapies for Musculoskeletal Tissue Repair. *Cell Stem Cell.* 2018.
108. Landers R, Pfister A, Hübner U, John H, Schmelzeisen R, Mülhaupt R. Fabrication of soft tissue engineering scaffolds by means of rapid prototyping techniques. *J Mater Sci.* 2002;

109. Wang Z, Samanipour R, Koo KI, Kim K. Organ-on-a-chip platforms for drug delivery and cell characterization: A review. *Sensors Mater.* 2015;
110. Mikos AG, Herring SW, Ochareon P, Elisseeff J, Lu HH, Kandel R, et al. Engineering complex tissues. In: *Tissue Engineering.* 2006.
111. Xu Y, Balooch G, Chiou M, Bekerman E, Ritchie RO, Longaker MT. Analysis of the material properties of early chondrogenic differentiated adipose-derived stromal cells (ASC) using an in vitro three-dimensional micromass culture system. *Biochem Biophys Res Commun.* 2007;
112. Turnbull G, Clarke J, Picard F, Riches P, Jia L, Han F, et al. 3D bioactive composite scaffolds for bone tissue engineering. *Bioact Mater.* 2018;3(3):278–314.
113. Dai R, Wang Z, Samanipour R, Koo KI, Kim K. Adipose-Derived Stem Cells for Tissue Engineering and Regenerative Medicine Applications. *Stem Cells International.* 2016.
114. Bi Y, Ehirchiou D, Kilts TM, Inkson CA, Embree MC, Sonoyama W, et al. Identification of tendon stem/progenitor cells and the role of the extracellular matrix in their niche. *Nat Med.* 2007;

Chapter 3

Tendon Tissue Engineering

3.1 Abstract

In this chapter, the peculiar organization of tendon biology and the mechanisms underlying natural tendon tissue healing are elucidated. Tendon injuries occurrences increase with the increase of aged population and active life style. The incidence rate ranges from 6 to 18 per 100 000 per year. To overcome the limited efficacy of current conventional treatments, both conservative and surgical, alternative approaches have been recently proposed. In this chapter, current advances and challenges in the development of alternative tissue engineering and regenerative medicine strategies are discussed. These strategies include the selection of appropriate stem cell type, growth factors and biomaterials, and their combination in static or dynamic cultures. Different scaffold fabrication strategies employed to imitate the particular features of tendon tissue are also discussed.

3.1 Basic science of tendon

3.1.1 Tendon structure and mechanical properties

Tendons are dense connective tissue that connect muscle to bone enabling movement of the body (1–3). Their fibrous-elastic structure transmits the force generated by muscle contraction directly to bone with minimal energy dispersion. The Achilles tendon, which is the strongest and largest tendon in the body, can sustain loads up to 17 times the body weight. Beside locomotion, tendons are involved in joint stabilization, shock adsorption and mechano-sensitivity for muscles (3). They are connected to muscles and bone by proximal insertions (myotendinous junctions) and distal insertions (osteotendinous junctions), respectively (4). Ligaments are connective tissues that connect bone to bone. They span a joint and are anchored to the bone to either end to ensure joint stability and support during motion (5). Ligament and tendon possess similar structure, extracellular matrix (ECM) content and some differences in cellular composition (Fig 3.1).

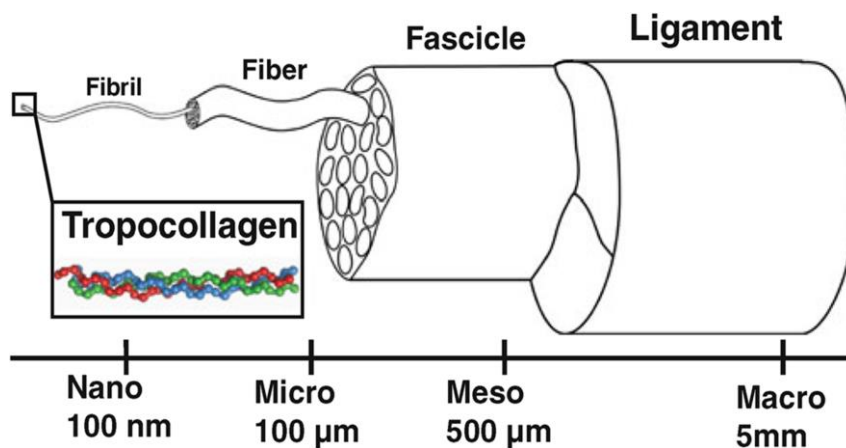


Figure 3.1. Ligament structure
Reprinted with permission from Lim et al (6).

Healthy tendon appears brilliant white with fibro-elastic texture (7). At a microscopic level, tendons are characterized by multiple layers of connective tissues that are predominantly composed of parallel, closely packed collagen elastic fibers (mainly type I and III collagens), ECM (mostly proteoglycans

responsible for the viscoelastic properties of tendons) and resident cells (tendon stem/progenitor cells –TSPCs- and tenocytes) organized in a hierarchical architecture. The smallest structural unit of tendon is tropocollagen, a single collagen molecule consisting of three polypeptide strands (alpha peptides) organized in a right handed triple helix stabilized by hydrogen bonds (3). Tropocollagen molecules aggregate progressively into fibrils stabilized by cross-linking bonds (aldol reaction) and then in fibers (8). Multiple bundles of fibrils and fibers are collected together by the endo- and epi-tenon carrying blood vessels, nerves and lymphatics to the deeper portion of the tendon. Finally, the paratenon (fatty areolar tissue) is considered as the outermost layer of the tendon. Figure 3.3 shows the histology of tendon highlighting the presence of highly aligned collagen fibers with interposed flattened parallel tenocytes.

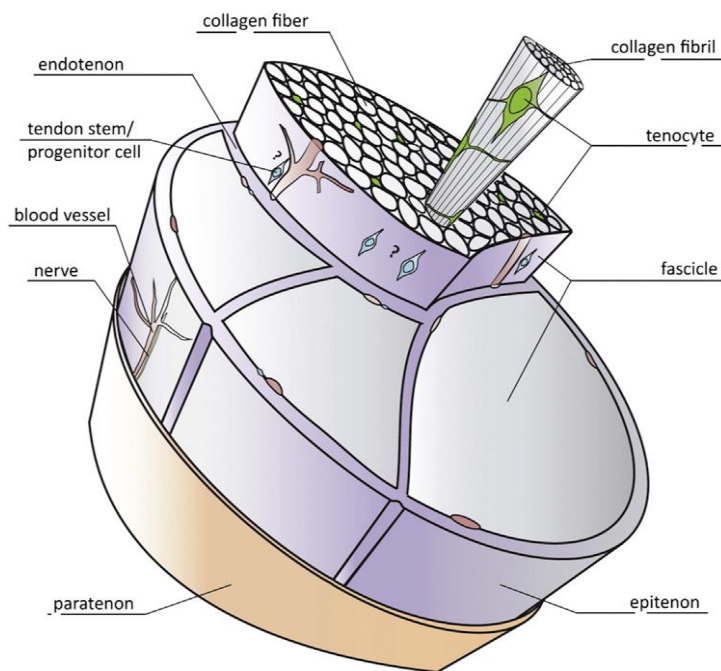


Figure 3.2. Tendon hierarchical structure

Tendon tissue is enveloped by loose connective tissue named paratenon and organized in fascicles of collagen fibrils and fibers delimited by the endotenon and epitenon, respectively. The main ECM component consist in collagen type I and III, meanwhile the cell component is present in low percentage and include mainly tenocytes and TSPCs which nature and behavior still remain to be clearly understood . Few vessels and nerves are also localized among tendon fascicles. Reprinted with permission from Bi et al (9).

The ultrastructure of tendon and ligaments guarantees high mechanical strength, tensile force and resilience preventing fiber separation and failure (7). Collagen

fibers are arranged longitudinally to the axis of tendon to provide good load capacity and resistance during movements. In particular, fibrils aggregates form a crimped structure that allows energy absorption (2). Each tendon is characterized by its own mechanical properties, i.e., stress-strain curve, stress and strain at break and Young's modulus (stiffness) (7). In the physiological loading range, tendon characteristic crimped fibers can be temporarily deformed allowing dissipation of energy and leading to straighten fibers. Within this region, tendon deforms in a linear fashion by the gliding of collagen molecules, resulting in fibers progressively becoming parallel to the direction of applied strain. This elastic behavior is maintained up to 4% of strain; then, microscopic and macroscopic (8-10% strain) failures can occur (Fig 3.4). For instance, the most commonly damaged tendon in sports injuries is Achilles tendon, which is characterized by a tensile strength of 1200 N and can bear load up to 3500 N (6).



Figure 3.3. Histology of tendon.

The collagen fibers of Achilles tendon are highly aligned with interposed flattened parallel tenocytes (arrows). Representative image, scale bar: 100 μm , reproduced by (6)

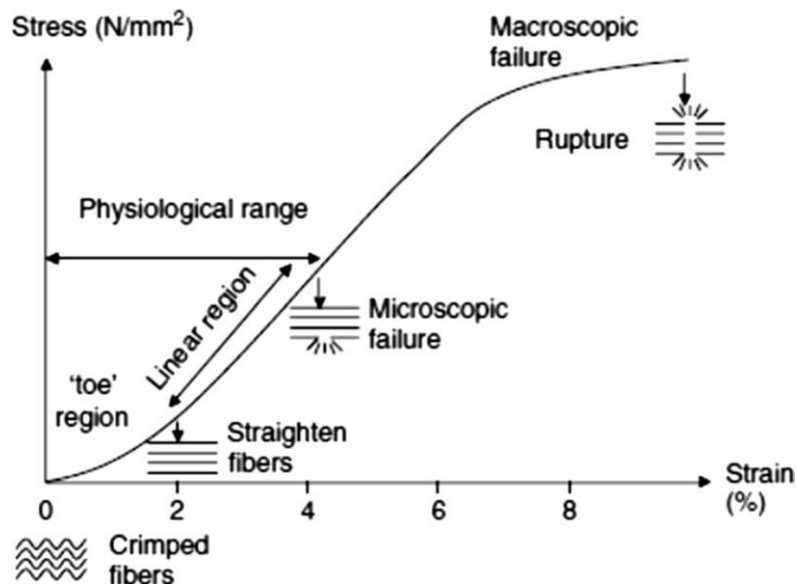


Figure 3.4. Stress–strain curve of tendon tissue.

Within the physiological loading range, elastic deformation of crimped collagen fiber bundles occurs. Then, loads within the non-physiological range result in microtears or rupture of fibers. Reproduced with permission from Trumbull et al (10).

Tendons are highly hydrated and contain approximately 70% of water (mostly associated with proteoglycans). Collagen type I is the most abundant ECM molecule of the tissue and represents about the 65-80% of the dry mass of tendon. Among other collagen types, collagen type III is the most important and it is normally abundant in endotenon and epitenon sheets. However, it is also found in large quantities in pathological tendons and represents the first collagen highly produced during tendon healing (8,11). Other components of tendon ECM are elastin, the ground substance and inorganic components. Elastic fibers ensure tissue flexibility and extensibility of collagen fibers, allowing crimp pattern recovery after stretching (12). The ground substance consists in hyaluronic acid, proteoglycans (i.e., decorin, laminin, aggrecan, biglycan, versican, fibromodulin, lumican) and glycoproteins (13). They confer visco-elastic properties to tendon tissue, provide protection against compressive forces and exert a lubricating role by retaining water molecules in the tissue (11,13). Altogether, ECM components are also responsible of the biochemical and biomechanical cues needed for the correct tissue morphogenesis, differentiation and homeostasis. The cellular components of tendon account for the lowest percentage in the tissue composition, about 5%, as shown in Figures 3.2 and 3.3. They include tendon stem/progenitor cells (TSPCs; discussed before in chapter 2) and terminally differentiated tenocytes. Both populations are responsible of ECM matrix production and

remodeling, including adaptation and tendon-related injuries (9). Other resident cells are chondrocytes, vascular cells and nervous cells, which are involved in fibrocartilage formation, tissue repair and pain perception, respectively (1,3).

3.1.2 Tendon healing

Tendon injuries are still a major challenge in orthopedics as well as a big burden in clinics. They represent about 45% of musculoskeletal lesions worldwide and is expected to quickly increase in the next decades along with the popularity of sport and the aging of population (14). The incidence rate ranges from 6 to 18 per 100 000 per year (15). The pathophysiology and healing mechanism of tendon still remain to be clearly understood so far. The difficulty in obtaining human tissues biopsies at early stages of tendon degeneration is one of the main reasons explaining this situation (11). To overcome this limit, *in vivo* studies were conducted on animal models of acute tendon ruptures or collagenase-induced tendinopathy (16,17). Tendon-related injuries are age-related disorders and have high incidence in athletes and active working people. They strongly influence the quality of life of patients who suffer of high impairments of motion and pain. The causing factors could be intrinsic, as genetics, age and nutrition, that are frequently associated to chronic injuries, and extrinsic like pharmacological therapy, or excessive or absence of mechanical loading that are related to acute injuries (6,7,11). The most common injured tendon is the Achilles tendon (18). During the pathological process, extensive ECM production by tenocytes, or maybe by erroneous differentiation of TSPCs, causing fatty degeneration and calcification accompanied by inflammation of sheath occur in tendon. However, the role of inflammation in pathogenesis rather than healing is still debated (6–8,11). The more accredited hypothesis is that, after injury, the healing process passes through four overlapping phases: inflammatory phase, reparative or proliferative phase and the consolidation and maturation remodeling phases (Fig. 3.5).

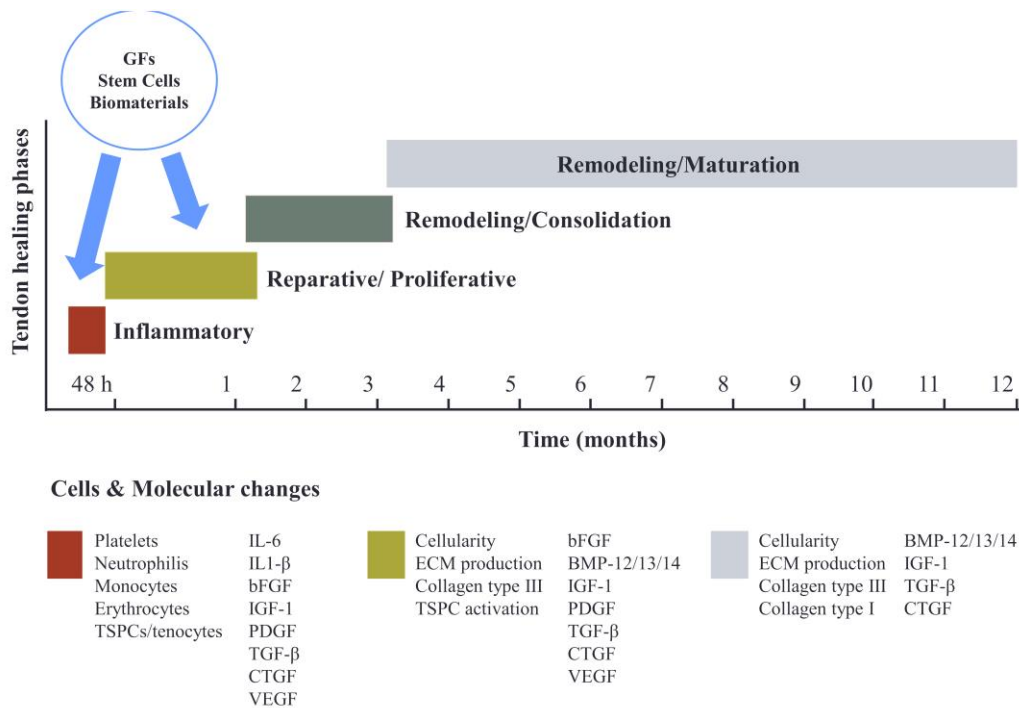


Figure 3.5. Tendon healing process.

The healing of injured tendons passes through four main overlapping phases that can take place with different duration and cellular and molecular changes. Tissue engineering approaches based on the use of growth factors (GFs), stem cells and biomaterials, alone or in combinations, are valuable alternatives to improve tendon healing. The first two phases (blue arrows) represent the most appropriate times for the application and depend on the type of GFs, stem cells or biomaterials used. Adapted with permission from Docheva et al (9)

Immediately after injury, the inflammatory phase begins with the release of chemotactic factors and cytokines for the recruitment of red blood cells and neutrophils followed by monocytes and macrophages. Secreted pro-inflammatory cytokines, such as interleukin (IL)-6 and IL-1 β , and a number of growth factors (GFs) including bFGF (basic fibroblast GF), CTGF (connective tissue GF), BMPs (bone morphogenetic proteins)-12, -13, and -14, TGF- β (transforming GF beta), IGF-1 (insulin-like GF-1), PDGF (platelet-derived GF) and VEGF (vascular endothelial GF), are released by invading inflammatory cells to induce novel blood vessel formation, tenocyte proliferation, synthesis of collagen type III and a further recruitment of inflammatory cells (6,8,19). After few days, the proliferative phase includes activation of tendon cell proliferation and abundant synthesis of ECM components, like proteoglycans and collagen type III with random arrangement. A scar-like tissue appears at the end of this phase. Almost 6-8 weeks after injury the remodeling phase starts and takes around 1-2 years

depending by the type of tendon and of patient's conditions. This phase is characterized in consolidation and maturation sub-stages. Consolidation consists in a decrease of cell proliferation and recruitment and of matrix production. Collagen type III is replaced by collagen type I and collagen fibers and tenocytes start to localize longitudinally along the axis of tendon, thus restoring tendon stiffness and tensile strength mechanical properties. Finally, maturation starts after 10 weeks accompanied by collagen fibers crosslinking and mature tendon formation. Cytokines and growth factors are involved during the entire healing process with different molecular effects, including collagen production, angiogenesis, regulations of proteinases, cell migration and proliferation (Fig 3.5) (8,20). However, especially in aged individuals the newly formed healed tendon possess lower biochemical and mechanical properties (i.e., strength (80%), stiffness (80%), stress (40%) and Young's modulus (40%) compared to pre-injured tendon) (21).

3.2 Conventional treatments

Currently the available treatments for the management of tendon/ligament disorders are conservative or surgical. The selected treatment approach generally depends on the characteristics of the tissue as well as the type and the severity of the damage. However, they usually do not allow successfully mid and long-term outcomes and injuries can evolve in severe forms of osteoarthritis (22). Generally, conservative approaches act only against symptoms to reduce pain and inflammation and include rest, non-steroidal therapy, pulsed electromagnetic field and shock waded therapy, cryotherapy, corticosteroids injection and laser therapy (7,23–25). For their high failure rates in the treatment of severe tendon injuries, such as those with complete rupture, surgery remains the treatment of choice. The main surgical repair techniques consist in re-suturing ruptured tendon ends, removal of the damaged tissue and tissue grafting in order to stabilize and improve articular functions and pain relief (26). Tissue graft can be autografts, allografts and xenografts. Autografts transplant part of a tissue in the body to another tissue in the same individual. The most common autograft is hamstring or patellar tendon used for anterior cruciate ligament (ACL) reconstruction with high success rate, almost 50% of patients, in the re-establishment of the pre-injured function state of the ligament (27). However, donor side morbidity, pain, joint instability and low mechanical performance are the detrimental long-term outcomes of this technique. Allografts, both artificial and biological devices, and xenografts reconstructions are alternative approaches that avoid donor side morbidity and improve knee stability and full well bearing (28). High failures, the risk of immune-reaction and zoonotic transmission as well as the low number of published scientific reports, limit the potential to effectively address the clinical outcomes of treated patients (22).

3.3 Tendon tissue engineering and regeneration

The scarce cellularity and vascularity of tendons is probably the main cause of the limited efficacy of the natural tendon healing. Tissue engineering and regenerative medicine approaches have been proposed as alternative therapy to obtain a functional tissue replacement able to sustain the native tendon healing and overcoming the limitations of tissue grafting (cp chapter 2). Tissue engineering for tendon includes the use of adequate cell types, scaffolds that should possess comparable mechanical properties and biologically active molecules for engineered tissue fabrication as illustrated in Figure 3.6.

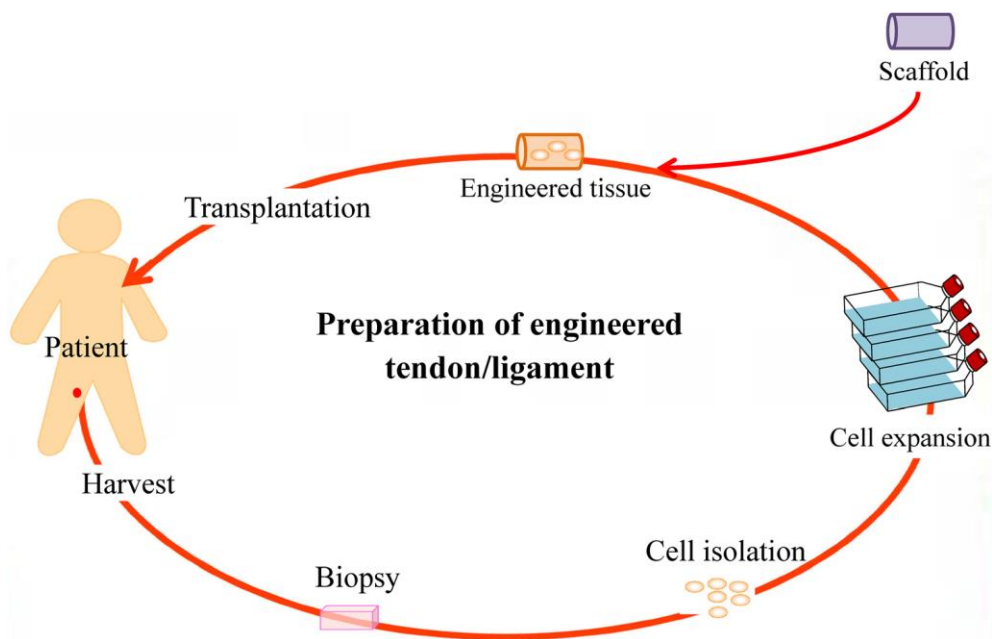


Figure 3.6. Tendon tissue engineering approach.
Reprinted with permission from Lim et al (6)

3.3.1 Cell sources

As illustrated before in chapter 2, TSPC populations possess the attractive features of mesenchymal stem cells (MSCs), including clonogenicity, multipotency and self-renewal capacity. Despite TSPCs could be use as autologous cell source for

tendon reconstruction, the low cellular yields and the potential donor side morbidity has limited their potential application in this field. Among MSCs source, cells derived from adult tissues, like bone marrow (BMSCs) and fat (ASCs), represent the favorite options since they can be easily harvested by a renewal or a waste tissue, thus avoiding the ethical concerns and the risk of tumorigenicity related to the use of embryonal and induced pluripotent stem cells (ESCs and iPSCs). Promising *in vitro* results demonstrated the tenogenic differentiation ability of BMSCs and ASCs through supplementation of the medium with GFs, such as BMP-12/14, IGF-1, that induced cellular expression of tendon-related markers, including collagen type I and III, scleraxis, decorin and tenascin C (29–32). Pretreating MSCs with selected GFs prior to their *in vivo* administration could improve tendon ECM production and ameliorate the healing process. Moreover, *in vivo* application of ASCs for the treatment of horse superficial digital flexor tendon (SDFT) has turned out to positively affect collagen type I expression and crosslinking and induce remodelling of scar tissue in SDFT lesion with less inflammatory infiltrate (33,34). The potential therapeutical effects of MSCs have been also reported in several clinic studies. For instance, injection of ASCs into tendon lesions in lateral epicondylitis of 12 patients showed promising results, including reduction of tendon defects and pain relief. Additionally, the combination of BMSCs transplantation and surgery of rotator cuff ruptures promoted faster healing rate by 6 months in comparison with the group treated with surgical repair only (35).

Despite the advancements in MSC use in regenerative medicine and their application in a number of clinical studies (mainly no tendon-related), further studies are needed to better understand the mechanisms underpinning tendon healing and regeneration, thus allowing a better spatio-temporal administration of therapeutics for successful cell-based therapy approach. Moreover, the scarce knowledge about tendon development and specific markers, and the lack of standardized protocols to induce tendon differentiation *in vitro*, are the main issues that research must face in order to progress in the understanding of tendon regeneration.

3.3.2 Effect of growth factors

In the last decade, a growing interest on platelet rich plasma (PRP) application has been registered for the treatment of tendon disorders. PRP has been already used in clinics to treat patients, as an autologous source of growth factors for the treatment of tendon injuries (21). PRP is a blood plasma with high concentration of platelets that contain various growth factors in large amount, including PDGF, IGF-1, bFGF and VEGF known to modulate healing in tendon (36). The process of harvest is very simple and inexpensive consisting in centrifugation of the whole blood to obtain the PRP fraction (Fig 3.7). Several devices for PRP preparation are already approved by the FDA. Preclinical studies have reported the efficacy of PRP in sustaining and promoting tendon regeneration and healing. However, only few studies have been performed in athletes, with often conflicting data, due also to the absence of PRP practical guidelines. PRP administration in ACL reconstruction or patellar tendinopathy has been observed to reduce pain, thickness of tendons and defect size. On the other hands, other studies did not report any improvement in healing after PRP administration (22–24). PRP contains a cocktail of growth factors but also others components like interleukins, chemokines, proteinases, inhibitors of proteinases, adhesion molecules, sphingolipids, thromboxanes, serotonin, calcium, and many other mediators (8,36). The variable composition and concentration of PRP together with the high inter-donor variability could explain the observed different responses to PRP treatments. For these reasons, a prospective randomized controlled trials using PRP standards with reproducible composition could be useful to overcome these limitations, obtain more accurate data and definitively clarify the potential of PRP to improve tendon regeneration.

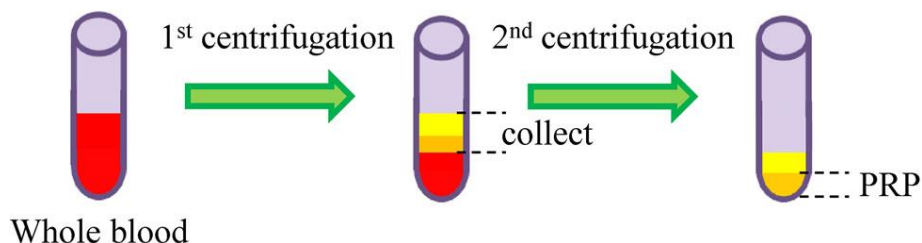


Figure 3.7. Preparation of platelet-rich plasma (PRP).
Reproduced with permission from Lim et al (6).

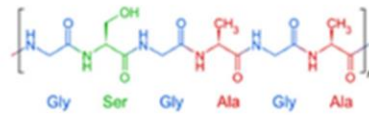
3.3.1 3D scaffold design and fabrication

As discussed before, the peculiar tendon architecture and its ECM composition are essential for tendon functionality, cell microenvironment modulation and for the mechano-sensitivity and mechano-responsive properties. Tendon tissue engineering strategies are designed to exactly resembling the native 3D structure and properties of the native tissue. To this aim, biomimetic materials are exploited to (i) provide cells with the specific topographical and biophysical cues of tendon microenvironment, thus allowing their activation, differentiation and functionality, and (ii) maintain suitable scaffolding and mechanical properties during tendon healing process. The localized delivery of growth factors previously encapsulated into the scaffold has been also investigated to increase the functionality of the 3D system (22,33,37–39).

Polymers employed in this technique can be natural-based, such as collagen, chitosan, hyaluronic acid and silk fibroin, or synthetic-based, e.g poly(ϵ -caprolactone) (PCL), poly(glycolide) (PLGA), poly(L-lactide) (PLA) or their combinations (22). Some of these materials were already known for their application in the neighboring fields of cartilage and bone tissue engineering. Natural polymers derive from renewable and abundant natural sources and are characterized by unique biodegradable and biochemical properties similar to living tissues (Fig 3.8). Owing to their similarity with the native ECM, natural polymers they can elude the immune system and avoid tissue inflammation (40).



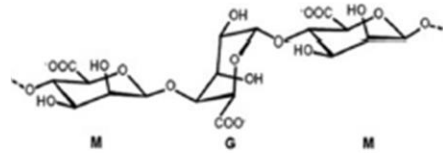
Bombyx mori silk cocoon



Silk fibroin



Brown algae



Alginate



Shrimp, crab and squid

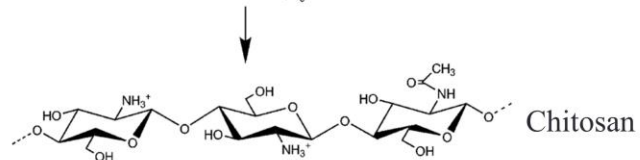
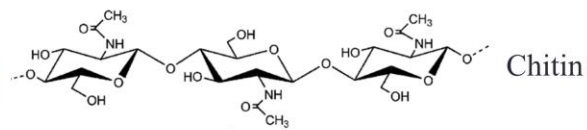


Figure 3.8. Natural polymers.

Examples of biopolymers derived from renewable resources and their respective chemical structures: silk fibroin protein, alginate and chitin/chitosan polysaccharides. Modified with permission from Pina et al (40).

Synthetic polymers are very attractive candidates for tissue engineering since they can be easily fabricated with inexpensive process and present tunable and reproducible chemical and mechanical properties. Scaffold fabrication techniques used for tendon tissue engineering include electrospinning, electrochemical alignment, knitting and freeze-drying. Table 3.1 summarizes the main biomaterials used in tendon tissue engineering, their scaffolding strategies and key advantages. Several *in vitro* and *in vivo* studies using animal models have demonstrated their promising effects for tendon regeneration (41–47). However, at present, the developed tendon tissue engineering approaches have not tested in human clinical trials yet (48).

Table 3.1 Scaffolding strategies for tendon tissue engineering

Origin	Biomaterial	Processing method	Advantages	Ref.
Natural	Collagen	Wet-spinning electrochemical alignment	Suitable mechanical properties Slow degradation rate Main ECM component	(41)
	Silk	Electrospinning Kitting	Good mechanical strength Slow degradation rate	(46)
	Alginate/CHT	Wet-spinning	Biocompatible and hydrophilic properties Sustain cell growth and collagen type I production	(42)
Synthetic	PLGA	Electrospinning	Easy to process Mass production with low cost	(43)
	PLLA	Melt-spinning		(39)
	PGA	Melt-spinning	High mechanical strength compared to natural polymers	(49)
	PCL	Freeze drying Electrospinning		(50)
Bio-artificial	PLCL/ Collagen	Electrospinning	Combination of the best properties of both natural and synthetic polymers	(51)
	PCL/CHT			(44)
	PCL/CHT/ CNC			(45)

Abbreviations: *PCL* poly(ϵ -caprolactone), *PLGA* poly(lactic-co-glycolic acid), *CHT* chitosan, *PLCL* poly(L-lactide-co- ϵ -caprolactone), *PLLA* poly(L-lactic acid), *CNC* cellulose nanocrystals

Among natural polymers, collagen has been widely explored for tendon reconstruction in the form of sponges, extruded collagen fibers or electrochemically-aligned meshes. Collagen 3D sponges could be obtained through freeze-drying method, which exploits ice-crystals as porogen for the fabrication of highly interconnected porous structures with good nutrient diffusion properties and cell penetration (52). For instance, collagen sponges cultured with BMSCs were employed to investigate the role of mechanical stimulation on the biomechanical properties of the resulting cellularized constructs (53). Mechanically stimulated bioengineered constructs (8 h/day at 2.4% strain and 1 min⁻¹ frequency) showed better mechanical properties (i.e., linear strength and

modulus) than the non-stimulated ones. Implantation of those stimulated constructs in the patellar tendon of rabbits confirmed their positive outcomes in terms of tissue remodeling. Silk fibroin, given its fibrous nature, degradability, low cost and with biocompatibility, low immunogenicity and tensile strength properties has been also largely used for biomedical applications. For instance, silk scaffolds, obtained by incorporating microporous silk sponges into knitted silk mesh to mimic tendon ECM, used in combination with BMSCs *in vitro* promoted cell proliferation and collagen synthesis (54). Then, their application for ACL reconstruction in rabbit models showed strong ECM production after 24 weeks of implantation, as well as good mechanical strength of the newly formed tissue and ligament-bone insertion reconstruction. In another study, the same tissue engineering strategy was applied to pig animal models, confirming previous results obtained in rabbits regarding the good mechanical strength of the regenerated ligament and proving the progressive degradation of the polymeric scaffolds upon implantation (47).

Recently, in a work by Lee et al, porcine decellularized tibialis tendons were re-cellularized with BMSCs and then stimulated in a bioreactor to biaxial cyclic loading for 7 days to reproduce ACL typical mechanical cues before their implantation in 24 pigs. The dynamic culture in the bioreactor increased tendon-related markers expression both at gene and protein levels and the further implantation *in vivo* restored 80% of the mechanical strength of natural ACL (55). In order to better replicate *in vitro* the physio-chemical properties of native tendon tissue, bioreactors and mechanical stresses have been demonstrated to effectively provide a dynamic environment to bioengineered constructs, thus stimulating engineered tendon tissue maturation which then will result in an enhanced tissue regeneration *in vivo* (56).

As tendon structure is mainly organized into linear and fibrillary collagen molecules, aligned nanofibers have been preferably explored because of their potential to mimic the tendon matrix architecture and provide topographical cues to promote cell alignment, stem cell differentiation, phenotype maintenance as well as matrix deposition. Recently, electrospinning and electrochemical alignment techniques combined with textile techniques have been extensively explored for the development of hierarchical scaffolds. Electrospinning allows the

production of long fibers ranging in diameter from nanometers to microns useful for tissue engineering applications (57,58).

In vitro biological tests on BMSCs cultured on electrochemically aligned collagen type I fibers evidenced the huge potential of the anisotropic structure to promote tenocyte-like cell morphology and matrix alignment, and to stimulate BMSCs to differentiate towards a tenogenic lineage (59). More recently, it has been demonstrated that electrospun silk/collagen blend scaffolds well support ASC viability, alignment and spreading with good biocompatibility and biodegradability properties suitable for tendon regeneration (60).

In the last decade, rapid prototyping or additive manufacturing technology have gain increase interests in tissue engineering for the capability to produce three-dimensional (3D) scaffold with high precision, reproducibility and controllable 3D ultrastructure. Among them, 3D bioprinting allows the fabrication of engineered tissue constructs with complex architecture by additive manufacturing of cells, biomaterials and growth factors, soluble molecules and drugs (1,2). Despite the conventional tissue engineering approach, the main advantage of this technique is represents by the possibility to obtain, in a high reproducibility and repeatability manner, a homogenous cell seeding by the precisely controlled placement of cells (61,62). In chapter 5, scientific and technological advancement of 3D bioprinting on cartilage and bone tissue engineering are discussed in detail, including the state-of-the-art technologies and pre-clinical applications. As reported below, intense development of 3D bioprinted engineered constructs has been focused for soft and hard tissue engineering (e.g., in bone and cartilage tissue engineering) whilst no application for engineered tendon substitutes has been reported in literature so far. In chapter 6, a first attempt to study *in vitro* 3D bioprinting of ASCs embedded in a natural-based hydrogel for tendon regeneration has been illustrated.

Despite the advancement on the field and the promising results obtained both *in vitro* and *in vivo*, the clinical translation of tendon tissue engineering approaches is still difficult as well as their scale-up production or standardization (22). Nevertheless, tendon tissue engineering approaches hold the potential to become the elective therapy for tendon disorder management in the future, although some

drawbacks and challenges still remain to be overcome. For instance, a better understanding of tendon biology and the pathophysiological mechanisms, the establishment of stem cell differentiation protocols, the identification of biomaterials and 3D scaffolding technologies, allowing the fine replication of tendon hierarchical and anisotropic architecture as well as of its biomechanical and biochemical cues, and a proper standardization of clinical trials are still open questions.

3.4 References

1. Kannus P. Structure of the tendon connective tissue. *Scand J Med Sci Sport*. 2000;
2. Franchi M, Trirè A, Quaranta M, Orsini E, Ottani V. Collagen structure of tendon relates to function. *TheScientificWorldJournal*. 2007.
3. Zabrzyński J, Łapaj, Paczesny, Zabrzyńska A, Grzanka D. Tendon — function-related structure, simple healing process and mysterious ageing. *Folia Morphologica (Poland)*. 2018.
4. O'Brien M. The anatomy of the achilles tendon. *Foot and Ankle Clinics*. 2005.
5. Frank CB. Ligament structure, physiology and function. *Journal of Musculoskeletal Neuronal Interactions*. 2004.
6. Lim WL, Liau LL, Ng MH, Chowdhury SR, Law JX. Current Progress in Tendon and Ligament Tissue Engineering. *Tissue Engineering and Regenerative Medicine*. 2019.
7. Sharma P, Maffulli N. Biology of tendon injury: Healing, modeling and remodeling. *Journal of Musculoskeletal Neuronal Interactions*. 2006.
8. Docheva D, Müller SA, Majewski M, Evans CH. Biologics for tendon repair. *Advanced Drug Delivery Reviews*. 2015.
9. Bi Y, Ehirchiou D, Kilts TM, Inkson CA, Embree MC, Sonoyama W, et al. Identification of tendon stem/progenitor cells and the role of the extracellular matrix in their niche. *Nat Med*. 2007;
10. Trumbull A, Subramanian G, Yildirim-Ayan E. Mechanoresponsive musculoskeletal tissue differentiation of adipose-derived stem cells. *BioMedical Engineering Online*. 2016.
11. Riley G. The pathogenesis of tendinopathy. A molecular perspective. *Rheumatology*. 2004.
12. Butler DL, Grood ES, Noyes FR, Zernicke RF. Biomechanics of ligaments and tendons. *Exerc Sport Sci Rev*. 1978;
13. Kjøer M. Role of Extracellular Matrix in Adaptation of Tendon and Skeletal Muscle to Mechanical Loading. *Physiological Reviews*. 2004.

14. Maffulli N, Wong J, Almekinders LC. Types and epidemiology of tendinopathy. *Clinics in Sports Medicine*. 2003.
15. Del Buono A, Volpin A, Maffulli N. Minimally invasive versus open surgery for acute Achilles tendon rupture: A systematic review. *Br Med Bull*. 2014;
16. Orfei CP, Lovati AB, Viganò M, Stanco D, Bottagisio M, Di Giancamillo A, et al. Dose-related and time-dependent development of collagenase-induced tendinopathy in rats. *PLoS One*. 2016;11(8).
17. Warden SJ. Animal models for the study of tendinopathy. *British Journal of Sports Medicine*. 2007.
18. Pedowitz D, Kirwan G. Achilles tendon ruptures. *Curr Rev Musculoskelet Med*. 2013;
19. Fenwick SA, Hazleman BL, Riley GP. The vasculature and its role in the damaged and healing tendon. *Arthritis Research*. 2002.
20. Evans CH. Cytokines and the role they play in the healing of ligaments and tendons. *Sports Medicine*. 1999.
21. Geremia JM, Bobbert MF, Casa Nova M, Ott RD, De Aguiar Lemos F, De Oliveira Lupion R, et al. The structural and mechanical properties of the Achilles tendon 2 years after surgical repair. *Clin Biomech*. 2015;
22. Santos ML, Rodrigues MT, Domingues RMA, Reis RL, Gomes ME. Biomaterials as Tendon and Ligament Substitutes: Current Developments. In 2017.
23. De Girolamo L, Stanco D, Galliera E, Viganò M, Lovati AB, Marazzi MG, et al. Soft-focused extracorporeal shock waves increase the expression of tendon-specific markers and the release of anti-inflammatory cytokines in an adherent culture model of primary human tendon cells. *Ultrasound Med Biol*. 2014;40(6).
24. de Girolamo L, Stanco D, Galliera E, Viganò M, Colombini A, Setti S, et al. Low Frequency Pulsed Electromagnetic Field Affects Proliferation, Tissue-Specific Gene Expression, and Cytokines Release of Human Tendon Cells. *Cell Biochem Biophys*. 2013;66(3).
25. Riley G. Tendinopathy - From basic science to treatment. *Nature Clinical Practice Rheumatology*. 2008.

26. Siegel L, Vandenakker-Albanese C, Siegel D. Anterior cruciate ligament injuries: Anatomy, physiology, biomechanics, and management. *Clinical Journal of Sport Medicine*. 2012.
27. Mascarenhas R, Tranovich MJ, Kropf EJ, Fu FH, Harner CD. Bone-patellar tendon-bone autograft versus hamstring autograft anterior cruciate ligament reconstruction in the young athlete: A retrospective matched analysis with 2-10 year follow-up. *Knee Surgery, Sport Traumatol Arthrosc*. 2012;
28. Liu ZT, Zhang XL, Jiang Y, Zeng BF. Four-strand hamstring tendon autograft versus LARS artificial ligament for anterior cruciate ligament reconstruction. *Int Orthop*. 2010;
29. Stanco D, Viganò M, Perucca Orfei C, Di Giancamillo A, Peretti GM, Lanfranchi L, et al. Multidifferentiation potential of human mesenchymal stem cells from adipose tissue and hamstring tendons for musculoskeletal cell-based therapy. *Regen Med*. 2015;10(6).
30. Violini S, Ramelli P, Pisani LF, Gorni C, Mariani P. Horse bone marrow mesenchymal stem cells express embryo stem cell markers and show the ability for tenogenic differentiation by in vitro exposure to BMP-12. *BMC Cell Biol*. 2009;
31. Tan SL, Ahmad RE, Ahmad TS, Merican AM, Abbas AA, Ng WM, et al. Effect of growth differentiation factor 5 on the proliferation and tenogenic differentiation potential of human mesenchymal stem cells in vitro. *Cells Tissues Organs*. 2012;
32. Park A, Hogan M V., Kesturu GS, James R, Balian G, Chhabra AB. Adipose-derived mesenchymal stem cells treated with growth differentiation factor-5 express tendon-specific markers. *Tissue Eng - Part A*. 2010;
33. Molloy T, Wang Y, Murrell GAC. The roles of growth factors in tendon and ligament healing. *Sports Medicine*. 2003.
34. Conze P, Van Schie HTM, Weeren R Van, Staszuk C, Conrad S, Skutella T, et al. Effect of autologous adipose tissue-derived mesenchymal stem cells on neovascularization of artificial equine tendon lesions. *Regen Med*. 2014;
35. Hernigou P, Flouzat Lachaniette CH, Delambre J, Zilber S, Duffiet P, Chevallier N, et al. Biologic augmentation of rotator cuff repair with mesenchymal stem cells during arthroscopy improves healing and prevents further tears: A case-controlled study. *Int Orthop*. 2014;

36. Stanco D, Viganò M, Croiset SJ, De Girolamo L. Applications and limits of platelet-rich plasma in sports related injuries. *J Biol Regul Homeost Agents*. 2012;26(2).
37. Klein MB, Yalamanchi N, Pham H, Longaker MT, Chang J. Flexor tendon healing in vitro: Effects of TGF- β on tendon cell collagen production. *J Hand Surg Am*. 2002;
38. Chan BP, Fu SC, Qin L, Lee KM, Rolf CG, Chan KM. Effects of basic fibroblast growth factor (bFGF) on early stages of tendon healing. A rat patellar tendon model. *Acta Orthop Scand*. 2000;
39. Sahoo S, Toh SL, Goh JCH. A bFGF-releasing silk/PLGA-based biohybrid scaffold for ligament/tendon tissue engineering using mesenchymal progenitor cells. *Biomaterials*. 2010;
40. Pina S, Ribeiro VP, Marques CF, Maia FR, Silva TH, Reis RL, et al. Scaffolding strategies for tissue engineering and regenerative medicine applications. *Materials*. 2019.
41. Gurkan UA, Cheng X, Kishore V, Uquillas JA, Akkus O. Comparison of morphology, orientation, and migration of tendon derived fibroblasts and bone marrow stromal cells on electrochemically aligned collagen constructs. *J Biomed Mater Res - Part A*. 2010;
42. Yoon JP, Lee CH, Jung JW, Lee HJ, Lee YS, Kim JY, et al. Sustained Delivery of Transforming Growth Factor β 1 by Use of Absorbable Alginate Scaffold Enhances Rotator Cuff Healing in a Rabbit Model. *Am J Sports Med*. 2018;
43. Leong NL, Arshi A, Kabir N, Nazemi A, Petrigliano FA, Wu BM, et al. In vitro and in vivo evaluation of heparin mediated growth factor release from tissue-engineered constructs for anterior cruciate ligament reconstruction. *J Orthop Res*. 2015;
44. Deepthi S, Nivedhitha Sundaram M, Deepti Kadavan J, Jayakumar R. Layered chitosan-collagen hydrogel/aligned PLLA nanofiber construct for flexor tendon regeneration. *Carbohydr Polym*. 2016;
45. Leroy A, Nottelet B, Bony C, Pinese C, Charlot B, Garric X, et al. PLA-poloxamer/poloxamine copolymers for ligament tissue engineering: Sound macromolecular design for degradable scaffolds and MSC differentiation. *Biomater Sci*. 2015;

46. Font Tellado S, Bonani W, Balmayor ER, Foehr P, Motta A, Migliaresi C, et al. Fabrication and Characterization of Biphasic Silk Fibroin Scaffolds for Tendon/Ligament-to-Bone Tissue Engineering. *Tissue Eng - Part A*. 2017;
47. Fan H, Liu H, Toh SL, Goh JCH. Anterior cruciate ligament regeneration using mesenchymal stem cells and silk scaffold in large animal model. *Biomaterials*. 2009;
48. U.S. National Institutes of Health. *ClinicalTrials.gov* Background. *ClinicalTrials.gov*. 2014.
49. Rothrauff BB, Coluccino L, Gottardi R, Ceseracciu L, Scaglione S, Goldoni L, et al. Efficacy of thermoresponsive, photocrosslinkable hydrogels derived from decellularized tendon and cartilage extracellular matrix for cartilage tissue engineering. *J Tissue Eng Regen Med*. 2018;
50. Leung M, Jana S, Tsao CT, Zhang M. Tenogenic differentiation of human bone marrow stem cells via a combinatory effect of aligned chitosan-poly-caprolactone nanofibers and TGF- β 3. *J Mater Chem B*. 2013;
51. Wu G, Deng X, Song J, Chen F. Enhanced biological properties of biomimetic apatite fabricated polycaprolactone/chitosan nanofibrous bio-composite for tendon and ligament regeneration. *J Photochem Photobiol B Biol*. 2018;
52. Schoof H, Apel J, Heschel I, Rau G. Control of pore structure and size in freeze-dried collagen sponges. *J Biomed Mater Res*. 2001;
53. Juncosa-Melvin N, Shearn JT, Boivin GP, Gooch C, Galloway MT, West JR, et al. Effects of mechanical stimulation on the biomechanics and histology of stem cell-collagen sponge constructs for rabbit patellar tendon repair. *Tissue Eng*. 2006;
54. Fan H, Liu H, Wong EJW, Toh SL, Goh JCH. In vivo study of anterior cruciate ligament regeneration using mesenchymal stem cells and silk scaffold. *Biomaterials*. 2008;
55. Lee K Il, Lee JS, Kang KT, Shim YB, Kim YS, Jang JW, et al. In Vitro and In Vivo Performance of Tissue-Engineered Tendons for Anterior Cruciate Ligament Reconstruction. *Am J Sports Med*. 2018;
56. Jaiswal D, Yousman LC, Neary M, Fernschild E, Zolnoski B, Katebifar S, et al. Tendon tissue engineering: biomechanical considerations. *Biomed Mater*. 2020;

57. Nivison-Smith L, Weiss AS. Alignment of human vascular smooth muscle cells on parallel electrospun synthetic elastin fibers. *J Biomed Mater Res - Part A*. 2012;
58. Domingues RMA, Gomes ME, Reis RL. The potential of cellulose nanocrystals in tissue engineering strategies. *Biomacromolecules*. 2014.
59. Kishore V, Bullock W, Sun X, Van Dyke WS, Akkus O. Tenogenic differentiation of human MSCs induced by the topography of electrochemically aligned collagen threads. *Biomaterials*. 2012;
60. Maghdouri-White Y, Petrova S, Sori N, Polk S, Wriggers H, Ogle R, et al. Electrospun silk-collagen scaffolds and BMP-13 for ligament and tendon repair and regeneration. *Biomed Phys Eng Express*. 2018;
61. Murphy S V., Atala A. 3D bioprinting of tissues and organs. *Nature Biotechnology*. 2014.
62. Kang HW, Lee SJ, Ko IK, Kengla C, Yoo JJ, Atala A. A 3D bioprinting system to produce human-scale tissue constructs with structural integrity. *Nat Biotechnol* [Internet]. 2016;34(3):312–9. Available from: <http://dx.doi.org/10.1038/nbt.3413>

PART II

Chapter 4

***In vitro* tenogenic differentiation of ASCs in GMP-compliant xenogenic-serum free media**

4.1 Abstract

Regenerative medicine approaches based on the use of patient-derived ASCs have been largely proposed in the last decades as alternative therapies to solve unmet clinical needs, including tendon injuries. For their application in clinical setting some standardization procedure are required to satisfy the safety, efficacy, reproducibility and quality of the procedure. For this reason, a key issue concerns the development of a clinical-grade medium for a pre-implant safe and efficient expansion and differentiation of stem cells. In this chapter, a GMP-compliant approach consisting of serum-free medium (SF) or a xenogenic-free human pooled platelet lysate medium (hPL) supplemented with a combination of soluble and growth factors was used to maintain the peculiar MSC features and to trigger ASC toward a tenocyte-like phenotype. The suitability of this approach on ASC cultures and tenogenesis induction is assessed by the evaluation of the typical MSC profile and by the expression of stemness and tendon-related markers during differentiation, respectively. The results highlight the potential applicability of both SF and hPL media in GMP-compliant approach to culture ASC and drive cell differentiation in vitro moving toward the application of ASCs in cell-based therapeutical approaches in clinical setting.

*Part of the results described in this chapter have been published in the manuscript titled “Tenogenic differentiation protocol in xenogenic-free media enhances tendon related marker expression in ASCs” authored by **Deborah Stanco**, Christian Caprara, Gianluca Ciardelli, Luca Mariotta, Mauro Gola, Greta Minonzio and Gianni Soldati in PLoS ONE, 2019, 14(2):e0212192 <https://doi.org/10.1371/journal.pone.0212192>.*

4.2 Introduction

Tendon injuries are still a major challenge in orthopedics as well as a big burden in clinics. They represent about 45% of musculoskeletal lesions worldwide and count approximately 2,000 new cases each year only in Switzerland (*statistique de l'assurance-accidents; www.unfallstatistik.ch*) with a mean insurance cost of 23,843 CHF that is expected to quickly increase in the next decades along with the popularity of sport and the aging of population (1). Tendons are ubiquitous, dense, regular connective tissue structures in the body, which definition derives from their anatomical position connecting muscle to bone (cp- chapter 3). They enable the transfer of mechanical load generated by a muscle to bone, resulting in stabilization or movement across a joint (2,3). The dry weight of normal tendons consists in extracellular matrix (ECM) composed mainly of collagen type I and III (4). The cellular component is scarce, accounting for only 5% of the tissue and consisting for the 95% in tenocytes that are terminally differentiated cells responsible for maintaining ECM homeostasis and collagen molecule synthesis (5,6). Over the last decade, a unique progenitor cell population named tendon stem/progenitor cells (TSPCs) was isolated. They possess self-renewal and multilineage differentiation potential and could be probably primarily involved in maintaining tissue homeostasis and in promoting repair after injury (7,8). ECM proteins play an important role on the regulation of the fate of stem cells within their niche by modulating the bioactivities of growth factors and cytokines to which ECM proteins often bind (7). Matrix metalloproteinases (MMPs) and the tissue inhibitors of metalloproteinases (TIMPs) are important regulator of ECM remodeling and their enzymatic activity imbalance may result in uncontrolled tendon damage (5,9,10). Natural healing in tendon occurs slowly due to its hypocellularity and hypovascularity. Moreover, it often fails to restore the functionality and biological properties proper of the tissue due to the erroneous formation of hypercellular scar tissue with impaired mechanical properties that can lead to reinjure (5,9,11). Several efforts have been done in the last years in the understanding of tendon biology and related pathogenesis, although knowledge in these fields still remains limited. In this regard, the difficulty in obtaining tendon biopsies is the main clinical problem since they are usually collected at the end-

stage of the injured condition (10,12). From these evidences, the need for an advanced therapy to address the underlying pathology by improving clinical, mechanical, and radiologic outcomes is evident. Recent studies have focused on improving the biological environment around the tendon itself through growth factor delivery or stem cell therapy (13–16). These regenerative medicine approaches aim to enhance the quality of healing tendons by inducing tissue self-regeneration. The choice of the most appropriate cell type is crucial for the final treatment outcomes; indeed, if the harvesting and culturing of terminally differentiated tenocytes have resulted to be inefficient for clinical applications due to their low *in vitro* proliferative capacity, mesenchymal stem cells (MSCs) represent a promising cell source for tendon tissue engineering (17–20). Under the authority of the International Society for Cellular Therapy (ISCT), researchers in the MSC field issued a bold statement defining the identity of MSCs as adherent cells to tissue culture polystyrene with a typical immunophenotype profile consisting in the positive expression for the surface antigens CD73, CD90, and CD105, the negative expression of hematopoietic and endothelial markers (CD14 or CD11b, CD19, CD45, CD79a) and HLA-DR markers, and the capacity to differentiate into osteoblasts, adipocytes, and chondrocytes under permissive conditions (cp. Chapter 2) (21). These adult stem cells produce relevant extracellular matrix proteins, such as collagens, rapidly proliferate and secrete growth factors and cytokines necessary for tissue regeneration and chemotactic molecules, which can recruit additional reparative cells into the lesion site. Moreover, since the hallmark symptoms of tendon injuries are pain and inflammation, the use of MSCs seems to be appropriate given their anti-inflammatory and immunomodulatory capacity (17,22–24).

The self-renewal and regenerative potential of adipose-derived stem cells (ASCs) have been intensively studied in the last decades for their use in regenerative medicine. These cells are present in abundance in the perivascular region of white adipose tissue and the easy and minimally invasive procedure for the harvest makes them as ideal cell-source in cell-based therapies (8,25,26). For this purpose, several facilities have been established as cell banks for the procurement and the storage of human ASCs. Over the past decade, international research efforts have established a wealth of basic science and pre-clinical evidence regarding the differentiation potential and regenerative properties of both freshly

processed, heterogeneous stromal vascular fraction (SVF) cells and culture-expanded, relatively homogeneous adipose-derived stem cells (20,27–30). A number of clinical trials involving ASCs in the treatment of various musculoskeletal disorders and autoimmune diseases are already ongoing (31). In my previous *in vitro* study, compared the multidifferentiative potential of patient derived ASCs and TSPCs demonstrating their similar MSC behavior which suggested the suitable use of ASCs for tendon treatment (8). In addition, some pre-clinical studies have recently demonstrated their efficacy in inducing the restoration and regeneration of tendons by improving tissue healing and enhancing new functional tendon formation together with reduction of inflammation (23,32,33). Moreover, some clinical studies have already assessed the safety use of ASC injections to treat tendinopathies (34,35). However, several challenges still remain to overcome. Firstly, the scientific community lacks a consensus about the exact composition of tenogenic inductive medium used for MSC differentiation. A variety of growth factors highly expressed during the tendon healing process, such as bone morphogenic proteins (BMPs), transforming growth factor beta (TGF- β), platelet-derived growth factor (PDGF), connective tissue growth factor (CTGF), has been used with promising results to trigger *in vitro* MSC differentiation toward the tendon lineage. The connective tissue growth factor (CTGF) is a cysteine-rich protein highly expressed at the early stage of tendon repair and it has been reported to induce collagen type I and tenascin-C expression in MSCs *in vitro* (36,37). The TGF- β signaling plays a crucial role in tendon development and healing. Specifically, TGF- β 3 is the main inducer of scleraxis (SCX), an early expressed tendon marker, and collagen production acting as a potential trigger of tenogenesis (38–41). Furthermore, BMP-12 has been shown to allow new connective tissue formation, improving tendon repair in several tendon injury models (42,43). In particular, BMP-12 promoted the expression of scleraxis at both mRNA and protein level during culture with canine or human ASCs (14,44). In addition, in combination with TGF- β 3, it turned out to effectively promote tenogenic differentiation of MSCs and tendon healing in *in vivo* injured models (45–47). Moreover, ascorbic acid is an essential factor of collagen fibrillogenesis during tendon development. Its combination with BMP-12 or CTGF was demonstrated to enhance the expression of SCX and collagen type I and III on human ASCs and TSPCs cultures (48–50).

Another key point in cell-based therapy regards the clinical-scale translation of MSC isolation and expansion procedures. Indeed, in the vast majority of cases reagents were derived from animal sources (i.e., fetal bovine serum-FBS) are used with the consequent risks of adverse cell and tissue responses and infection occurrences by non-human pathogens (51,52). Moreover, the Food and Drug Administration (FDA) drafted strictly controls the use of xenoproducts and regulated cell therapy products to ensure safety in patients (53). Common alternatives were found in the direct use of human serum and platelet-derived products. However other concerns, such as safety and lot-to-lot variability, remains to be solved (54,55). For these reasons, the ideal culture system suitable for cell-based therapy should be a xenogenic- and serum-free medium with a chemically defined composition.

Given these assumptions, in order to move toward the clinical scale-up of the use of ASCs in regenerative cell-based therapy for injured-tendon treatment, the objectives of this study were: i) to design a GMP-compliant protocol for ASCs culture and expansion *in vitro* able to maintain their MSC properties; ii) to develop a tenogenic inductive medium, and iii) to characterize the ability of differentiated ASCs to produce tendon ECM components. For these purposes, the culture of ASCs with a novel chemically defined serum free and xenogenic-free medium (SF) and human platelet lysate (hPL) medium was evaluated. In particular, the SF medium, already protected by a patent released from SSCF cell-bank institute (PCT/EP2013/072738), consisted of essential amino acids, inorganic salts and other components, along with an optimized mix of recombinant human growth factors already known to be essential for MSC expansion. Alternatively, hPL medium is commercially available and made up of a pool of human platelet lysates derived from more than 300 donors to minimize the intrinsic donor variability. Cell morphology, immunophenotype, viability and expression of proliferative (Ki67 and PCNA) and stem-cell (KLF4, OCT4 and NANOG) markers were measured in ASCs cultured in both hPL and SF (hPL-ASCs and SF-ASCs, respectively). Then, for TENO-induced ASCs we use for the first time a blend of ascorbic acid and CTGF, TGF β -3, BMP-12 supplementation (hPL-TENO and SF-TENO, respectively) for 1, 3, 7 and 14 days. Their tenogenic differentiation was evaluated by quantifying the expression of the tendon-related markers scleraxis (SCX), tenomodulin (TNMD), tenascin (TNC), cartilage

oligomeric matrix protein (COMP), metalloproteinases (MMP3 and MMP13), tissue inhibitor of metalloproteinase (TIMP-2) and the ability of cells to produce a tendon-like extracellular matrix. Finally, to better mimic the tendon tissue environment all cultures were conducted in flask surfaces coated with collagen type I, which is the major tendon ECM component.

4.3 Materials and Methods

4.3.1 SVF isolation and cryopreservation

Adipose-derived stem cells were isolated from subcutaneous adipose tissue harvested during aesthetic liposuction of 4 healthy human donors (n=4) after signed an informed consent declaration. The procedure for ASC isolation, expansion and characterization was already GMP compliant and in accordance with the SOPs (standard operating procedures) released from the Swiss Stem Cell Foundation (SSCF) and approved by the Ethical Committee of the Canton Ticino, Switzerland (CE 2961). Stromal vascular fraction (SVF) isolation procedure was protected by a patent already deposited by SSCF (Patent PCT/EP2012/069261) and published (56). In Figure 4.1 the isolation and characterization of SVF fraction is illustrated. Briefly, to discard the hydrophilic phase from the tissue, two washings were performed using Dulbecco's Phosphate Buffered Saline (DPBS with Ca^{2+} and Mg^{2+} , Gibco, Life Technologies, Oregon, USA) in a 100 ml syringe (BBraun Medical AG, Melsungen, Germany) and placed in a support to maintain vertical position for few minutes. Upon removal of the aqueous phase, adipose tissue was digested with Liberase MNP-S (Roche Applied Science, Basel, Switzerland) at a final concentration of 0.28 Wunsch U/ml diluted in DPBS (with Ca^{2+} and Mg^{2+}) and incubated at 37 °C for 45 minutes in a thermo-heated stirring plate. After, DPBS (without Ca^{2+} and Mg^{2+} , Gibco, Life Technologies, Oregon, USA) supplemented with 1% albumin (CSL Behring AG, Bern, Switzerland) was added to interrupt the enzymatic reaction and the resulting solution was strongly mixed to separate the hydrophilic phase from the hydrophobic one. Then, the lower layer, which contained SVF cells, was collected into a conical 50 ml centrifuge tube (Falcon, Corning Science, México) washed with 1% albumin solution in DPBS and filtered through a 100 μm and a 40 μm sieves (BD Falcon, Basel, Switzerland). Finally, SVF was centrifuged at 400 g at room temperature for 5 minutes and the collected cells were resuspended in 5% human albumin solution (CSL Behring AG, Switzerland). Cell counting and cell viability of SVF cells were immediately assessed using an automated propidium iodide-based cell counting device (Nucleocounter NC-100, Chemometec A/S, Denmark).

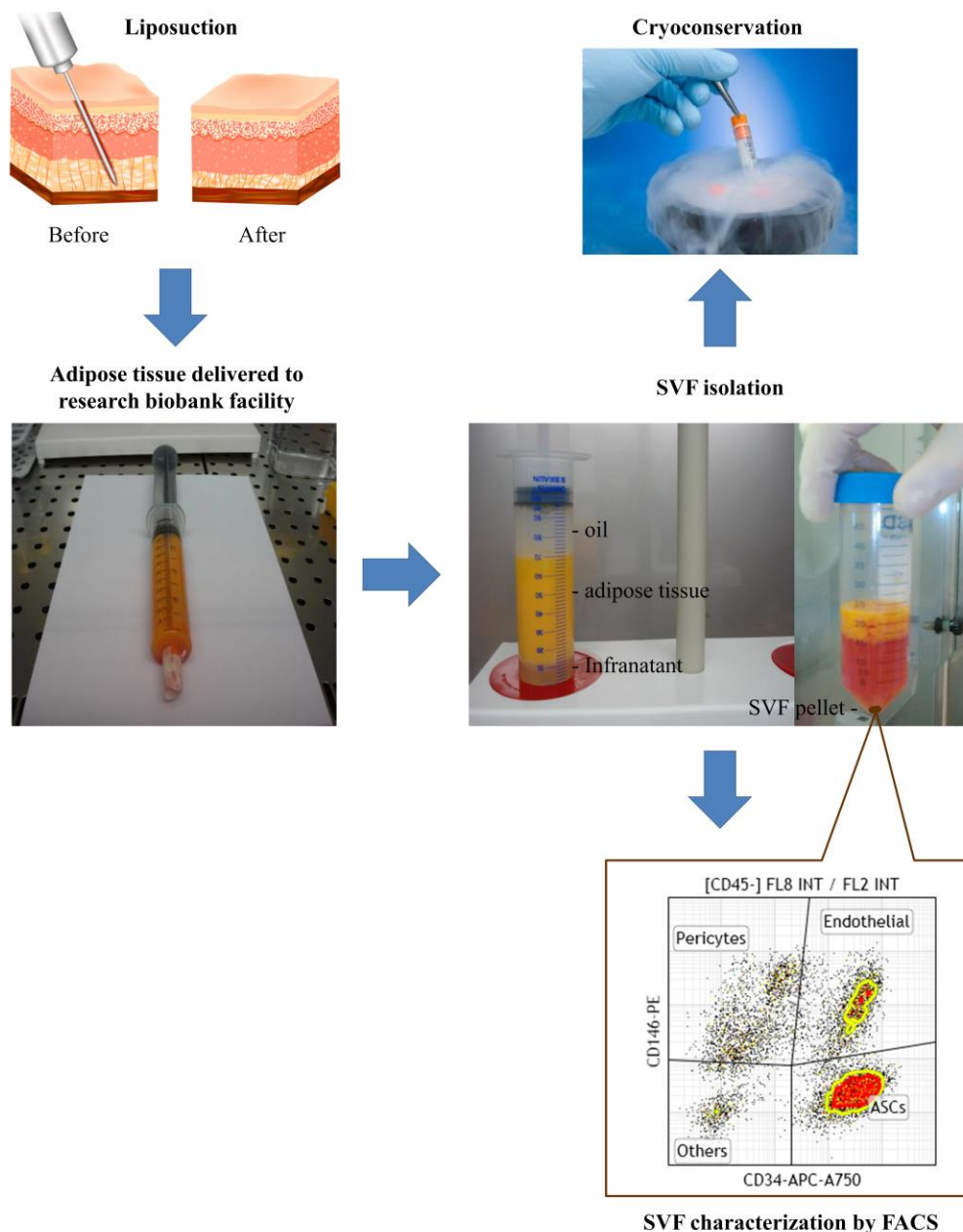


Figure 4.1. Schematic diagram depicting SVF isolation and characterization.

Lipoaspiration of subcutaneous fat was performed in clinic and delivered to the research biobank facility of SSCF followed by separation into layers of oil (discarded), aspirated adipose tissue, and infranatant (blood, plasma and anesthetic). After enzymatic digestion, the stromal vascular fraction (SVF) was isolated from the pellet obtained by centrifugation and the cells were counted and then characterized by FACS analysis demonstrating the unique surface antigen profile of ASCs (CD34⁺), pericytes (CD146⁺) and endothelial cells (CD45⁺). Finally, SVF can be cryopreserved in vapour phase nitrogen.

The cryopreservation of SVF cells was performed by centrifugation for 5 minutes at 400 g after their suspension into a 2 ml cryovial (Nalgene, Thermo Fisher Scientific, Waltham, USA) with an ice-cold solution of 1% albumin solution, 5.5% ME₂SO and 4.5% dextran-40 (Cryosure DEX-40, WAK-Chemie Medical

GmbH, Germany) in MEM alpha (PAA Laboratories, Austria) to avoid loss of cells and maintain viability. Finally, a programmable freezer (Consartic GmbH, Germany) was used under the following conditions: from 4 °C to 0 °C in 6 minutes, then hold for 15 minutes at 0 °C. From 0 °C to -2 °C in 9 minutes and then hold at -2 °C for 2 minutes. From -2 °C to -35 °C in 25.5 minutes and finally, from -35 °C to -100 °C in 13 minutes. Cryovials were then transferred into vapor nitrogen for long-term storage.

4.3.2 Xenogenic-free culture of isolated ASCs

For SVF cell expansion, after thawing cells were cultured in flasks (Nunc, Thermo Fisher Scientific, USA) at cell density of 3×10^3 cells/cm² in medium consisting of 5% pooled human platelet lysate (hPL, Stemulate, Cook Regentec, USA) in α MEM medium without nucleosides with GlutamaxTM (Fisher Scientific, USA) supplemented of 100 μ g/ml Primocin (InvivoGen, USA), as previously described (58). The medium was changed every 3 days. When cells reached 80–90% confluence, after approximately 7 days of culture, they were detached by incubation with TrypLE Select (Gibco) for 3 minutes at 37 °C in incubator. The number of collected cells and their viability were assessed through an image cytometer based on fluorescence from the fluorescent dye propidium iodide (PI) (Nucleocounter NC-100, ChemoMetec A/S, Denmark) and the “PI-exclusion” method (Figure 4.2). After 3 passages in culture, ASCs were plated on pre-coated collagen I culture flasks (Corning, USA) at 3×10^3 cells/cm² cell density and cultured in two different xenogenic free media: i) the low percentage hPL medium (1% hPL, Stemulate, Cook Regentec) (hPL-ASCs) or ii) in the SSCF serum free medium (SF-ASCs). The percentage of hPL supplementation was selected according to manufacturer’s instructions in order to avoid differences based on the content of mitogenic growth factors and soluble molecules between the two media (data not shown). The formulation of SF medium consisted in Ham’s F12/IMDM (1:1) medium supplemented with 0.1 μ g/ml Primocin, 2 mM L-alanyl-L-glutamine, 50 μ g/ml L ascorbic acid-2-phosphate (Sigma Aldrich), 5 μ g/ml human ITS supplement premix (BD Life Sciences), 250 μ g/ml human albumin 5% solution (CSL Behring AG), 50 ng/ml human thyroglobulin (Millipore SAS, Calbiochem, USA), and 10 ng/ml of the growth factors b-FGF,

PDGF-AB, PDGF-BB, TGF- β 1 (all from ProSpec-Tany TechnoGene Ltd, Israel). hPL-ASCs and SF-ASCs were detached at 1, 7 and 14 days and then analyzed for cell count and viability as described before.

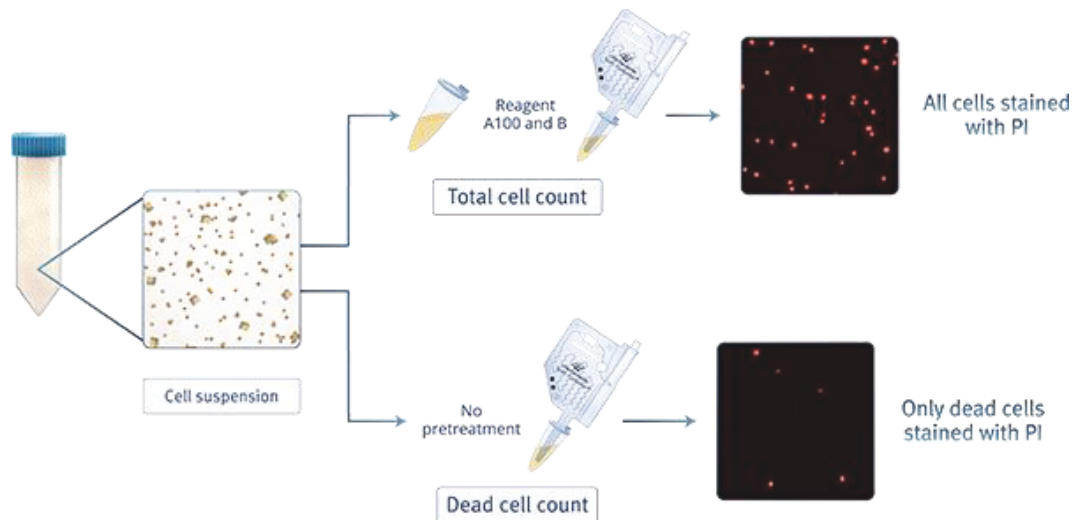


Figure 4.2. Determination of the number of viable cells with NucleoCounter

According to manufacturer's instructions, after cell lysis to induce cell membrane rupture, all cell nuclei become susceptible to PI staining and the total cell count can be read. On the other hand, non-viable cells are already permeable to PI before the lysis procedure. Hence, in this case the staining with PI results in a non-viable cell count. Finally, cell viability of a sample is determined using the total cell count and the count of non-viable cells.

4.3.3 Tenogenic differentiation protocol in xenogenic-free media

Tenogenic differentiation induction was performed in both hPL-ASC and SF-ASC populations at passage 4 (hPL-TENO and SF-TENO, respectively). In particular, cells were seeded in collagen I coated-well plates or culture flasks (Corning, USA) at a cell density of 3×10^3 cells/cm² and then cultured in hPL or SF medium supplemented with 50 μ g/ml Ascorbic acid (AA; Sigma Aldrich), 50 ng/ml BMP-12, 100 ng/ml CTGF and 10 ng/ml TGF- β 3 (all from Peptrotech, UK). The medium was changed twice a week. Cells cultured in hPL or SF medium without any further supplementation were used as control (hPL-CTRL, SF-CTRL).

4.3.4 Immunophenotype characterization

ASC identification and their absolute number were evaluated in the fresh SVF fraction. In particular, staining of 5×10^5 SVF cells was performed incubating them with the following monoclonal antibodies: CD146-PE, CD34-APC-A750,

CD45-KrO (Beckman Coulter, Switzerland), Syto 40 (Life Technologies, USA) to exclude cellular debris and 7-amino-actinomycin D (7-AAD, Beckman Coulter) to assess cell viability (59). After 20 minutes of incubation, erythrocytes were lysed using Versalysse lysing solution (Beckman Coulter). For the direct evaluation of the absolute number of ASCs, Flow-Count Fluorospheres (Beckman Coulter) were added in the tube for the FACS analysis. Finally, ASCs were identified as negative for the CD45 and CD146 marker expression and positive for the superficial antigen CD34, as shown in Figure 4.1 (59,60).

In order to characterize ASCs cultured in the xenogenic-free media as proposed by the Mesenchymal and Tissue Stem Cell Committee of the International Society for Cellular Therapy, the immunophenotype of P4 ASCs cultured in hPL or SF xenogenic-free medium was evaluated (21). Firstly, 5×10^5 cells were washed from the culture medium with PBS^{+/+} and then incubated with LIVE/DEAD fixable stain (Life Technologies) at room temperature in the dark for 30 minutes to exclude fluorescent dead cells. Then, hPL-ASCs and SF-ASCs were stained with control antibodies IgG1-FITC, IgG3-PE, IgG1-PC5, IgG1-PC7, IgG1-APC, IgG1-APC-A750, IgG1-KrO (all from Beckman Coulter) or with CD73-FITC, CD31-FITC (BD Biosciences, USA), CD105-PE, CD90-PC5, CD13-PC7, CD44-APC-A750, CD45-KrO (Beckman Coulter). Before measurement, cells were resuspended in IOTest 3 Fixative Solution (Beckman Coulter).

The superficial expression of the specific tendon-related marker tenomodulin (TNMD) in both hPL- and SF- cultured ASCs after 7 and 14 days of differentiation was also assessed by FACS. Incubation of 2.5×10^5 CTRL and TENO cells with anti-human polyclonal tenomodulin antibody (ab203676, Abcam) was performed for 1 hour at 4 °C in the dark. Then, they were stained with the secondary goat polyclonal antibody Alexa Fluor® 488 (ab150077, Abcam). The background fluorescence emission by death cells was excluded by DAPI viability dye (Beckman Coulter) staining.

All flow cytometry analyses were performed using a Navios 3-lasers/10-channels flow cytometer (Beckman Coulter), and data were analyzed with Kaluza software (Beckman Coulter).

4.3.5 Cell viability

Cell counting and viability of ASCs cultured in all media conditions were assessed at 1, 7 and 14 days of culture using the automated propidium iodide-based cell counting device (Nucleocounter NC-100, ChemoMetec A/S) as previously described. Furthermore, Alamar Blue Assay (Thermo Fisher Scientific, USA) was performed in both undifferentiated and differentiated hPL-ASCs and SF-ASCs at 1, 4 and 7 days of culture to detect cell metabolic activity (61). This bioassay incorporates a fluorometric/colorimetric growth indicator based on detection of metabolic activity. Specifically, the oxidation-reduction indicator resazurin is a proven cell viability indicator that emits fluorescence and changes color in response to chemical reduction in resorufin of growth medium resulting from cell growth (62). Moreover, Alamar is not cytotoxic allowing monitoring of cell growth of the same cell cultures over time. At the day of the evaluation cells were incubated with Alamar Blue (1:10 dilution in MEM α) for 4 hours at 37 °C in the dark. Then, supernatants were transferred to black-bottom 96-well plates and emitted fluorescence was read with an Enspire plate reader (Perkin Elmer, USA).

4.3.6 RNA reverse transcription

The RNeasy Mini Kit (Qiagen, Hilden, Germany) was used according to manufacturer's instructions for total RNA extraction from ASCs at 1, 3, 7 and 14 days of differentiation. Then, the quantification of extracted RNA was determined spectrophotometrically for each sample with a Jenway Genova spectrophotometer (Bibby Scientific Limited, United Kingdom). Finally, reverse transcription of RNA in the respective cDNA was performed using a Maxima H Minus First Strand cDNA Synthesis Kit (Thermo Scientific, USA) with oligodT and random hexamer primers according to manufacturer's instructions. The resulting cDNA was diluted to a final concentration of 5 ng/ μ l and then stored at -80°C until use.

4.3.7 Quantitative Real-Time Polymerase Chain Reaction

Quantitative real-time polymerase chain reaction (qPCR) analysis was performed by SYBR Green technology based on the principle that fluorescence can be measured at the end of each amplification cycle for relative or absolute

quantification of DNA content. The fluorescent dye binds the double-stranded DNA molecules. Reactions were set up for 10 ng of cDNA in a final volume of 20 μ l in a 96-well plate (Bio-Rad, Hercules, USA) and processed in a CFX Connect Real Time PCR Detection System (Bio-Rad, Hercules, USA). The PCR master mix consisting in 1 x SsoAdvanced SYBR Green Supermix (Bio-Rad, Hercules, USA), 250 nM forward primer, 250 nM reverse primer, up to 20 μ l with nuclease-free water. Primers were designed by primer-BLAST (NCBI, USA), within the sequences of a panel of genes (SCX, TNC, DCN, COMP, COL1A1, COL3A1, MMP3, MMP13, TIMP2, KLF4, NANOG, Ki67, PCNA), on an exon-exon junction in order to prevent genomic DNA amplification. To analyze the relative expression of different genes, three housekeeping genes were chosen (GAPDH, GUSB and YWHAZ) and the geometric mean of their Ct values was calculated. A negative sample (without cDNA) was used to verify the absence of nucleic acid contaminations. A cDNA sample composed of a mix of various cell extracts, calibrator (CAL), was run of every 96-well plate to normalize each gene expression level. Thermocycler chain reaction consisted of an initial hot start cycle at 95 °C for 30 seconds followed by 45 amplification cycles resulting in a denaturation step at 95 °C for 10 seconds and an annealing-extension phase at 60 °C for 30 seconds. For melt-curve evaluation at the end of the analysis, the temperature was raised from 65 °C to 95 °C at rate of 0.5 °C every 5 seconds. For all samples, reactions were performed in duplicate. The Ct values were recorded with a threshold of 3000 relative fluorescence units and the relative gene expression was defined as $2^{-\Delta Ct}$. Results are expressed as average \pm standard deviation relative to CAL expression. Primers used in this work are listed in Table 4.1.

Table 4.1. Primers used in this study.

Gene Name	Sequence 5'-3'	Type	Amplicon length (bp)	Accession number
<i>GAPDH</i>	5:TTCGTCATGGGTGTGAACCA	Housekeeping	142	NM_002046.3
	3:CTGTGGTCATGATGAGTCCTTCCA			
<i>GUSB</i>	5:CTCATTGGAAATTTGCCGAATTTT	Housekeeping	81	NM_000181.3
	3:CCGAGTGAAGATCCCTTTTTA			
<i>YWHAZ</i>	5:TGGCTCGAGAATACAGAGAG	Housekeeping	99	NM_001135699
	3:GTGAAGCATTGGGGATCAAG			
<i>SCX</i>	5: CAGCGGCACACGGCGAAC	Tendon	163	BK000280
	3: CGTTGCCAGGTGCGAGATG			
<i>TNC</i>	5:CCACAATGGCAGATCCTTCT	Tendon	118	NM_002160
	3: GTTAACGCCCTGACTGTGGT			
<i>DCN</i>	5:CTCTGCTGTTGACAATGGCTCTCT	Tendon	256	NM_001920
	3:TGGATGGCTGTATCTCCAGTACT			
<i>COMP</i>	5:AGAAGTCCTATCGTTGGTTCC	Tendon	104	NM_000095
	3: CAAGACCACGTTGCTGTC			
<i>COL1A1</i>	5:CCAGAAGAACTGGTACATCAGCAA	Tendon	70	NM_000088.3
	3: CGCATACTCGAACTGGAATC			
<i>COL3A1</i>	5:GGGAACATCCTCCTTCAACA	Tendon	183	NM_000090.3
	3:GCAGGGAACAACCTTGATGGT			
<i>MMP3</i>	5:CTGTTGATTCTGCTGTTGAG	Tendon	126	NM_002422.4
	3:AAGTCTCCATGTTCTCTAACTG			
<i>MMP13</i>	5: AAGACTTCCAGGAATTGGTGA	Tendon	126	NM_002427.4
	3: GGCATGACGCGAACAATACG			
<i>TIMP2</i>	5: ATCTCATTGCAGGAAAGCCG	Tendon	103	NM_003255.4
	3: AGGCTCTTCTTCTGGGTGGT			
<i>KLF4</i>	5: AAGAGTCCCATCTCAAGGCACA	Stemness	90	NM_001314052 .1
	3: GGGCGAATTTCCATCCACAG			
<i>NANOG</i>	5: CAACTGGCCGAAGAATAGCAATG	Stemness	110	NM_001297698 .1
	3: TGGTTGCTCCAGGTTGAATTGTT			
<i>Ki67</i>	5: AGCAAGCACTTTGGAGAGCA	Proliferation	89	NM_001145966 .1
	3: CATTGCTCAGCCTTCTTTGG			
<i>PCNA</i>	5: GTAGTAAAGATGCCTTCTGGTG	Proliferation	189	NM_002592.2
	3: TCTCTATGGTAACAGCTTCTC			

Abbreviations: F, Forward Primer; R, Reverse Primer

4.3.8 Immunofluorescence staining

To assess the expression of the transcription factor scleraxis, P4 hPL- and SF-ASCs were plated at a cell density of 3×10^3 cells/cm² on 22 mm pre-coated collagen I German Glass coverslip (Corning) and then induced toward tenogenic lineage as described before. For immunofluorescence staining, cells at 3 days of differentiation were fixed with 4% paraformaldehyde in PBS. After washing (3X) in PBS, permeabilization of the membranes was performed with 0.5% Triton X-100 in PBS-tween (PBST) and the unspecific binding blocked with bovine serum albumin (BSA from Sigma Aldrich). Immunostaining using 1:100 goat anti-human scleraxis (sc-87425, Santa Cruz Biotechnology) was performed overnight at 4 °C. Samples were incubated with the secondary antibody using 1:1000 Alexa Fluor 488 rabbit anti-goat IgG (Invitrogen) for 1 hour at room temperature; then, cell nuclei were counterstained with DAPI (BDBioscience). Finally, immunostained samples were observed and photographed under a fluorescence microscope (Zeiss Axiophot).

4.3.9 Sirius Red staining

Sirius red staining was performed to visualize the total collagen production after 7 days of differentiation in undifferentiated and differentiated cells previously seeded in collagen I coated 24-well plates (Corning) at a cell density of 3×10^3 cells/cm². At the day of the experiment, each sample was fixed in Bouin's solution (Bouin's Fixative, Electron Microscopy Sciences, USA) for 1 hour and collagen fibers were stained with 0.1% Sirius Red saturated in picric acid (Sigma). To visualize collagen matrix deposition under polarized light microscopy (63).

4.3.10 Statistical Analysis

Data were expressed as means \pm standard deviation (sd). The normal distribution of values was assessed by the Kolmogorov–Smirnov normality test. Statistical analyses were performed using the Student's t-test for data with a normal distribution and the Wilcoxon test for data with a non-normal distribution (GraphPad Prism v7.00; GraphPad Software, USA) (20).

4.4 Results and Discussion

4.4.1 Human ASCs features in xenogenic-free media

ASCs were isolated from 4 healthy female donors after liposuction of the subcutaneous adipose tissue with a cellular yield of $2.9 \pm 1.5 \times 10^5$ ASCs per ml of raw adipose tissue. Isolated ASCs at passage 4 were placed in flasks coated with collagen type I, the most abundant ECM component of tendon, and cultured with xenogenic-free and serum-free hPL or SF medium. As depicted in Figure 4.3, cells appeared viable and with the typical fibroblastic-like morphology similarly to ASCs cultured in the standard medium condition (SC-ASCs) consisting in MEM-alpha supplemented with 10% FBS. According to the International Society for Cell Therapy (ISCT) standards, the expression of typical MSCs superficial markers was also evaluated (21,32). Both hPL-ASCs and SF-ASCs expressed a typical MSC immunophenotype profile. They resulted negative (< 5%) for the endothelial marker CD31 and the hematopoietic antigen CD45, whilst a high percentage of cells (> 95%) expressed antigens CD105, CD90 and CD73, as well as the stromal markers CD13 and CD44 with no statistical significant differences due to the culture conditions (Fig. 4.4). These findings were in accordance with previous studies which reported that ASCs cultured in serum-free medium maintained the surface marker expression profile characteristic of MSCs (64,65).

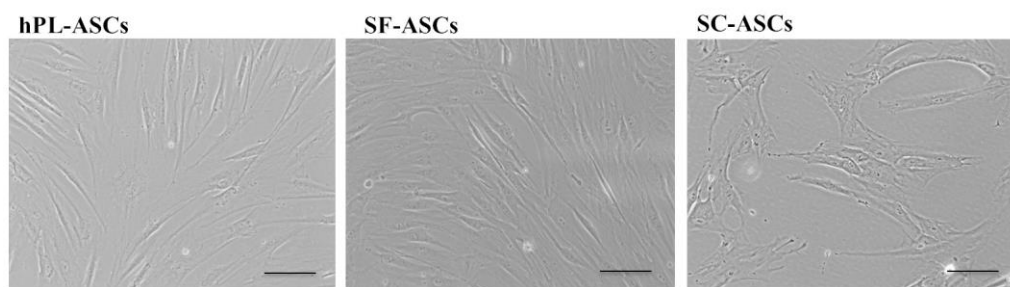
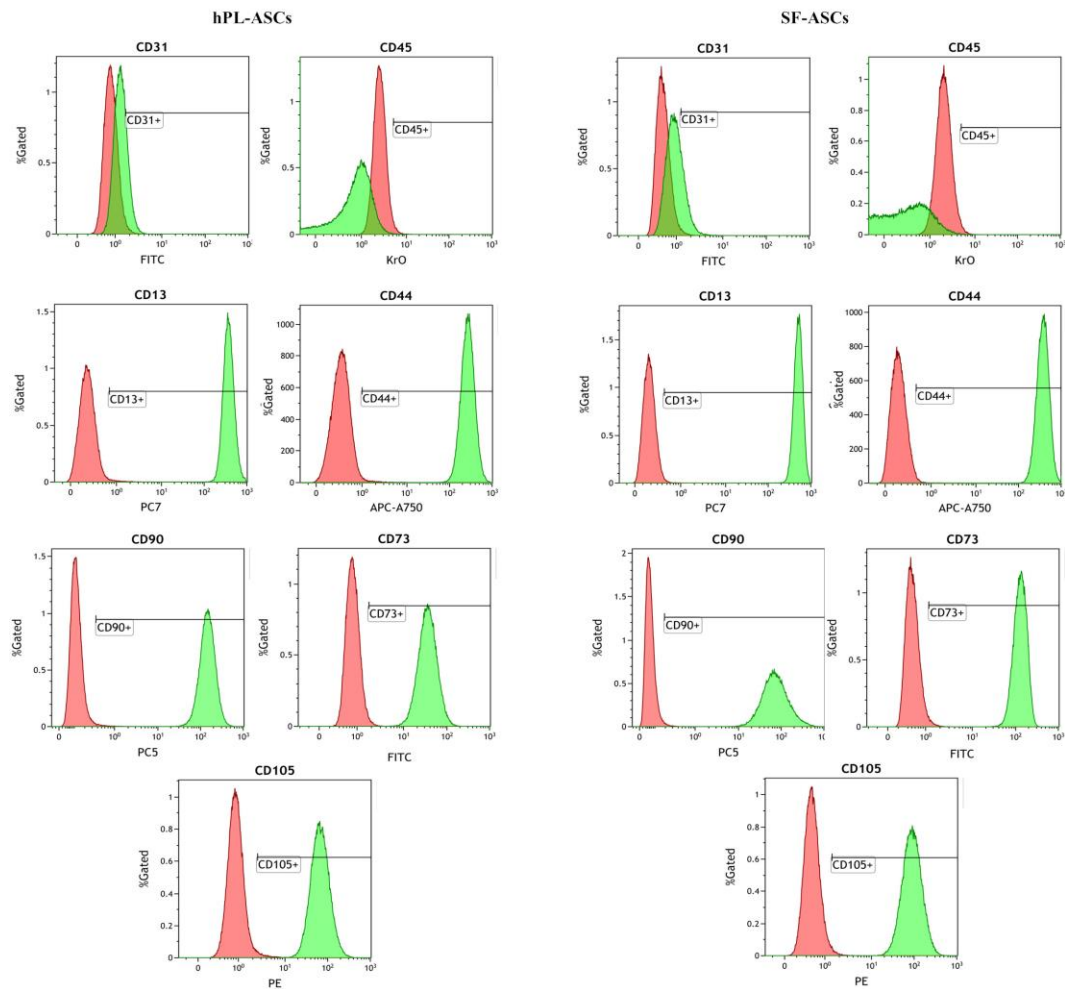


Figure 4.3. Morphological appearance.

Representative micrographs of ASCs at passage 4 cultured in hPL and SF media (hPL-ASCs and SF-ASCs) in comparison with ASCs cultured in standard laboratory condition (SC-ASCs) consisting in MEM-alpha as growth medium supplemented with 10% FBS provided by Sigma Aldrich (optical microscopy: 10X; scale bar 200 μ m).



Percentage of positive cells by FACS analysis for specific MSC markers

	CD31	CD45	CD13	CD44	CD90	CD73	CD105
hPL-ASCs	15.3±6.6%	0.2±0.1%	100.0±0.0%	100.0±0.0%	99.9±0.1%	99.9±0.0%	99.9±0.1%
SF-ASCs	15.5±7.9%	0.4±0.2%	100.0±0.0%	100.0±0.0%	100.0±0.1%	99.9±0.0%	99.9±0.0%

Figure 4.4. Immunophenotype profile of hPL-ASCs and SF-ASCs

FACS analysis illustrating the percentage of hPL-ASCs and SF-ASCs cells negative for the endothelial marker CD31 and the hematopoietic antigen CD45 and positive for the typical mesenchymal stem cell surface markers CD13, CD44, CD90, CD73 and CD105 (red: isotypic control, green: ASCs); table reports the quantification of the above depicted markers expressed as mean ± sd (n=4).

In order to investigate the impact of both serum-free and tenogenic cell culture conditions on cell behavior, morphological and cellular viability analyses were then performed. First of all, as shown in Figure 4.5, CTRL and TENO hPL-ASCs and SF-ASCs appeared viable and elongated with the typical fibroblastic-like shape morphology at 3 days of cell culture and then tenogenic induction did not induce any sign of suffering at the cellular level on both hPL-TENO and SF-TENO ASCs. Moreover, these cells, showed slight appearance differences already

at 3 days of differentiation, with a more rounded shape and higher cytoplasmic content in comparison to the respective undifferentiated control cells.

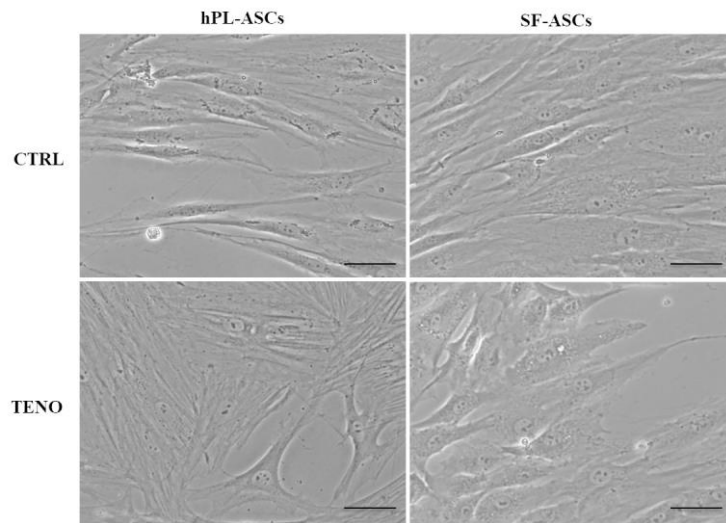


Figure 4.5. Cell morphological appearance during tenogenic induction compared to undifferentiated cells cultured in CTRL conditions.

Representative micrographs of CTRL and TENO hPL-ASCs and SF-ASCs at 3 days of cell culture (optical microscopy 20x; scale bar 200 μ m).

In accordance with these qualitative observations, the percentage of viable cells was very high ($> 85\%$) in all culture conditions at all the investigated time points, with no significant differences (Fig. 4.6 A). Surprisingly, cells cultured in SF-CTRL were characterized by higher metabolic activity and proliferation ability respect to hPL-cultured cells (Fig. 4.6 B). Indeed, cell viability in SF-CTRL cell culture conditions showed increases of $+105\%$ ($p<0.05$) and $+169\%$ ($p<0.01$) in comparison to what observed in hPL-CTRL cells at 7 and 14 days, respectively. Furthermore, media supplementation with AA, BMP-12, CTGF and TGF- β 3 soluble factors induced increases on cell viability of both TENO hPL-ASCs and SF-ASCs in comparison to the CTRL conditions. In detail, both TENO hPL-ASCs and SF-ASCs showed increases in cell viability of $+60\%$ ($p<0.01$) compared to their respective CTRLs, without any significant difference between the two investigated serum free media. All these results demonstrated the success of culturing ASCs on a biocompatible surface coated with collagen type I molecules in the presence of a unique xenogenic- and serum-free culture medium (SF) or in hPL supplemented medium. Indeed, cells showed the peculiar features of progenitor cells including the typical fibroblastic spindle-like morphology and the

stem cell markers expression in accordance with the minimal criteria for defining multipotent MSCs (21).

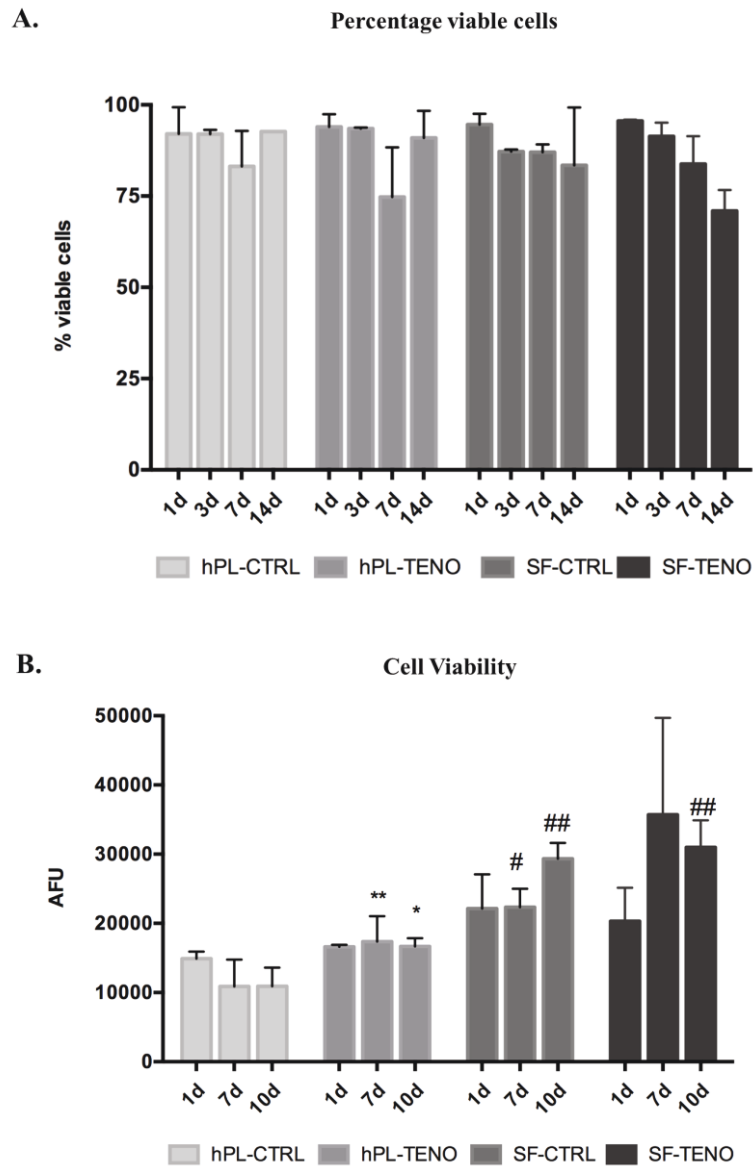


Figure 4.6. Cell Viability.

A. Percentage of viable hPL- and SF-ASCs at passage 4 cultured in CTRL and TENO conditions for 1, 3, 7 and 14 days (n=3). Data were expressed as average \pm standard deviation of percentage of viable cells. **B.** Cell viability of hPL- and SF-ASCs cultured in CTRL and TENO conditions at 1, 7 and 10 days of cell cultured (n=3). Data were expressed as average \pm standard deviation of arbitrary fluorescence units (AFU). * $p < 0.05$, ** $p < 0.01$ for TENO vs CTRL cells; # $p < 0.05$, ## $p < 0.01$ for hPL-ASCs vs SF-ASCs.

In order to thoroughly investigate the influence of culture conditions on cell proliferation and on the differentiate state of cells, gene expression of Ki67, proliferating cell nuclear antigen (PCNA), embryonic stem cell markers Kruppel-like factor 4 (KLF4), octamer-binding transcription factor 4 (OCT4) and NANOG, was evaluated (Fig 4.7 and Fig 4.8).

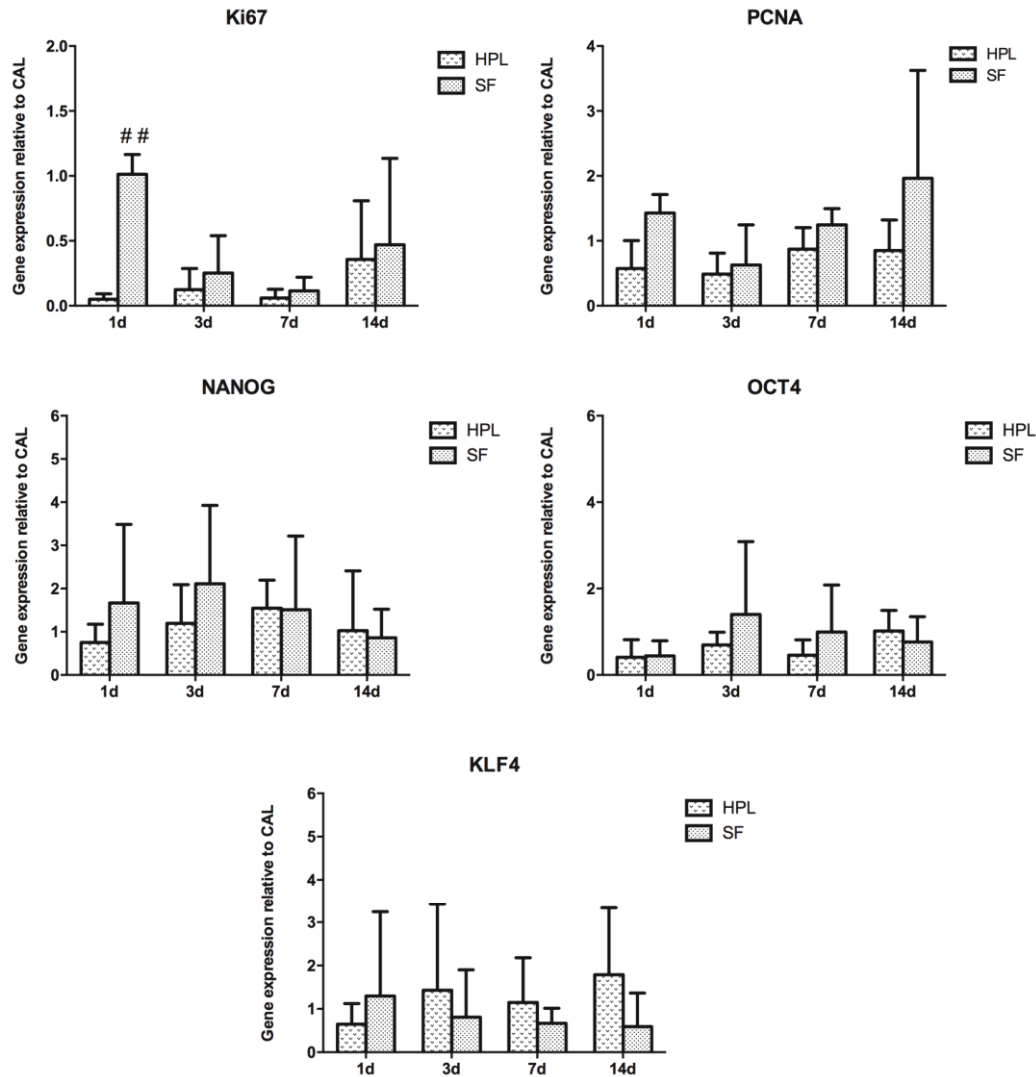


Figure 4.7. Gene expression of cell proliferation and embryonic stem cell markers in control media conditions

Relative gene expression of Ki67, PCNA, NANOG, OCT4, KLF4 in hPL- and SF-cultured ASCs at 1, 3, 7 and 14 days of cell culture (n=4). The housekeeping GAPDH, GUSB and YWHAZ genes were used for data normalization expressed as relative to the calibrator (CAL). ## p<0.01 for hPL-ASCs vs SF-ASCs.

The level of mRNA of Ki67 observed in SF-ASCs (SF-CTRL) at day 1 was 2-fold higher respect to hPL-ASCs (hPL-CTRL) (p<0.01, Fig 4.7). Concerning the expression of PCNA, NANOG, OCT4 and KLF4 genes, no significant differences were observed between hPL-CTRL and SF-CTRL media at all time points (Fig 4.7). After tenogenic induction, the expression of both Ki67 and PCNA were up-regulated already at early time points in both hPL-TENO and SF-TENO with respect to their corresponding CTRLs. Nevertheless, these differences were not statistically significant, probably due to the high inter-donor variability (Fig 4.8).

In particular, TENO differentiated ASCs in hPL medium showed the highest levels of Ki67 at 3 days with fold change increases versus CTRL of 6.5 ± 3.1 , whilst at the same time point the expression of PCNA was higher in TENO-SF ASCs in comparison to CTRL (Fig 4.8B). Concerning the expression of stem cell markers, KLF4 levels were significantly decreased at all the investigated time points with the minimum observed at 3 days in both hPL-TENO (3d: -0.94; $p < 0.05$) and SF-TENO (3d: -0.87) ASCs with respect to CTRL cells and with no significant differences induced by the kind of xeno-free medium used to culture the cells (Fig 4.8). On the other hand, the expression of OCT4 and NANOG was similar in TENO- and CTRL-cultured cells and without any significant difference between hPL and SF cell culture media (Fig 4.8). These data demonstrate the feasibility of the chemically defined SF medium to sustain ASC growth in culture and to maintain their MSCs characteristics *in vitro*. Indeed, both hPL-ASCs and SF-ASCs exhibited a specific MSC immunophenotype profile and expressed the transcription factors which are essential for the maintenance of self-renewal potential and pluripotency in embryonic stem cells, such as KLF4, OCT4 and NANOG (21,66). Moreover, the further tenogenic induction did not negatively affect ASC viability during the culture.

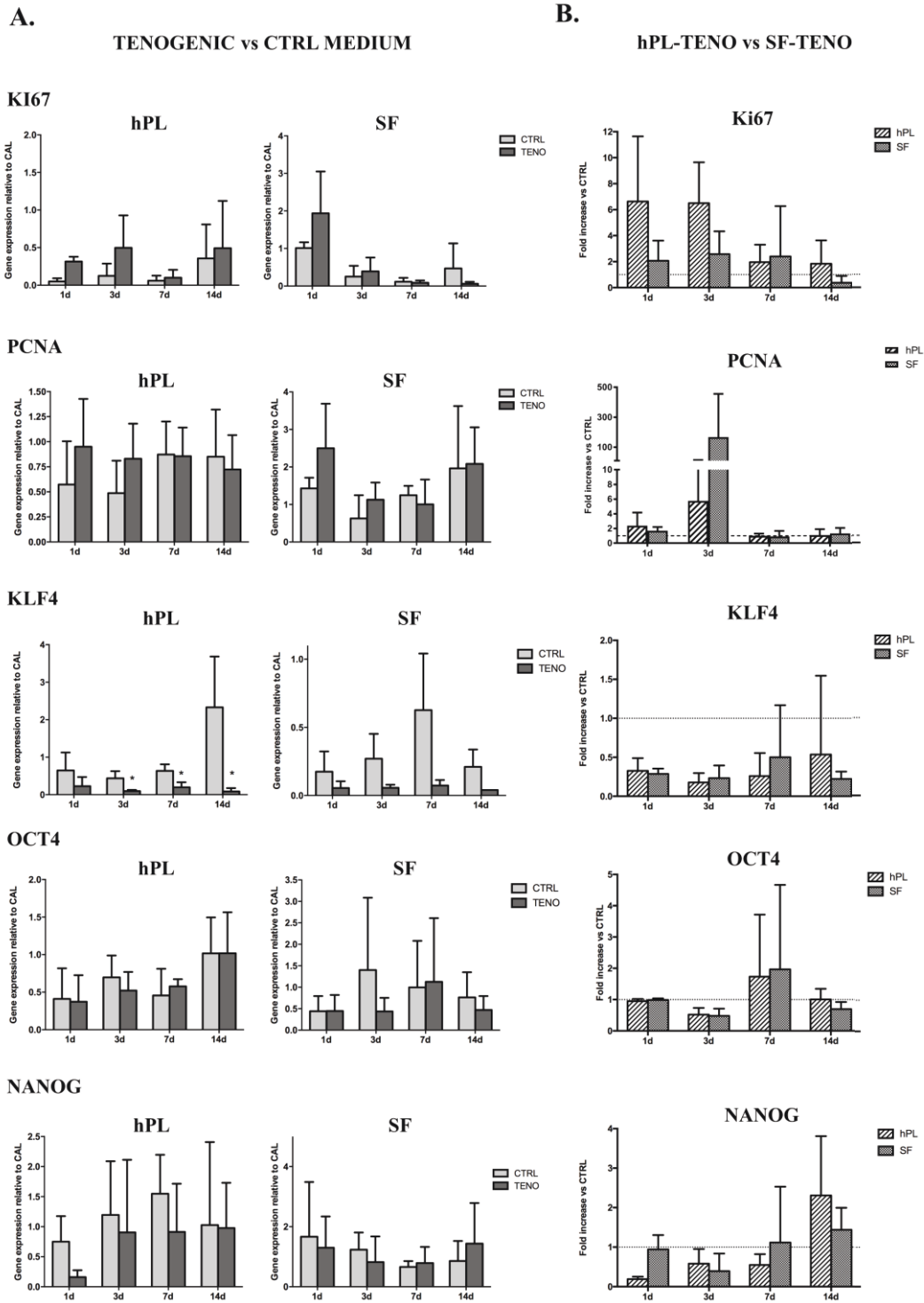


Figure 4.8. Gene expression of cell proliferation and embryonic stem cell markers after tenogenic differentiation and in CTRL cell culture conditions.

(A) Effect of tenogenic induction on Ki67, PCNA, OCT4, KLF4 and NANOG gene expression in hPL- and SF-ASCs cultured in CTRL and TENO conditions at 1, 3, 7 and 14 days of cell culture (n=4). Data were normalized against the expression of the housekeeping GAPDH, GUSB and YWHAZ genes and expressed as relative to the calibrator (CAL). * p<0.05 for TENO vs CTRL cells. (B) Normalized values of hPL-TENO and SF-TENO to their corresponding CTRL. Data expressed as average fold increase \pm standard deviation compared with the respective CTRL cells (dashed line means equal).

4.4.2 Evaluation of SCX, COL1A1, COL3A1, COMP and MMPs gene expression in SF-TENO and hPL-TENO ASCs

Biochemical induction was performed for 14 days using ascorbic acid, BMP-12, CTGF and TGF- β 3 growth factors known to be naturally involved in the early phases of tendon genesis and during tissue repair. Moreover, both CTRL and TENO ASCs were cultured on flasks coated with collagen type I, with the aim to replicate *in vitro* the physiological ECM cues typical of tendon microenvironment. ASC differentiative potential was evaluated by monitoring the relative gene expression of markers of tendon development pathway (e.g., SCX), and of tendon and extracellular matrix related genes (e.g., DCN, TNC, COL1A1, COL3A1, COMP, the metalloproteinases MMP-3 and MMP-13 and the tissue inhibitor protein TIMP-2) at 1, 3, 7 and 14 days of cell culture. The extracellular matrix (ECM) microenvironment is essential for stem cells maintenance and normal tissue development and homeostasis. In tendons, ECM is mainly composed by collagen type I and III and in minor percentage of elastin embedded in a proteoglycan-water matrix, proteoglycans, glycosaminoglycans and structural glycoproteins (40). Tendon architecture comprises few cells, namely tenocytes and a small niche of tendon-derived stem cells interspersed within the ECM, responsible for maintaining tissue homeostasis and collagen molecules synthesis (8, 41). Metalloproteinase (MMP) enzymes have an important role in tendon matrix remodelling, being responsible for the degradation of collagen and proteoglycans, including secreted collagenases (i.e., MMP13) and stromelysins (i.e., MMP-3) which enzymatic activity is balanced by the tissue inhibitors of metalloproteinases (TIMPs) (1, 2).

As shown in Figure 4.9A, TENO differentiated hPL- and SF-ASCs exhibited statistically significant increases of 2.7 and 5.3 times ($p < 0.05$) respectively, in the mRNA level of SCX already after 1 day of differentiation, in comparison to CTRL-cultured cells. This trend was maintained over time in both hPL- and SF-TENO ASCs with fold increases of 6.4 and 3.5 at 3 days ($p < 0.01$), 10.0 and 1.7 at 7 days ($p < 0.05$) and 11.7 and 1.6 at 14 days ($p < 0.05$), respectively, in comparison with CTRL-cultured cells. In particular, a time-dependent SCX up-regulation was observed in hPL-TENO that at 14 days cell culture showed a 21-fold change increase, which turned to be significantly higher than what observed in SF-TENO at the same time point ($p < 0.05$) (Fig. 4.9B). The same Figure also report the

expression of the later markers of tenogenic differentiation tenascin-C (TNC) and decorin (DCN), a proteoglycan involved in collagen type I and III fibrils organization (Fig. 4.9A, 4.8B). However, only slight but not significant increases in their expression were observed in TENO-differentiated ASC populations compared to CTRL-cultured cells (Fig. 4.9A, 4.9B). In this regard, Goncalves et al reported that the up-regulation of these genes started from 21 days of human ASC differentiation *in vitro* in a cell culture medium supplemented with EGF and bFGF growth factors (49). Hence, in the present study, despite the different composition of the differentiative medium, 14 days of differentiation could be not enough to drive TNC and DCN gene expression.

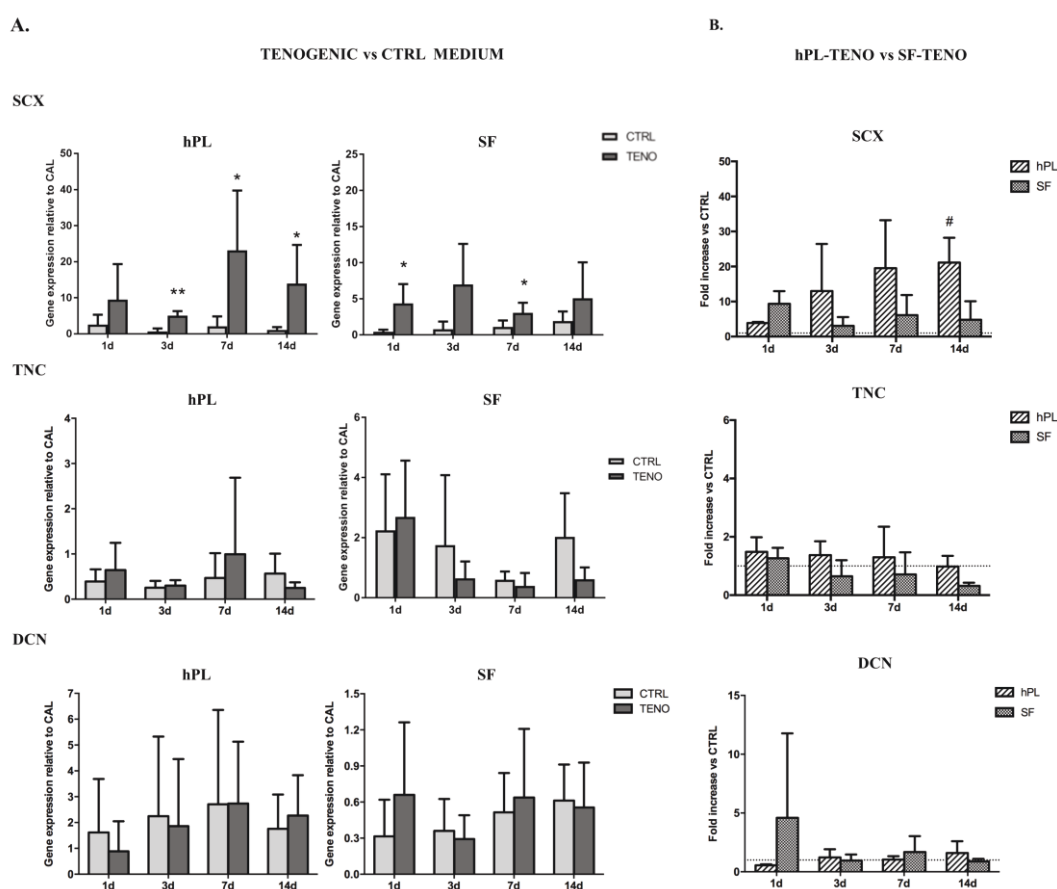


Figure 4.9. Scleraxis, tenascin-C and decorin expression.

A. SCX, TNC and DCN gene expression in hPL- and SF-ASCs cultured in CTRL and TENO conditions at 1, 3, 7 and 14 days of cell culture (n=4). Data normalized against housekeeping GAPDH, GUSB and YWHAZ gene expression and expressed as relative to the calibrator (CAL). * $p < 0.05$, ** $p < 0.01$ for TENO vs CTRL cells. B. Comparison in gene expression between hPL-TENO and SF-TENO. Data were expressed as average fold increase \pm standard deviation compared to the respective CTRL cells (dashed line set at 1). # $p < 0.05$ for hPL vs SF.

Interestingly, levels of collagen type I and III mRNA were significantly higher after culture in tenogenic media in both hPL and SF conditions, in comparison with undifferentiated CTRL cells (Fig. 4.10A, 4.10B). Similarly to SCX expression, a time-dependent up-regulation of COL1A1 and COL3A1 was observed in hPL-TENO ASCs with a maximum peak at 14 days and statistically significant ($p < 0.05$) fold increases of 4.4 and 3.1 compared to hPL-CTRL ASCs (Fig. 4.10A). On the other hand, SF-TENO ASCs showed higher increases of these markers already at day 1 compared to undifferentiated CTRL cells (fold increases of 1.9 and 1.8 for COL1A1 and COL3A1, respectively). COL1A1 over-expression was then maintained until 14 days when SF-TENO showed a significant 1-fold increase ($p < 0.05$) relative to CTRL cells. On the other hand, at the same time point, COL3A1 levels resulted similar to what observed in CTRL cells. As shown in Figure 4.10B, COL1A1 expression did not show significant differences between hPL-TENO and SF-TENO over time, with the exception of 7 days of tenogenic induction ($p < 0.05$). Tenogenic induction in both xeno-free conditions was able to induce also a strong time-dependent up-regulation of the gene encoding for another ECM protein, i.e., the cartilage oligomeric matrix protein (COMP). Indeed, starting from 1 day of differentiation, both hPL-TENO and SF-TENO showed a 17.9 ($p < 0.05$) and 24.0-fold increase, respectively, in COMP expression compared to CTRL cells, reaching a 99.0 and 31.8 fold increase respectively at day 14 of differentiation (Fig. 4.9 A). Moreover, the fold change increases observed at all time points in hPL-TENO seemed to be higher with respect to what observed in SF-TENO, although this differences were not statistically significant (Fig. 4.10B). Previous other reports indicated a positive correlation between COMP expression *in vivo* and the healthy tendon healing (67,68). In addition, COMP involvement as enhancer of the kinetics of collagen fibrillogenesis has been also demonstrated (67,68). For this reason, the here observed up-regulation of COMP at the gene level during ASC differentiation could be relevant *in vivo* and clinically beneficial for tendon recovery.

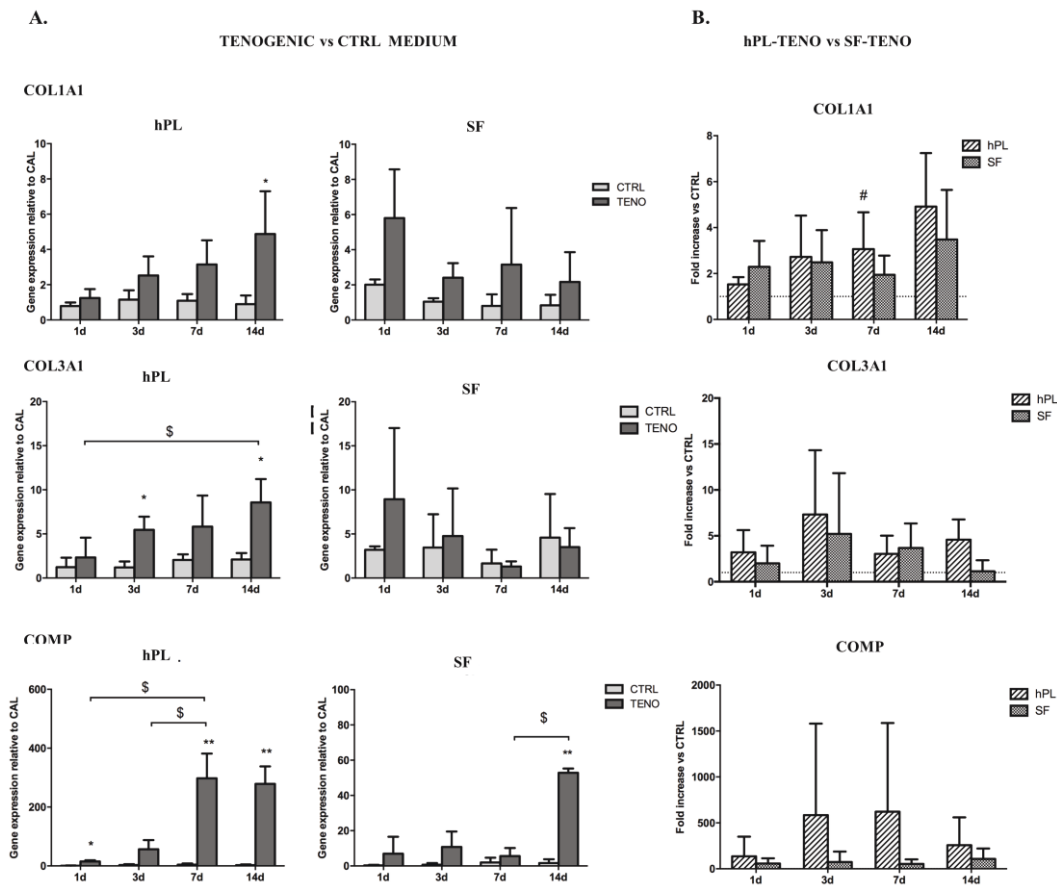


Figure 4.10. Collagen type I, type III and COMP gene expression.

A. COL1A1, COL3A1 and COMP gene expression in hPL- and SF-ASCs cultured in CTRL and TENO conditions at 1, 3, 7 and 14 days of cell culture (n=4). Data were normalized against the expression of the housekeeping GAPDH, GUSB and YWHAZ genes and expressed as relative to the calibrator (CAL). * $p < 0.05$, ** $p < 0.01$ for TENO vs CTRL cells; \$ $p < 0.05$ for differences between time-points. (B) Comparison of COL1A1, COL3A1 and COMP gene expression in hPL-TENO and SF-TENO ASCs. Data are expressed as average fold increase \pm standard deviation compared to the respective CTRL cells (dashed line set at 1). # $p < 0.05$ for hPL versus SF.

Finally, the expression of the matrix remodeling proteins MMP-3, MMP-13 and TIMP-2 was evaluated in all ASC cultures and reported in Figure 4.11. Levels of MMP-3 mRNA were significantly higher in hPL-TENO ASCs compared to hPL-CTRL cells, with 2.1 and 4.4 fold increases after day 1 and 3 of differentiation, respectively. Differently, SF-TENO ASCs exhibited fold increases of 8.6 ($p < 0.05$) and 27.6 ($p < 0.05$) in MMP-3 expression with respect to SF-CTRL ASCs, at 7 and 14 days cell culture, respectively (Fig. 4.11A). Moreover, the over-expression of MMP-3 measured in SF-TENO ASCs at 14 days of differentiation was also significantly higher ($p < 0.05$) with respect to what observed in hPL-TENO ASCs (Fig. 4.11B). Concurrently, a statistically significant over-expression of MMP-13 gene was observed in both hPL-TENO and SF-TENO ASCs starting from 3 days of differentiation, in comparison to CTRL cells ($p < 0.05$) (Fig. 4.11A). In this case, hPL-TENO ASCs showed higher fold change increases in MMP-13 gene

expression levels compared to SF-TENO ASCs (Fig. 4.11B). Moreover, TIMP-2 gene expression was up-regulated only in differentiated hPL cells, showing a slight fold increase at 7 days (0.6) and 14 days (0.4) in comparison to CTRL cells, even if these differences were not statistically significant (Fig. 4.11A, 4.11B).

Overall these results demonstrated the efficiency of these investigated tenogenic media to positively drive prompt increases of the transcription factor scleraxis as well as strong over-expression of the others tendon-related markers COL1A1, COL3A1, COMP, MMP3 and MMP13 in ASCs.

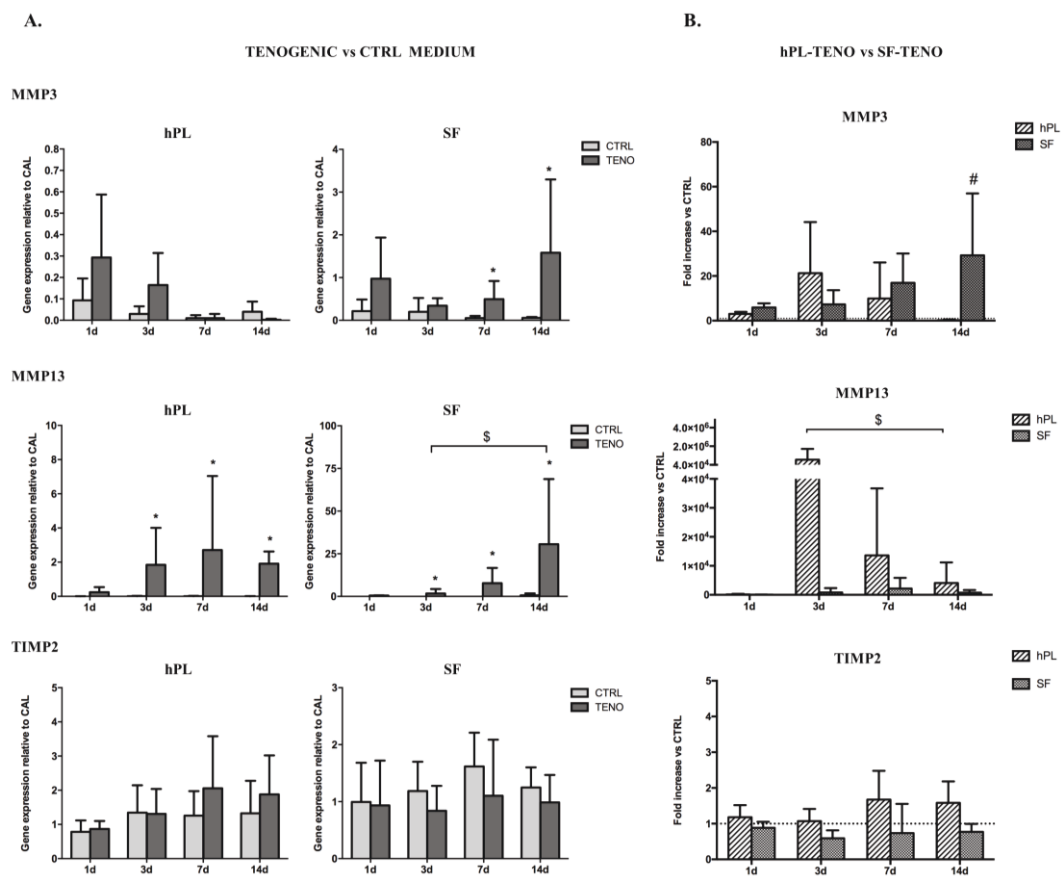


Figure 4.11. MMP3, MMP13 and TIMP2 gene expression.

(A) MMP3, MMP13 and TIMP2 gene expression in hPL- and SF-ASCs cultured in CTRL and TENO conditions at 1, 3, 7 and 14 days of cell culture (n=4). Data were normalized against the expression of the housekeeping GAPDH, GUSB and YWHAZ genes and expressed as relative to the calibrator (CAL). * $p < 0.05$ for TENO vs CTRL cells; \$ $p < 0.05$ for differences between time-points. (B) Comparison in MMP3, MMP13 and TIMP2 gene expression between hPL-TENO and SF-TENO ASCs. Data expressed as average fold increase \pm standard deviation compared with the respective CTRL cells (dashed line set at 1). # $p < 0.05$ for hPL vs SF.

4.4.3 Collagen matrix deposition and expression of scleraxis and tenomodulin

Beside the observation of the unique gene expression profile exhibited by TENO-differentiated ASCs, the specific protein expression of important tendon-related markers was also evaluated in order to determine a functional activity of the cells. In particular, staining of scleraxis, collagen and tenomodulin was performed. Since the early mRNA up-regulation shown before, scleraxis expression was observed already at day 3 of TENO-induction in both hPL- and SF-ASCs. Figure 4.12 reports the positive immunofluorescence staining of scleraxis (green) resulting specifically only in teno-induced cells. Confirming this cell behavior, after 7 days of differentiation with tenogenic medium, cells were able to produce massive collagen matrix depots in both hPL and SF media (Fig. 4.12).

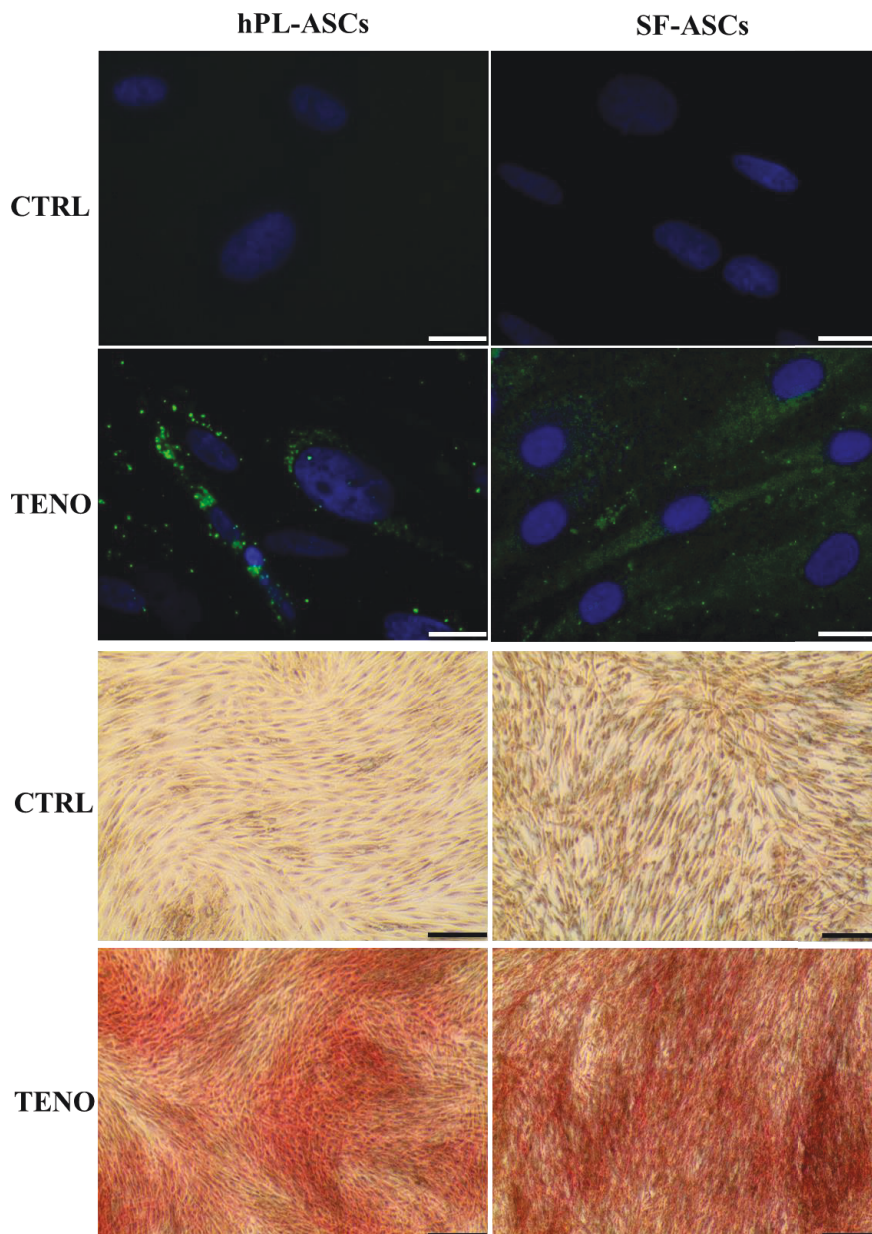


Figure 4.12. Scleraxis expression and collagen matrix deposition after tenogenic differentiation.

Upper four panels show representative micrographs of scleraxis immunostaining visualized as green in CTRL- and TENO-cultured cells at 3 days of cell culture (the nuclei were stained with DAPI, blue) captured by fluorescence microscope (40x; scale bar 20 μm). Four panels on the bottom show representative images of collagen matrix deposition after staining with Sirius Red (10x; scale bar 100 μm) evaluated at 7 days of hPL- and SF-ASCs culture in CTRL and TENO conditions.

During the early stage of tendon development, scleraxis expression is crucial to drive the tendon/ligament primordium formation and then the presence of tenomodulin (TNMD) expression allows maturation of tendons and ligaments (44,69). In particular, tenomodulin is a type II transmembrane glycoprotein responsible for the regulation of the proliferation of mature differentiated tenocytes as well as of matrix organization (44). Importantly, Jiang et al observed

enhancement of cell proliferation, tendon-related marker gene expression and novel tendon-like tissue formation after overexpression of tenomodulin in murine mesenchymal stem cells both *in vitro* and *in vivo* (70). In a recent work (published after this study) sorted TNMD-positive hASCs showed a more prominent expression of tendon-related markers when cultured in a tenogenic media containing TGF- β 3 or GDF-5 (BMP-12) growth factors in comparison with unsorted cells (71). In accordance with these reports, the protein expression on cell surface of tenomodulin was evaluated by cytofluorimetric analysis in both differentiated and undifferentiated hPL- and SF-ASCs at 7 and 14 days of culture (Fig. 4.13). Interestingly, a very low percentage of undifferentiated cells was positive for TNMD staining at both 7 and 14 days of culture, with a similar behavior of hPL-CTRL ($6.0 \pm 2.6\%$) and SF-CTRL ($6.9 \pm 2.9\%$) ASCs. Importantly, differentiated TNMD-positive ASCs showed a 2-fold increase with respect to control at 14 days cell culture. Indeed, culture in the tenogenic media induced evident increases in tenomodulin expression, with no differences between hPL-TENO and SF-TENO ASC populations. Indeed, at 7 and 14 days of differentiation, TNMD-positive hPL-TENO cells were $18.0 \pm 7.3\%$ and $14.4 \pm 13.1\%$, respectively, with an increase of $+66.4\%$ and $+57.0\%$ with respect to what observed in hPL-CTRL at the same time points. The same trend was observed in SF-TENO ASCs that showed significant increases of $+26\%$ and $+58\%$ ($p < 0.05$) in the expression of tenomodulin at 7 and 14 days of differentiation, respectively, in comparison with SF-CTRL cells.

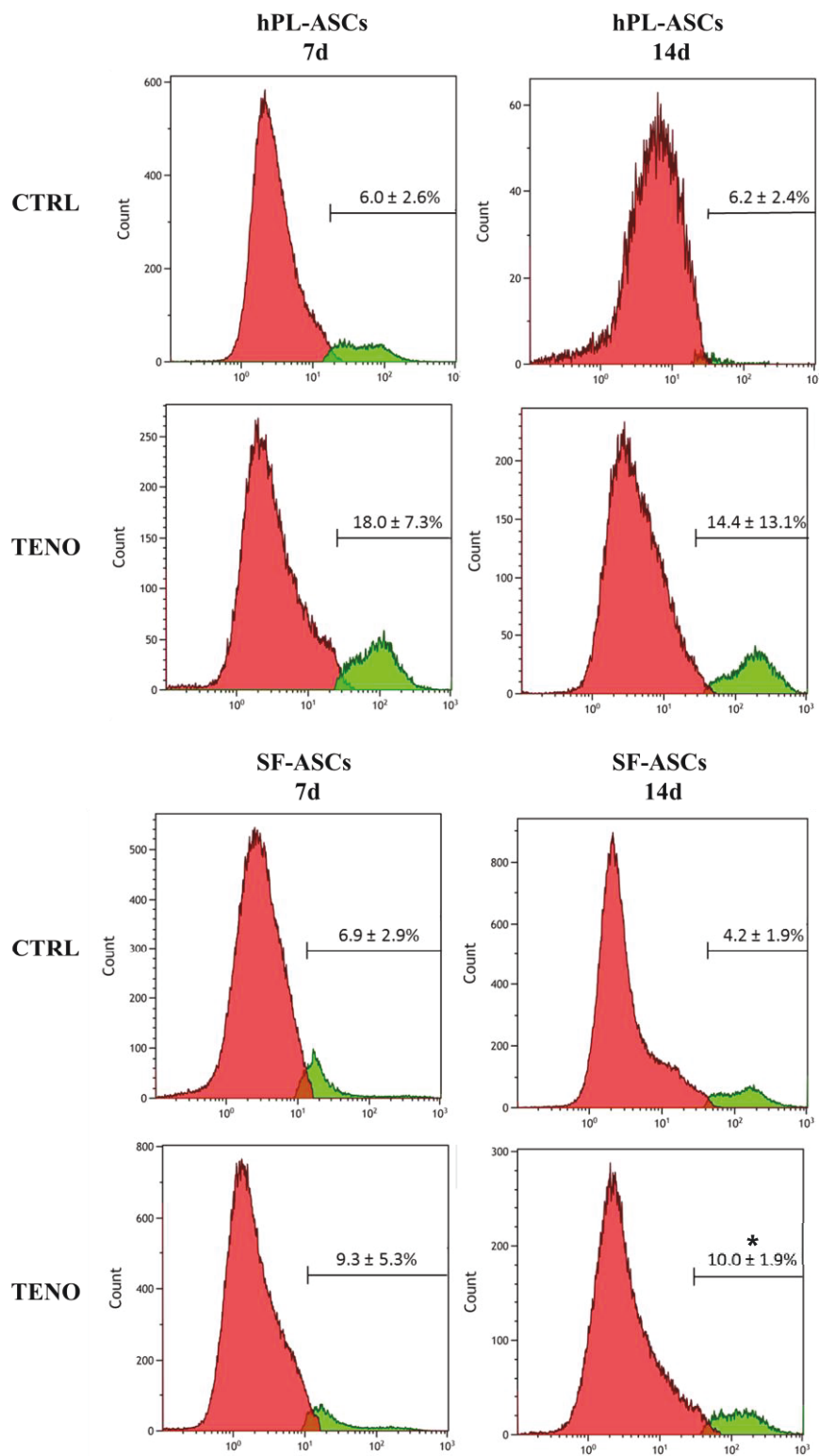


Figure 4.13. Tenomodulin expression on ASC surfaces.

Representative graphs show the percentage of positive (green) and negative (red) subpopulation of hPL-ASCs and SF-ASCs for tenomodulin (TNMD) surface expression at 7 and 14 days of culture in CTRL and TENO media. Data related to three ASC populations are expressed as mean ± standard deviation (n=3). * p<0.05 for TENO vs CTRL cells.

4.5 Conclusions

Regenerative medicine approaches based on the use of patient-derived ASCs have been largely proposed in the last decades as alternative therapies to solve unmet clinical needs, including tendon injuries. For their application in clinical setting some standardization procedure are required to satisfy the safety, efficacy, reproducibility and quality of the procedure. For this reason, a key issue regards the development of a clinical-grade medium for a pre-implant safe and efficient expansion of stem cells. To the best of our knowledge, this was the first study focused on the development of a unique xenogenic and serum free protocol to *in vitro* induce human ASC differentiation toward tenogenic lineage for the translational use in clinic. The GMP compliant approach used in this study has been already published (56) and consisted in the development of a xenogenic and serum-free medium supplemented with a combination of growth factors able to induce the tenogenic differentiation of ASCs *in vitro*. The chemically defined SF medium was suitable to maintain viability and MSC features of ASCs in culture and could be employed in possible future regenerative medicine applications to growth cells *in vitro* in order to obtain the cell number required for their *in vivo* implantation. Moreover, AA, TGF- β 3, BMP-12 and CTGF soluble factors turned out to trigger the differentiation of ASCs toward a tenocyte-like profile in both hPL and SF media. Indeed, they showed significant high gene expression levels of the tendon associated markers SCX, COL1A, COL3A1, COMP, MMP3 and MMP13 in comparison to undifferentiated cells. Confirming these data, TENO-differentiated cells showed also specific protein expression of scleraxis and tenomodulin and produced abundant collagen matrix, i.e., the major ECM constituent of tendon. ASCs cultured in the commercial hPL supplemented medium expressed higher levels of tendon-related marker expression. Contrary to SF medium, that is chemically defined and standardized, the nature of hPL supplementation consisted in a pool of platelet lysates derived from 300 donors. This observation could explain a certain intrinsic lot-to-lot variability of hPL medium and thus the differences observed between hPL-ASCs and SF-hASCs in terms of gene expression profile. Moreover, one limitation of the study is the high

inter-donor variability of ASCs that often represents a critical point when dealing with primary cells.

In conclusion, altogether these results suggested that AA, TGF- β 3, BMP-12 and CTGF soluble factors are involved in tendon development and repair process, eliciting stem cells in their niche and then providing insights of the earliest events of tendon development. Importantly, the demonstration of the suitability of the here-investigated GMP-compliant approach to drive cell differentiation *in vitro* is a crucial step toward the application of ASCs in cell-based therapeutical approaches in the clinics.

4.6 References

1. Maffulli N, Wong J, Almekinders LC. Types and epidemiology of tendinopathy. *Clinics in Sports Medicine*. 2003.
2. Birch HL. Tendon matrix composition and turnover in relation to functional requirements *INTERNATIONAL JOURNAL OF EXPERIMENTAL PATHOLOGY*. *Int J Exp Path*. 2007;
3. Hodgson R, O'Connor PJ, Grainger AJ. Tendon and ligament imaging. *British Journal of Radiology*. 2012.
4. Kannus P. Structure of the tendon connective tissue. *Scand J Med Sci Sport*. 2000;
5. Sharma P, Maffulli N. Biology of tendon injury: Healing, modeling and remodeling. *Journal of Musculoskeletal Neuronal Interactions*. 2006.
6. Stanco D, Viganò M, Perucca Orfei C, Di Giancamillo A, Thiebat G, Peretti G, et al. In vitro characterization of stem/progenitor cells from semitendinosus and gracilis tendons as a possible new tool for cell-based therapy for tendon disorders. *Joints*. 2014;2(4).
7. Bi Y, Ehreichiou D, Kilts TM, Inkson CA, Embree MC, Sonoyama W, et al. Identification of tendon stem/progenitor cells and the role of the extracellular matrix in their niche. *Nat Med*. 2007;
8. Stanco D, Viganò M, Perucca Orfei C, Di Giancamillo A, Peretti GM, Lanfranchi L, et al. Multidifferentiation potential of human mesenchymal stem cells from adipose tissue and hamstring tendons for musculoskeletal cell-based therapy. *Regenerative Medicine*. 2015.
9. Riley G. The pathogenesis of tendinopathy. A molecular perspective. *Rheumatology*. 2004.
10. Riley G. Tendinopathy - From basic science to treatment. *Nature Clinical Practice Rheumatology*. 2008.
11. Yang G, Rothrauff BB, Tuan RS. Tendon and ligament regeneration and repair: Clinical relevance and developmental paradigm. *Birth Defects Research Part C - Embryo Today: Reviews*. 2013.
12. Obaid H, Connell D. Cell therapy in tendon disorders: What is the current evidence? *Am J Sports Med*. 2010;

13. Filardo G, Di Matteo B, Kon E, Merli G, Marcacci M. Platelet-rich plasma in tendon-related disorders: results and indications. *Knee Surgery, Sports Traumatology, Arthroscopy*. 2018.
14. Gaspar D, Spanoudes K, Holladay C, Pandit A, Zeugolis D. Progress in cell-based therapies for tendon repair. *Advanced Drug Delivery Reviews*. 2015.
15. Tang JB, Zhou YL, Wu YF, Liu PY, Wang XT. Gene therapy strategies to improve strength and quality of flexor tendon healing. *Expert Opinion on Biological Therapy*. 2016.
16. Raabe O, Shell K, Fietz D, Freitag C, Ohrndorf A, Christ HJ, et al. Tenogenic differentiation of equine adipose-tissue-derived stem cells under the influence of tensile strain, growth differentiation factors and various oxygen tensions. *Cell Tissue Res*. 2013;
17. Gimble JM, Katz AJ, Bunnell BA. Adipose-derived stem cells for regenerative medicine. *Circulation Research*. 2007.
18. J. Braga Osorio Gomes Salgado A, L. Goncalves Reis R, Jorge Carvalho Sousa N, M. Gimble J, J. Salgado A, L. Reis R, et al. Adipose Tissue Derived Stem Cells Secretome: Soluble Factors and Their Roles in Regenerative Medicine. *Curr Stem Cell Res Ther*. 2010;
19. Loebel C, Burdick JA. Engineering Stem and Stromal Cell Therapies for Musculoskeletal Tissue Repair. *Cell Stem Cell*. 2018.
20. Stanco D, Caprara C, Ciardelli G, Mariotta L, Gola M, Minonzio G, et al. Tenogenic differentiation protocol in xenogenic-free media enhances tendon-related marker expression in ASCs. *PLoS One*. 2019;14(2).
21. Dominici M, Le Blanc K, Mueller I, Slaper-Cortenbach I, Marini FC, Krause DS, et al. Minimal criteria for defining multipotent mesenchymal stromal cells. The International Society for Cellular Therapy position statement. *Cytotherapy*. 2006;
22. Bagnaninchi PO, Yang Y, El Haj AJ, Maffulli N. Tissue engineering for tendon repair. *British journal of sports medicine*. 2007.
23. Barco R, Encinas C, Valencia M, Carrascal MT, García-Arranz M, Antuña S. Use of adipose-derived stem cells in an experimental rotator cuff fracture animal model. *Rev Española Cirugía Ortopédica y Traumatol (English Ed)*. 2015;

24. Shen H, Korpakakis I, Havlioglu N, Linderman SW, Sakiyama-Elbert SE, Erickson IE, et al. The effect of mesenchymal stromal cell sheets on the inflammatory stage of flexor tendon healing. *Stem Cell Res Ther.* 2016;
25. Zuk PA, Zhu M, Ashjian P, De Ugarte DA, Huang JI, Mizuno H, et al. Human adipose tissue is a source of multipotent stem cells. *Mol Biol Cell.* 2002;
26. Baer PC, Geiger H. Adipose-derived mesenchymal stromal/stem cells: Tissue localization, characterization, and heterogeneity. *Stem Cells International.* 2012.
27. Bellotti C, Stanco D, Ragazzini S, Romagnoli L, Martella E, Lazzati S, et al. Analysis of the Karyotype of Expanded Human Adipose-Derived Stem Cells for Bone Reconstruction of the Maxillo-Facial Region. *Int J Immunopathol Pharmacol.* 2013;26.
28. de Girolamo L, Viganò M, Galliera E, Stanco D, Setti S, Marazzi MG, et al. In vitro functional response of human tendon cells to different dosages of low-frequency pulsed electromagnetic field. *Knee Surgery, Sport Traumatol Arthrosc.* 2015;23(11).
29. Arrigoni E, Lopa S, De Girolamo L, Stanco D, Brini AT. Isolation, characterization and osteogenic differentiation of adipose-derived stem cells: From small to large animal models. *Cell Tissue Res.* 2009;
30. De Girolamo L, Stanco D, Salvatori L, Coroniti G, Arrigoni E, Silecchia G, et al. Stemness and Osteogenic and Adipogenic Potential are Differently Impaired in Subcutaneous and Visceral Adipose Derived Stem Cells (ASCs) Isolated from Obese Donors. *Int J Immunopathol Pharmacol.* 2013;26.
31. U.S. National Institutes of Health. *ClinicalTrials.gov Background.* *ClinicalTrials.gov.* 2014.
32. Chen HS, Su YT, Chan TM, Su YJ, Syu WS, Harn HJ, et al. Human adipose-derived stem cells accelerate the restoration of tensile strength of tendon and alleviate the progression of rotator cuff injury in a rat model. *Cell Transplant.* 2015;
33. Mora MV, Antuña SA, Arranz MG, Carrascal MT, Barco R. Application of adipose tissue-derived stem cells in a rat rotator cuff repair model. *Injury.* 2014;

34. Lee SY, Kim W, Lim C, Chung SG. Treatment of Lateral Epicondylitis by Using Allogeneic Adipose-Derived Mesenchymal Stem Cells: A Pilot Study. *Stem Cells*. 2015;
35. Pak J, Chang JJ, Lee JH, Lee SH. Safety reporting on implantation of autologous adipose tissue-derived stem cells with platelet-rich plasma into human articular joints. *BMC Musculoskelet Disord*. 2013;
36. Lee CH, Shah B, Moiola EK, Mao JJ. CTGF directs fibroblast differentiation from human mesenchymal stem/stromal cells and defines connective tissue healing in a rodent injury model. *J Clin Invest*. 2010;
37. Chen CH, Cao Y, Wu YF, Bais AJ, Gao JS, Tang JB. Tendon Healing In Vivo: Gene Expression and Production of Multiple Growth Factors in Early Tendon Healing Period. *J Hand Surg Am*. 2008;
38. Schneider PRA, Buhrmann C, Mobasheri A, Matis U, Shakibaei M. Three-dimensional high-density co-culture with primary tenocytes induces tenogenic differentiation in mesenchymal stem cells. *J Orthop Res*. 2011;
39. Park BS, Kim WS, Choi JS, Kim HK, Won JH, Ohkubo F, et al. Hair growth stimulated by conditioned medium of adipose-derived stem cells is enhanced by hypoxia: Evidence of increased growth factor secretion. *Biomed Res*. 2010;
40. Klein MB, Yalamanchi N, Pham H, Longaker MT, Chang J. Flexor tendon healing in vitro: Effects of TGF- β on tendon cell collagen production. *J Hand Surg Am*. 2002;
41. Pryce BA, Watson SS, Murchison ND, Staverosky JA, Dünker N, Schweitzer R. Recruitment and maintenance of tendon progenitors by TGFB signaling are essential for tendon formation. *Development*. 2009;
42. Lou J, Tu Y, Burns M, Silva MJ, Manske P. BMP-12 gene transfer augmentation of lacerated tendon repair. *J Orthop Res*. 2001;
43. Wolfman NM, Hattersley G, Cox K, Celeste AJ, Nelson R, Yamaji N, et al. Ectopic induction of tendon and ligament in rats by growth and differentiation factors 5, 6, and 7, members of the TGF- β gene family. *J Clin Invest*. 1997;
44. Shukunami C, Takimoto A, Oro M, Hiraki Y. Scleraxis positively regulates the expression of tenomodulin, a differentiation marker of tenocytes. *Dev Biol*. 2006;

45. James R, Kumbar SG, Laurencin CT, Balian G, Chhabra AB. Tendon tissue engineering: Adipose-derived stem cell and GDF-5 mediated regeneration using electrospun matrix systems. *Biomed Mater.* 2011;
46. Leung M, Jana S, Tsao CT, Zhang M. Tenogenic differentiation of human bone marrow stem cells via a combinatory effect of aligned chitosan-poly-caprolactone nanofibers and TGF- β 3. *J Mater Chem B.* 2013;
47. Manning CN, Kim HM, Sakiyama-Elbert S, Galatz LM, Havlioglu N, Thomopoulos S. Sustained delivery of transforming growth factor beta three enhances tendon-to-bone healing in a rat model. *J Orthop Res.* 2011;
48. Liu J, Tao X, Chen L, Han W, Zhou Y, Tang K. CTGF positively regulates BMP12 induced tenogenic differentiation of tendon stem cells and signaling. *Cell Physiol Biochem.* 2015;
49. Gonçalves AI, Rodrigues MT, Lee SJ, Atala A, Yoo JJ, Reis RL, et al. Understanding the role of growth factors in modulating stem cell tenogenesis. *PLoS One.* 2013;
50. Shen H, Gelberman RH, Silva MJ, Sakiyama-Elbert SE, Thomopoulos S. BMP12 induces tenogenic differentiation of adipose-derived stromal cells. *PLoS One.* 2013;
51. Spina A, Montella R, Liccardo D, De Rosa A, Laino L, Mitsiadis TA, et al. NZ-GMP approved serum improve hDPSC osteogenic commitment and increase angiogenic factor expression. *Front Physiol.* 2016;
52. Desiderio V, De Francesco F, Schiraldi C, De Rosa A, La Gatta A, Paino F, et al. Human Ng2⁺ adipose stem cells loaded in vivo on a new crosslinked hyaluronic acid-lys scaffold fabricate a skeletal muscle tissue. *J Cell Physiol.* 2013;
53. Halme DG, Kessler DA. FDA regulation of stem-cell-based therapies. *N Engl J Med.* 2006;
54. Bieback K, Hecker A, Kocaömer A, Lannert H, Schallmoser K, Strunk D, et al. Human alternatives to fetal bovine serum for the expansion of mesenchymal stromal cells from bone marrow. *Stem Cells.* 2009;
55. Schallmoser K, Strunk D. Preparation of pooled human platelet lysate (pHPL) as an efficient supplement for animal serum-free human stem cell cultures. *J Vis Exp.* 2009;

56. Stanco D, Caprara C, Ciardelli G, Mariotta L, Gola M, Minonzio G, et al. Tenogenic differentiation protocol in xenogenic-free media enhances tendon-related marker expression in ASCs. *PLoS One*. 2019;
57. Shukla L, Morrison WA, Shayan R. Adipose-Derived Stem Cells in Radiotherapy Injury: A New Frontier. *Front Surg*. 2015;
58. Pirrone C, Gobbetti A, Caprara C, Bernardini G, Gornati R, Soldati G. Chondrogenic potential of hASCs expanded in flask or in a hollow-fiber bioreactor. *J Stem Cell Res Med*. 2017;
59. G. M, M. C, L. M, M. G, M. Z, E. G, et al. Frozen adipose-derived mesenchymal stem cells maintain high capability to grow and differentiate. *Cryobiology*. 2014.
60. Bourin P, Bunnell BA, Casteilla L, Dominici M, Katz AJ, March KL, et al. Stromal cells from the adipose tissue-derived stromal vascular fraction and culture expanded adipose tissue-derived stromal/stem cells: A joint statement of the International Federation for Adipose Therapeutics and Science (IFATS) and the International So. Cytotherapy. 2013;
61. Giannasi C, Pagni G, Polenghi C, Niada S, Manfredi B, Brini A, et al. Impact of Dental Implant Surface Modifications on Adhesion and Proliferation of Primary Human Gingival Keratinocytes and Progenitor Cells. *Int J Periodontics Restorative Dent*. 2018;
62. Lancaster, M. V. and Fields RD. Antibiotic and cytotoxic drug susceptibility assays using resazurin and poisoning agents. United States Pat. 1995;
63. SWEAT F, PUCHTLER H, ROSENTHAL SI. SIRIUS RED F3BA AS A STAIN FOR CONNECTIVE TISSUE. *Arch Pathol*. 1964;
64. Lindroos B, Boucher S, Chase L, Kuokkanen H, Huhtala H, Haataja R, et al. Serum-free, xeno-free culture media maintain the proliferation rate and multipotentiality of adipose stem cells in vitro. *Cytotherapy*. 2009;
65. Patrikoski M, Juntunen M, Boucher S, Campbell A, Vemuri MC, Mannerström B, et al. Development of fully defined xeno-free culture system for the preparation and propagation of cell therapy-compliant human adipose stem cells. *Stem Cell Res Ther*. 2013;
66. Nichols J, Zevnik B, Anastassiadis K, Niwa H, Klewe-Nebenius D, Chambers I, et al. Formation of pluripotent stem cells in the mammalian embryo depends on the POU transcription factor Oct4. *Cell*. 1998;

67. Halász K, Kassner A, Mörgelin M, Heinegård D. COMP acts as a catalyst in collagen fibrillogenesis. *J Biol Chem.* 2007;
68. Södersten F, Hulténby K, Heinegård D, Johnston C, Ekman S. Immunolocalization of collagens (I and III) and cartilage oligomeric matrix protein in the normal and injured equine superficial digital flexor tendon. *Connect Tissue Res.* 2013;
69. Schweitzer R, Chyung JH, Murtaugh LC, Brent AE, Rosen V, Olson EN, et al. Analysis of the tendon cell fate using Scleraxis, a specific marker for tendons and ligaments. *Development.* 2001;
70. Jiang Y, Shi Y, He J, Zhang Z, Zhou G, Zhang W, et al. Enhanced tenogenic differentiation and tendon-like tissue formation by tenomodulin overexpression in murine mesenchymal stem cells. *J Tissue Eng Regen Med.* 2017;
71. Gonçalves AI, Berdecka D, Rodrigues MT, Eren AD, de Boer J, Reis RL, et al. Evaluation of tenogenic differentiation potential of selected subpopulations of human adipose-derived stem cells. *J Tissue Eng Regen Med.* 2019;

Chapter 5

3D bioprinting technology: current advances and limits for bone and cartilage tissue engineering applications and its mapping by TIM

5.1 Abstract

The development of 3D-bioprinting in tissue engineering application could allow faster tissue substitutes fabrication with increased complexity, resolution, and functionality, contributing toward providing personalized regenerative solutions. 3D bioprinting has particularly advanced in the orthopaedic field, especially in custom-made prostheses and implants for bone and cartilage tissue engineering. On the other hand, to our knowledge, biofabrication strategies to treat tendon injuries have not been explored so far. Many ongoing research efforts are aimed at obtaining 3D tissue-grafts of greater complexity with better ability to mimic tissue behavior *in vivo*. In this chapter scientific and technological advancement of 3D bioprinting on cartilage and bone tissue engineering are reviewed, including the state-of-the-art technologies and pre-clinical applications. Advantages and challenges are indicated for each technology. Moreover, the monitoring of 3D bioprinting in terms of principal actors involved worldwide in scientific and patent productions was allowed by using the unique Tool for Innovation Monitoring (TIM) software. TIM is a tool developed by the Joint Research Center (JRC) of the European Commission to perform bibliometric analyses, track changes and monitoring about emerging technologies that are still far away from the market and thus employed commercially.

Results from TIM showed a map confirmed the positive trend, in the last decade, in the development of 3D bioprinting technology worldwide, above all in terms of scientific production, and identified USA and China as the main best performing countries in terms of both scientific production and patent released.

*Part of the results described in this chapter are described in the manuscript in preparation entitled “3D bioprinting for orthopaedic applications: advances, challenges and regulatory considerations” authored by **Deborah Stanco**, Patricia Urbán, Salvatore Tirendi, Gianluca Ciardelli, Josefa Barrero for the submission on Bioprinting.*

5.2 Introduction

Three dimensional (3D) bioprinting technology allows the fabrication of engineered tissue constructs with complex 3D structures by additive manufacturing of cells, biomaterials and growth factors, soluble molecules and drugs (1,2). In contrast the conventional tissue engineering methods, the advantage of this technique is represented by the possibility to obtain, in a high reproducibility and repeatability manner, a homogenous cell seeding by the precisely controlled placement of cells over the scaffold. Hence, the high printing resolution enables the production of functional tissue constructs with morphological, biological and mechanical characteristics that highly resemble the native target tissue cues (1,3,4). In particular, the specific 3D architecture such as external shape, pore size, pore interconnectivity, internal microarchitecture and topology cannot be achieved using traditional tissue engineering approaches (1,5). For these reasons, 3D bioprinting together with the advancement of medical imaging, such as magnetic resonance imaging (MRI) or computer tomography (CT), could offer customized products with clinically relevant size, overcoming the limited organ availability of transplant, and thus potentially bring healthcare in the era of personalized medicine (Figure 5.1) (6,7).

In the orthopaedic field, the use of 3D (bio)printing (with and without cells) has been recently explored to obtain customized prosthetics and implants for patient-specific therapy and to potentially regenerate tissues, in particular for bone and cartilage disorders (8,9). More than 300 articles, including *in vitro* and pre-clinical studies have been revised in this chapter, revealing the growing interest in printing cells for the repair of large tissue defects in that area. However, for what concerns 3D bioprinting application in the orthopaedic field, they are limited to bone, cartilage and osteochondral tissues, with only one report about tendon tissue, i.e. muscle-tendinous junction (cp chapter 6), and still no applications in clinical setting (10,11).

This chapter summarizes the best achievements in the production of 3D bioprinted bone and cartilage substitutes as well as limits and advances of the printing protocols, biomaterials and cell sources. From a social and economic point of view, the early identification and the monitoring of new emerging technology,

like 3D bioprinting, makes important to understand how this scientific and technological advancements can impact on society and human health in the future (1,12–14). In this contest, beyond the classical consultation of experts in specific fields, the Joint Research Centre (JRC) of the European Commission has recently developed a new software Tool for Innovation Monitoring (TIM). TIM allows bibliometric analysis and the extraction of accurate, target and timely information derived by scientific production, patent release and EU funded projects (13,14). In this chapter, the intense research & development activity about 3D bioprinting worldwide was also analyzed by the use of TIM.

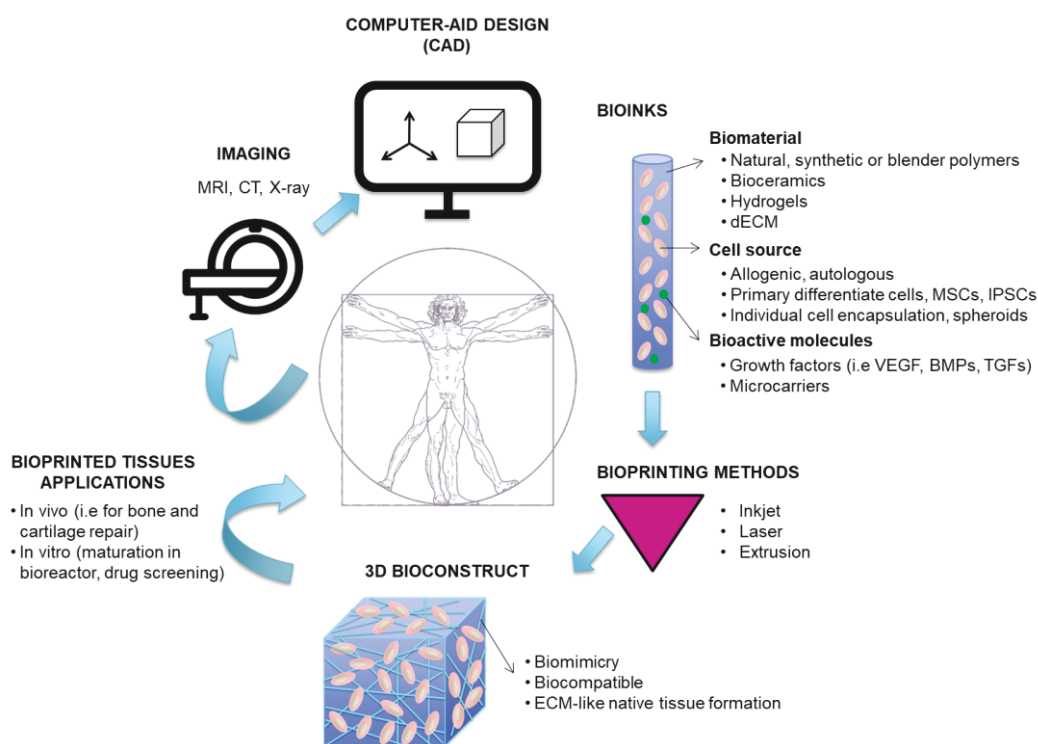


Figure 5.1. 3D bioprinting strategy

The diagnostic images of the damaged patient's tissue are collected using CT and/or MRI scans and then used to design the bioprinted tissue construct by CAD. The composition of the bioink made from biomaterials and cells is crucial to suit the specific characteristics of the target tissue. Biomaterials can be natural- or synthetic-based or derived from decellularized extracellular matrix (dECM). Cells can be isolate from the same patient (autologous) or from another individual (allogenic) and often consisting in mesenchymal stem cells (MSCs) or induced pluripotent stem cells (iPSCs). The presence of growth factors like vascular endothelial growth factor (VEGF), bone morphogenic proteins (BMPs), and tissue growth factor (TGF) could be employed to drive cell differentiation and proliferation. Then, bioprinting of these components includes the inkjet, laser or extrusion-based methods. The final 3D customized bioconstruct could be implant *in vivo* or culture in a bioreactor for tissue maturation *ex-vivo* before transplantation or alternative used as diagnostic tool applications.

5.3 Research strategy

The impact of the innovation of 3D bioprinting technology in the healthcare system was evaluated by analyzing efforts in biomedical translational research for bone and cartilage tissue engineering. In particular, the biomedical literature search of relevant articles was assessed applying specific keywords combined with boolean operators: ("3D bioprinting" OR "bioprinting") AND ("bone OR cartilage") in PUBMED search (Figure 5.2). The searches were performed between January and May 2019 and the language was limited to English. Since bioprinting is still in its initial stage of development, no restrictions to publication year were applied. Additional papers were identified through automated database notifications of new publications according to our search terms until September 2019. The evolution of this technology was tracked also by Tools for Innovation Monitoring (TIM) (13,14). A specific search string with selected keywords and boolean operators, listed in Figure 5.2, was used to collect data or documents from different sources in a limited included from December to April 2019. In particular, TIM search is based on the simultaneous search from three databases: Scopus database as source of peer-reviewed scientific journals (15); the Community Research and Development Information Service (CORDIS) the primary source of European Commission results for research funded projects by the EU's framework programs for research and innovation (FP1 to Horizon 2020) (from cordis.europa.eu) and Patstat the international database of patent data (from epo.org/searching-for-patents/business/patstat.html#tab-1). After data monitoring and collection, TIM allows to organize and visualize as networks of specific sub-datasets.



	STRATEGY
 Scientific advances in bone and cartilage TE	PUBMED
	"bio printing" OR "bio-printing" OR "bioprinting" <u>AND</u> bone OR cartilage OR tendon OR orthopedic
 Interests in academia and healthcare sector	TIM
	"bio printing" OR "bio-printing" OR "bioprinting" OR "bio-ink" OR bioink <u>AND</u> health OR medicine OR medical OR eye OR skin OR heart OR vessel OR blood OR cardiovascular OR "regenerative medicine" OR urology OR "plastic surgery" OR bone OR cartilage

Figure 5.2. Search strategy

The selected keywords and boolean operators used for the PUBMED and TIM search.

5.4 Results and Discussion

5.4.1 Basic aspects of 3D bioprinting technology

Bioink components include biomaterials, cells and bioactive molecules. Cell sources for bioprinting may be allogeneic or autologous; among these, mesenchymal stem cells (MSCs) and induced pluripotent stem cells (IPSCs) are largely employed. The presence of bioactive molecules such as growth factors could be employed to drive cell differentiation and proliferation. The different steps of the process and their components will be discussed below.

The bioink has the role of mimicking the tissue-specific extracellular matrix (ECM) components to offer an optimal environment for cell survival, proliferation and maturation. At the same time, the bioink should possess proper mechanical and viscoelastic properties to ensure print accuracy and post-printing stability (1). Common biomaterials include synthetic or natural polymers, hydrogels and decellularized extracellular matrix (dECM) components.

Hydrogels are often used as bioinks due to their biocompatibility and unique chemical and physical properties, such as high water content, nutrient and oxygen diffusion or *in vivo* biodegradability of the polymeric matrix. Moreover, the majority of them possess specific cell-binding sites promoting cell attachment, spreading and differentiation. Both natural and synthetic polymers (and their combination) have been employed for the synthesis of hydrogels (4,16). Natural polymers more predominantly used are gelatin, collagen or alginate and deriving from natural sources and have the notable property to resemble the physiological ECM cues. The use of the natural ECM as hydrogel for 3D bioprinting was developed by Pati and colleagues (17,18). In their studies, decellularized extracellular matrices derived from cartilage, adipose and heart tissues were developed as temperature-sensitive hydrogels to maintain MSC viability and multipotency after bioprinting. Synthetic polymers such as poly(lactic-co-glycolic acid) (PLGA), poly-caprolactone (PCL) and poly(lactic-co-glycolic acid) are generally used to provide mechanical strength to the construct and for their tunable composition and properties. Other synthetic materials often employed consist in calcium phosphate (CaP), tri-calcium phosphate (TCP) and hydroxyapatite (HA), alone or by their combination, for their biocompatible and

osteoinductive properties (2). The combination of natural with synthetic polymers allows to modulate specific mechanical properties of the hydrogel such as elasticity and stiffness as well as to support cell adhesion and proliferation, to improve biodegradability, biocompatibility, thermal and conductive properties (4,16,19). Recently, the use of nanocellulose has been considered for their characteristics that include not only their natural origin and the high water content, but also their nanofibrillar composition that highly resemble collagen fibril network, mechanical strength and shear thinning properties, as also discussed in chapter 6 (20–23).

The choice of the appropriate cell type represents another crucial issue for a functional bioprinted construct. Cells for bioprinting should be able to proliferate maintaining their own phenotype and guiding the new tissue formation. Current options from bioprinting cells include: (i) cells embedded into a hydrogel that is often loaded with bioactive molecules and growth factors to aid cell metabolism, (ii) cells individually encapsulated in microcarriers or (iii) cell aggregates (spheroids) which are deposited using extrusion printers and are allowed to self-assemble into the desired 3-D structure (1,5,24–27).

MSCs represent the most suitable cell source for tissue regeneration approaches like bioprinting for several reasons (discussed in detail in chapter 2). Firstly, they have unique self-renewal ability and the capacity to differentiate into a variety of cell types, such as osteoblasts, adipocytes, chondrocytes, tenocytes and skeletal myocytes. In addition, they possess immunomodulatory properties, they have shown the capacity to secrete protective biological factors and they can be easily purified from different tissues (such as bone marrow, adipose tissue or umbilical cord). Moreover, their therapeutic effect has been thoroughly explored in a number of human clinical trials (1,28), their use is considered safe, and ethical concerns present for embryonic and pluripotent stem cells do not apply for MSCs. On the other hand, the bioprinting of terminally differentiated cell lines like osteoblasts and chondrocytes has been explored, but their limited lifespan and the invasive surgical procedure needed for harvesting them represent the major limitations for their use (29).

Beyond cell-laden scaffolds characteristics, parameters such as the printing resolution, placement accuracy, amount of printed layers, dimension and consumed printing time should be taken into consideration during the 3D

bioprinting process (2). Common methods used to produce 3D bioproducts include (i) inkjet, (ii) laser and (iii) extrusion-based bioprinting are showed in Figure 5.3 (1,2,7,16,30).

(i) Inkjet-based bioprinting uses thermal, piezoelectric or electromagnetic forces to deposit small bioink droplets from a print head nozzle. This method is widely employed because it is easy to use, low cost and highly versatile. It allows printing many materials with high resolution and speed (1,31). Nonetheless, tissue fabrication using this method presents limitations such as frequent nozzle clogging, thermal and mechanical stress on cells, poor cell density and non-uniform droplet size.

(ii) Laser bioprinting is a scaffold-free technique able to print cells in a very high density using laser energy to transfer and encapsulate them from a donor slide within droplets of biomaterial toward a collector slide (32,33). Despite the high print accuracy and 3D structure resolution of this method, cell survival is low and the printing process is expensive and time consuming. In this context, stereolithography or digital light processing represent reliable alternatives to overcome these limitations. These techniques employ ultraviolet or visible light to solidify a liquid with photopolymeric properties to layer-by-layer manufacturing the 3D construct (34,35). However, further technical developments of laser-based techniques are needed in order to achieve large and more complex tissue reconstruction.

(iii) Extrusion-based bioprinting employs different nozzles to extrude the bioink driven by pneumatic or mechanical pressure. It is the most commonly used technique nowadays due to its very high resolution and the possibility to print high viscosity bioinks such as complex polymers and cell spheroids (30,36–38). One of its major disadvantages is associated with shear-stress during printing, which may affect cell viability (39).

Volumetric printing technologies have emerged recently, enabling the creation of entire objects at once in a short time (i.e. several seconds), rather than using layer-by-layer additive manufacturing. A centimeter-scale cell-laden hydrogel has been generated using this technique at an unprecedented printing velocity (40). However, this technology is still in its infancy and further studies are needed for upscaling the production of hydrogel-based constructs and to evaluate their biological activity *in vivo*.

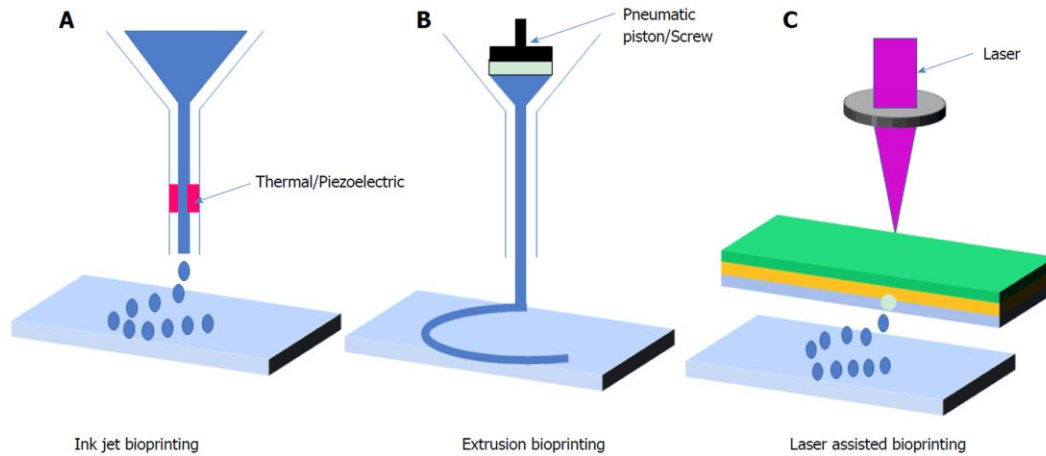


Figure 5.3. Classification of bioprinting techniques.

Schematic diagram of the three major bioprinting techniques. A. Inkjet-based printing; B. Extrusion-based printing; C. Laser-based bioprinting (41).

5.4.2 Advances in bone repair

Bone defects and injuries resulting from aging, trauma, infection, disease or failed arthroplasty often require tissue reconstruction using a graft or metal implants (42). However, these techniques show often limited efficacy due to several reasons, such as scarce bone substitute availability, donor site morbidity, poor tissue integration, fatigue fractures, immune response activation or infections (43–45). Over the past decades, extensive attention has been given to 3D-printed scaffolds for bone tissue regeneration due to their 3D structure with desirable porosity and mechanical properties that can mimic the natural trabecular bone. However, current tissue engineering applications still lack the ability to organize cells within a 3D scaffold and to reproduce the microstructure of native tissues. Bioprinting is expected to be a powerful tool for bone tissue engineering, since it can build 3D constructs to reproduce the bone microstructure. Moreover, bioprinting has the potential to enhance bone repair clinical outcomes since it could overcome some of current bone graft side adverse effects.

An overview of recent *in vitro* and *in vivo* studies using 3D bioprinting for bone tissue engineering applications is shown in table 1 (7,26,46–59). Considerable work has been done to develop functional models of bone tissues in laboratories. For instance, some authors have used composite-hydrogel printed MSCs using

laser-based bioprinting to treat *in situ* cranial defects in mouse (51). Keriquel et al. use a composite-hydrogel characterized by two phases to resemble the bone ultra-structure and its mechanical resistance and osteoconductivity properties. The phase of collagen type I mimics the organic part of the bone and a second phase of nano-hydroxyapatite represents the mineral content (51). After 42 days post-implantation, the research group showed cell proliferation and good effects in enhancing bone regeneration. Other groups have explored the use of a composite of synthetic polymeric membrane (PCL/PLGA/TCP), hydroxyapatite and growth factors (such as platelet rich plasma (PRP) and bone morphogenetic protein-2 (BMP-2)) to elicit cell differentiation and bone tissue formation *in vitro* and *in vivo* (46,54,55,57,59–64). Moreover, pre-vascularization strategies aiming to resemble the highly vascularized nature of bone have been also developed using vascular endothelial growth factors (VEGF) and endothelial cells (ECs) (26,50,52,65). For instance, Anada et al. used GelMA hydrogel as a matrix with calcium phosphate materials (peripheral octacalcium phosphate, OCP) in which MSCs-ECs were co-cultured to drive osteogenic differentiation and blood vessel-like structures formation. In particular, the research group produced a biomimetic dual ring structure using stereolithography for the precise positioning of cells and OCP material into GelMA hydrogels, showing good results in term of capillary-like structure formation already after 1 day of culture (50).

The fabrication of a suitable 3D construct for the regeneration of the osteochondral bone which is present in joints regions, such as the knee, is particularly challenging. For these applications, the different hierarchical and organizational structure of this tissue, which is composed by abundant articular cartilage and subchondral bone region, has to be mimicked. With this purpose, Shim et al. developed a multi-head tissue/organ building system (MtoBS), which is an extrusion-based able to dispense biomaterials with completely different rheology properties and different cell types (53). Using this system, Shim et al. fabricated a poly-(ϵ -caprolactone) framework to confer structural strength to the construct, which was covered with two different cell-laden hydrogels. The obtained 3D bioprinted construct contained two different cell types (osteoblasts and chondrocytes) to resemble the osteochondral nature of the bone. Both cell types not only retained their initial position and viability, but also proliferated up to 7 days after being dispensed. More recently, Kang et al. developed another

multi cartridge system, the integrated tissue organ printer (ITOP), to produce multiple tissue constructs of any shape with clinically relevant size and structural integrity. Authors reported high cell viability and density *in vitro* and a newly formed vascular network throughout the entire implantation in mice, showing the potential of their system to treat mandible and calvarian bone defects *in vitro* and *in vivo* (7). Kang et al. demonstrated the capabilities of the ITOP system by fabricating mandible and calvarian bone, cartilage and skeletal muscle.

Table 5.1 Recent *in vitro* and *in vivo* studies using 3D bioprinting for bone tissue engineering applications

Biomaterials and GFs	Cells	Main results	References
Extrusion-based bioprinting			
Alginate/gelatin/bioglass	Osteoblasts	Increased cell proliferation and mineralization by adding bioglass to the hydrogel.	<i>Wenz et al.</i> (58)
Alginate/gelatin/HA	ASCs	Structure integrity maintained for 28 days in culture, intense matrix formation and upregulation of osteogenic markers.	<i>Wang et al.</i> (57)
Alginate/GelMA/HA	BMSCs	Long-term structural integrity and high cell viability after 3days of <i>in vitro</i> culture.	<i>Wüst et al.</i> (55)
Alginate/gelatin/polyP-Ca ²⁺ complex	Osteoblasts	Improved cell proliferation and significant matrix deposition due to the calcium salt from polyP-Ca ²⁺ complex.	<i>Neufurth et al.</i> (56)
Alginate/PCL	Pre-osteoblasts, Chondrocytes	Maintained their cell viability and proliferation in culture of encapsulated cells dispensed into the pores of a pre-formed PCL framework.	<i>Shim et al.</i> (53)
Bioglass/gliadin/PCL	Pre-osteoblasts	Scaffold with controllable architecture, high compressive strength, proper degradability and biocompatible. Osteogenesis <i>in vivo</i> after implantation in rabbit femoral bone defect.	<i>Zhang et al.</i> (49)
Chitosan, Chitosan/HA, Alginate, Alginate/HA	Osteoblasts	The combination of Chitosan/HA showed improved cell viability, proliferation and differentiation.	<i>Dermitaş et al.</i> (59)
Collagen/PCL-HA/TCP + rhBMP-2 or PRP	Osteoblasts	The addition of PRP showed higher cellular activities and mineralisation for bone tissue regeneration in Collagen/PCL-HA/TCP biocomposites, compared to the addition of rhBMP-2.	<i>Kim et al.</i> (46)
Gelatin/silicate nanoparticles + VEGF	HUVECs and BMSCs	Constructs with high structural stability, cell survival and proliferation <i>in vitro</i> .	<i>Byambaa et al.</i> (48)

Table 5.1 continued

Biomaterials and GFs	Cells	Main results	References
GelMA/Pluronic F-127	BMSCs	Total bone formation, increased vascularisation and implant remodelling observed after implantation in rat femoral bone defect.	<i>Daly et al.</i> (26)
Matrigel	ECs and BMSCs	Bone and vessel formation in printed grafts after subcutaneous implantation in immunodeficient mice.	<i>Fedorovich et al.</i> (61)
PCL/ β -TCP	Fibroblasts, Pre-osteoblasts	Excellent cell affinity and mechanical properties of the membrane. Enhancement of bone formation after implantation in alveolar bone defect in beagles.	<i>Shim et al.</i> (47)
PCL/CB[6]/DAH-HA+TGF β /Atelocollagen + rhBMP-2	hTMSCs	Cytocompatible multi-layered 3D construct capable of inducing cell differentiation <i>in vitro</i> . <i>In vitro</i> and <i>in vivo</i> osteochondral tissue formation.	<i>Shim et al.</i> (54)
PCL/TCP/Pluronic F-127	hAFMSCs	Formation of new vascularized bone tissue with no necrosis, after 5 months of calvarian bone reconstruction <i>in vivo</i> .	<i>Kang et al.</i> (7)
Stereolithography			
GelMa/OCP	HUVECs and BMSCs	Bone-like tissue and capillary-like structure formation after 1 day of <i>in vitro</i> culture.	<i>Anada et al.</i> (50)
Laser Bioprinting			
nHA-collagen	BMSCs	Proliferation of printed MSCs and improved bone regeneration 42 days post-implantation in the calvarian bone defect mouse model.	<i>Keriquel et al.</i> (32)

Abbreviations: [ECs] endothelial cells, [BMSCs] bone marrow-derived mesenchymal stem cells, [PCL] poly(caprolactone), [CB(6)] Cucurbit[6]uril, [DAH-HA] 1,6-diaminohexane-conjugated hyaluronic acid, [hTMSCs] human nasal inferior turbinate tissue-derived mesenchymal stromal cells, [TGF β] transforming growth factor, [rhBMP-2] recombinant human bone morphogenetic protein-2, [GelMa] gelatin methacrylamide, [HA] hydroxyapatite, [polyP-Ca²⁺ complex] calcium salt of polyphosphate-calcium complex, [ASCs] adipose derived mesenchymal stem cells, [TCP] tricalcium phosphates, [hAFMSCs] human Amniotic fluid-derived mesenchymal stem cells, [PRP] platelet rich plasma, [VEGF] vascular endothelial growth factor, [HUVECs] Human umbilical vein endothelial cells, [OCP] peripheral octacalcium phosphate.

5.4.3 Advances in cartilage repair

Cartilage is a dense connective avascular tissue with limited self-repair ability, which is frequently damaged as a result of trauma and degenerative joint diseases such as osteoarthritis. Osteoarthritis is characterized by a progressive loss of articular cartilage and causes pain, impaired function, limited range of motion, stiffness, catching, locking and joint enlargement or swelling (66). In the last decades, the poor outcome of standard surgical joint replacements has triggered the development of alternative approaches including cell-based therapies and tissue engineering. Autologous chondrocyte implantation (ACI) was the first cell-based approach used to treat cartilage defects, but it presented drawbacks such as limited availability and lifespan of chondrocytes. Further disadvantages include the high cost and length of the procedure and patient discomfort related to surgery (67–69). Concurrently, the intra-articular injection of MSCs has gained popularity as emerging regime for cartilage regeneration. The safety, feasibility and efficacy of MSCs for regeneration of human articular cartilage has been investigated in more of 50 clinical trials to date (70).

Cartilage repair with a personalised engineered tissue resembling the native cartilage directly into the site of lesion is a very attractive approach. However, it remains a significant challenge due to cartilage complex zonal organization, which plays an important role in the structure and function of the tissue. Some recent studies based on bioprinting were conducted to obtain the ideal graft, which would be able to integrate in the host tissue and to closely mimic the native cartilage. Moreover, the graft should maintain cartilage zonal organization, such as hyaline cartilage of articulating surface of bones or fibrocartilage of meniscus, as well as its ECM composition and mechanical properties.

An overview of recent studies using different biomaterials and cells for 3D bioprinting of cartilage is presented in Table 2 (7,17,71–80). The choice of the proper cell type and biomaterial is crucial to achieve cartilage-like tissue formation. In fact, it has been demonstrated that natural hydrogels such as agarose, alginate and gelatin methacrylamide (GelMa) drive differently MSCs phenotype and differentiation after 28 days *in vitro* culture (75). MSCs cultured with alginate and agarose hydrogels showed higher cell viability and hyaline-like cartilage formation with predominant expression of collagen type II. When

culturing MSCs in GelMA bioconstructs, a fibrocartilage-like tissue formation was observed, with higher expression of collagen type I and II.

Cui et al. bioprinted poly(ethylene glycol) dimethacrylate (PEGDMA) with human chondrocytes using a layer-by-layer assembly to repair defects in osteochondral plugs *in vitro*. They achieved good chondrocyte viability and mechanical properties similar to native human articular cartilage with cartilage ECM protein expression as collagen type II, aggrecan and glycosaminoglycans (GAGs) (71).

Some studies were performed to generate human scale tissue constructs with complex architectures and high structural integrity. Kang et al. demonstrated to develop a complex, human ear-shaped construct containing cartilage tissue with histological and mechanical characteristics of human auricles after maturation *in vivo* (7). They used a ITOP technology for the delivery of bioink, which consisted of different hydrogels (gelatin, fibrinogen and HA) and rabbit ear chondrocytes. More recently, a PCL microchamber system has been proposed to engineer scaled-up tissues with native-like collagen anisotropies. Using the PCL microchamber system, it has been possible to support the formation of oriented arrays of MSCs aggregates to produce cartilage tissues with a collagen network organization mimicking the native tissue, with a parallel orientation in the superficial zone and random-perpendicular organization in the middle and deep zones (72).

The intra-operative application of 3D bioprinting has been recently explored with the development of the Biopen. This hand-held device allows the delivery of the bioscaffold and cultured cells directly into the defect site in a single surgical session. Moreover, it allows the reconstruction of different tissues by printing multiple layers using different biomaterials and/or cells, simply by changing cartridges. The biopen integrates in one single component bioink chambers, a multi- injet extruder nozzle, a light source to catalyze phase transformation of the ink and a motorized extrusion system (81). Moreover, the internal structure of the nozzle was designed to contain the bioink comprising living cells in an inner core, which is protected by a shell of a more robust biomaterial. The *in vivo* application of the Biopen was investigated by Di Bella and colleagues to treat *in situ* chondral defects in sheeps (76). The bioink 'core' was filled with allogeneic infrapatellar adipose-derived stem cells (ASCs) and HA- GelMa hydrogel (hyaluronic acid

and gelatin methacrylamide), which was surrounded by an outer shell of HA-GelMa bioink and the photoinitiator. The results of this pilot study show that real-time, safe, *in vivo* bioprinting is a feasible to regenerate articular cartilage in a large animal model. Moreover, better overall macroscopic and microscopic cartilage characteristics were observed with Biopen-when compared to pre-constructed 3D bioscaffolds, microfractures and untreated controls at the time points studied.

Table 5.2 Recent *in vitro* and *in vivo* studies using 3D bioprinting for cartilage tissue engineering applications

Biomaterials and GFs	Cells	Main results	Ref.
Extrusion-based bioprinting			
Agarose, Alginate, GelMA and PEGMA + TGFβ3	BMSCs	High levels of MSC viability observed post-printing in all bioinks. Alginate and agarose hydrogels supported the development of hyaline-like cartilage phenotype. GelMA and PEGMA-based hydrogel supported the development of fibrocartilage-like tissue.	<i>Daly et al.</i> (82)
Collagen type II hydrogel	Chondrocytes	Stable cell distribution patterns throughout the culture period with formation of new ECM with gradient distribution.	<i>Ren et al.</i> (74)
dECM/PCL	hTMSCs	High cell viability and significant chondrogenic differentiation <i>in vitro</i> .	<i>Pati et al.</i> (18)
GelMA	ACPCs, BMSCs and Chondrocytes	Neo-cartilage synthesis in layered co-cultures in a zonal-like architecture <i>in vitro</i> .	<i>Levato et al.</i> (77)
GelMA/HAMA	IFP-MSCs	Rapid generation of Core/Shell GelMa/HAMA bioscaffolds with high modulus and cell viability.	<i>Duchi et al.</i> (79)
HAMA/GelMA	IFP-MSCs	Intraoperative bioprinting using the 'biopen' to treat chondral defect in sheeps showed better macroscopic and microscopic cartilage characteristics.	<i>Di Bella et al.</i> (76)
PCL/Alginate + TGFβ3	Chondrocytes	Enhanced cartilage tissue and type II collagen fibril formation after four weeks of implantation in nude mice.	<i>Kundu et al.</i> (73)
PCL/Pluronic F-127	Chondrocytes	High cell viability, new cartilage tissue formation and increase of GAG content <i>in vivo</i> of human ear-shaped cartilage constructs.	<i>Kang et al.</i> (7)
SA, SA/COL, SA/AG	Chondrocytes	SA/COL showed better cell adhesion, proliferation and cartilage-specific gene expression. SA/COL also suppressed the de-differentiation of chondrocytes and preserved their phenotype.	<i>Yang et al.</i> (78)

Table 5.2 continued

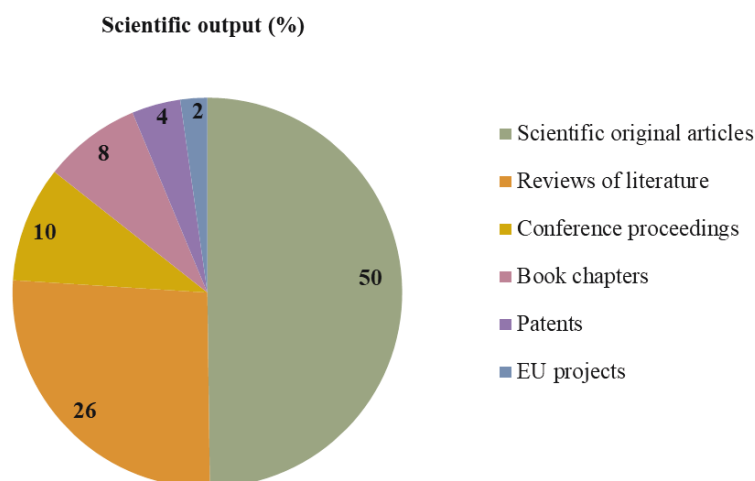
Biomaterials and GFs	Cells	Main results	Ref.
Inkjet-based bioprinting			
PCL microchambers	BMSCs and Chondrocytes	PCL microchambers promoted growth and fusion of cellular spheroids. Formation of stratified cartilage with collagen fibre architecture, composition and biomechanical properties comparable to the native tissue.	<i>Daly et al. (72)</i>
Stereolithography			
GelMA, HAMA	Chondrocytes	Both materials supported cartilage ECM formation and recovery of chondrocyte phenotype <i>in vitro</i> . Influence of cell density on the differentiation pattern.	<i>Lam et al. (80)</i>

Abbreviations: [TGF β -3] Transforming growth factor-3, [GelMa] Gelatin methacrylamide, [PEGMA] Poly(ethylene glycol) methacrylate, [BMSCs] Bone marrow-derived mesenchymal stem cells, [HAMA] hyaluronic acid methacrylate, [IFP-MSCs] infrapatellar fat pad derived mesenchymal stem cells, [ACPCs] Cartilage-resident chondroprogenitor cells, [SA] Sodium Alginate, [COL] collagen, [AG] agarose, [PEGDMA] Poly(ethylene glycol) dimethacrylate, [PCL] poly(caprolactone).

5.4.4 TIM analysis

Three-dimensional bioprinting has the potential to radically transform the health industry and will generate major economic and social impacts (83–86).

In order to identify scientific and technology trends, main actors, countries or regions in specific scientific and technological areas, the knowledge landscape of 3D bioprinting as emerging technology was analyzing using the TIM tool. After a selection of keywords regarding bioprinting and bioinks in health, medical and regenerative medicine sectors for bone and cartilage tissues, TIM collected information related to scientific publications, patents and European projects by databases Scopus, PatStat and Cordis, respectively. A collection of 717 documents were recorded and shown in Figure 5.4.



Type of Document	Number (total 717)
Scientific original articles	357
Reviews of literature	188
Conference proceedings	69
Book chapters	58
Patents	29
EU projects	16

Figure 5.4. TIM platform (Scopus, Patstat, Cordis) search.
Type of documents collected by TIM on 3D bioprinting.

The majority of records were scientific publications that counted 672 documents in which the 50% of original articles, 26% of review of literature, 10% of conference proceedings documents and 8% of book chapters. Surprisingly, patents and related EU projects counted less than 5% (29 and 16 documents, respectively). A certain delay between the research & the development of a new technique/process and the final functional innovative product ready to be patented is expected. Based on the current standings of technology, it would take at least few years of research and development, to have marketable products for 3D bioprinting and bioprinted tissue-constructs that fulfill the ethical and legal requirements to their use in humans.

According to these results, as shown in Figure 5.5, the scientific production and research networks involved in 3D bioprinting technology are constantly increasing in the last decade. In particular, the growing interest in this field is

evident since 2014, assuming an exponential trend until the date of measurements (April 2019), in terms of number of scientific publications released.

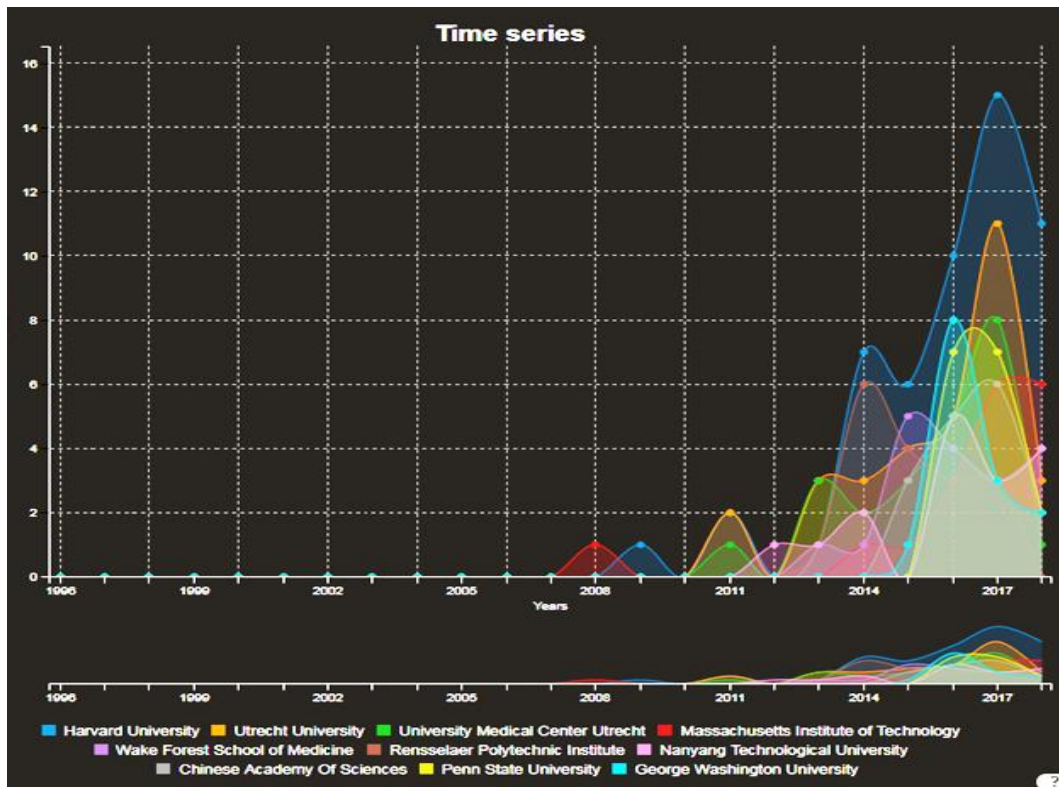


Figure 5.5. Scientific publication production trend from 2007 to 2019

Contributions on scientific publications regarding 3D bioprinting released by Universities and Institutions.

As shown in Figure 5.5, the most prolific countries and institutions in terms of scientific output in the 3D bioprinting application are the United States of America (USA) and in particular Harvard University, Massachusetts Institute of Technology and Wake Forest School of Medicine. The second best performing country is China with the China Nanyang Technological University (Singapore) and Chinese Academy of Science. In Europe, the Netherlands was the country with the highest scientific production with Utrecht University and University Medical Center Utrecht. Furthermore, Figure 5.6 represents the network analysis that allow to organize data based on the location of entities that are publishing, patenting or are beneficiaries of EU projects, the collaborations among these entities and journal categories of publishing.

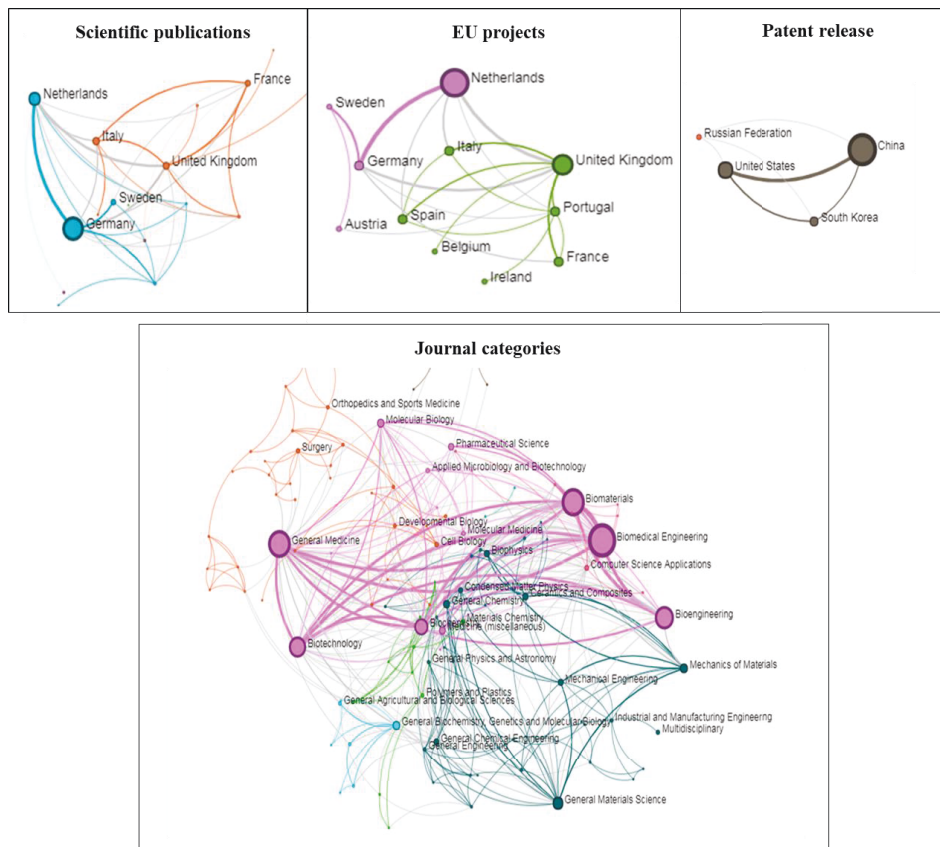


Figure 5.6. Network analyses.

Data visualization by network for what concern scientific publications, EU funded projects, patent release and journal categories for publication. The size of the nodes expresses the number of documents retrieved for an organization, location, topic or other; edges (lines between two nodes) the co-occurrence in the same documents and the edge thickness is relative to number of documents in common; different colors show the communities of nodes that tend to appear more together than with the others.

For what concern the European network, the node size revealed that Germany and Netherlands are the countries mainly involved in scientific production and for the access to EU funding. Moreover, they actively collaborating each other in these fields as they linked from the same colored edges. United Kingdom is the second country for its presence in European projects and their activity is mainly linked with Italy, Spain, Portugal and France. Interestingly, for what concern the ability in patent depositing, China is the most prolific country followed by USA and South Korea. Finally, TIM analysis showed the journal categories mainly involved for the scientific communication that included Biomedical Engineering, Biomaterials, General Medicine, Bioengineering and Biotechnology as predominant journals.

5.5 Conclusions

3D bioprinting has particularly advanced in the orthopaedics field, especially in custom-made prostheses and implants for bone and cartilage tissue engineering. Many ongoing research efforts are aimed at obtaining 3D tissue-grafts of greater complexity with better ability to mimic tissue behavior *in vivo*. Hydrogel-based matrices have received considerable interest as tissue scaffolds due to their biocompatibility and structural similarities to natural ECM. The use of composite materials combining polymer and ceramic biomaterials has shown to improve biomaterial strength and biodegradability while inducing an adequate host immune response. Furthermore, there is a growing use of dECM in scaffolds, hydrogels and bioinks due to its resemblance with the native ECM. With regard to the type of cells used in the bioink, mesenchymal stem cells derived from bone marrow and adipose tissue are the most widely and successfully used in bioprinting. Notable success has already been achieved using extrusion-based bioprinting with alginate carriers and scaffold-free bioinks for cartilage and bone tissue bioprinting. However, there are still some limitations to overcome before this technology reaches clinical application, e.g. the standardization of the bioprinting process, scaffold production and cell source selection in order to achieve better reproducibility of the process.

The growing interest in 3D bioprinting was confirmed also by results obtained using the recent TIM platform, that showed a progressive increase in the research & development activity in the healthcare field (including orthopaedics), in the last decade. This positive trend was mainly derived by the intensive scientific production worldwide with particular attention by USA and China countries. Moreover, as 3D bioprinting is an emerging technology in the early stage of development, it is probably premature to observe also a high number of patents released in that field.

5.6 References

1. Murphy S V., Atala A. 3D bioprinting of tissues and organs. *Nat Biotechnol* [Internet]. 2014;32(8):773–85. Available from: <http://dx.doi.org/10.1038/nbt.2958>
2. Huang Y, Zhang XF, Gao G, Yonezawa T, Cui X. 3D bioprinting and the current applications in tissue engineering. *Biotechnol J*. 2017;12(8).
3. Turnbull G, Clarke J, Picard F, Riches P, Jia L, Han F, et al. 3D bioactive composite scaffolds for bone tissue engineering. *Bioact Mater*. 2018;3(3):278–314.
4. Zhang L, Yang G, Johnson BN, Jia X. Three-dimensional (3D) printed scaffold and material selection for bone repair. *Acta Biomater* [Internet]. 2019;84(November):16–33. Available from: <https://doi.org/10.1016/j.actbio.2018.11.039>
5. Moroni L, Boland T, Burdick JA, De Maria C, Derby B, Forgacs G, et al. *Biofabrication: A Guide to Technology and Terminology*. Trends in Biotechnology. 2018.
6. Gomes ME, Rodrigues MT, Domingues RMA, Reis RL. Tissue engineering and regenerative medicine: new trends and directions - A year in review. *Tissue Eng - Part B Rev*. 2017;23(3):211–24.
7. Kang HW, Lee SJ, Ko IK, Kengla C, Yoo JJ, Atala A. A 3D bioprinting system to produce human-scale tissue constructs with structural integrity. *Nat Biotechnol* [Internet]. 2016;34(3):312–9. Available from: <http://dx.doi.org/10.1038/nbt.3413>
8. Lai Y, Li Y, Cao H, Long J, Wang X, Li L, et al. Osteogenic magnesium incorporated into PLGA/TCP porous scaffold by 3D printing for repairing challenging bone defect. *Biomaterials*. 2019;
9. Liu D, Fu J, Fan H, Li D, Dong E, Xiao X, et al. Application of 3D-printed PEEK scapula prosthesis in the treatment of scapular benign fibrous histiocytoma: A case report. *J Bone Oncol*. 2018;
10. <https://clinicaltrials.gov>. <https://ClinicalTrials.gov>. U.S. National Institutes of Health. 2019.
11. Merceron TK, Burt M, Seol YJ, Kang HW, Lee SJ, Yoo JJ, et al. A 3D bioprinted complex structure for engineering the muscle-tendon unit.

- Biofabrication [Internet]. 2015;7(3):35003. Available from:
<http://dx.doi.org/10.1088/1758-5090/7/3/035003>
12. Kang HW, Lee SJ, Ko IK, Kengla C, Yoo JJ, Atala A. A 3D bioprinting system to produce human-scale tissue constructs with structural integrity. *Nat Biotechnol.* 2016;
 13. Moro A, Boelman E, Joanny G, Lopez-Garcia J. A bibliometric-based technique to identify emerging photovoltaic technologies in a comparative assessment with expert review. *Renew Energy.* 2018;
 14. Moro A, Joanny G, Moretti C. Emerging technologies in the renewable energy sector: A comparison of expert review with a text mining software. *Futures.* 2020;
 15. Elsevier. Scopus | The largest database of peer-reviewed literature. About Scopus. 2017.
 16. Aljohani W, Ullah MW, Zhang X, Yang G. Bioprinting and its applications in tissue engineering and regenerative medicine. *Int J Biol Macromol* [Internet]. 2018;107(PartA):261–75. Available from:
<https://doi.org/10.1016/j.ijbiomac.2017.08.171>
 17. Pati F, Jang J, Ha DH, Won Kim S, Rhie JW, Shim JH, et al. Printing three-dimensional tissue analogues with decellularized extracellular matrix bioink. *Nat Commun* [Internet]. 2014;5:1–11. Available from:
<http://dx.doi.org/10.1038/ncomms4935>
 18. Pati F, Song TH, Rijal G, Jang J, Kim SW, Cho DW. Ornamenting 3D printed scaffolds with cell-laid extracellular matrix for bone tissue regeneration. *Biomaterials.* 2015;
 19. Ashammakhi N, Hasan A, Kaarela O, Byambaa B, Sheikhi A, Gaharwar AK, et al. Advancing Frontiers in Bone Bioprinting. *Adv Healthc Mater.* 2019;8(7):1–24.
 20. Bäckdahl H, Helenius G, Bodin A, Nannmark U, Johansson BR, Risberg B, et al. Mechanical properties of bacterial cellulose and interactions with smooth muscle cells. *Biomaterials.* 2006;
 21. Siqueira P, Siqueira É, de Lima AE, Siqueira G, Pinzón-Garcia AD, Lopes AP, et al. Three-dimensional stable alginate-nanocellulose gels for biomedical applications: Towards tunable mechanical properties and cell growing. *Nanomaterials.* 2019;

22. Mertaniemi H, Escobedo-Lucea C, Sanz-Garcia A, Gandía C, Mäkitie A, Partanen J, et al. Human stem cell decorated nanocellulose threads for biomedical applications. *Biomaterials*. 2016;
23. Nguyen D, Hgg DA, Forsman A, Ekholm J, Nimkingratana P, Brantsing C, et al. Cartilage Tissue Engineering by the 3D Bioprinting of iPS Cells in a Nanocellulose/Alginate Bioink. *Sci Rep*. 2017;
24. Colosi C, Shin SR, Manoharan V, Massa S, Costantini M, Barbetta A, et al. Microfluidic Bioprinting of Heterogeneous 3D Tissue Constructs Using Low-Viscosity Bioink. *Adv Mater*. 2016;
25. Ayyildiz-Tamis D, Avcı K, Deliloglu-Gurhan SI. Comparative investigation of the use of various commercial microcarriers as a substrate for culturing mammalian cells. *Vitr Cell Dev Biol - Anim*. 2014;
26. Daly AC, Pitacco P, Nulty J, Cunniffe GM, Kelly DJ. 3D printed microchannel networks to direct vascularisation during endochondral bone repair. *Biomaterials*. 2018;162:34–46.
27. Sart S, Agathos SN, Li Y. Engineering stem cell fate with biochemical and biomechanical properties of microcarriers. *Biotechnol Prog*. 2013;
28. Leberfinger AN, Ravnic DJ, Dhawan A, Ozbolat IT. Concise Review: Bioprinting of Stem Cells for Transplantable Tissue Fabrication. *Stem Cells Translational Medicine*. 2017.
29. Dimri GP, Lee X, Basile G, Acosta M, Scott G, Roskelley C, et al. A biomarker that identifies senescent human cells in culture and in aging skin in vivo. *Proc Natl Acad Sci U S A*. 1995;
30. Ashammakhi N, Hasan A, Kaarela O, Byambaa B, Sheikhi A, Gaharwar AK, et al. Advancing Frontiers in Bone Bioprinting. *Advanced Healthcare Materials*. 2019.
31. Gao G, Cui X. Three-dimensional bioprinting in tissue engineering and regenerative medicine. *Biotechnol Lett*. 2016;38(2):203–11.
32. Keriquel V, Oliveira H, Rémy M, Ziane S, Delmond S, Rousseau B, et al. In situ printing of mesenchymal stromal cells, by laser-assisted bioprinting, for in vivo bone regeneration applications. *Sci Rep*. 2017;
33. Koch L, Gruene M, Unger C, Chichkov B. Laser Assisted Cell Printing. *Curr Pharm Biotechnol*. 2013;
34. Kim SH, Yeon YK, Lee JM, Chao JR, Lee YJ, Seo YB, et al. Precisely

- printable and biocompatible silk fibroin bioink for digital light processing 3D printing. *Nat Commun.* 2018;
35. Lim KS, Levato R, Costa PF, Castilho MD, Alcala-Orozco CR, Van Dorenmalen KMA, et al. Bio-resin for high resolution lithography-based biofabrication of complex cell-laden constructs. *Biofabrication.* 2018;
 36. Cohen DL, Malone E, Lipson H, Bonassar LJ. Direct freeform fabrication of seeded hydrogels in arbitrary geometries. *Tissue Eng.* 2006;
 37. Iwami K, Noda T, Ishida K, Morishima K, Nakamura M, Umeda N. Bio rapid prototyping by extruding/aspirating/refilling thermoreversible hydrogel. *Biofabrication.* 2010;
 38. Bishop ES, Mostafa S, Pakvasa M, Luu HH, Lee MJ, Wolf JM, et al. 3-D bioprinting technologies in tissue engineering and regenerative medicine: Current and future trends. *Genes and Diseases.* 2017.
 39. Chang R, Nam J, Sun W. Effects of dispensing pressure and nozzle diameter on cell survival from solid freeform fabrication-based direct cell writing. *Tissue Eng - Part A.* 2008;
 40. Bernal PN, Delrot P, Loterie D, Li Y, Malda J, Moser C, et al. Volumetric Bioprinting of Complex Living- Tissue Constructs within Seconds. *Adv Mater.* 2019;(August):1904209.
 41. Kumar SA, Delgado M, Mendez VE, Joddar B. Applications of stem cells and bioprinting for potential treatment of diabetes. *World Journal of Stem Cells.* 2019.
 42. Ashman O, Phillips AM. Treatment of non-unions with bone defects: Which option and why? *Injury.* 2013;
 43. Reichert JC, Saifzadeh S, Wullschlegler ME, Epari DR, Schütz MA, Duda GN, et al. The challenge of establishing preclinical models for segmental bone defect research. *Biomaterials.* 2009;
 44. Yunus Basha R, Sampath SK, Doble M. Design of biocomposite materials for bone tissue regeneration. *Materials Science and Engineering C.* 2015.
 45. Dabrowski B, Swieszkowski W, Godlinski D, Kurzydowski KJ. Highly porous titanium scaffolds for orthopaedic applications. *J Biomed Mater Res - Part B Appl Biomater.* 2010;
 46. Kim WJ, Jang CH, Kim GH. Optimally designed collagen/polycaprolactone biocomposites supplemented with controlled

- release of HA/TCP/rhBMP-2 and HA/TCP/PRP for hard tissue regeneration. *Mater Sci Eng C*. 2017;
47. Shim JH, Won JY, Park JH, Bae JH, Ahn G, Kim CH, et al. Effects of 3D-printed polycaprolactone/ β -tricalcium phosphate membranes on guided bone regeneration. *Int J Mol Sci*. 2017;18(5).
 48. Byambaa B, Annabi N, Yue K, Trujillo-de Santiago G, Alvarez MM, Jia W, et al. Bioprinted Osteogenic and Vasculogenic Patterns for Engineering 3D Bone Tissue. *Adv Healthc Mater*. 2017;
 49. Zhang Y, Yu W, Ba Z, Cui S, Wei J, Li H. 3D-printed scaffolds of mesoporous bioglass/ gliadin/polycaprolactone ternary composite for enhancement of compressive strength, degradability, cell responses and new bone tissue ingrowth. *Int J Nanomedicine*. 2018;13:5433–47.
 50. Anada T, Pan CC, Stahl AM, Mori S, Fukuda J, Suzuki O, et al. Vascularized bone-mimetic hydrogel constructs by 3D bioprinting to promote osteogenesis and angiogenesis. *Int J Mol Sci*. 2019;
 51. Keriquel V, Oliveira H, Rémy M, Ziane S, Delmond S, Rousseau B, et al. In situ printing of mesenchymal stromal cells, by laser-assisted bioprinting, for in vivo bone regeneration applications. *Sci Rep*. 2017;7(1):1–10.
 52. Fedorovich NE, Wijnberg HM, Dhert WJA, Alblas J. Distinct tissue formation by heterogeneous printing of osteo-and endothelial progenitor cells. *Tissue Eng - Part A*. 2011;
 53. Shim JH, Lee JS, Kim JY, Cho DW. Bioprinting of a mechanically enhanced three-dimensional dual cell-laden construct for osteochondral tissue engineering using a multi-head tissue/organ building system. *J Micromechanics Microengineering*. 2012;
 54. Shim JH, Kim SE, Park JY, Kundu J, Kim SW, Kang SS, et al. Three-dimensional printing of rhBMP-2-loaded scaffolds with long-term delivery for enhanced bone regeneration in a rabbit diaphyseal defect. *Tissue Eng - Part A*. 2014;
 55. Wüst S, Godla ME, Müller R, Hofmann S. Tunable hydrogel composite with two-step processing in combination with innovative hardware upgrade for cell-based three-dimensional bioprinting. *Acta Biomater*. 2014;
 56. Neufurth M, Wang X, Schröder HC, Feng Q, Diehl-Seifert B, Ziebart T, et al. Engineering a morphogenetically active hydrogel for bioprinting of

- bioartificial tissue derived from human osteoblast-like SaOS-2 cells. *Biomaterials*. 2014;
57. Wang X, Tolba E, Der HCS, Neufurth M, Feng Q, Diehl-Seifert BR, et al. Effect of bioglass on growth and biomineralization of saos-2 cells in hydrogel after 3d cell bioprinting. *PLoS One*. 2014;
 58. Wenz A, Borchers K, Tovar GEM, Kluger PJ. Bone matrix production in hydroxyapatite-modified hydrogels suitable for bone bioprinting. *Biofabrication*. 2017;
 59. TT D, G I, M G. A bioprintable form of chitosan hydrogel for bone tissue engineering. *Biofabrication*. 2017;
 60. Shim JH, Won JY, Park JH, Bae JH, Ahn G, Kim CH, et al. Effects of 3D-printed polycaprolactone/ β -tricalcium phosphate membranes on guided bone regeneration. *Int J Mol Sci*. 2017;
 61. Fedorovich NE, Schuurman W, Wijnberg HM, Prins HJ, Van Weeren PR, Malda J, et al. Biofabrication of osteochondral tissue equivalents by printing topologically defined, cell-laden hydrogel scaffolds. *Tissue Eng - Part C Methods*. 2012;
 62. Nie H, Wang CH. Fabrication and characterization of PLGA/HAp composite scaffolds for delivery of BMP-2 plasmid DNA. *J Control Release*. 2007;
 63. Shi S, Cheng X, Wang J, Zhang W, Peng L, Zhang Y. RhBMP-2 microspheres-loaded chitosan/collagen scaffold enhanced osseointegration: An experiment in dog. *J Biomater Appl*. 2009;
 64. Daly AC, Freeman FE, Gonzalez-Fernandez T, Critchley SE, Nulty J, Kelly DJ. 3D Bioprinting for Cartilage and Osteochondral Tissue Engineering. *Adv Healthc Mater*. 2017;6(22):1–20.
 65. K erour dan O, Hakobyan D, R emy M, Ziane S, Dusserre N, Fricain JC, et al. In situ prevascularization designed by laser-assisted bioprinting: Effect on bone regeneration. *Biofabrication*. 2019;
 66. Zengerink M, Struijs PAA, Tol JL, van Dijk CN. Treatment of osteochondral lesions of the talus: A systematic review. *Knee Surgery, Sport Traumatol Arthrosc*. 2010;
 67. Brittberg M, Lindahl A, Nilsson A, Ohlsson C, Isaksson O, Peterson L. Treatment of deep cartilage defects in the knee with autologous

- chondrocyte transplantation. *N Engl J Med*. 1994;
68. Benya PD, Padilla SR, Nimni ME. Independent regulation of collagen types by chondrocytes during the loss of differentiated function in culture. *Cell*. 1978;
 69. Peterson L, Vasiliadis HS, Brittberg M, Lindahl A. Autologous chondrocyte implantation: A long-term follow-up. *Am J Sports Med*. 2010;
 70. U.S. National Institutes of Health. *ClinicalTrials.gov Background*. *ClinicalTrials.gov*. 2014.
 71. Cui X, Breitenkamp K, Finn MG, Lotz M, D'Lima DD. Direct human cartilage repair using three-dimensional bioprinting technology. *Tissue Eng - Part A*. 2012;18(11–12):1304–12.
 72. Daly AC, Kelly DJ. Biofabrication of spatially organised tissues by directing the growth of cellular spheroids within 3D printed polymeric microchambers. *Biomaterials*. 2019;
 73. Kundu J, Shim JH, Jang J, Kim SW, Cho DW. An additive manufacturing-based PCL-alginate-chondrocyte bioprinted scaffold for cartilage tissue engineering. *J Tissue Eng Regen Med*. 2015;
 74. Ren X, Wang F, Chen C, Gong X, Yin L, Yang L. Engineering zonal cartilage through bioprinting collagen type II hydrogel constructs with biomimetic chondrocyte density gradient. *BMC Musculoskelet Disord*. 2016;
 75. Daly AC, Critchley SE, Rencsok EM, Kelly DJ. A comparison of different bioinks for 3D bioprinting of fibrocartilage and hyaline cartilage. *Biofabrication*. 2016;8(4).
 76. Di Bella C, Duchi S, O'Connell CD, Blanchard R, Augustine C, Yue Z, et al. In situ handheld three-dimensional bioprinting for cartilage regeneration. *J Tissue Eng Regen Med*. 2018;12(3):611–21.
 77. Levato R, Webb WR, Otto IA, Mensinga A, Zhang Y, van Rijen M, et al. The bio in the ink: cartilage regeneration with bioprintable hydrogels and articular cartilage-derived progenitor cells. *Acta Biomater*. 2017;
 78. Yang X, Lu Z, Wu H, Li W, Zheng L, Zhao J. Collagen-alginate as bioink for three-dimensional (3D) cell printing based cartilage tissue engineering. *Mater Sci Eng C [Internet]*. 2018;83(June 2017):195–201. Available from: <https://doi.org/10.1016/j.msec.2017.09.002>

79. Duchi S, Onofrillo C, O'Connell CD, Blanchard R, Augustine C, Quigley AF, et al. Handheld Co-Axial Bioprinting: Application to in situ surgical cartilage repair. *Sci Rep.* 2017;7(1):1–12.
80. Lam T, Dehne T, Krüger JP, Hondke S, Endres M, Thomas A, et al. Photopolymerizable gelatin and hyaluronic acid for stereolithographic 3D bioprinting of tissue-engineered cartilage. *J Biomed Mater Res - Part B Appl Biomater.* 2019;
81. O'Connell CD, Di Bella C, Thompson F, Augustine C, Beirne S, Cornock R, et al. Development of the Biopen: A handheld device for surgical printing of adipose stem cells at a chondral wound site. *Biofabrication.* 2016;
82. Andrew CD, Susan EC, Emily MR, Daniel JK. A comparison of different bioinks for 3D bioprinting of fibrocartilage and hyaline cartilage. *Biofabrication.* 2016;
83. Rodríguez-Salvador M, Rio-Belver RM, Garechana-Anacabe G. Scientometric and patentometric analyses to determine the knowledge landscape in innovative technologies: The case of 3D bioprinting. *PLoS One.* 2017;12(6).
84. Sheehan T, Mironov V, Kasyanov V, Markwald RR. Recent patents and trends in bioprinting. *Recent Patents on Biomedical Engineering.* 2011.
85. Lee Ventola C. Medical applications for 3D printing: Current and projected uses. *P T.* 2014;
86. Yoo SS. 3D-printed biological organs: Medical potential and patenting opportunity. *Expert Opinion on Therapeutic Patents.* 2015.

Chapter 6

3D Bioprinting of Adipose-derived Stem Cells with Nanocellulose- Alginate bioink for tendon tissue Engineering applications

6.1 Abstract

Given the biomechanical role of tendon tissue, defining the best combination of cells and biomaterials are key challenges for the development of tendon tissue engineering strategies. Three-dimensional (3D) bioprinting represents a promising tool for bioengineered cell-laden constructs fabrication by precise and controlled cell positioning and customized 3D scaffold design. In this chapter, 3D bioprinting of ASCs within a nanofibrillar cellulose (NFC) and alginate (A) bioink well suited with the regenerative and immunomodulatory properties of human ASCs. The combination of biochemical and mechanical stimuli allowed to efficiently drive cell differentiation towards the tendon lineage with no signs of ASC inflammatory response to the 3D NFC/A substrate ensuring the safety of these xenogenic-free and FDA approved biomaterials as well as of the GMP-compliant tenogenic differentiation protocol.

*Part of the results described in this chapter will be including in the manuscript in preparation entitled “Tenogenic differentiation of human adipose-derived stem cell-laden in the nanocellulose/alginate hydrogel after 3D bioprinting” authored by **Deborah Stanco**, Monica Boffito, Alessia Bogni, Luca Puricelli, Josepha Barrero, Gianni Soldati and Gianluca Ciardelli for the submission in the special issue "Tendon/Ligament Reconstruction by Tissue Engineering" at the The International Journal of Molecular Sciences.*

6.2 Introduction

The inability of native tendon to *de novo* synthesize its extracellular matrix (ECM) is expected to be overcome by cell-based tissue engineering that aims to deliver adequate, regeneration-competent cells to the injured tendon enabling the restoration of its functions (1). Tissue engineering (TE) approaches apply biology and engineering principles combining cells, biomaterials and signaling factors (2). As a biological building block, cells play a primary role in the development and maintenance of tendon extracellular matrix (ECM) homeostasis; biomaterials properly micro-fabricated into scaffolds mimic the natural microenvironment and provide mechanical-physical support to cells; signaling factors as growth factors progressively guide tissue development.

As previously reported, adipose derived stem cells (ASCs) have the potential to be employed for tendon TE as they are an efficient and safe tool to modulate the microenvironment of the tendon niche *in vitro* and to reduce inflammation improving tendon healing *in vivo*. Although the optimum conditions to drive tendon cell differentiation have not been identified yet, several attempts have been made on ASC *in vitro* using growth factors (3–6), mechanical cues (7) or combination of mechanical and biochemical stimuli (8). Nanofiber materials have been proposed as suitable scaffolds for tendon TE since their natural microporous structure and composite properties resembling the ultrastructure of tendon, provide cell-cell interactions and porosity to encourage remodeling (9). Cell substrates can be based on synthetic or natural polymers or a combination of both to mimic ECM composition and the multiple hierarchical collagen fibrous structure proper of tendon tissue (10). For instance, Yang et al. recently reported the design of a multilayered fiber-hydrogel scaffold to closer mimic the tendon structure by simultaneous co-electrospinning of poly-caprolactone (PCL) and methacrylated gelatin. The combination of nanofibrous structures and hydrogels provided the aligned topographical cues and contributed to the tenogenic differentiation of the embedded ASCs (11). However, conventional fabrication techniques, such as electrospinning, electrochemical alignment, knitting and freeze-drying, are less practical in terms of clinical translation as well as their scale up production or standardization (10). Moreover, the traditional tissue-

engineered construct production, consisting in the manual cell seeding over the scaffold, possesses several limitations including a non-homogenous cell distribution, the inability to spatially distribute multiple cell types, and the poor control over scaffold microarchitecture.

Three-dimensional (3D) bioprinting represents a promising tool that can potentially overcome these limitations allowing 3D complex cell culture system fabrication with precise and controlled cell positioning, which finally results in bioengineered cell-laden constructs (12). Among the available printing systems (cp chapter 5), the extrusion-based method allows the microfabrication of complex structures combining different cell types and materials into a bioink that can be printed with high cell densities but low speed and resolution (13). To date, the literature reports only one study applying 3D bioprinting for muscle-tendon junction TE (14). In this work, the authors employed an integrated organ printing (IOP) system to fabricate a muscle-tendon unit construct composed of four different elements: two thermoplastic structural polymers, to resemble elasticity and stiffness of muscle and tendon, were used as a scaffolds for the bioprinting of two cell-laden hydrogels that provided terminally differentiated myoblasts on the muscle part and fibroblasts at the tendon part. After 7 days of culture in FBS standard medium, collagen type I deposition at the tendon side of the construct was observed.

In such a context characterized by a scarce number of reports concerning tendon tissue engineering based on 3D bioprinting systems, the study here presented was designed to evaluate the 3D bioprinting of ASCs and their differentiation towards a tenogenic phenotype. To this aim ASCs were embedded into a commercially available bioink (Laminik+, Cellink) composed of nanofibrillar cellulose (NFC) and alginate (A) combining with a blend of ECM-laminin proteins to support cellular response. No published data are available to date concerning this bioink. Nanofibrillar cellulose and alginate are natural, xenogenic-free and FDA-compliant materials which make them very attractive for biomedical applications. Nanofibrillar cellulose has been successfully employed as reinforcing agent in many biodegradable polymeric compositions for their high tensile strength properties, capacity to retain water and tunable surface chemistry properties (15). Moreover, their fibrillary structure, resemble the collagen fibrils of tendon. Alginate has been widely used in cell encapsulation, cell transplantation and tissue

engineering; it forms stable gels in the presence of certain divalent cations, such as calcium ions, and provides a biocompatible environment suitable for downstream processes such as *in vitro* cell culture or *in vivo* experiments (16). Only recently, few studies have been done to investigate the 3D bioprinting feasibility of NFC/A hydrogel for cartilage TE. In detail, the bioink turned out to allow the 3D bioprinting of the desired architecture structures and to support proliferation and differentiation towards the chondrogenic lineage of the encapsulated chondrocytes or induced pluripotent stem cells (iPSCs) (17–20).

To the best of our knowledge, NFC/A hydrogels have never been used to bioprint ASCs and drive tenogenic differentiation. First, in this study, in order to identify an appropriate environment for cell survival and proliferation, printability of the bioink, morphological properties of the printed scaffolds as well as the appropriate cell density for the printing process in terms of cell viability and proliferation were evaluated. Moreover, the ability of ASCs embedded in the 3D NFC/A constructs to differentiate toward tendon lineage was assessed using the biochemical induction of TENO medium established before in 2D cell culture conditions (cp chapter 4) consisting in the xenogenic serum-free culture media supplemented with a mixture of growth factors and soluble factors (BMP-12, CTGF, TGF- β 3 and ascorbic acid) (4). The combination of biochemical and physical (i.e, morphological and mechanical) cues in the tenogenic induction of 3D cell-constructs were then evaluated in term of cell morphology and expression of specific tendon-related markers.

6.3 Materials and Methods

6.3.1 Bioink characteristics

The bioink (Laminink+, Cellink, Sweden) consists in a mixture of nanocellulose fibers (NFC) and alginate (A) with the addition of the ECM proteins laminin 111, 121, 411 and 521 (Fig 6.1). It is a commercial available product delivered in a sterile 3 ml cartridge, and tested to have an endotoxin level < 40 EU/ml and pH range of 6.5-7.4. Unfortunately no further specifications about fabrication method and concentration of the components have been provided from the manufacturer.



Figure 6.1. 3D printing equipment

From the left the 3D bioprinter BIOIX, the Laminink+ bioink and the crosslinking agent all provided by Cellink (Sweden).

6.3.2 3D printing of nanocellulose-alginate scaffolds

In this study, a micro-extrusion based three-syringe cell bioprinter (BioX, Cellink) was used to print the NFC/A scaffolds. The scaffold design model used in this work was a square 5 X 5 X 1 mm with 200 μ m layer height and nozzle diameter and 20% infill density determined by the G-Code file of the printing device software (Fig 6.2). To repeat the same methodology used to bioprinting cells, the injectable ink was prepared by mixing 1 ml of hydrogel with 100 μ l of Minimum

Essential Medium (MEM) α without nucleosides with Glutamax or Hanks' Balanced Salt (HBSS⁺⁺) solution with calcium and magnesium (both by Thermofisher Scientific, USA) that were then thoroughly mixed by connecting two luer lock syringes. To allow printability, the prepared ink was introduced into a sterilized 3 ml polyethylene injection cartridge (Cellink) then fixed into the printing device previously sterilized with own UV light (Fig 6.3). After G-Code model selection, scaffolds were printed layer-by-layer via ink extrusion as a fiber in a 24 multi-well plate at room temperature (about 25 °C). Typically, air pressure was set to 9-14 kPa, speed was 5 mm/s, and nozzle size 27 gauges. The projected area of each scaffold was 5 X 5 mm and scaffolds consisted of 5 layers. Nanocellulose-alginate scaffolds were immersed in 5 mM CaCl₂ solution (Cellink) for 5 min to crosslink alginate, thus stabilizing the porous structure. Then scaffolds were washed three times with HBSS⁺⁺ solution to remove residual CaCl₂. In order to evaluate fidelity to the CAD model and repeatability of the printing process, line width was measured for six cross-linked scaffolds after printing using the software ImageJ.

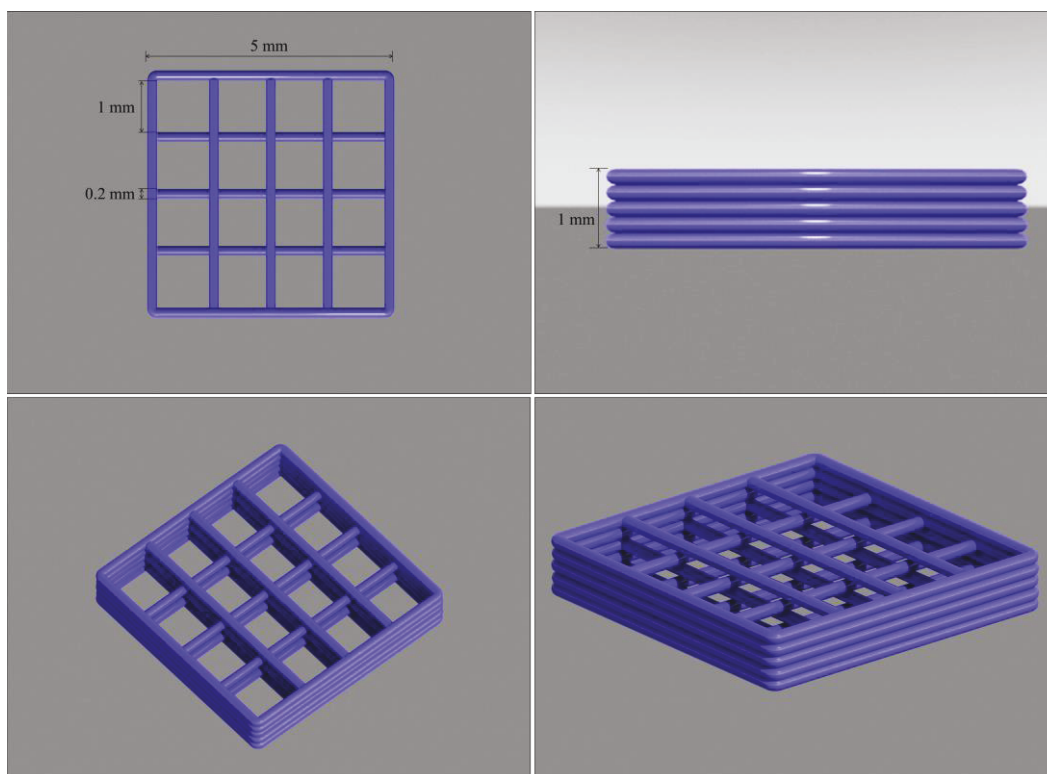


Figure 6.2. 3D scaffold design

Upper panels show top (left) and side (right) view, bottom panels show perspective projection images of the 3D NFC/alginate scaffold.

6.3.3 Rheological characterization of the bioink

Rheological characterization of the NFC/A bioink was conducted using a stress-controlled rheometer (MCR302 Anton Paar) equipped with a Peltier system for temperature control and a 25 mm parallel-plate geometry. In detail, the native bioink was characterized before crosslinking by rheological strain sweep and frequency sweep tests at 25 °C, that is the cartridge and printing platform temperature during the layer-by-layer deposition. In detail, strain sweep test was conducted at constant frequency (1 Hz) within the strain range from 0.01 and 500% with the aim to define the linear viscoelastic (LVE) region and Yield Stress (YS, i.e., the value of shear stress at the maximum of Loss Modulus) that characterized the bioink. Then, frequency sweep test was conducted within the LVE by varying angular frequency within the range 0.1-100 rad/s. The same characterizations were also conducted on cross-linked bioink to assess the effects of the crosslinking process on the rheological properties of the gel. Cross-linked gel was also characterized at 37 °C that is its temperature in incubator during 3D cell cultures. Before each test, the bioink was deposited on the bottom plate of the rheometer at 25 °C and left to equilibrate for 10 minutes at the testing temperature before the analysis. In order to test the cross-linked bioink, the hydrogel was crosslinked for 5 minutes according to supplier's instruction and then equilibrated at the testing temperature for 10 minutes and finally tested.

6.3.4 Swelling ratio

The fluid content of the prepared hydrogel scaffolds (N=6) was measured immediately after gelation (0h) and after 24 hour incubation in culture medium (500 µl/scaffold). At each time point, scaffolds were slightly dried with a filter paper to remove surplus aqueous medium and weighed (W_s). Then samples were dried at 50 °C in a dryer for 30' and weighed again (W_d). The swelling capacity of the hydrogels was estimated using equation (1):

$$\text{Swelling \%} = \frac{(W_s - W_d)}{W_d} \times 100$$

6.3.5 Cell isolation and culture expansion

Human adipose-derived stem cells were isolated from subcutaneous adipose tissue of healthy donors undergoing liposuction and their characterization is already reported elsewhere (4). All the medical procedures were approved by the Ethical Committee of the Canton Ticino, Switzerland (CE 2961). All subjects were in good health and provided their written consent before participating to the study. The collected stromal vascular fractions were plated at a cell density of 10^4 cells/cm² and cultured in the 5% hPL xenogenic-free expansion medium consisting in α MEM without nucleosides with Glutamax (Fisher Scientific, USA) supplemented with 5% pooled human platelet lysate (hPL, Stemulate, Cook Regentec, USA), 100 Units/ml Penicillin and 100 Units/ml of Streptomycin (Fisher Scientific, USA). The medium was changed every three to four days and passaged upon reaching 90%. After approximately 7 days of culture, cells were harvest by trypsin treatment (0.5% trypsin/0.2% EDTA; Sigma-Aldrich, USA) for 5 minutes and then counted by trypan blue exclusion. To obtain the number of cells needed for the 3D bioprinting experiments, the cells were plated in the 5% hPL xenogenic-free expansion medium on T150 cell culture flasks (Nunc) at a cell density of 3000 cell/cm². For cryopreservation cells were centrifuged at 400 g for 5 minutes, resuspended in an ice-cold solution of 1% albumin solution, 5.5% ME₂SO and 4.5% dextran-40 (Cryosure DEX-40, WAK-Chemie Medical GmbH, Germany) in α MEM and transferred into a 2 ml cryovial (Nalgene, Thermo Fisher Scientific, Waltham, USA). As previously described, cells were frozen by means of a programmable freezer (Consartic GmbH, Germany) under the following conditions: from 4 °C to 0 °C in 6 minutes, then hold for 15 minutes at 0 °C. From 0 °C to -2 °C in 9 minutes and then kept at -2 °C for 2 minutes. From -2 °C to -35 °C in 25.5 minutes and finally, from -35 °C to -100 °C in 13 minutes (4). Cryovials were then transferred into liquid nitrogen for long-term storage. After thawing, cells at passage 3 (N=4) were analyzed to mycoplasma detection. Samples were prepared by collecting 500'000 ASCs and their supernatant of three days of culture, which were then analyzed by Mycoplasma Diagnostic Service (Minerva Analytix GmbH, Germany). All samples resulted negative to mycoplasma contamination (data not shown). For 3D bio-printing experiments ASC populations at passage 4 were used.

6.3.6 Bioprinting of ASCs

For the bioprinting of cellularized constructs, ASCs at passage 4 (n=3) were resuspended within the bioink (Laminink+) in a ratio of 1:9 at a final concentration of 3, 6 or 9 x 10⁶ ml⁻¹ of ASCs/ml of bioink (N=3) to test the effect of different cell densities on cell viability and morphology after printing. To this aim, pellets were resuspended in 100µl of CTRL medium consisting in MEMα without nucleosides with Glutamax (Fisher Scientific) supplemented with 2% pooled human platelet lysate (hPL, Stemulate, Cook Regentec, USA), 100 Units/ml of Penicillin and Streptomycin (Fisher Scientific). Afterwards, ASC suspensions were gently mixed within 1 ml of bioink at room temperature (about 25 °C) by sterile luer locks syringes, until homogeneous, then dispensed in an empty cartridge and finally fixed into the printing device. After scaffold design selection, cell-laden scaffolds were printed layer-by-layer in 24 multi-well plates. Table 6.1 summarizes the detailed printing and crosslinking parameters.

Table 6.1. 3D bioprinting parameters

List of materials and methods used for 3D bioprinting of ASCs in the NFC/A hydrogel.

MATERIAL	
Trade name	Cellink Laminink+
Composition	Nanofibrillar cellulose, alginate, laminin proteins
MIXING PARAMETERS	
Ratio*	9:1
Material Temperature (°C)	22-25
Nozzle (gauge)	27
PRINTING PARAMETERS	
Pressure (kPa)	9-14
Speed (mm/sec)	5
Bioink Temperature (°C)	22-25
CROSSLINKING PARAMETERS	
Method	5 mM CaCl ₂
Time (min)	5

*ratio of biomaterial to cell suspension in the respective cell culture medium

The bioprinting parameters were established as listed below. The ratio between material and cells, as well as the nozzle diameter, were kept constant, and the printing pressure was adjusted as required in the range of 9-14 kPa. After crosslinking, the cell-laden scaffolds were cultured for 14 days in CTRL medium consisting of MEM α without nucleosides with Glutamax (Fisher Scientific, USA) supplemented with 2% pooled human platelet lysate (hPL, Stemulate, Cook Regentec, USA), 100 Units/ml Penicillin and 100 Units/ml of Streptomycin (Fisher Scientific, USA) at 37 °C 5% CO₂ in humidified incubator. The schematic illustration of the bioprinting process including bioink preparation is depicted in Figure 6.3.

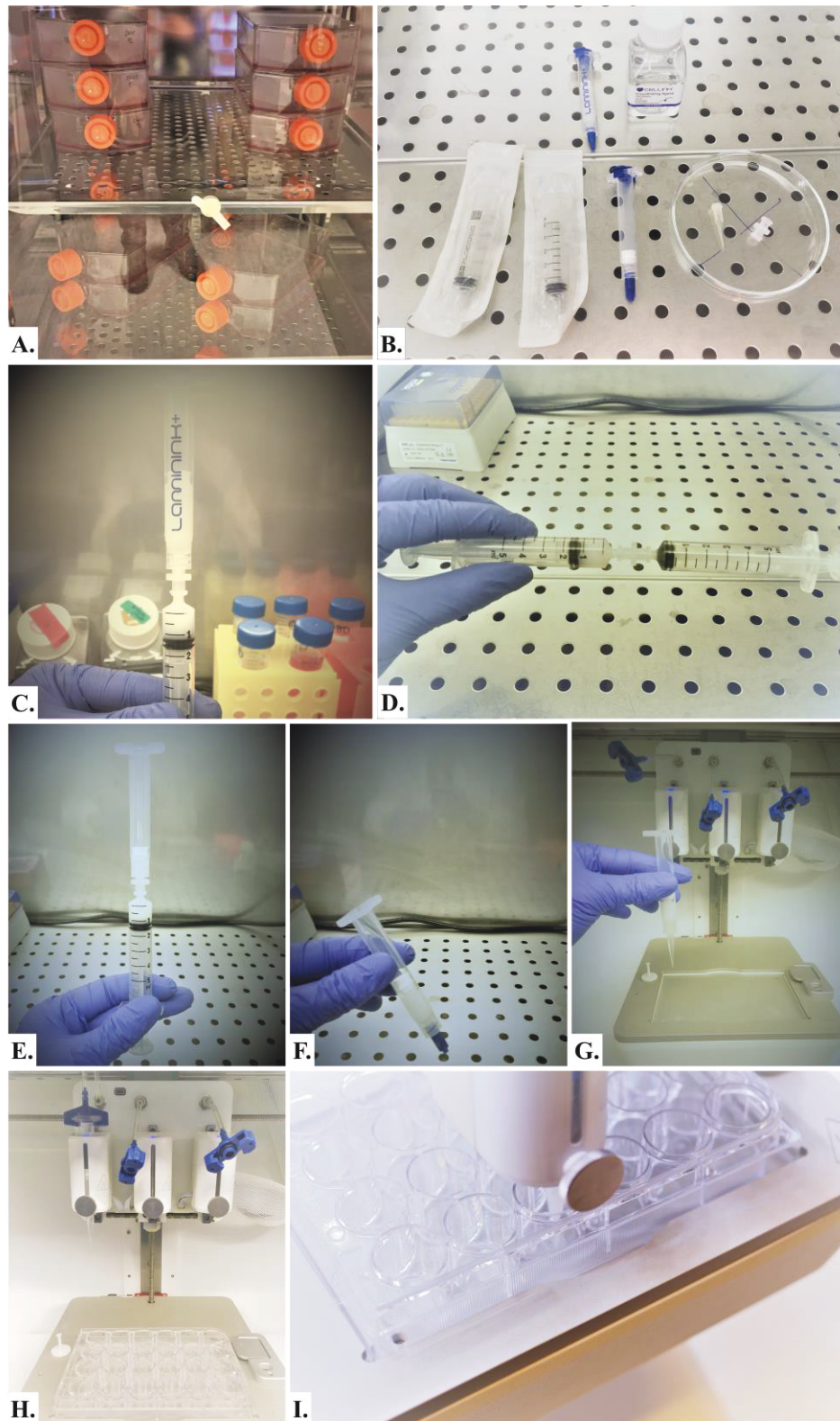


Figure 6.3. 3D bioprinting procedure.

A. ASCs at passage 3 cultured in T150 flasks at 37 °C 5% CO₂ in humidified incubator to obtain the cell number needed for printing; **B.** materials and reagents needed for 3D bioprinting, including the Laminink+ bioink, the crosslinking reagent, two luer lock syringes, an empty cartridge, the sterile 27G nozzle and luer lock connector; **C. D.** mixing of 1 ml of bioink with 100 µl of cellular suspension; **E.** filling of an empty cartridge with the homogenous bioink suspension; **F.** cartridge plugging on the bottom to reduce air bubbles; **G.** insertion of the prepared cartridge into the 3D printing device; **H. I.** 3D bioprinting of ASC laden-NFC/A in 24 multi-well plate.

6.3.7 Cell Viability

Fluorescence-based live and dead assay was used to evaluate the cell viability in the bioprinted 3D cell-laden scaffolds at 1, 3, 7 and 14 days in all culture conditions. The simultaneous use of two fluorescent dyes allows a two-color discrimination of the population of living cells from the dead-cell population. In particular, after washing with HBSS twice, samples were stained using 20 mg/ml fluorescein diacetate (FDA) and 1.6 mg/ml propidium iodide (PI) (both from Sigma-Aldrich) in MEM α , for 5 min at room temperature (RT) in the dark. When FDA stains viable cells the non-fluorescent FDA was converted by the cells into the green fluorescent metabolite fluorescein and visualized as green fluorescence under Green Fluorescent Protein (GFP) channel (Emission: 525 nm). This esterase fluorescent-based method is commonly used as a cell viability assay. In contrast, the nuclei staining dye PI cannot pass through a viable cell membrane. It reaches the nucleus by passing through disordered areas of dead cell membranes, and intercalates with the DNA double helix of dead cells and interacts with nucleotides to emit fluorescence visualized under mCherry Fluorescent Protein channel (Emission: 630 nm). Fluorescent microscopy Zeiss Axiovert Apotome was used to visualize the living and dead cells and three representative images were taken from each scaffold (magnification of 10X).

Quantitative analysis of cell viability and proliferation was performed in all 3D culture conditions by Alamar Blue Assay (Thermo Fisher Scientific, USA) at 1, 3, 7 and 14 days of culture after printing (21). This bioassay incorporates a fluorometric/colorimetric growth indicator based on the detection of metabolic activity. Specifically, the oxidation-reduction indicator resazurin is a proven cell viability indicator that emits fluorescence and changes color as response to chemical reduction in resorufin of growth medium resulting from cell growth (22). Moreover, Alamar is not cytotoxic allowing monitoring of cell growth of the same cell cultures over time. At the day of the evaluation cells were incubated with Alamar Blue (1:10 dilution in MEM α) for 4 hours at 37 °C in the dark. Then, supernatants were transferred to black-bottom 96-well plates and emitted fluorescence was read with Enspire plate reader (Perkin Elmer, USA).

6.3.8 Scanning electron microscopy (SEM)

Porosity and the ultrastructure morphology of fabricated scaffolds were assessed by scanning electron microscopy (Thermofisher-FEI Nova NanoLab 600 DualBeam). Due to the aqueous hydrogel's nature and the need to perform SEM analysis on dried samples, scaffolds were subjected to two different drying procedures (Freeze Drying (FD) and Crytical Point Dryer (CPD)) aiming to preserve the scaffold microstructure. Freeze drying (also known as lyophilisation) was conducted by first freezing samples in liquid nitrogen, and then dehydrating them in a vacuum so that the frozen water sublimates directly from solid to gas. In particular, here samples were freeze dried at room temperature and 20 mbar pressure overnight in a CHRIST CMC1 freeze dryer (23). Differently, for Critical Point Drying, samples were first dehydrated in 30, 50, 75, 95 and 100% ethanol solutions and then transferred to the critical point dryer (K850 Quantum Design GmbH, Germany). Dried scaffolds were mounted on self-adhesive carbon disks and sputter-coated with a conductive thin layer of gold using a magnetron sputtering reactor equipped with a pure Au target and operated in DC mode with bias voltage of 150 V (Leybold), in order to avoid accumulation of static electric charge, and consequently interference with the incoming electron beam during SEM imaging and at the same time preserving the relevant morphological and topographical features. The microscope was driven with an acceleration voltage of 5.0 kV detecting secondary electrons, working distance (WD) of 5 mm and spot size (SS) of 98 pA, using 70x, 113x, 300x, 1000x, 5000x, 800x and 8000x magnifications scale. Cell distribution in the scaffolds was visualized after 14 days of culture by fixation of the samples in 4% formaldehyde (Sigma Aldrich) for 1 hour at RT. Dried samples were obtained by dehydration in ethanol gradient series followed by critical point dryer and then visualized as above.

6.3.9 Tenogenic differentiation

For tenogenic differentiation evaluation, cell-loaded hydrogel at 6.0×10^6 ASC/ml concentration was used and 3D printed scaffolds were cultured in CTRL medium at 37 °C 5% CO₂ as described before. The day after, tenogenic differentiation of the 3D ASC-laden scaffolds was induced by culturing them in TENO medium consisting in CTRL medium supplemented with 50 µg/ml Ascorbic acid (AA;

Sigma Aldrich), 50 ng/ml BMP-12, 100ng/ml CTGF and 10 ng/ml TGF- β 3 (all from PeptoTech, UK). The differentiation was induced up to 14 days of culture changing the medium twice a week. Cells cultured in CTRL medium without any further supplementation were also used as control (4).

6.3.10 Immunofluorescence staining

Cell morphology appearance in both CTRL- and TENO-cultured 3D cell-laden constructs was evaluated after 14 days of cell culture by assessing the distribution of F-actin in fixed cells through the use of fluorescently conjugated phalloidin. Cells constructs were fixed with 4% paraformaldehyde in HBSS, then washed three times with HBSS and permeabilized with 0.5% Triton X-100 in HBSS (HBSST). After three washes with HBSS, samples were stained with 1:100 DAPI (Invitrogen) for 15 min at RT in the dark and then washed as before. Constructs were stained for 20 min at 37 °C in the dark using 1:40 Alexa Fluor 488 phalloidin antibody (Invitrogen, Thermo Fisher Scientific), then washed three times with HBSS and prepared for cryo-section. Samples were embedded in tissue freezing medium (Leica, Germany) and then frozen at -20°C . The frozen samples were transversally cryo-sectioned along microgrooves to 50 μm sections using a cryostat (Leica CM 1800). Six sections for each sample were observed and photographed under a fluorescence microscope (Zeiss Axiovert Apotome).

Expression of the transcription factor scleraxis and the extracellular matrix protein collagen type III was assessed by immunofluorescence staining after 14 days of 3D cell-laden constructs culture in both CTRL and TENO cell culture medium. Cells in the constructs were fixed with 4% paraformaldehyde in HBSS, then washed three times with HBSS, permeabilized with 0.5% Triton X-100 in HBSS (HBSST) and blocked with bovine serum albumin (BSA; from Sigma Aldrich). Immunostaining was performed overnight at 4 °C using 1:100 goat anti-human Scleraxis (HPA043183, Sigma Aldrich) and 1:500 rabbit anti-human Collagen III (PA5-34787, Invitrogen). Cells were washed three times in HBSST, incubated for 1 hour at room temperature with 1:1000 Alexa Fluor 488 rabbit anti-goat IgG (Invitrogen) and cell nuclei were counterstained with 1:100 DAPI (Invitrogen). Immunostained constructs were cryo-sectioned as shown before and six 50 μm sections for each sample were observed and photographed under a fluorescence microscope (Zeiss Axiovert Apotome).

6.3.11 Cytokines release

To identify biomarkers of inflammation, GM-CSF, IFN- γ , IL-2, IL-4, IL-6, IL-8, IL-10 and TNF- α were analyzed by measuring the secreted amount in the supernatant of both CTRL- and TENO-cultured cell-laden constructs after 3, 7 and 14 days of culture. Conditioned medium of samples treated with 20 ng/ml LPS (Lipopolysaccharides; Invitrogen) for 24h were used as positive control.

Cytokines release was tested through multiplex-enzyme linked immunosorbent assay (ELISA) by using a Bio-Plex Pro Human Cytokine 8-plex assay. Each experimental sample was run in a biological duplicate. Cytokines were measured with a Bio-Plex200 System using the Bio-Plex Manager™ software. All reagents and instruments including Washing Station and Shaker Incubator were from BIORAD (USA).

6.3.12 Statistical analysis

Data are expressed as means \pm standard deviations. The normal distribution of values was assessed by the Kolmogorov–Smirnov normality test. Statistical analyses were performed using the Student's t-test for data with a normal distribution and the Wilcoxon test for data with a non-normal distribution (GraphPad Prism v6.00; GraphPad Software, USA).

6.4 Results and Discussion

6.4.1 Characterization of the nanocellulose-alginate hydrogel

Successful and reliable bioprinting results from high printing resolution and fidelity, a homogeneous cell distribution and high cell viability post-printing (24). Various factors such as good mechanical, biodegradable and biocompatible properties of biomaterial as well as appropriate viscosity, surface tension, and cross-linking kinetics are important to determine printing accuracy and cell loading capacity of a bioink. A proper balance between physico-mechanical and biological properties of the selected biomaterial is needed to ensure high cell viability, differentiation and migration of seeded cells, as well as nutrient and oxygen diffusion in the bioprinted construct (25). Here the viscoelastic properties of the NFC/A hydrogel were rheologically analyzed at 25 °C to thoroughly characterize it at the printing temperature. First, strain sweep test was conducted for bioink characterization in terms of resistance to deformation. Figure 6.4B reports the trends of Storage and Loss Moduli (G' and G'' , respectively) as a function of applied strain within the range 0.01-500%. The CNF/alginate hydrogel exhibited the typical behavior of structured materials with G' initially constant up to a critical strain value (i.e., γ_L 1.8 %), which identifies the limiting value of the linear viscoelastic (LVE) region. Within the LVE region the characterized sample exhibited the typical behavior of a gel system ($G' > G''$). At strain higher than γ_L , G' started to decrease, while G'' initially slightly increased and then decreased, as a consequence of a slight strain hardening effect. For strain values within γ_L and the strain at G'/G'' crossover (i.e., 11.6%), micro-cracks appeared within the sample, progressively leading to the complete mechanical failure of the gel with the appearance of macro-cracks and the sample behaving as a solution ($G'' > G'$). Gel Yield Stress resulted to be 38.7 Pa. Frequency sweep test (Figure 6.4A) further confirmed the gel state of the investigated sample at 25 °C. Indeed, Storage Modulus trend turned out to be independent over angular frequency within the investigated range, as typical of fully developed gel systems. Complex viscosity linearly decreased with increasing angular frequency from 0.1 to 100 rad/s (Figure 6.4C), suggesting that the bioink possessed a shear thinning behavior, which is a key feature for printable formulations (26).

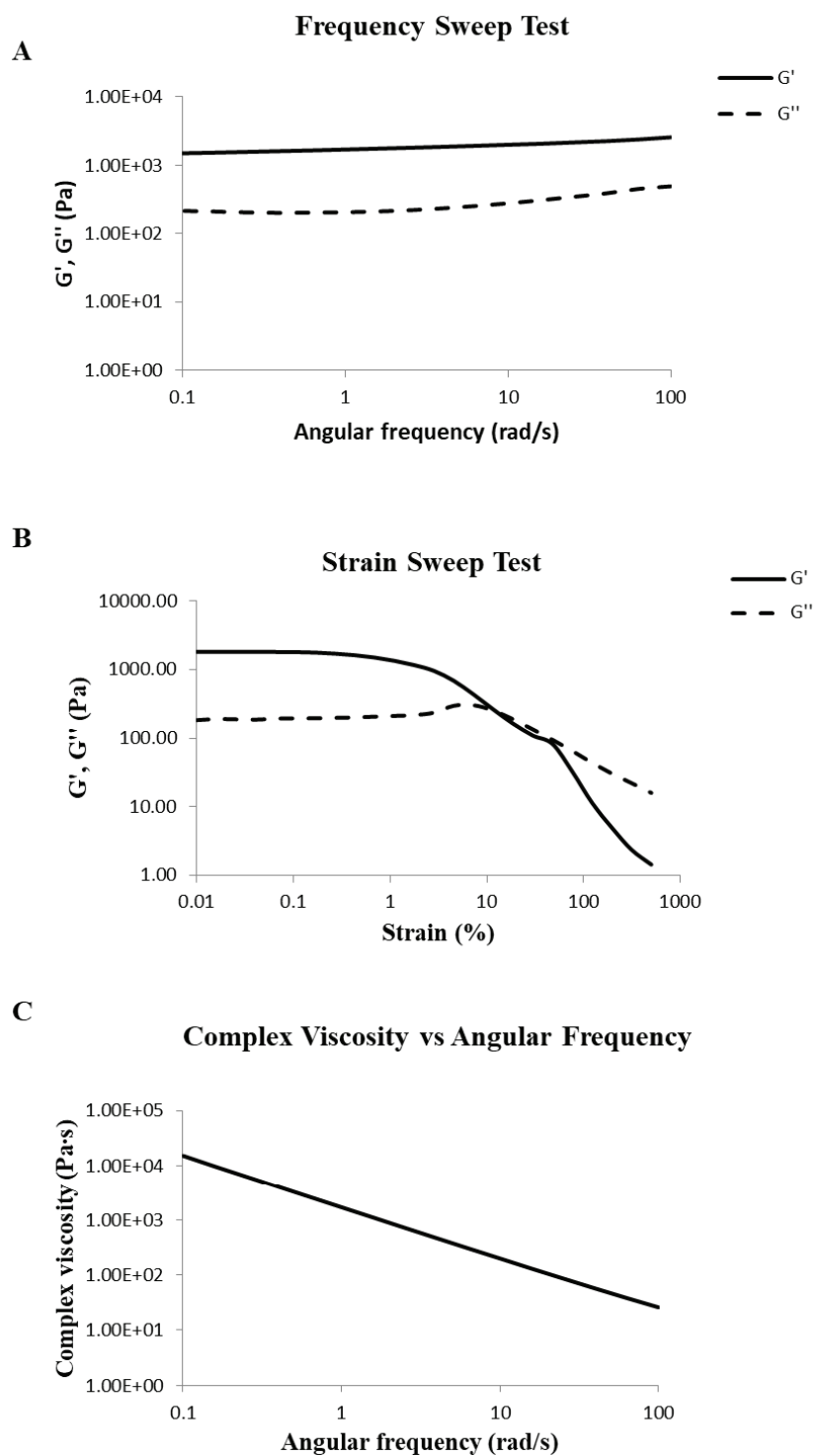


Figure 6.4. Rheological characterization of the bioink
 Storage (G') and loss (G'') moduli trends as a function of **A.** applied strain and **B.** angular frequency, both at 25 °C. **C)** Complex viscosity trend as a function of angular frequency.

The same characterizations were performed also on cross-linked gel (Figure 6.5). Both strain sweep and frequency sweep tests confirmed the successful crosslinking of the gel, with a significant increase in both G' and G'' . For instance, G' value at 0.01 % applied strain increased from 20200 Pa to 26900 Pa.

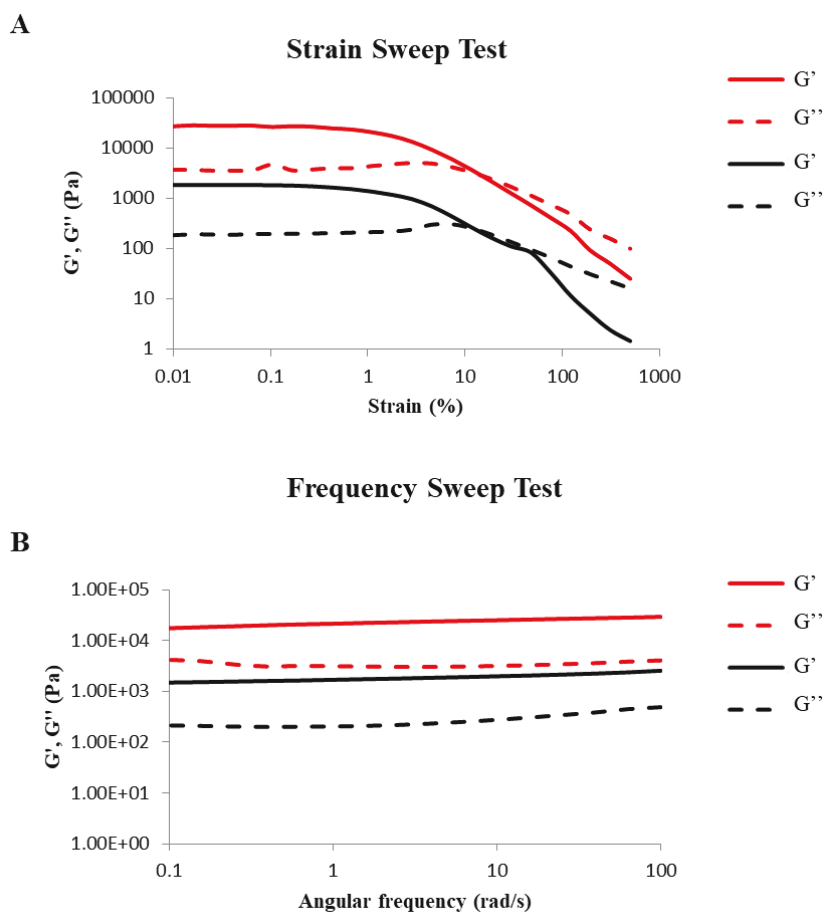


Figure 6.5. Rheological characterization of the bioink before and after cross-linking.

A. Storage (G') and loss (G'') moduli trends as a function of applied strain at 25 °C for the bioink before (black) and after (red) crosslinking. **B.** Storage (G') and loss (G'') moduli trends as a function of angular frequency at 25 °C for the bioink before (black) and after (red) crosslinking.

No significant changes in γ_L value were observed upon crosslinking (γ_L value slightly decreased from 1.8% to 1.1%).

On the other hand, Yield stress increased of one order of magnitude, from 38.7 Pa to 40.4 Pa. As expected, the crosslinking procedure improved the overall mechanical properties of the sample which still remain in the gel state (i.e., $G' > G''$, G' independent over angular frequency). Cross-linked gel was further characterized at 37 °C, which will be the real working temperature of the printed constructs. Both strain sweep and frequency sweep tests evidenced the capability of cross-linked gel to keep its mechanical properties constant, with no thermo-responsiveness (Figure 6.6).

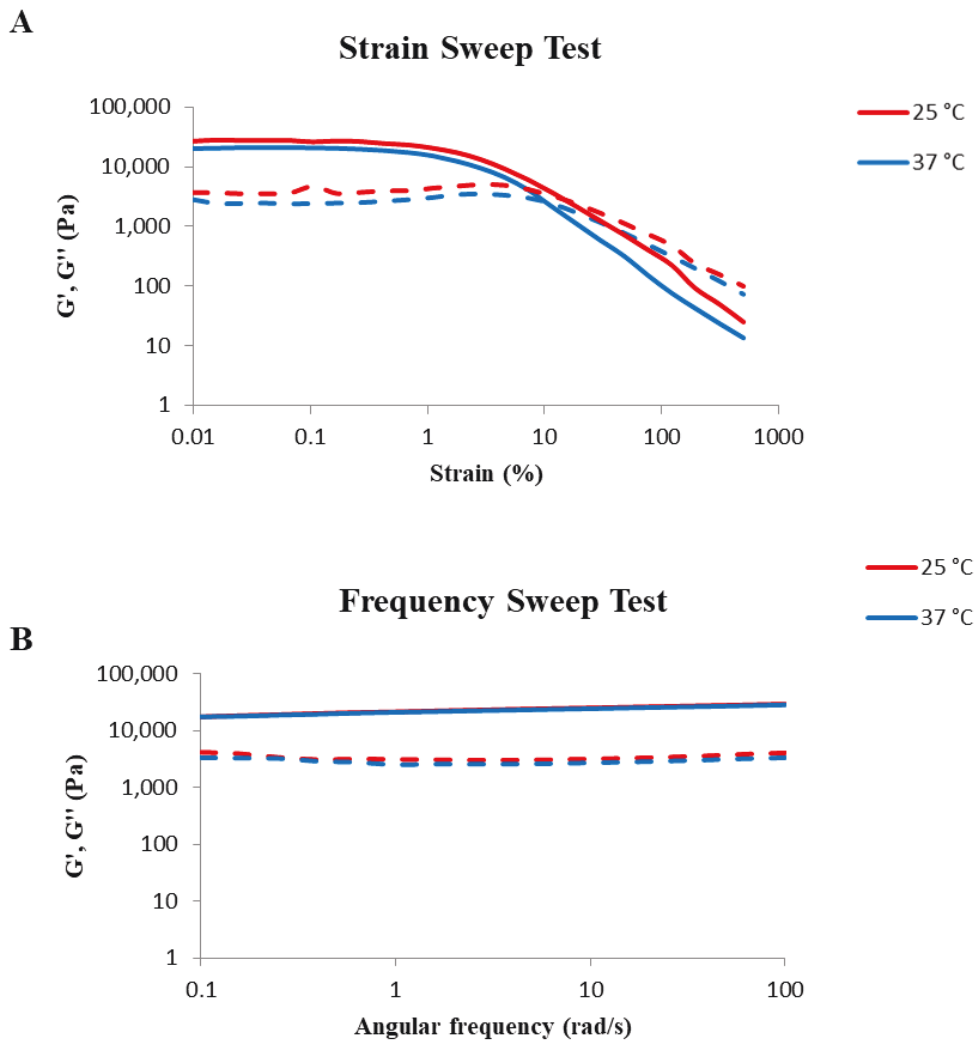


Figure 6.6. Rheological characterization of cross-linked bioink at 25 °C and 37 °C
A. Storage (G' , continuous line) and loss (G'' , dashed line) moduli trends as a function of applied strain at 25 °C and 37 °C. **B.** Storage (G' , continuous line) and loss (G'' , dashed line) moduli trends as a function of angular frequency at 25 °C and 37 °C.

6.4.2 Characterization of the 3D NFC/A scaffold

The printing parameters were set in order to obtain NFC/A scaffolds with 5 X 5 X 1 mm dimension. In order to achieve good shape fidelity of the resulting scaffolds, adequate mechanical properties and the preservation of the cell function, printing parameters were set as listed in table 1.

In particular, the precise positioning of the bioink was allowed by conical nozzle of 200 μm of diameter (27 gauge) and cell viability in the printed construct was ensured by maintaining low pressure (9-14 kPa) and speed (5 mm/sec) of deposition, which minimized shear stress and thus cell damage (27). As a result of

the printing and crosslinking processes, small 3D square shaped structures of gels were obtained, as shown in Figure 6.7 panels A-C.

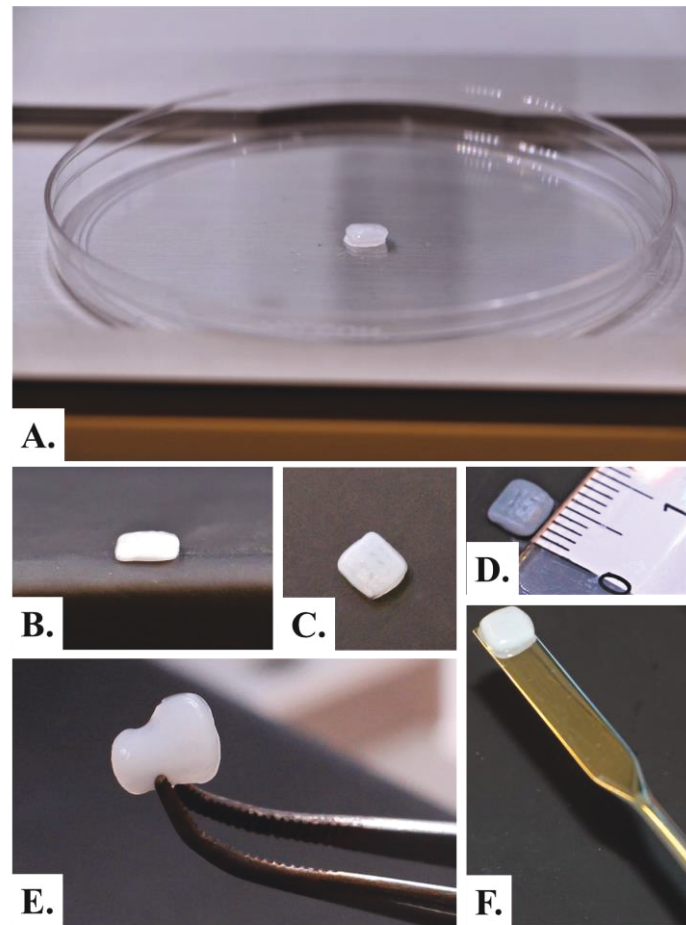


Figure 6.7. 3D printed NFC/A scaffold

A-C. Photographs of 3D printed scaffolds; **D.** the dimension of the scaffold was measured after cross-linking. **E.** The shape of the scaffold deforms while squeezing and **F.** it is restored after squeezing.

Although, it is known that alginate possesses low viscosity itself, the combination with nanocellulose in the bioink allows to achieve a good structural integrity (17,25). Macroscopically, printed scaffolds appeared opaque, white and well defined in terms of structure with an average width of 5.72 ± 0.62 mm (measured with Image J software); they deformed while squeezing and were easily handle using a spatula (Figure 6.7F). However, air bubbles in the bioink that could form during its preparation, or clogging of the nozzle sometimes occurred affecting the resulting shape. In case of these events, a non-continuous bioink deposition was observed and imperfections and structural interruptions in the scaffold were produced as depicted in the upper panels of Figure 6.8. Moreover, measurements

of single filaments evidenced a width of 1.10 ± 0.21 mm, with an increase of +81% in terms of expected with respect to their nominal dimension (0.2 mm). One explanation of this observation could be found in the low viscosity of alginate component. Indeed, as shown in the lower panels of Figure 6.8, alginate may tend to slightly collapse outside of the deposited filament, thus increasing its width (Figure 6.8). All these features can affect the good fabrication reproducibility of 3D printed NFC/A scaffolds.

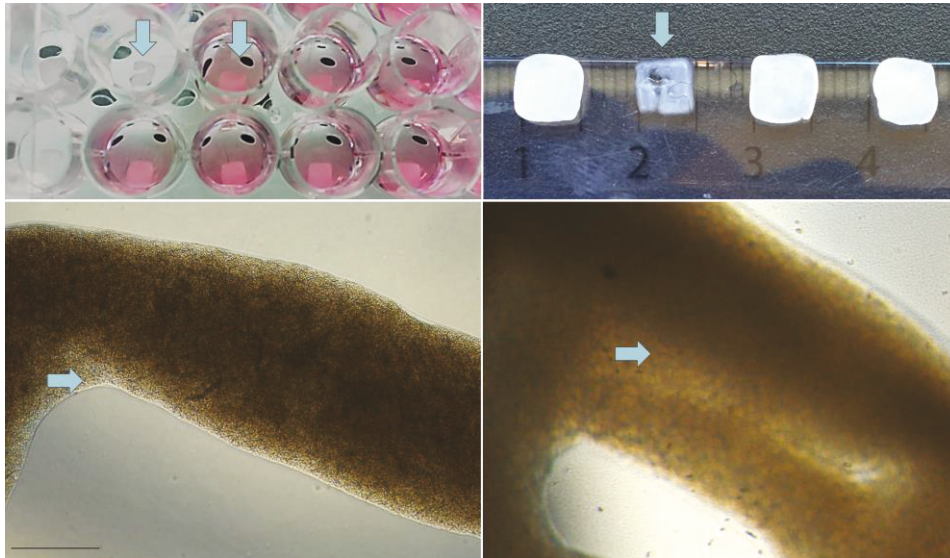


Figure 6.8. Artefacts formation during printing.

Arrows in upper panels show interruptions and imperfections resulting from the presence of air bubbles in the bioink or nozzle clogging events. Lower panels show microphotographs of the perimeter (left) and partial grid (right) of the cross-linked first layer of the scaffold (magnification 4x; scale bar 500 μ m). Arrows indicate non-homogenous bioink probably due to a sort of phase-separation between alginate and NFC.

Therefore, to evaluate the microstructure and porosity of the NFC/A 3D scaffold after printing, SEM imaging was performed on samples dried through Freeze Drying (FD) and Critical Point Dryer (CPD) techniques. Indeed, the high water content of hydrogel matrices represents one of the most challenging barriers to preserve native structural arrangement in the aqueous system (28). The analysis of hydrated materials by electron microscopy at ambient temperatures presents some problems due to their vacuum operating conditions causing liquid water to evaporate and thus altering the hydrogel structure. However, a reduction of evaporation can be performed by operating at low temperatures, but water can exist in many polymorphic crystalline structures which may detrimentally affect the structure of materials due to their lower density (hence higher volume) than

liquid water. Using critical point dryer technology the water in the constructs is replaced using liquid carbon dioxide (CO₂) at 32°C of critical temperature with pressure around 1,200 psi. At this temperature, liquid CO₂ changes to vapor without change of density. This avoids the surface tension effects, which distort specimen morphology and ultrastructure. Since CO₂ is not sufficiently miscible with water it is necessary to use intermediate fluids, such as ethyl alcohol, which are miscible with both water and CO₂. As show in Figure 6.9 CPD-SEM images clearly visualized the ultrastructure organization of the scaffold. Filament surface appeared highly porous with the typical cellulose fibrillary morphology in a nanometer range (40.41 ± 35.76 nm of diameter), which is important to assist nutrients and oxygen supply to the encapsulated cells. On the other hand, SEM images obtained by FD method resulted less effective to show the ultrastructure morphology of fibers since they appeared smoother and less defined in their nanostructure.

Critical point dryer method

Freeze dryer method

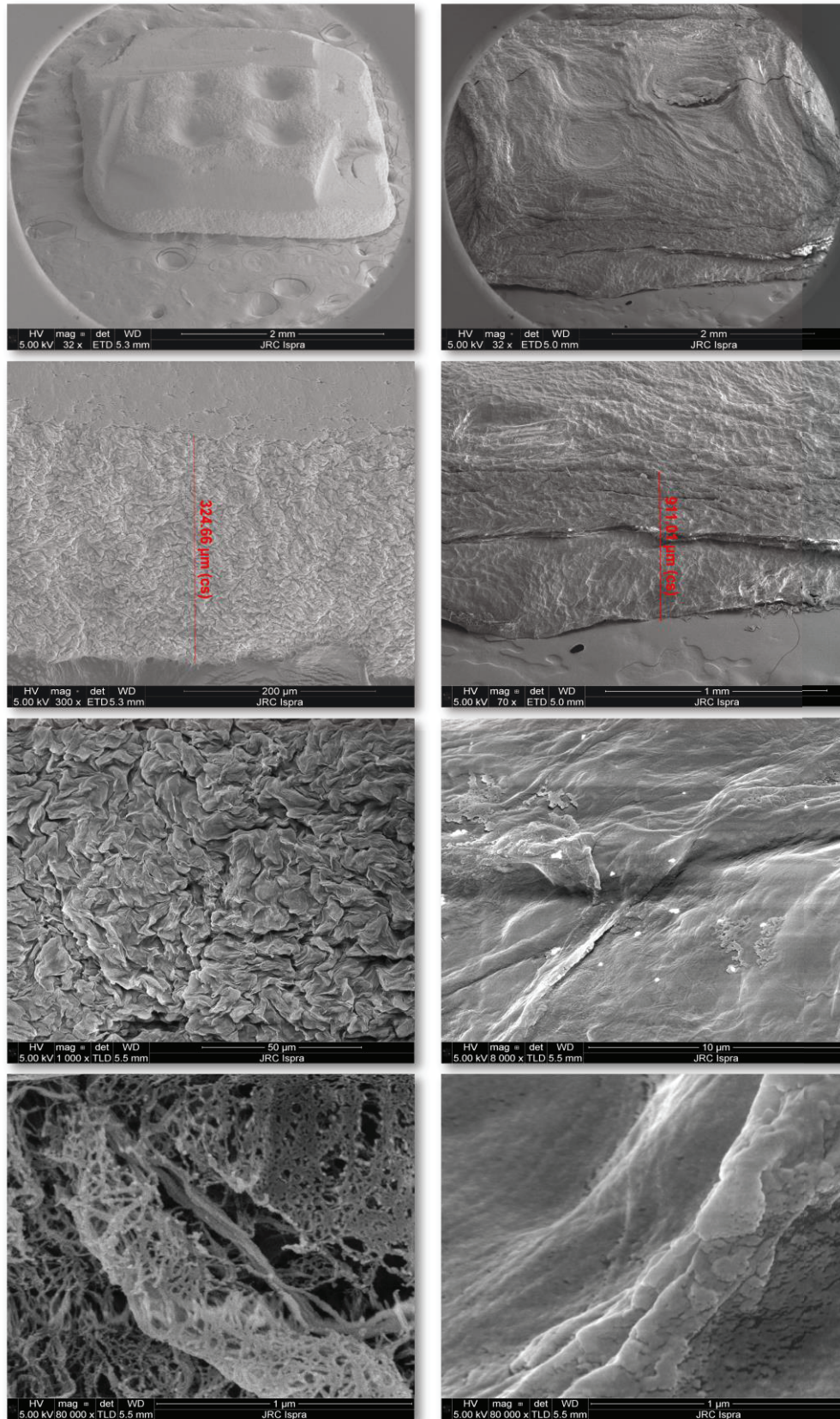


Figure 6.9. Ultrastructure morphology of the scaffold

Scanning Electron Microscopy (SEM) micrographs of 3D NFC/alginate hydrogel scaffolds dried with critical point dryer and freeze dryer techniques. Surface appearance of scaffolds after printing visualized at the top and side views.

Hydrophilicity of the scaffold is another critical feature in the evaluation of biomaterials for tissue engineering. Indeed, this feature strongly influences scaffold capability to absorb body fluids and diffuse cell nutrients and metabolites. The hydrophilicity of the nanofiber scaffold was determined by measuring the swelling ratio (29). As shown in Figure 6.10A, the average swelling ratio of as-prepared NFC/A scaffolds after crosslinking and 10 min washing in HBSS^{+/+} at RT was 311.3 ± 137.8%.

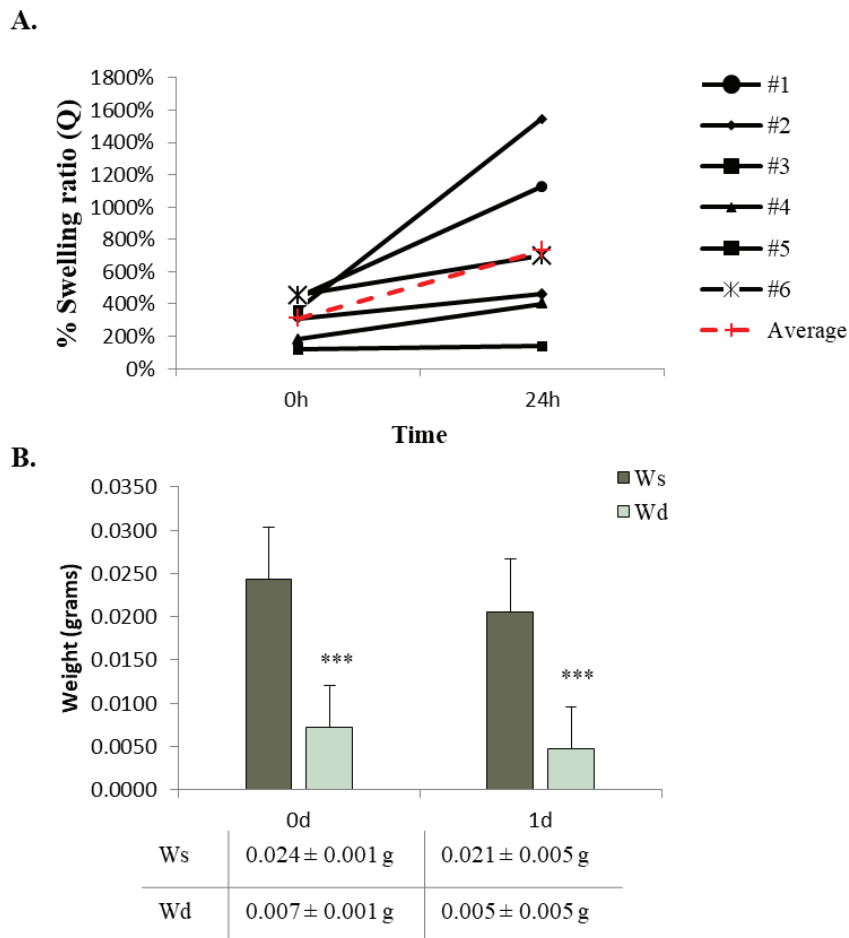


Figure 6.10. Swelling ratio

A. Swelling ratio (%) of each NFC/A scaffold (N=6) and average swelling ratio at 0 and 24 hours after printing. **B.** Average mass (g) of wet (*Ws*) and dried (*Wd*) scaffolds (***) p<0.001) at 0 and 24 hours after printing.

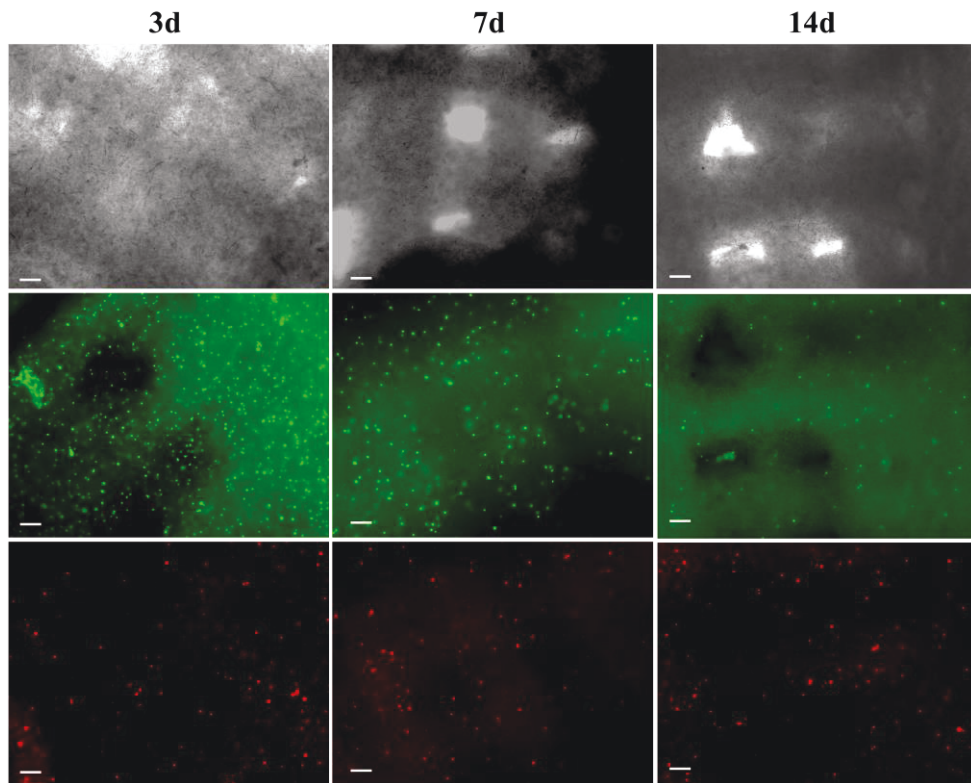
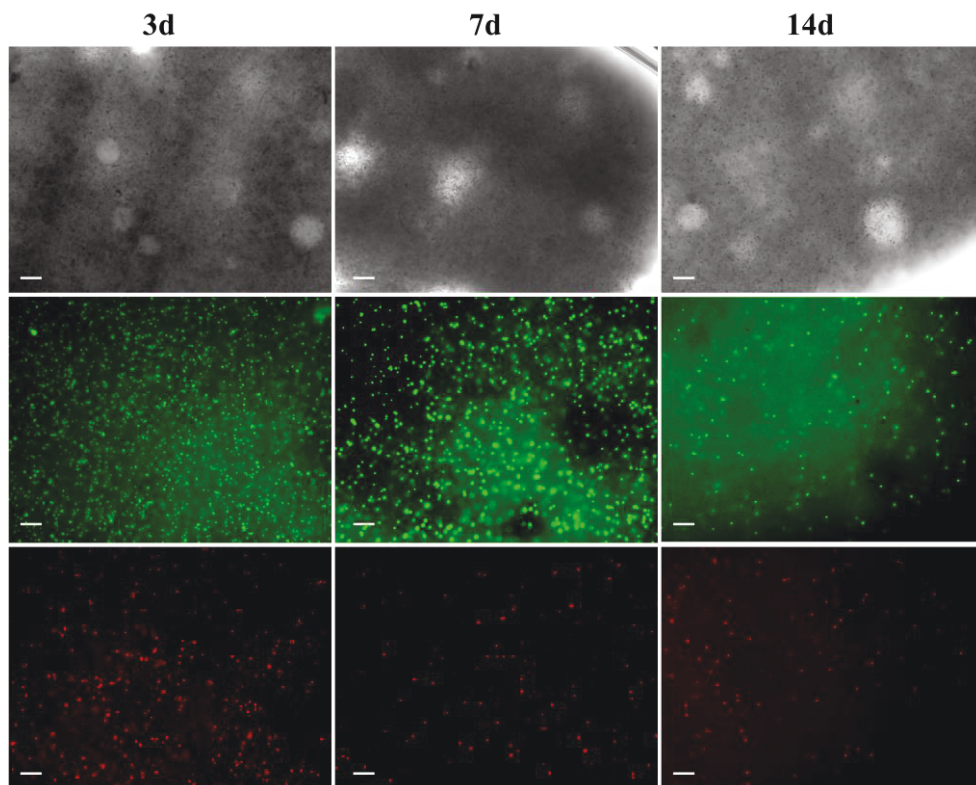
Then, after 24 hours sample incubation in HBSS^{+/+} at 37 °C it increased (+134.3%) with no statistically significant differences. Moreover, the weight of the wet scaffolds after printing and at 24 hours of immersion in HBSS^{+/+} (Fig.6.10B) was similar among scaffolds and significantly decreased (p<.001)

after drying (*Wd*) and not significant differences were observed after 24 hours, suggesting successful cross-linking phase of alginate. These data reflect the high hydrophilicity of the hydrogel resulting immediately after 3D printing indicating their potential use for tissue engineering applications in clinical trials.

6.4.3 Viability of embedded ASCs within NFC/A hydrogel

Bioink printability and cell viability are both crucial parameters for successful bioprinting and development of specific tissue substitutes. A suitable viscosity of the gel construct is required to achieve printing fidelity as well as high cell viability post printing (30). Viscosity of the bioink can vary based on both the mechanical properties of the biomaterial and on the cell density employed for bioprinting (31,32). An optimal cell concentration is essential to guarantee construct functionality in terms of cell survival after printing, cell proliferation and differentiation. Indeed, an erroneous cell density can lead to scarce cell viability and proliferation with consequent poor tissue integration and ingrowth in the construct (33). Cell density can vary according to the tissue; for instance, a cell density between 5 and 10 x 10⁶ cells/ml has been identified as the optimal value for bone tissue engineering (34–36). In this study, bioprinting of ASCs (N=3) was performed using three different cell densities, i.e., 3.0, 6.0 and 9.0 x 10⁶ /ml of NFC/A bioink. Considering an average number of 20 bioconstructs produced from 1 ml of bioink, each 3D printed construct was estimated to contain approx. 1.5, 3.0 and 4.5 x 10⁵ cells, depending on the cell density of the starting bioink (i.e., 3.0, 6.0 and 9.0 x 10⁶ cells/ml, respectively). After printing, the viability of ASCs within the construct was evaluated after 1, 7 and 14 days of cell culture. Results of cell viability assay based on the fluorescence of the live and dead stained cells are shown in Figure 6.11. The different seeding densities appeared to be proportional to the number of ASCs present in the constructs without great impact on their viability. Cells appeared rounded and showed a very high cell viability at all time points of culture after bioprinting, as highlighted by the higher number of green cells visualized in the cell-laden constructs in comparison with fewer red cells. No significant difference due to the different cell concentration in the starting bioink was observed. The same trend was maintained also after 7 days of culture since a very high number of live cells and only some dead cells were displayed in 3D cell-constructs without significant

differences among the three cell densities teste. At 14 days, the viability remained significantly high but it decreased in comparison with early time points in all printing conditions. These data suggested a good survival rate of ASCs after printing and the suitability of the set printing parameters for the microfabrication of cellularized constructs.

A $3.0 \times 10^6 / \text{ml}$ **B** $6 \times 10^6 / \text{ml}$ 

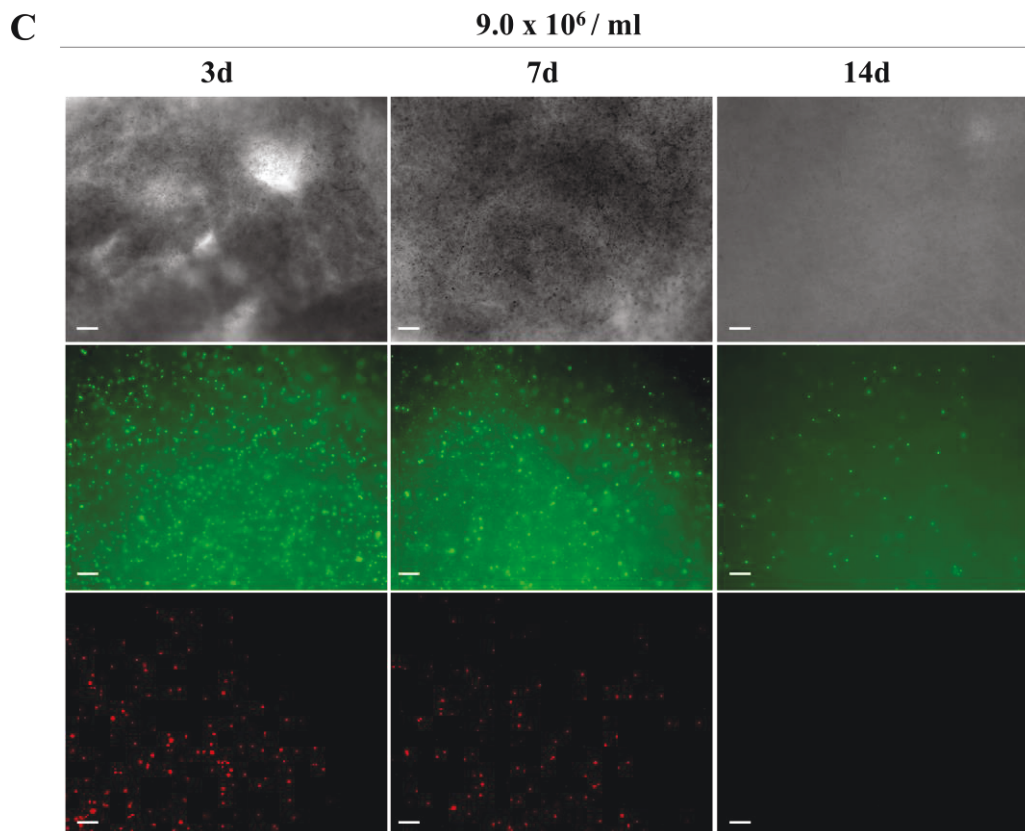


Figure 6.11. Live-dead staining of ASCs printed in the NFC/A hydrogel at different cell densities

Representative images showing bright field, live (green) and dead (red) cells encapsulated in the scaffolds at cell densities of **A.** 3.0×10^6 , **B.** 6.0×10^6 and **C.** 9.0×10^6 cells/ml of bioink after 3, 7 and 14 days of cell culture (4X magnification; scale bar $10\mu\text{m}$).

To validate live-dead staining results and to assess the proliferation rate, Alamar blue assay was employed as a quantitative evaluation and more accurate approach. It is a proven cell viability indicator that exploits the natural reducing power of living cells to convert resazurin to the fluorescent molecule, resorufin. Results from Alamar assay were in agreement with live-dead staining. Indeed, as shown in Figure 6.12A, ASCs possessed high cell viability in all 3D cell-constructs already 3 days after bioprinting without differences based on initial cell concentration in the bioink. In particular, ASCs printed at the cell density of $6.0 \times 10^6/\text{ml}$ showed higher cell viability with increases of +60% and +65% at 3 and 7 days, respectively, in comparison with the lowest dose of printed cells as well as increase of +18% at 3 days in respect to constructs with the highest cell density. All these results, clearly demonstrated the biocompatibility of the bioink, which turned out to be a well suited hydrogel of the 3D bioprinting of ASCs.

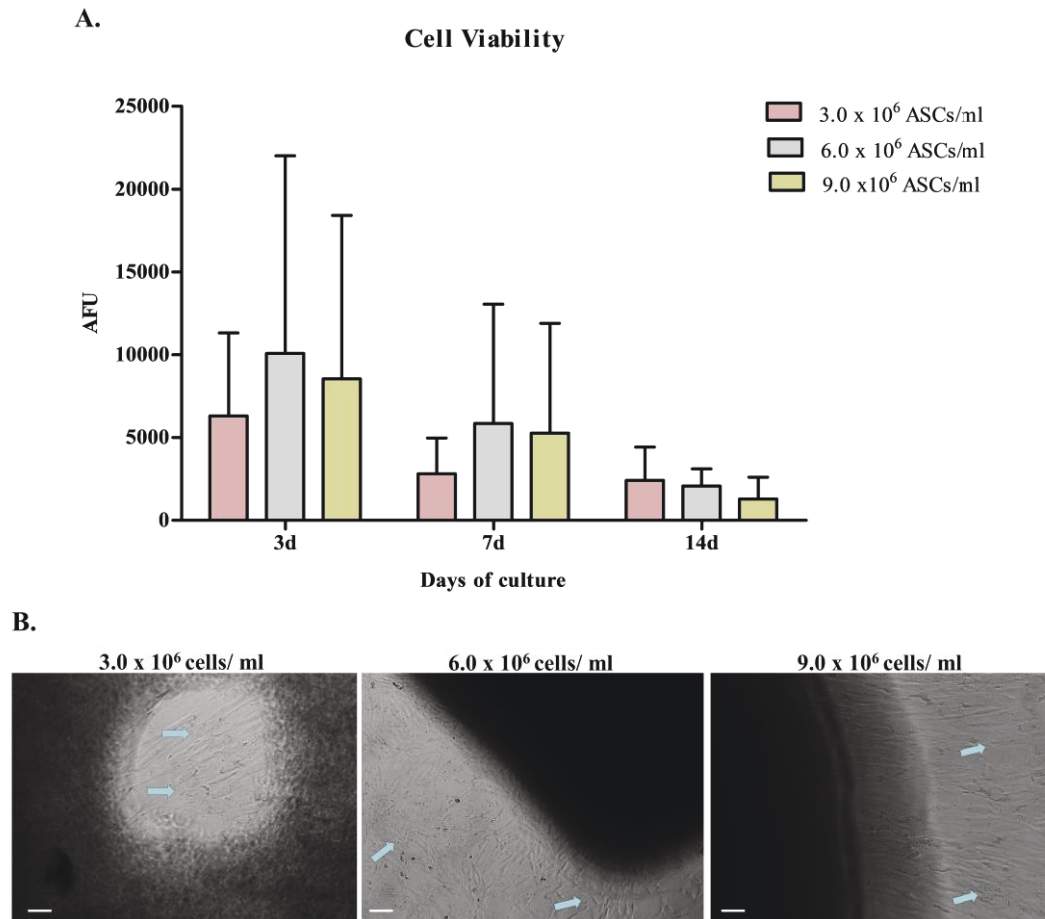


Figure 6.12. Cell viability of ASCs in the NFC/A hydrogel

A. Cell viability of ASCs encapsulated in the scaffolds at 3.0×10^6 , 6.0×10^6 and 9.0×10^6 cells/ml of bioink at 3, 7 and 14 days after bioprinting ($n=3$). Data were expressed as average \pm standard deviation of arbitrary fluorescence units (AFU). **B.** Micrographs showing adherent ASCs on the well plate surface (blue arrows) at 7 days of culture after bioprinting in the NFC/A hydrogel (10X magnification, scale bar 10 μ m).

These findings are also confirmed by previous published studies that reported high cell viability and proliferation post-printing of chondrocytes and induced pluripotent stem cells embedded in a NFC/A bioink (17–20). However, with the progress of the culture, embedded ASCs showed a decrease of cell metabolic activity in the NFC/A constructs in any seeded density. Moreover, ASCs with the typical fibroblastic morphology were adherent at the bottom surface of the well plates, suggesting their migration out of the construct as shown in Figure 6.12B. These results could suggest the matrix characteristics such as pore size or pore interconnectivity not allow a proper cell attachment and proliferation (37). The importance of the pore size of scaffolds to ensure cell bio-adhesion, proliferation and differentiation is well recognized. Recently, it has been suggested that gel

pore size must be sufficiently small to allow mechanical integrity but enough void space should be available to accomplish cell growth and nutrient diffusion within the tissue construct (38,39). According to this, Novikova et al. reported that MSCs from bone marrow cultured in an alginate hydrogel appeared as atypical cells with spherical shape with an inhibited metabolic activity (40). Other studies reported that NFC/A hydrogels do not allow or inhibit proliferation and growth of several different types of cells (20,41). For instance, Müller et al. also reported significant decrease in cell proliferation of chondrocytes embedded in a NFC/A hydrogel (20).

In order to study the capability of the NFC/A hydrogel to hold ASC 3D cell culture, the morphological cell appearance in the nanostructure of the scaffold was evaluated by SEM. As showed in Figure 6.13A.

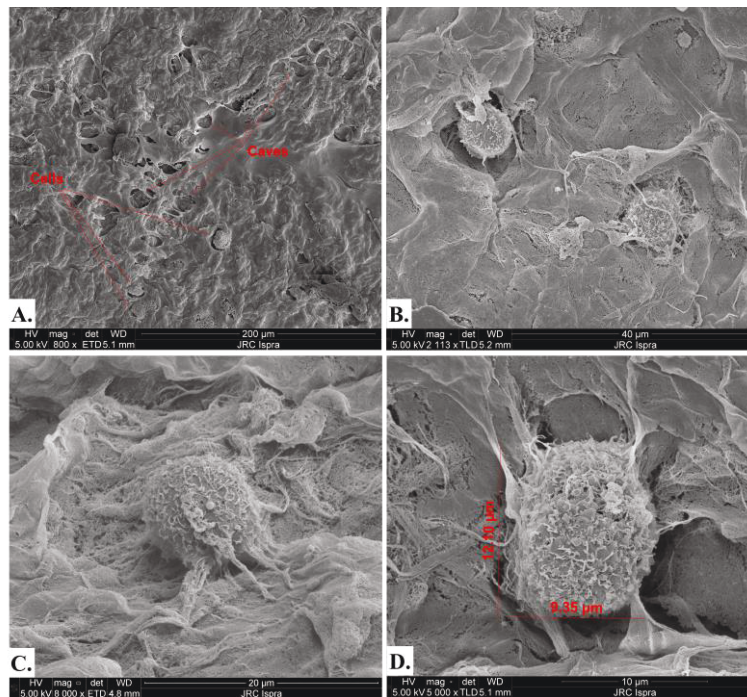


Figure 6.13. ASC distribution in the NFC/A hydrogel

Micrographs obtained by SEM showing **A.** the cell distribution on the 3D cell construct surface and caves; **B-D.** cell appearance in the 3D culture condition.

After 14 days of culture 3D bioprinted ASCs were homogenously distributed over the surface of the scaffolds. Moreover, some rounded caves on the surface of the scaffolds were also visualized and they may represent the area where cells attached before flushing out from the 3D structure. It is interesting to observe, from a closer view, cells on the gels presenting rough surface textures (Figure

6.13B) and cytoskeleton filaments interacting with the surrounding area. This behavior is an important indicator that scaffolds provided a good environment for cells to migrate and interact with each other (42).

6.4.4 Tenogenic potential of the 3D ASC NFC/A constructs

Tenogenic differentiation of stem cells, and thus the regenerative ability of tendon, is based on matrix stiffness, mechanical forces and biochemical inducing signals. Matrix stiffness of stem cell niche plays an important role in regulating the proliferation and differentiation of mesenchymal stem cells (MSCs) including adipose derived stem cells (43). It was found that a low matrix stiffness is correlated with pathological tendon tissue and erroneous differentiation of tendon derived stem cell (TDSCs) (44). Conversely, higher expression of tenogenic related markers were found in normal tendon ECM with higher matrix stiffness (45). Most of the studies in 2D and 3D conditions have been performed with tendon derived stem cells; however, the optimal culture conditions that drive tenogenic cell differentiation of MSCs have not been identified yet. Nonetheless, adipose-derived stem cells constitute an interesting candidate for tendon tissue engineering as already reported in previous *in vitro* and *in vivo* studies (4,46). In order to study the influence of both biochemical and mechanical stimuli on the tenogenic differentiative capability of 3D bioprinted ASCs within the NFC/A matrix, TENO serum-free culture media containing the mixture of selected growth factors and soluble molecules (BMP-12, CTGF, TGF- β 3 and ascorbic acid) (cp chapter 3) was supplied to the 3D printed constructs the day after bioprinting and cell viability, morphology and tendon-related protein expression were observed over time (4). Constructs were also cultured in CTRL medium as control condition. First, cell viability in terms of survival and metabolic/proliferation activity of 3D bioprinted ASCs cultured in CTRL and TENO conditions, was evaluated after 1, 3, 7 and 14 days using both the fluorescence-based live and dead and Alamar blue assays (Figure 6.14 and 6.15). At all time-points most of the entrapped cells (over 90%) successfully survived in both CTRL and TENO conditions (Fig 6.14). However, as showed in Figure 6.15, cell viability progressively decreased over time up to 7 days, without any significant difference between CTRL- and TENO-cultured ASCs. In particular, CTRL-cultured

constructs showed significant decrease in cell viability of 12.1% ($p < 0.05$) and 32.6% ($P < 0.01$) after 3 and 7 days, respectively, compared to cell viability at day 1. Similarly, decreases of 22.0% after 3 days ($p < 0.05$) and 46.6% at 7 days were observed also in TENO-cultured constructs with respect to 1 day.

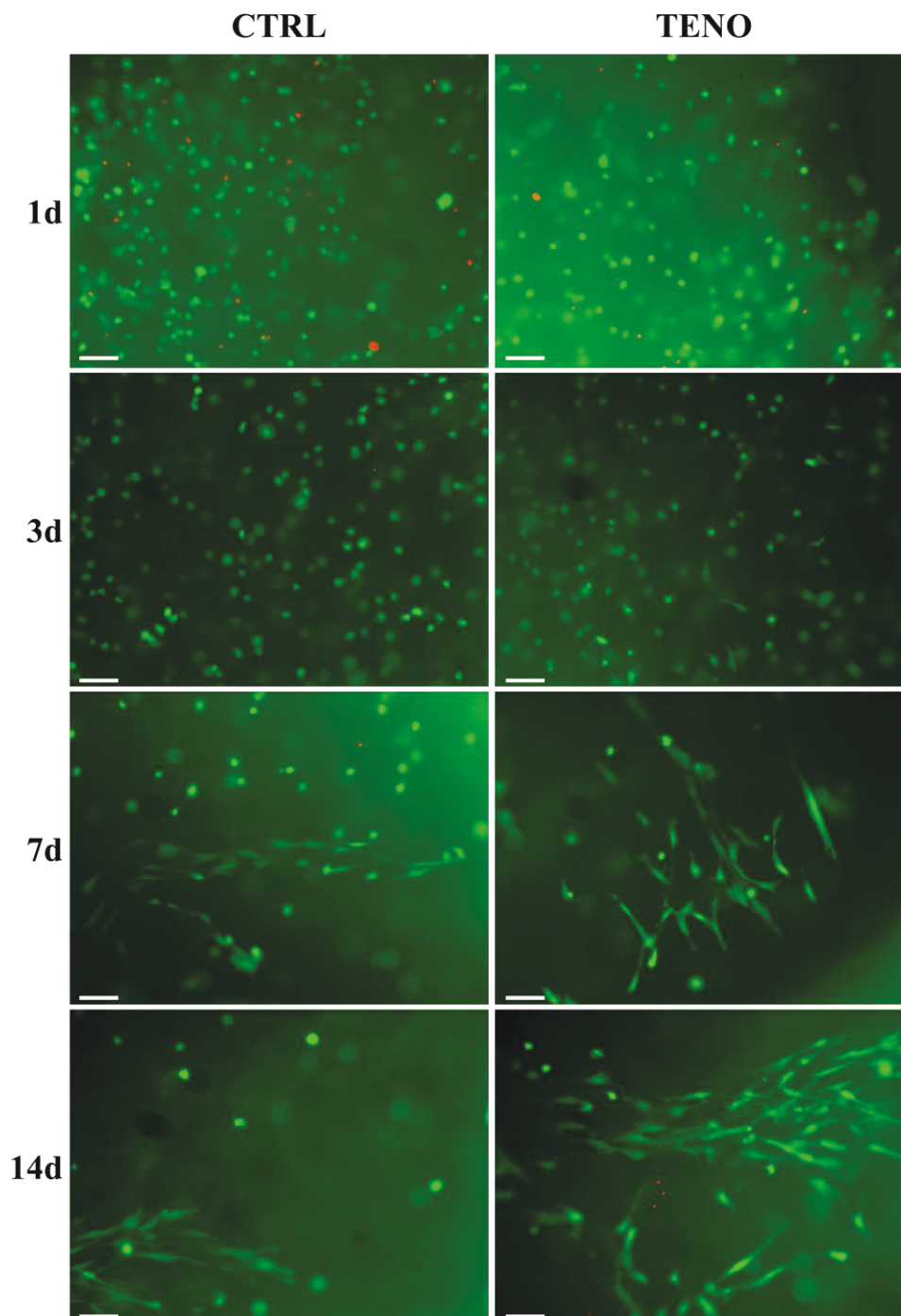


Figure 6.14. Live and dead staining of CTRL- and TENO-cultured 3D bioprinted constructs
Representative images of live (green) and dead (red) cells encapsulated in the scaffolds and cultured in CTRL and TENO medium after 1, 3, 7 and 14 days of cell culture (10X magnification; scale bar 10 μ m).

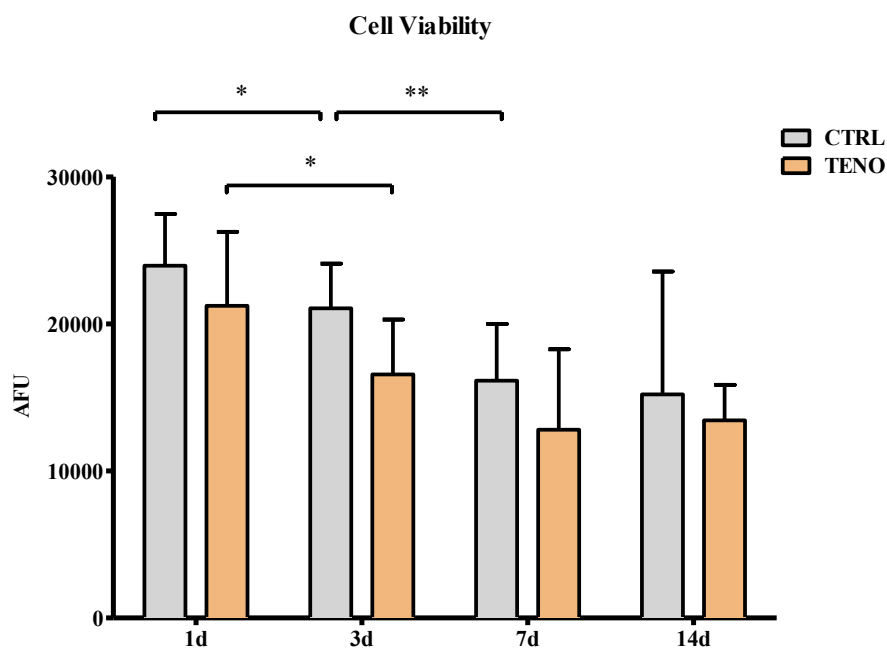


Figure 6.15. Cell viability of CTRL- and TENO-cultured ASCs printed in the NFC/A hydrogel

Cell viability of encapsulated ASCs at 1, 3, 7 and 14 days of cell culture. Data were expressed as average \pm standard deviation of arbitrary fluorescence units (AFU). Level of significance: ** $p < 0.01$, * $p < 0.05$.

Finally, at 7 and 14 days cell culture no further decrease was observed in cell viability, without any significant difference between CTRL- and TENO-cultured constructs. Interestingly, as shown in Figure 6.14, at both 7 and 14 days, 3D printed ASCs showed an evident cell spreading and orientation towards a preferred direction, probably induced by the bioprinting process, with no differences induced by the culture medium. Hence, ASCs were able to activate cellular membrane proteins (ion channels) to trigger signaling pathway to better accommodate in the interconnected pores of the nanofibrillar structure of the scaffold, allowing cell spreading.

The visualization of actin cytoskeleton expression by ASCs embedded in the NFC/A matrix partially confirmed the spreading activity of cells (Fig 6.16). Indeed, as shown in Figure 6.16, at 14 days of cell culture, encapsulated cells showed actin filament prolongations that spread in the 3D environment of the scaffold. Interestingly, TENO-cultured cells seemed to exhibit a more pronounced expression of actin filaments that appeared in greater number on cell surfaces in comparison to what observed in undifferentiated cells (i.e, CTRL-cultured cells). Despite this behavior, cells appeared not fully elongated, as shown before in live and dead images, and most of them still possessed a round morphology.

Nevertheless, it should be considered that cytoskeleton images were captured from scaffold slices at different deeper levels of the 3D structure, representing a more realistic and accurate cell behavior inside the construct, with respect to the top view which characterize live and dead images.

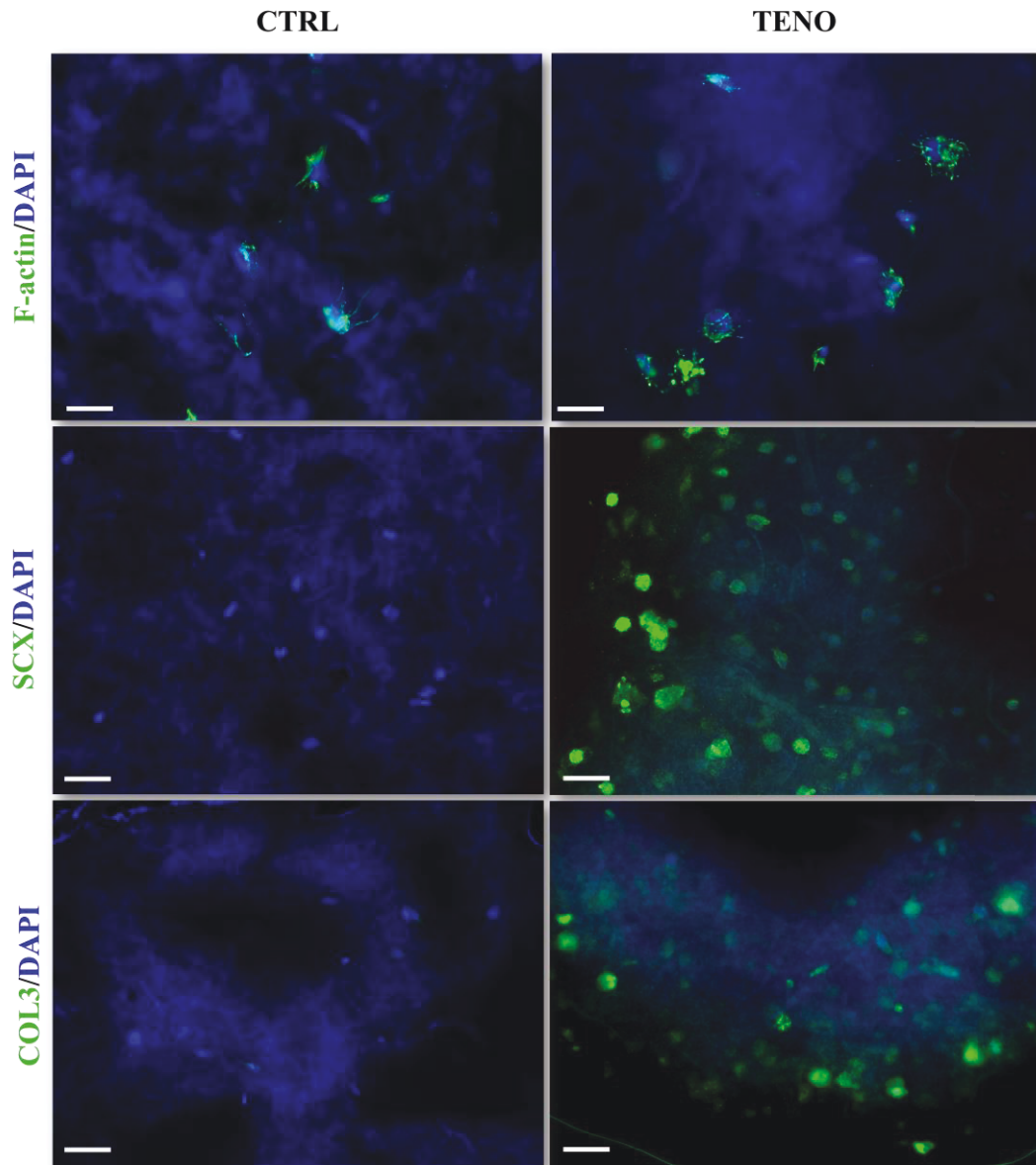


Figure 6.16. Fluorescence imaging

From the top, cytoskeleton imaging of both CTRL- and TENO-cultured ASCs embedded in NFC/A stained with phalloidin (green) for F-actin detection and counterstained with DAPI to visualize cell nuclei (blue) (32X magnifications; 10 μ m scale bar); expression on tendon-related markers scleraxis (SCX) at day 3 and collagen type III (COL3), at day 14 of differentiation were visualized with Alexa-fluor 488 (green) and counterstained with DAPI to visualize cell nuclei (blue) in both CTRL- and TENO-cultured ASCs embedded in NFC/A constructs (20X magnification; 10 μ m scale bar).

Further investigations about the role of actin cytoskeleton during tendon development and tenogenic differentiation to establish effective regenerative strategies are needed. In this context, indeed, it has been recently demonstrated the central role of actin cytoskeleton in cell's contractile machinery and in the elastic modulus during early tendon development (47). It is strictly involved in the typical crimp collagen pattern formation of tendon ECM and in the mechanical properties of mature tendon tissue acting both as mechano-transducer and signaling actor (48–50). Indeed, the contact sites of cells to ECM, called focal adhesions, take place through transmembrane proteins called integrin allowing specific recognition of various ECM proteins, e.g., fibrinogen, collagen, vitronectin, and laminin (51). After the ligation of integrins with ECM proteins, many structural and signaling proteins are recruited to focal adhesions, including kinases, e.g., FAK, integrin-linked kinase, and phosphatase. Since integrin itself lacks enzymatic activity, these signaling proteins at focal adhesions are crucial to transfer extracellular mechanical information inside the cells. For instance, FAK interacts with integrin receptors and ECM proteins to sense the mechano-environment (51). For these reasons, laminin proteins present within the NFC/A bioink exert an important role in supporting cell adhesion and proliferation. Moreover, they act as differentiative cues for embedded ASCs. Other reports demonstrated also the key role of matrix stiffness in the modulation of tendon derived stem cells (TDSCs) proliferation and differentiation by FAK or its downstream signaling molecular ERK1/2 activation (52). In particular, the phosphorylation of FAK and ERK1/2 were enhanced in TDSCs culture on stiff gelatin hydrogels and inhibited by matrices exhibiting lower stiffness. The phenomenon was especially obvious on polystyrene culture plate and in accordance to ASC behavior which showed faster growth rate on stiff substrate compared to soft ones (53). Nevertheless, it has been recently reported that stem cell types derived from soft tissues as umbilical cord stem cells, lose cell proliferation ability if the stiffness of the matrix increases (54). This effect could indicate that stem cell proliferation is regulated by the matrix stiffness of the substrates. In this study, the expression of the well-recognized tendon-related proteins was detected in both CTRL- and TENO-cultured cell constructs. Immunofluorescence analysis was performed to assess the presence of scleraxis and collagen type III at day 3 and 14 days of differentiation, respectively, and the

representative images are shown in Figure 6.16. Scleraxis (SCX) is a transcription factor continuously expressed from earlier differentiative stages for mature tendons development and regulation (4,55). Collagen type III (COL3) is one the major component of the ECM of tendon and ligament tissue and a late marker of tendon differentiation (56,57). Interestingly, already after 3 days of differentiation, a high number of TENO-differentiated cells specifically expressed SCX whilst undifferentiated-CTRL cells were not able to express this transcription factor. Moreover, at 14 days COL3 was significantly expressed in TENO-cultured cell constructs in comparison to CTRL ones. These findings are in agreement with the previous *in vitro* study on the tenogenic differentiation of ASCs in 2D-condition (cp. chapter 3) (4).

6.4.5 Inflammatory response

Undifferentiated mesenchymal stem cells secrete a broad panel of growth factors and cytokines with trophic, immunomodulatory, antiapoptotic and proangiogenic properties. This effect is closely related to the ASC's secretome and the soluble factors released, such as hepatocyte growth factor (HGF), granulocyte and macrophage colony stimulating factors (GM-CSF), interleukins (ILs) 6, 7, 8 and 11, tumor necrosis factor-alpha (TNF- α), vascular endothelial growth factor (VEGF), brain derived neurotrophic factor (BDNF), nerve growth factor (NGF), adipokines and others (58). For a safe therapeutic application of ASCs in tissue engineering strategies it is important to consider also the scaffold environment as another tool to control the immunomodulatory character of ASCs. For what concerns the safety of the nanofibrillar cellulose, previous *in vitro* studies reported no pro-inflammatory cytokine secretion by macrophages (59,60). Kilroy et al. observed that ASCs respond to an inflammatory stimulus, such as lipopolysaccharide (LPS) increasing their secretion of both hematopoietic (GM-CSF and IL-7) and proinflammatory (ILs 6, 8, 11 and TNF- α) cytokines. Herein the supernatants of both CTRL- and TENO-cultured ASCs embedded in the NFC/A hydrogel were collected during culture at day 3, 7 and 14 and the content of GM-CSF, IFN- γ , IL-2, IL-4, IL-6, IL-8, IL-10 and TNF- α cytokines involved in several different processes of inflammation were analyzed by Enzyme Linked Immunoabsorbent Assay (ELISA). The supernatant of cell-constructs treated for

24 hours with LPS was used as positive control. Neither GM-CSF, IFN- γ , IL-2, IL-4, IL-10 and TNF- α cytokines was detected in the conditioned medium from undifferentiated and differentiated 3D ASC constructs (data not shown). On the other hand, as shown in Figure 6.17, increases of IL-6 and IL-8 were observed at all time points in both CTRL- and TENO-cultured ASC constructs without any difference based on the culture conditions.

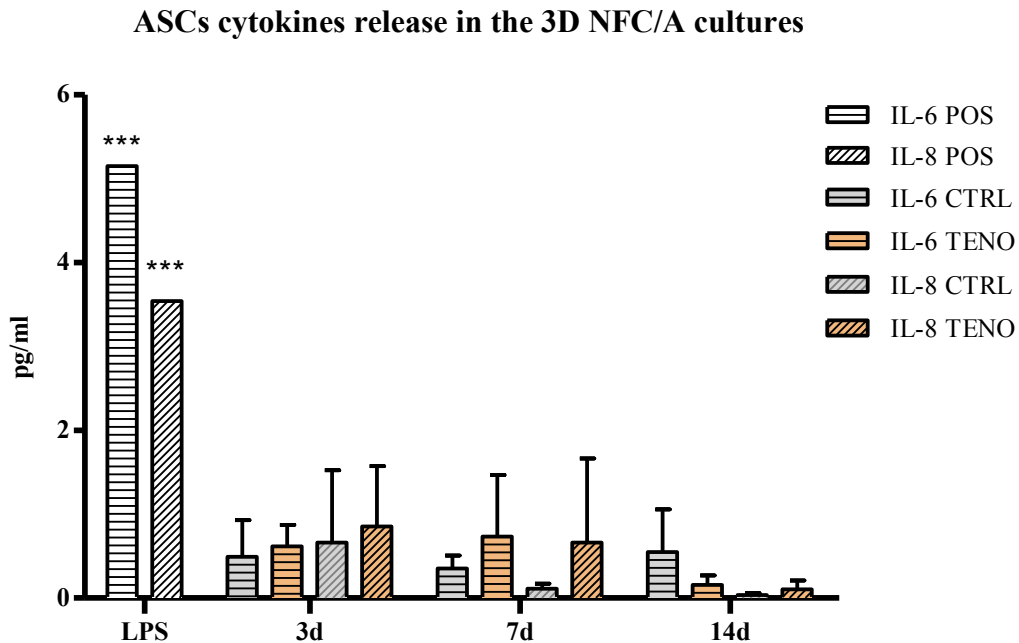


Figure 6.17. ASC cytokines release in the 3D NFC/A cultures. Comparison of the supernatant media collected after 3, 7 and 14 days of both undifferentiated (CTRL) and differentiated (TENO) ASC constructs. Positive control was obtained from supernatant media of ASC constructs treated with LPS for 24 hours. Level of significance *** $p < 0.001$ vs the respective no-LPS stimulated ASC constructs.

Moreover, levels of these secreted cytokines reached maximal mean levels at less than 1 pg/ml values that were significantly lower than what was observed in the respective LPS treated group ($p < 0.001$). Indeed, the LPS stimulation of ASCs embedded in the NFC/A hydrogel induced a greater production of the cytokines involved in inflammatory modulation and wound healing, as IL-8 and IL-6 (61,62). These findings represent, to our knowledge, the first attempt to investigate the influence of NFC/A hydrogel and tenogenic medium on cytokine release of ASCs. It was found that NFC/A hydrogel is a safe and suitable material for cell-therapy applications since it does not induce any significant inflammatory response to ASCs. However, further investigations on the complete panels of

cytokines released from ASCs after bioprinting could give more insight about their potential in tendon tissue engineering. For instance, Martaniemi et al reported analysis of 60 cytokines involved in several different processes as immunomodulation, angiogenesis or differentiation in the conditioned medium of ASCs cultured on native nanofibrillated cellulose with glutaraldehyde cross-linked threads (NFC-X) (63). Comparing the cytokines levels found in the supernatant of ASCs cultured on plastic with NFC-X cultures they reported that, while NFC-X did not influence the type of molecules secreted, higher levels of molecules involved in tissue regeneration and wound healing as IL-8, Acrp30 or ENA-78 were secreted by hASC cultured over NFC-X.

6.5 Conclusions

Given the biomechanical role of tendon tissue, defining the best combination of cells and biomaterials are key challenges that bioengineers should address. Cells have a primary role in maintaining tendon ECM homeostasis, while biomaterials should possess several requirements in term of mechanical, structural and biological properties as they could also modulate cell proliferation and differentiation. Several key issues must be considered, such as the lack of standardized protocols defining the resolution of the printing process, the definition of adequate differentiation protocols of MSCs and their bioactivity in cellularized-constructs.

To address these challenges, we showed that ASCs were embedded into a NFC/A hydrogel providing a xenogeneic-free tool for delivering stem cells into injured areas in a precise manner that might be useful to improve healing in tendon, thus opening new possibilities in personalized medicine. In fact, for the first time, we evaluated the ASC behaviour, after embedding into a NFC/A hydrogel and bioprinting into square grid structures, in terms of cell viability, proliferation, differentiation and inflammatory response. The influence of cell seeding density into the bioink on cell behaviour upon printing was also assessed. Primary human adipose derived stem cells showed high survival rate after printing and cell viability in 3D culture was not influenced by cell seeding density in the starting bioink, demonstrating its potential as cell-carriers for the fabrication of 3D tissue constructs. However, cell viability decreases were observed until 7 days of culture in both CTRL- and TENO-cultured ASCs. In this regards, future studies with lower cell density ($< 1.0 \times 10^6$ cells/ml) could be conducted to investigate if the major oxygen and nutrient availability within the constructs allows higher cell growth until 14 days. At the same time, since stiffness of the matrix plays a key role in stem cell communication, proliferation and maturation, further study concerning the use of different crosslinked alginate ratio within the construct as well as different concentration of nanocellulose and alginate in the bioink could be useful to better understand this cellular behavior.

Finally, the 3D environment well suited with the regenerative and immunomodulatory properties of human ASCs. In fact, the combination of

biochemical and mechanical stimuli allowed to efficiently driving cell differentiation toward tendon lineage, as demonstrated by the specific and strong expression of the early marker (scleraxis) and the late marker (collagen type III). Moreover, the absence of ASC inflammatory response to the 3D NFC/A substrate represents another insight that ensures the safety of these xeno-free FDA approved materials and of the xenogenic free-tenogenic differentiation protocol. In conclusion, all these findings represent a first proof-of-concept to the possible development of ASC-laden 3D bioprinted constructs for tendon tissue engineering. The evaluation of MSCs in the 3D environment is another key issue to better understand their natural behavior in the tissue-like construct contributing to the advancement of the knowledge concerning stem cell biology. Critical challenges still remain to be addressed to apply 3D bioproducts in clinical setting, such as construct fabrication, standardized markers for cell viability and functionality in the 3D-construct, and standardization of bioprinting parameters. As emerging field, the way toward the *ad-hoc* cell-laden implant development is in its infancy and further studies including the *in vivo* functionality demonstration are still to address.

6.6 References

1. Costa-Almeida R, Calejo I, Gomes ME. Mesenchymal stem cells empowering tendon regenerative therapies. *International Journal of Molecular Sciences*. 2019.
2. Langer R, Vacanti JP. Tissue engineering. *Science* (80-). 1993;
3. Stanco D, Viganò M, Perucca Orfei C, Di Giancamillo A, Thiebat G, Peretti G, et al. In vitro characterization of stem/progenitor cells from semitendinosus and gracilis tendons as a possible new tool for cell-based therapy for tendon disorders. *Joints*. 2014;2(4).
4. Stanco D, Caprara C, Ciardelli G, Mariotta L, Gola M, Minonzio G, et al. Tenogenic differentiation protocol in xenogenic-free media enhances tendon-related marker expression in ASCs. *PLoS One*. 2019;14(2).
5. Stanco D, Viganò M, Perucca Orfei C, Di Giancamillo A, Peretti GM, Lanfranchi L, et al. Multidifferentiation potential of human mesenchymal stem cells from adipose tissue and hamstring tendons for musculoskeletal cell-based therapy. *Regen Med*. 2015;10(6).
6. Mizuno H, Tobita M, Uysal C. Concise Review : Adipose-Derived Stem Cells as a Novel Tool for. *Stem Cells*. 2012;
7. Laranjeira M, Domingues RMA, Costa-Almeida R, Reis RL, Gomes ME. 3D Mimicry of Native-Tissue-Fiber Architecture Guides Tendon-Derived Cells and Adipose Stem Cells into Artificial Tendon Constructs. *Small*. 2017;
8. Raabe O, Shell K, Fietz D, Freitag C, Ohrndorf A, Christ HJ, et al. Tenogenic differentiation of equine adipose-tissue-derived stem cells under the influence of tensile strain, growth differentiation factors and various oxygen tensions. *Cell Tissue Res*. 2013;
9. Sengupta D, Waldman SD, Li S. From in vitro to in situ tissue engineering. *Ann Biomed Eng*. 2014;
10. Santos ML, Rodrigues MT, Domingues RMA, Reis RL, Gomes ME. Biomaterials as Tendon and Ligament Substitutes: Current Developments. In 2017.
11. Yang G, Lin H, Rothrauff BB, Yu S, Tuan RS. Multilayered polycaprolactone/gelatin fiber-hydrogel composite for tendon tissue

- engineering. *Acta Biomater.* 2016;
12. Murphy S V., Atala A. 3D bioprinting of tissues and organs. *Nature Biotechnology.* 2014.
 13. Hölzl K, Lin S, Tytgat L, Van Vlierberghe S, Gu L, Ovsianikov A. Bioink properties before, during and after 3D bioprinting. *Biofabrication.* 2016.
 14. Merceron TK, Burt M, Seol YJ, Kang HW, Lee SJ, Yoo JJ, et al. A 3D bioprinted complex structure for engineering the muscle-tendon unit. *Biofabrication* [Internet]. 2015;7(3):35003. Available from: <http://dx.doi.org/10.1088/1758-5090/7/3/035003>
 15. Kargarzadeh H, Mariano M, Huang J, Lin N, Ahmad I, Dufresne A, et al. Recent developments on nanocellulose reinforced polymer nanocomposites: A review. *Polymer.* 2017.
 16. Henriksson I, Gatenholm P, Hägg DA. Increased lipid accumulation and adipogenic gene expression of adipocytes in 3D bioprinted nanocellulose scaffolds. *Biofabrication.* 2017;
 17. Markstedt K, Mantas A, Tournier I, Martínez Ávila H, Hägg D, Gatenholm P. 3D bioprinting human chondrocytes with nanocellulose-alginate bioink for cartilage tissue engineering applications. *Biomacromolecules.* 2015;
 18. Möller T, Amoroso M, Hägg D, Brantsing C, Rotter N, Apelgren P, et al. In Vivo Chondrogenesis in 3D Bioprinted Human Cell-laden Hydrogel Constructs. *Plast Reconstr Surg - Glob Open.* 2017;5(2):1–7.
 19. Nguyen D, Hgg DA, Forsman A, Ekholm J, Nimkingratana P, Brantsing C, et al. Cartilage Tissue Engineering by the 3D Bioprinting of iPS Cells in a Nanocellulose/Alginate Bioink. *Sci Rep.* 2017;
 20. Müller M, Öztürk E, Arlov Ø, Gatenholm P, Zenobi-Wong M. Alginate Sulfate–Nanocellulose Bioinks for Cartilage Bioprinting Applications. *Ann Biomed Eng.* 2017;
 21. Giannasi C, Pagni G, Polenghi C, Niada S, Manfredi B, Brini A, et al. Impact of Dental Implant Surface Modifications on Adhesion and Proliferation of Primary Human Gingival Keratinocytes and Progenitor Cells. *Int J Periodontics Restorative Dent.* 2018;
 22. Lancaster, M. V. and Fields RD. Antibiotic and cytotoxic drug susceptibility assays using resazurin and poisoning agents. *United States Pat.* 1995;

23. Osorio M, Fernández-Morales P, Gañán P, Zuluaga R, Kerguelen H, Ortiz I, et al. Development of novel three-dimensional scaffolds based on bacterial nanocellulose for tissue engineering and regenerative medicine: Effect of processing methods, pore size, and surface area. *J Biomed Mater Res - Part A*. 2019;
24. Chung JHY, Naficy S, Yue Z, Kapsa R, Quigley A, Moulton SE, et al. Bio-ink properties and printability for extrusion printing living cells. *Biomater Sci*. 2013;
25. Aljohani W, Ullah MW, Zhang X, Yang G. Bioprinting and its applications in tissue engineering and regenerative medicine. *Int J Biol Macromol* [Internet]. 2018;107(PartA):261–75. Available from: <https://doi.org/10.1016/j.ijbiomac.2017.08.171>
26. Corker A, Ng HCH, Poole RJ, García-Tuñón E. 3D printing with 2D colloids: Designing rheology protocols to predict “printability” of soft-materials. *Soft Matter*. 2019;
27. Pati F, Jang J, Ha DH, Won Kim S, Rhie JW, Shim JH, et al. Printing three-dimensional tissue analogues with decellularized extracellular matrix bioink. *Nat Commun* [Internet]. 2014;5:1–11. Available from: <http://dx.doi.org/10.1038/ncomms4935>
28. Aston R, Sewell K, Klein T, Lawrie G, Grøndahl L. Evaluation of the impact of freezing preparation techniques on the characterisation of alginate hydrogels by cryo-SEM. *European Polymer Journal*. 2016.
29. Sharma C, Dinda AK, Potdar PD, Chou CF, Mishra NC. Fabrication and characterization of novel nano-biocomposite scaffold of chitosan-gelatin-alginate-hydroxyapatite for bone tissue engineering. *Mater Sci Eng C*. 2016;
30. Ouyang L, Yao R, Zhao Y, Sun W. Effect of bioink properties on printability and cell viability for 3D bioplotting of embryonic stem cells. *Biofabrication*. 2016;
31. Guillotin B, Souquet A, Catros S, Duocastella M, Pippenger B, Bellance S, et al. Laser assisted bioprinting of engineered tissue with high cell density and microscale organization. *Biomaterials*. 2010;
32. Xu T, Jin J, Gregory C, Hickman JJ, Boland T. Inkjet printing of viable mammalian cells. *Biomaterials*. 2005;

33. Cidonio G, Glinka M, Dawson JI, Oreffo ROC. The cell in the ink: Improving biofabrication by printing stem cells for skeletal regenerative medicine. *Biomaterials*. 2019.
34. Nicodemus GD, Bryant SJ. Cell encapsulation in biodegradable hydrogels for tissue engineering applications. *Tissue Engineering - Part B: Reviews*. 2008.
35. Luo F, Hou TY, Zhang ZH, Xie Z, Wu XH, Xu JZ. Effects of Initial Cell Density and Hydrodynamic Culture on Osteogenic Activity of Tissue-Engineered Bone Grafts. *PLoS One*. 2013;
36. Daly AC, Pitacco P, Nulty J, Cunniffe GM, Kelly DJ. 3D printed microchannel networks to direct vascularisation during endochondral bone repair. *Biomaterials*. 2018;162:34–46.
37. Piras CC, Fernández-Prieto S, De Borggraeve WM. Nanocellulosic materials as bioinks for 3D bioprinting. *Biomaterials Science*. 2017.
38. Liu M, Dai L, Shi H, Xiong S, Zhou C. In vitro evaluation of alginate/halloysite nanotube composite scaffolds for tissue engineering. *Mater Sci Eng C*. 2015;
39. Siqueira P, Siqueira É, de Lima AE, Siqueira G, Pinzón-Garcia AD, Lopes AP, et al. Three-dimensional stable alginate-nanocellulose gels for biomedical applications: Towards tunable mechanical properties and cell growing. *Nanomaterials*. 2019;
40. Novikova LN, Mosahebi A, Wiberg M, Terenghi G, Kellerth JO, Novikov LN. Alginate hydrogel and matrigel as potential cell carriers for neurotransplantation. *J Biomed Mater Res - Part A*. 2006;
41. Schmidt SK, Schmid R, Arkudas A, Kengelbach-Weigand A, Bosserhoff AK. Tumor Cells Develop Defined Cellular Phenotypes After 3D-Bioprinting in Different Bioinks. *Cells*. 2019;
42. Kirdponpattara S, Khamkeaw A, Sanchavanakit N, Pavasant P, Phisalaphong M. Structural modification and characterization of bacterial cellulose-alginate composite scaffolds for tissue engineering. *Carbohydr Polym*. 2015;
43. Wang T, Lai JH, Han LH, Tong X, Yang F. Chondrogenic differentiation of adipose-derived stromal cells in combinatorial hydrogels containing cartilage matrix proteins with decoupled mechanical stiffness. *Tissue Eng -*

Part A. 2014;

44. Dirrachs T, Quack V, Gatz M, Tingart M, Kuhl CK, Schrading S. Shear Wave Elastography (SWE) for the Evaluation of Patients with Tendinopathies. *Acad Radiol.* 2016;
45. Liu C, Luo JW, Zhang KK, Lin LX, Liang T, Luo ZP, et al. Tendon-derived stem cell differentiation in the degenerative tendon microenvironment. *Stem Cells Int.* 2018;
46. Kokubu S, Inaki R, Hoshi K, Hikita A. Adipose-derived stem cells improve tendon repair and prevent ectopic ossification in tendinopathy by inhibiting inflammation and inducing neovascularization in the early stage of tendon healing. *Regen Ther.* 2020;
47. Schiele NR, Von Flotow F, Tochka ZL, Hockaday LA, Marturano JE, Thibodeau JJ, et al. Actin cytoskeleton contributes to the elastic modulus of embryonic tendon during early development. *J Orthop Res.* 2015;
48. Herchenhan A, Kalson NS, Holmes DF, Hill P, Kadler KE, Margetts L. Tenocyte contraction induces crimp formation in tendon-like tissue. *Biomech Model Mechanobiol.* 2012;
49. Arnoczky SP, Tian T, Lavagnino M, Gardner K. Ex vivo static tensile loading inhibits MMP-1 expression in rat tail tendon cells through a cytoskeletonally based mechanotransduction mechanism. *J Orthop Res.* 2004;
50. Zhou J, Kim HY, Davidson LA. Actomyosin stiffens the vertebrate embryo during crucial stages of elongation and neural tube closure. *Development.* 2009;
51. Lu S, Wang Y. Single-cell imaging of mechanotransduction in endothelial cells. In: *Progress in Molecular Biology and Translational Science.* 2014.
52. Liu C, Luo JW, Liang T, Lin LX, Luo ZP, Zhuang YQ, et al. Matrix stiffness regulates the differentiation of tendon-derived stem cells through FAK-ERK1/2 activation. *Exp Cell Res.* 2018;
53. Zhang T, Lin S, Shao X, Shi S, Zhang Q, Xue C, et al. Regulating osteogenesis and adipogenesis in adipose-derived stem cells by controlling underlying substrate stiffness. *J Cell Physiol.* 2018;
54. Xu J, Sun M, Tan Y, Wang H, Wang H, Li P, et al. Effect of matrix stiffness on the proliferation and differentiation of umbilical cord mesenchymal stem cells. *Differentiation.* 2017;

55. Schweitzer R, Chyung JH, Murtaugh LC, Brent AE, Rosen V, Olson EN, et al. Analysis of the tendon cell fate using Scleraxis, a specific marker for tendons and ligaments. *Development*. 2001;
56. Bi Y, Ehrchiou D, Kilts TM, Inkson CA, Embree MC, Sonoyama W, et al. Identification of tendon stem/progenitor cells and the role of the extracellular matrix in their niche. *Nat Med*. 2007;
57. Hoffmann A, Gross G. Tendon and ligament engineering in the adult organism: Mesenchymal stem cells and gene-therapeutic approaches. *International Orthopaedics*. 2007.
58. J. Braga Osorio Gomes Salgado A, L. Goncalves Reis R, Jorge Carvalho Sousa N, M. Gimble J, J. Salgado A, L. Reis R, et al. Adipose Tissue Derived Stem Cells Secretome: Soluble Factors and Their Roles in Regenerative Medicine. *Curr Stem Cell Res Ther*. 2010;
59. Čolić M, Mihajlović D, Mathew A, Naseri N, Kokol V. Cytocompatibility and immunomodulatory properties of wood based nanofibrillated cellulose. *Cellulose*. 2015;
60. Vartiainen J, Pöhler T, Sirola K, Pylkkänen L, Alenius H, Hokkinen J, et al. Health and environmental safety aspects of friction grinding and spray drying of microfibrillated cellulose. *Cellulose*. 2011;
61. Reckhenrich AK, Kirsch BM, Wahl EA, Schenck TL, Rezaeian F, Harder Y, et al. Surgical sutures filled with adipose-derived stem cells promote wound healing. *PLoS One*. 2014;
62. Lin Z-Q, Kondo T, Ishida Y, Takayasu T, Mukaida N. Essential involvement of IL-6 in the skin wound-healing process as evidenced by delayed wound healing in IL-6-deficient mice. *J Leukoc Biol*. 2003;
63. Mertaniemi H, Escobedo-Lucea C, Sanz-Garcia A, Gandía C, Mäkitie A, Partanen J, et al. Human stem cell decorated nanocellulose threads for biomedical applications. *Biomaterials*. 2016;

PART III

Chapter 7

The regulatory framework and available standards for 3D bioprinted products

7.1 Abstract

Beyond the scientific and technical challenges, 3D bioprinting has been identified as a new technology requiring specific health regulatory frameworks. The main challenges identified by regulators are defining and categorising the products that result from the various sequential phases in 3D bioprinting, identifying afterwards the regulations that would be applicable throughout the whole process. In this chapter the careful examination of the existing regulatory pathways in the EU indicated that a 3D bioprinted product would be classified as a tissue engineered combined medicinal product that would fall under the scope of the ATMP Regulation. Other regulations would apply at different steps of the bioprinting process, but existing regulatory frameworks do not account for the differences between 3D printing and conventional manufacturing methods.

*Part of the results described in this chapter are described in the manuscript in preparation entitled “3D bioprinting for orthopaedic applications: advances, challenges and regulatory considerations” authored by **Deborah Stanco**, Patricia Urbàn, Salvatore Tirendi, Gianluca Ciardelli, Josefa Barrero, for the submission on *Bioprinting Journal**

7.2 Classification of 3D bioprinted products under EU regulatory framework

The application of 3D bioprinting in the biomedical field has an enormous potential to improve healthcare but it also brings significant challenges from the regulatory perspective. Recent discussions in the International Coalition of Medicines Regulatory Authorities (ICMRA) recognized 3D bioprinting as a particularly disruptive technology for regulatory systems (1). An in-depth analysis showing how the current European legislative framework may be affected by the emergence of 3D bioprinting for medical purposes was released by the European Parliamentary Research Service in 2018 (2). The main regulatory challenges identified in this analysis were defining and categorizing the products and processes in 3D bioprinting; and therefore, identifying the relevant regulations that would be applicable throughout the whole process. The appropriate product category designation would also determine the necessary marketing authorization procedures and the liability regime for manufacturers in case of defective products.

A 3D bioprinted product could potentially be considered either a medical device or an accessory to a medical device, an Advanced Therapy Medicinal Product or a medicinal product. The European Medicines Agency (EMA) has issued a scientific recommendation on the classification of viable cells cultured within a 3D structure that is part of the finished product. In that particular case, it was considered that the product would fall within the definition of a tissue engineered product, combined Advanced Therapy Medicinal Product (ATMP) (3). In accordance with this recommendation, a 3D bioprinted meniscus composed of a scaffold seeded with different cells derived from the patient pluripotent stem cells would be likely classified also as a combined ATMP (4) in Europe; but the scaffold should also demonstrate compliance with the applicable regulation for medical devices (MDR) (5).

7.2.2 EMA's approach to regulating combined ATMPs

ATMPs are a special class of medicines (including gene therapies, somatic cell therapies and tissue engineered products) that are governed by Regulation 1394/2007 in Europe (4). Despite that nowadays it is common to have combinations of medicines and devices a classification list of "combination ATMP products" does not exist, yet. Therefore, each classification is performed by EMA on a case-by-case basis and the border between combined or non-combined ATMPs is often subject to discussion during classification procedures (6).

The whole product considered a combined ATMP shall be subject to final evaluation by EMA via the centralized procedure for premarket approval, as stated in Article 9 of the ATMP Regulation. The Committee for Advanced Therapies (CAT) is responsible for assessing the quality, safety and efficacy of ATMPs. The CAT prepares a draft opinion on each ATMP application submitted to EMA, before the Committee for Medicinal Products for Human Use (CHMP) adopts a final opinion on the marketing authorization of the product concerned (4). EMA also manages the coordination of the consultation with the Notified Body in charge of the conformity assessment of the medical device, and should recognise the results of the assessment of the medical device (7,8). The specific requirements for the authorization of ATMPs-containing devices are listed in Article 7 of the ATMP Regulation: ~~For~~ "ATMPs containing medical devices, biomaterials, scaffolds or matrices, a description of the physical characteristics and performance of the product and a description of the product design methods, in accordance with Annex I to Directive 2001/83/EC." (4).

It is important to note that the medical device should retain its original form and function to be considered as an "integral part" of the final product to classify that product as a combined ATMP. For instance, the CAT committee considered that pancreatic beta cells embedded in an alginate matrix for the treatment of diabetes were somatic cell therapy medicinal products, and not combined ATMPs. This was because the alginate matrix was reworked by the cells during culture to support the biological characteristics and functional activities of the cells and the matrix function was no longer considered to be linked to its structural properties (6). Therefore, by analogy, it could be possible that a 3D bioprinted product would not be considered a combined ATMP but a tissue-engineered product.

7.2.3 Other applicable regulations through the 3D bioprinting process

Furthermore, other legislations are relevant at different steps of the production of 3D bioprinted products. We have gone through the whole 3D bioprinting process and identified the applicable legislations in the following steps: (i) pre-printing, (ii) printing process and (iii) final bioprinted product (Figure 7.1).

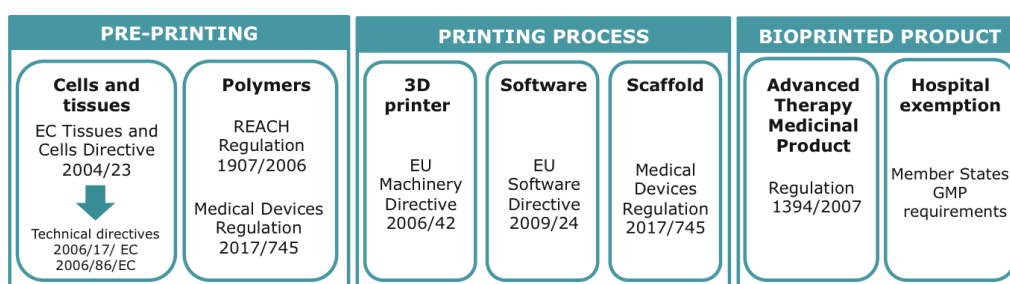


Figure 7.1. Applicable regulations through the 3D bioprinting process

Based on the different stage of production of the final 3D bioproduct different regulations are involved. They are here summarized in the main three stage of the bioprinting process: pre-printing process, printing process and bioprinted production. Good manufacturing practice (GMP).

(i) Pre-printing

Cells are the core element of the bioprinting process, and the legal framework defining the safety and quality standards for tissues and cells is set out in the European Union Tissue and Cells Directive (Directive 2004/23/EC) (9). This Directive is applied through two separate implementing Directives: the First Technical Directive, covering the steps of donation, procurement, and testing of tissue and cells and the Second Technical Directive covering their storage and distribution (10). When appropriate, additional requirements from ATPMs Regulation 1394/2007 should be included.

The REACH Regulation 1907/2006 for the Registration, Evaluation, Authorisation and Restriction of Chemicals (11) apply to all chemical substances, such as natural or synthetic polymers used for cell culture or in the bioink. Moreover, the polymeric matrix in which cells are cultured, can also fall under the provisions of the Medical Devices Regulation (5).

(ii) Printing process

The 3D printer itself would be considered as an advanced manufactured technology, which would fall under the scope of the EU Machinery Directive 2006/42 with its own quality and safety requirements (12).

With regard to the 3D printing software, a distinction must be made according to the intended purpose. When a software is intended to be used for therapeutic or diagnostic purposes (for instance, preoperative or surgical planning), it would qualify as a stand-alone medical device under the new EU MDR (5). In that case, the software is subject to safety and performance requirements, and would fall into the same category as the device. However, 3D design software is not classified as a medical device since it is only used for the production of the device and does not have a specific medical purpose. Therefore, the EU Software Directive 2009/24 would apply.

If present, the scaffold used for bioprinting would constitute a medical device in accordance with Article 2 of MDR and it would need to be compliant with the medical devices regulation (5). In the new MDR there is a clarification on mass-produced products that need to be adapted to a patient that changes the concept of custom-made products, custom-made devices are created only once from scratch following the prescription of the practitioner (5). For instance, a 3D-printed implant that is printed with the manufacturer's standard procedure and that afterwards is adapted to the patient following the indications of the practitioner would not be any more considered as a custom-made device but a mass-produced product. Therefore, a conformity assessment procedure needs to be undertaken for that scaffold in order to get a CE mark for that intended use by a Notified Body. Custom-made devices need to be compliant with less constraining requirements such as the general obligations of manufacturers described in Article 10 and General Safety and Performance Requirements in Annex I. These obligations include conformity assessment procedures in order to fulfill safety and performance requirements but do not include CE marking.

(iii) Final bioprinted product

Lastly, as already described before, the final 3D bioprinted product has to be approved; most probably by EMA following the centralized route for ATMPs. However, in order to facilitate access of patients to new treatments for unmet

medical needs, the ATMP Regulation includes a "hospital exemption" for products not intended to be marketed (13). This provision is made for ATMPs that are: (I) prepared on a non-routine basis, and (II) used within the same Member State in a hospital under the exclusive responsibility of a medical practitioner, and (III) comply with an individual medical prescription, (IV) for a custom-made product for an individual patient. In that case, the EU medicines legislation would not apply and a national competent authority would have to authorize the manufacturing of such products, which must comply with the same national requirements concerning good manufacturing practice and pharmacovigilance applicable to authorized medicinal products (14). 3D bioprinted products could eventually fall under the hospital exemption, even if this should not be the main route for their commercialization. However, the meaning of "non-routine basis" and "custom-made" are not specified in the regulation and there is a lack of a harmonized approach for the application of the exemption among different European countries (15,16). In fact, the hospital exemption was the topic triggering most responses and with more conflicting views manifested during the public consultation of the ATMP Regulation (17).

7.3 Regulatory framework for 3D bioprinting outside Europe

To our knowledge, there is also a lack of specific regulatory frameworks or guidance documents for bioprinting products outside Europe. The US Food and Drug Administration and Health Canada have released guidance documents with recommendations for additive manufactured medical devices (18,19), but there is not specific reference to bioprinting in these guidance documents. Australia has proposed a regulatory scheme for personalized medical devices including 3D-printed devices, which has recently been under consultation (20). This proposed reform to the regulation of medicines and medical devices specifically mentions 3D Bioprinting or printing of patient specific implants that incorporate human origin material. In the particular case of medical devices that contain human origin material (either viable or non-viable) as a component (not wholly comprised of) they would not be regulated as biologicals but as Class III medical devices with a biological component. Also South Korea and Japan have provided some specific regulatory guidance applicable to 3D bioprinting (21).

7.3.1 Available standards

Another challenge for both regulators and manufacturers pertains to the limited standards that are available covering additive manufacturing and bioprinting. Discussions within the ICMRA highlighted the importance of the adoption and update of established standards to ensure the quality, comparability, stability, safety and effectiveness of bioprinted products (1). These standards would include Good Manufacturing Practice (GMP), International Council of Harmonisation standards (ICH), International Standardisation Organisation (ISO) or ASTM (American Society for Testing and Materials) International standards.

The ASTM Committee F04 on Medical and Surgical Materials and Devices has published several working items related to 3D Bioprinting such as New Test Methods for Printability of Bioinks and Biomaterial Inks (WK65680), in collaboration with the Standards Coordinating Body for Gene, Cell, and Regenerative Medicines and Cell-Based Drug Discovery (SCB). This test method

aims at comparing printability and help to establish reproducibility and quality control between different material lots or manufacturers. Recently, another test method has been released on Printability of Bioinks for Extrusion-based Bioprinting (ASTM WK72274). This standard is focused on two test methods to evaluate printability of bioinks made of any material, including material inks without cells, used during extrusion-based bioprinting. ASTM efforts are also addressed at the development of a guidance document providing material properties and compositions that promote survival of living cells contained bioinks (ASTM WK65681 - New Guide for Bioinks and biomaterial inks used in bioprinting). The SCB is also coordinating two standards projects on (1) bioprinter software and data governance and (2) bioprinting hardware and component specifications, to develop guidelines for the calibration, compatibility, and interoperability of bioprinter hardware and related components ISO and ASTM International have a coordinated effort for the development of standards in additive manufacturing and have jointly crafted the Additive Manufacturing Standards Development Structure. This framework structure is aimed at identifying standards-related gaps and needs, prioritise standards areas and improve usability and acceptance among the 3D printing community, including manufacturers, entrepreneurs, consumers and others. Based on this structure, standards are developed at three levels: (i) General standards (such as concepts, common requirements, guides or safety) (ii) Standards for categories of materials or processes and (iii) Standards for a specific material, process or application. In each level, there is a division for feedstock materials, process/equipment and finished parts. Although these standards are not specific for bioprinting, they could be useful for the development and implementation of a standardized methodology for the characterisation of 3D bioprinted products.

7.4 Conclusions

Beyond the scientific and technical challenges, 3D bioprinting has been identified as a disruptive technology for traditional health regulatory systems since different aspects of 3D bioprinting could lead to regulatory oversight. Careful examination of the existing regulatory paths in the EU indicated that a 3D bioprinted product would be classified as a tissue engineered combined medicinal product that would fall under the scope of the ATMP Regulation. Other regulations would apply at different steps of the bioprinting process, but existing regulatory frameworks do not account for the differences between 3D printing and conventional manufacturing methods.

To truly facilitate the development of these innovative products while protecting patients, there is need for adequate standards to ensure that a bioprinted product would be reproducible, with high quality, effective and safe. As an emerging field with different manufacturers and researchers developing products independently, there is still a lack of bioprinting-specific standards. A detailed analysis of the suitability of existing standards from other sectors would be relevant to enlarge the portfolio of available standards for bioprinting. Such cross-fertilization, in terms of learning from the methodologies and guidelines existing in other fields, would support a smooth and safe translation of these products to clinical applications. Moreover, a close collaboration between academia, industry and regulators will be essential to move the field forward to facilitate patient access to these new products.

7.5 References

1. ICMRA Innovation Project 3D Bio-Printing Case Study: Summary of Discussions and Considerations for the New Informal Innovation. 2019;
2. Kritikos M. 3D bio-printing for medical and enhancement purposes: Legal and ethical aspects. 2018.
3. European Medicines Agency; Inspections Pharmacovigilance Human Medicines Committees & Division. Scientific recommendation on classification of advanced therapy medicinal products [Internet]. EMA/665239/2017. 2017. Available from: http://www.ema.europa.eu/ema/index.jsp?curl=pages/regulation/general/general_content_000296.jsp&mid=WC0b01ac058007f4bc
4. European Union. Regulation (EC) No 1394/2007 of the European Parliament and of the Council of 13 November 2007 on advanced therapy medicinal products. Off J Eur Union. 2007;L 324/121.
5. Regulation (EU) 2017/745 of the European Parliament and of the Council of 5 April 2017 on medical devices. 2017.
6. European Medicines Agency; Committee for Advanced Therapies. Reflection paper on classification of advanced therapy medicinal products Reflection paper on classification of Advanced Therapy Medicinal Products Table of contents. 2015;
7. European Medicines Agency; Committee for Advanced Therapies. Procedural advice on the evaluation of advanced therapy medicinal product in accordance with article 8 of Regulation (EC) No 1394/2007. 2009;EMA/630043/2008.
8. European Medicines Agency; Committee for Advanced Therapies. Procedural advice on the evaluation of combined advanced therapy medicinal products and the consultation of Notified Bodies in accordance with Article 9 of Regulation (EC) No . 1394 / 2007. EMA/354785/2010. 2011.
9. Directive 2004/23/EC of the European Parliament and of the Council of 31 March 2004 on setting standards of quality and safety for the donation, procurement, testing, processing, preservation, storage and distribution of

- human tissues and cells. Off J Eur Union. 2004;L 102/48-58.
10. Li P, Faulkner A. 3D Bioprinting Regulations: A UK/EU Perspective. *Eur J Risk Regul.* 2017;8(2):441–7.
 11. Regulation (EC) No 1907/2006 of the European Parliament and of the Council of 18 December 2006 concerning the Registration, Evaluation, Authorisation and Restriction of Chemicals (REACH). OJ L 396 [Internet]. 2006; Available from: <https://eur-lex.europa.eu/legal-content/EN/TXT/PDF/?uri=CELEX:02006R1907-20140410&from=EN>
 12. Kritikos M. 3D bio-printing for medical and enhancement purposes: Legal and ethical aspects [Internet]. 2018. Available from: [http://www.europarl.europa.eu/RegData/etudes/IDAN/2018/614571/EPRS_IDA\(2018\)614571\(ANN2\)_EN.pdf](http://www.europarl.europa.eu/RegData/etudes/IDAN/2018/614571/EPRS_IDA(2018)614571(ANN2)_EN.pdf)
 13. Eder C, Wild C. Technology forecast: advanced therapies in late clinical research, EMA approval or clinical application via hospital exemption. *J Mark Access Heal Policy.* 2019;7(1):1600939.
 14. European Medicines Agency. Advanced therapy medicines: exploring solutions to foster development and expand patient access in Europe Outcome of a multi-stakeholder meeting with experts and regulators held at EMA. 2016;(June):EMA/345874/2016. Available from: www.ema.europa.eu/contact
 15. Cuende N, Boniface C, Bravery C, Forte M, Giordano R, Hildebrandt M, et al. The puzzling situation of hospital exemption for advanced therapy medicinal products in Europe and stakeholders' concerns. *Cytotherapy.* 2014;16(12):1597–600.
 16. Detela G, Lodge A. EU Regulatory Pathways for ATMPs: Standard, Accelerated and Adaptive Pathways to Marketing Authorisation. *Mol Ther - Methods Clin Dev.* 2019;13(June):205–32.
 17. European Commission. Regulation (EC) No. 1394/2007 on advanced therapy medicinal products. Summary of the responses to the public consultation. 2013.
 18. US FDA. Technical Considerations for Additive Manufactured Medical Devices - Guidance for Industry and Food and Drug Administration Staff. 2017.
 19. Health Canada. Draft Guidance Document - Licensing Requirements for

- Implantable Medical Devices MAnufactured by 3D printing. 2018;1–9.
20. Therapeutic Goods Administration Department of Health. Consultation: Proposed regulatory scheme for personalised medical devices , including 3D-printed devices. 2019;
 21. Gilbert F, O'Connell CD, Mladenovska T, Dodds S. Print Me an Organ? Ethical and Regulatory Issues Emerging from 3D Bioprinting in Medicine. *Sci Eng Ethics*. 2018;24(1):73–91.

Conclusions and future perspectives

In this thesis the development and validation of a GMP-compliant xenogenic free medium for culture ASCs was obtained and exploited to induce ASCs toward tenogenic differentiation *in vitro* in both 2D and 3D (on bioprinted scaffold) conditions.

First, cryopreserved ASCs cultured xenogenic and serum-free media, serum free (SF) or human-platelet lysate (hPL) medium, were found suitable to grow cells *in vitro* maintaining the specific MSC features of ASCs such as fibroblast-like morphology, the expression of MSC surface antigens and of early stemness and proliferative markers. Moreover, the SF medium suits perfectly the requirements about standardization of culture protocol and xenogenic free products considering its chemically defined nature obtained avoiding the use of animal-derived serums. The tenogenic induction protocol developed here consists in a unique, and for the first time adopted, TENO medium with a blend of AA, TGF β 3, BMP-12 and CTGF growth factors and molecules involved in tendon development and healing process, that was able to strongly trigger tenogenesis of ASCs in both hPL and SF conditions for 14 days of culture. In particular, significant higher gene expression levels of the tendon associated markers, such as scleraxis (SCX), collagen type I/III (COL1A1, COL1A3), cartilage oligomeric matrix protein (COMP) and metalloproteinase-3/13 (MMP-3, MMP-13) were observed in both differentiated SF and hPL ASCs in comparison to the respective undifferentiated cells. In order to confirm these data at the protein levels, specific expression of scleraxis and tenomodulin were also detected by immunofluorescence-based assays, and abundant collagen matrix deposition detected with colorimetric staining.

Beside, a first proof-of-concept to the development of ASC-laden 3D bioprinted xenogenic-free constructs with FDA-compliant bioink for tendon tissue engineering was achieved. In particular, a mixture of nanocellulose fibers (NFC) and alginate (A) with the addition of the ECM proteins, laminin 111, 121, 411 and 521, showed good visco-elastic properties that permitted the printing of a 3D square grid structure (5 x 5 x 1 mm) with sufficient resolution. Bioprinted ASCs

in high cell densities (3, 6 and 9.0×10^6 cell/ml bioink) showed high survival rate after printing and high cell viability demonstrating the possibility to employ the NFC/A scaffold as cell-carrier to deliver and retain viable and functional human ASCs at the site of tendon damage in order to enhance tissue specific ECM production and tissue regeneration. Indeed, the combination with biochemical stimuli *in vitro* triggered tenogenesis of bioprinted ASCs. Differentiated ASC-constructs showed specific early expression of scleraxis and later of collagen type III. Furthermore, the nanofibrillar and microporous structure of NFC/A hydrogel resembles the microarchitecture of tendon realising a physical and mechanical biomimetic environment in which ASCs could adhere, spread and, probably, also migrate. The absence of ASC inflammatory response to the 3D NFC/A substrate represents another evidence of the safety of these xeno-free FDA approved materials and of the xeno-free tenogenic differentiation protocol.

Results achieved provide substantial evidence of the suitability of the xenogenic-free TENO medium to promote tenogenic differentiation of ASCs in both 2D and 3D conditions. Furthermore, the bioprinting of ASCs within a 3D structure made of natural-based hydrogel successfully provide an ideal environment for the transplanted cells, able to support their viability and functionality. Importantly, the demonstration of the suitability of the here-investigated GMP-compliant approaches is a crucial step toward the clinical application of bioprinted ASCs for tendon therapeutic approaches. The development of these innovative biological products, either stem cells alone or in combination with biomaterials through processing with additive manufacturing technologies, is strictly demanding adequate standards to ensure reproducible, high quality, effective and safe treatments with high translational potential.

Further studies, based on different bioprinting strategies, such as low cell density of printing and/or different composition of nanocellulose and alginate in the bioink could better clarify the behaviour of cells after printing in order to prolong as much possible the ASCs viability in the NFC/A scaffold. Moreover, since the mechano-responsiveness nature of tendon tissue, in order to better resemble the natural tendon microenvironment, future investigations may elucidate the mechanical response of the 3D ASC-constructs in terms of tenogenic differentiative ability by dynamic cultures using a bioreactor.

